



An experimental overview of the Scalar Boson

Lydia Iconomidou-Fayard



Comprendre le monde, construire l'avenir®

The topics of this Lecture

Goal: Describe the main tools that have been necessary for the Scalar Boson Discovery

The LHC machine

The ATLAS and CMS experiments

The particle signatures in the detectors

The main Higgs decay channels

The Scalar Boson passport:
Its mass, its couplings, its properties

Results from both experiments
(more on ATLAS....)



1964 : Brout Englert Higgs
And Kibble, Hagen, Guralnik

Introduction of a scalar field
with non-zero vacuum
expectation value after a
temperature $T > T_c$

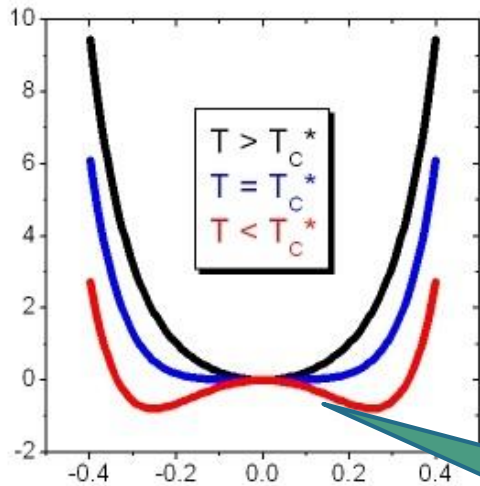


1964 : Brout Englert Higgs
And Kibble, Hagen, Guralnik

Introduction of a scalar field
with non-zero vacuum
expectation value after a
temperature $T > T_c$



$$V(\phi^*\phi) = -\mu^2(\phi^*\phi) + \lambda^2(\phi^*\phi)^2$$



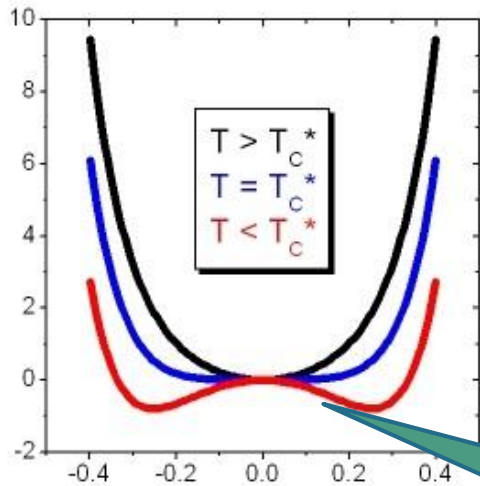
Vacuum: $dV(\phi^*\phi) = 0$
For $v = \sqrt{-\mu^2/\lambda} = 246.2 \text{ GeV}$

1964 : Brout Englert Higgs
And Kibble, Hagen, Guralnik



Introduction of a scalar field
with non-zero vacuum
expectation value after a
temperature $T > T_c$

$$V(\phi^*\phi) = -\mu^2(\phi^*\phi) + \lambda^2(\phi^*\phi)^2$$



Vacuum: $dV(\phi^*\phi) = 0$
For $v = \sqrt{-\mu^2/\lambda} = 246.2 \text{ GeV}$

Implications for the Electroweak Interactions

→ The fundamental particles, appearing in the lagrangian initially with zero mass, become massive through their interaction with the scalar field.

→ Gluons and photons remain massless

→ The EW intermediate bosons W and Z become heavy

The seventies

1967 : Glashow, Weinberg and Salam

Standard Model is published, integrating the Brout-Englert-Higgs mechanism
Prediction of W and Z boson masses. The Higgs mass remains unknown



The seventies

7

1967 : Glashow, Weinberg and Salam

Standard Model is published, integrating the Brout-Englert-Higgs mechanism
Prediction of W and Z boson masses. The Higgs mass remains unknown

1973 : Discovery of the neutral currents
at CERN- Gargamelle detector



Ydla Iconomidou-Fayard

The seventies

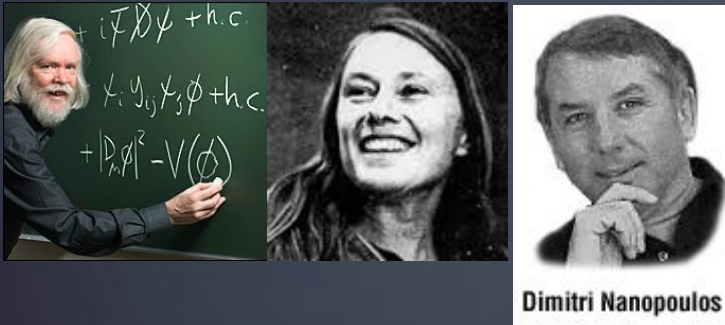
1967 : Glashow, Weinberg and Salam

Standard Model is published, integrating the Brout-Englert-Higgs mechanism
Prediction of W and Z boson masses. The Higgs mass remains unknown



1973 : Discovery of the neutral currents
at CERN- Gargamelle detector

1976: First phenomenological analysis of Higgs decays



We should perhaps finish with an apology and a caution. We apologize to experimentalists for having no idea what is the mass of the Higgs boson, unlike the case with charm^{3),4)} and for not being sure of its couplings to other particles, except that they are probably all very small. For these reasons we do not want to encourage big experimental searches for the Higgs boson, but we do feel that people performing experiments vulnerable to the Higgs boson should know how it may turn up.

The seventies

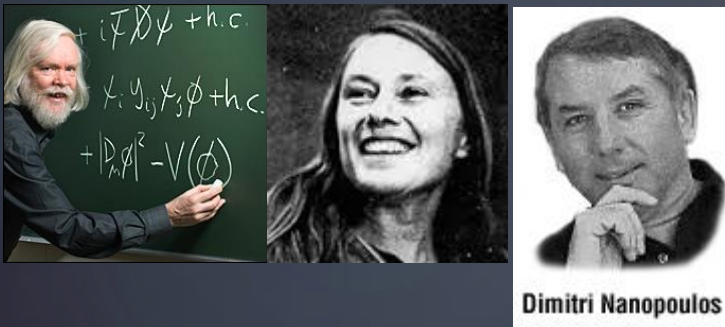
1967 : Glashow, Weinberg and Salam

Standard Model is published, integrating the Brout-Englert-Higgs mechanism
Prediction of W and Z boson masses. The Higgs mass remains unknown



1973 : Discovery of the neutral currents at CERN- Gargamelle detector

1976: First phenomenological analysis of Higgs decays



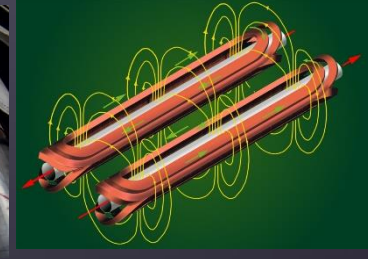
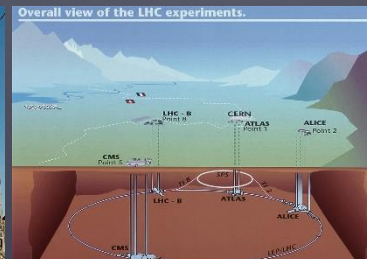
Dimitri Nanopoulos

We should perhaps finish with an apology and a caution. We apologize to experimentalists for having no idea what is the mass of the Higgs boson, unlike the case with charm^{3),4)} and for not being sure of its couplings to other particles, except that they are probably all very small. For these reasons we do not want to encourage big experimental searches for the Higgs boson, but we do feel that people performing experiments vulnerable to the Higgs boson should know how it may turn up.

1983 : Discovery of W⁺- and Z bosons at CERN- UA1 & UA2 detectors, with the predicted masses

Indirect proof for the mechanism

The main tool : The Large Hadron Collider at CERN



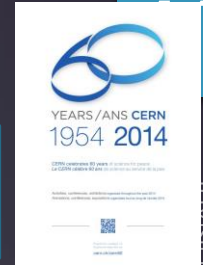
The CERN laboratory

Founded in 1954. Constructed around the French-Swiss frontier

Today

- 21 member-states
- 6 observers
- 42 collaborators
- 17 contacts

10000 scientists from 113 Universities



Lydia Iconomidou-Fayard
2015

The CERN laboratory

Founded in 1954. Constructed around the French-Swiss frontier

Today

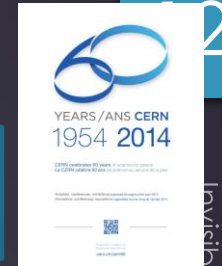
- 21 member-states
- 6 observers
- 42 collaborators
- 17 contacts



10000 scientists from 113 Universities

A series of major discoveries

- 1) Discovery of Neutral currents 1973
- 2) Discovery of W & Z bosons 1983
- 3) Search and measurement of the Direct CP violation in the Kaon system (1988-2001)
- 4) Number of lepton families (LEP, 1991)
- 5) Prediction of the top mass (LEP)
- 6) Evidence and Study of the quark-gluon plasma
- 7) Creation of anti-Hydrogen in the lab (2002)
- 8) The Scalar Boson (2012)



The LHC genesis

~1980

Brainstorming on CERN's future

1984

1992

1994

1995

1996



The LHC genesis

~1980

Brainstorming on CERN's future

1984

ECFA starts thinking about a proton collider to install in the LEP tunnel

1992

1994

1995

1996



The LHC genesis

~1980

Brainstorming on CERN's future

1984

ECFA starts thinking about a proton collider to install in the LEP tunnel

1992

First LOIs of experiments for LHC. Feasibility studies for the machine

1994

December : CERN Council approves the LHC Construction in 2 steps

1995

1996



The LHC genesis

~1980

Brainstorming on CERN's future

1984

ECFA starts thinking about a proton collider to install in the LEP tunnel

1992

First LOIs of experiments for LHC. Feasibility studies for the machine

1994

December : CERN Council approves the LHC Construction in 2 steps

1995

June: Japan becomes observer of CERN and approves financial contribution for LHC construction

1996

Invisibles 2015, Lydia Iconomidou-Foyard
16/06/2015



Daruma doll

The LHC genesis

17

~1980

Brainstorming on CERN's future

1984

ECFA starts thinking about a proton collider to install in the LEP tunnel

1992

First LOIs of experiments for LHC. Feasibility studies for the machine

1994

December : CERN Council approves the LHC Construction in 2 steps

1995

June: Japan becomes observer of CERN and approves financial contribution for LHC construction

1996

February : CMS and ATLAS experiments approved

March: India and Russia announce financial support to LHC

December: Canada contributes to LHC . Cooperation protocol with US



Daruma doll

Invisibles 2015, Lydia Iconomidou-Foxard
16/06/2015

The LHC genesis

18

~1980

Brainstorming on CERN's future

1984

ECFA starts thinking about a proton collider to install in the LEP tunnel

1992

First LOIs of experiments for LHC. Feasibility studies for the machine

1994

December : CERN Council approves the LHC Construction in 2 steps

1995

June: Japan becomes observer of CERN and approves financial contribution for LHC construction

1996

February : CMS and ATLAS experiments approved

March: India and Russia announce financial support to LHC

December: Canada contributes to LHC . Cooperation protocol with US

Thanks to the contributions of non-member states , the Council approves the LHC construction in a single step



Daruma doll

Invisibles 2015, Lydia Iconomidou-Foxard
16/06/2015

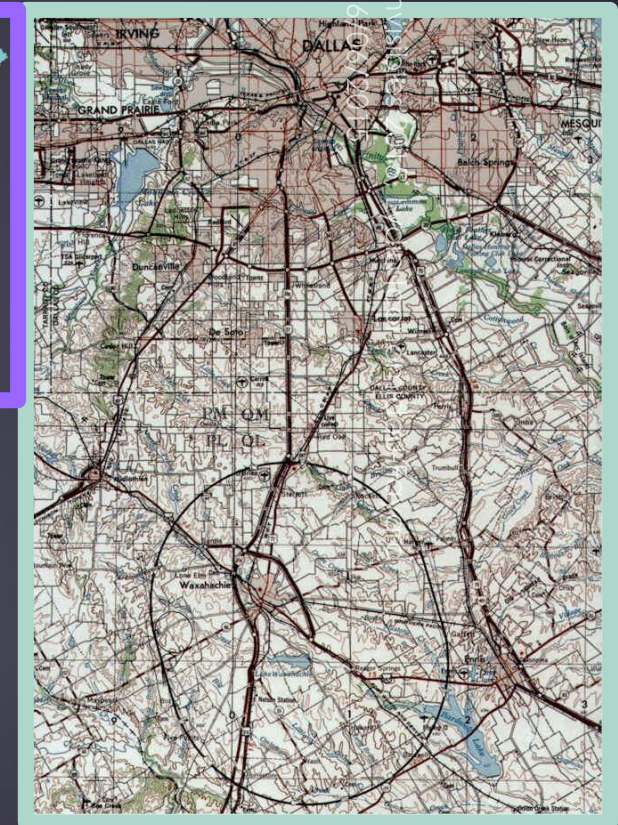
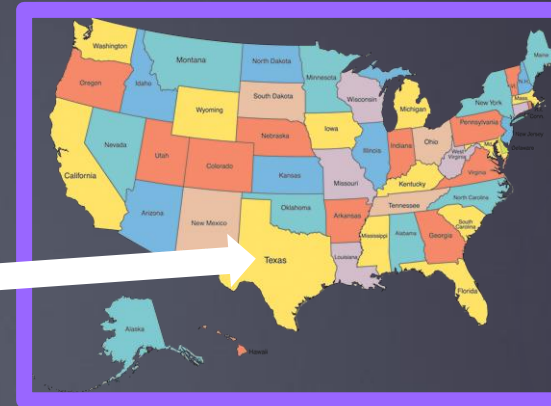
Remember: The short life of SSC (1983-1993)

The American project

19

Tunnel with circumference of 87Km, project started in 1983. Foreseen energy 20TeV per beam.

- ▶ Construction began at Waxahachie, Texas in 1990.



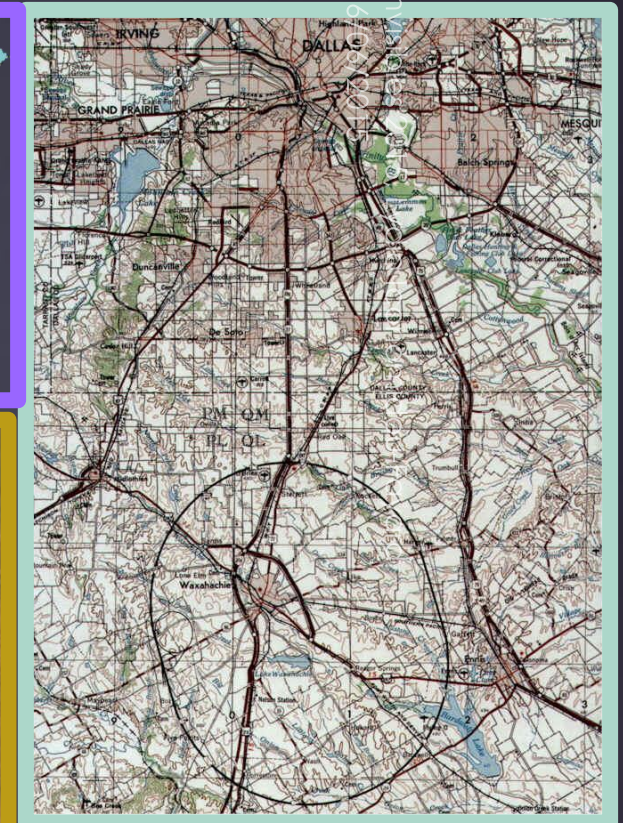
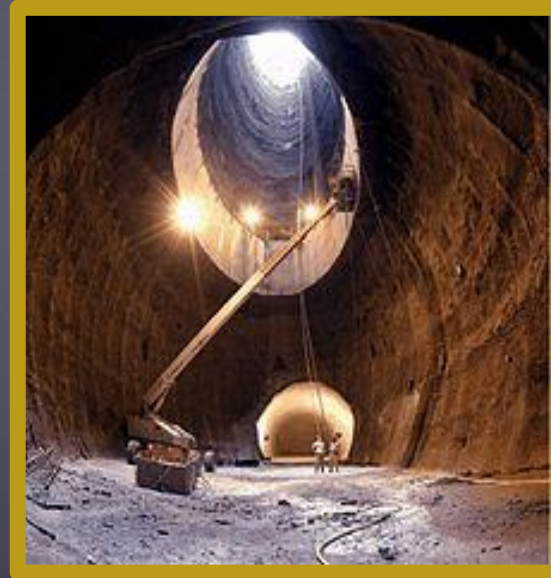
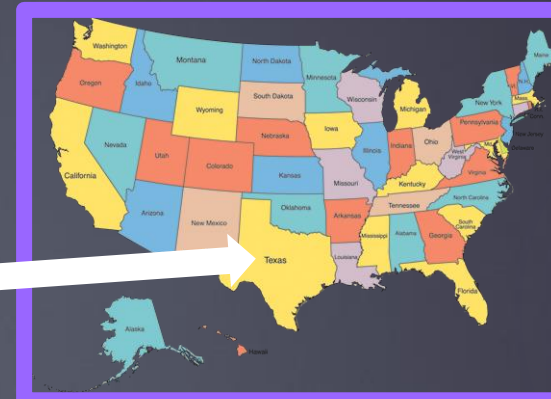
Remember: The short life of SSC (1983-1993)

The American project

20

Tunnel with circumference of 87Km, project started in 1983. Foreseen energy 20TeV per beam.

- ▶ Construction began at Waxahachie, Texas in 1990.
- ▶ Excavation of ~20Km of tunnel, construction of magnets, buildings in place, hire physicists.



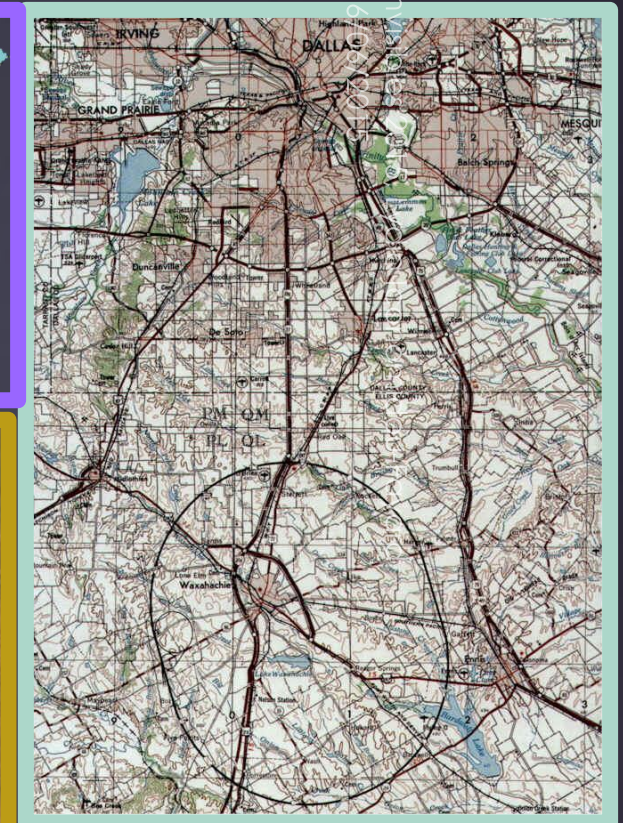
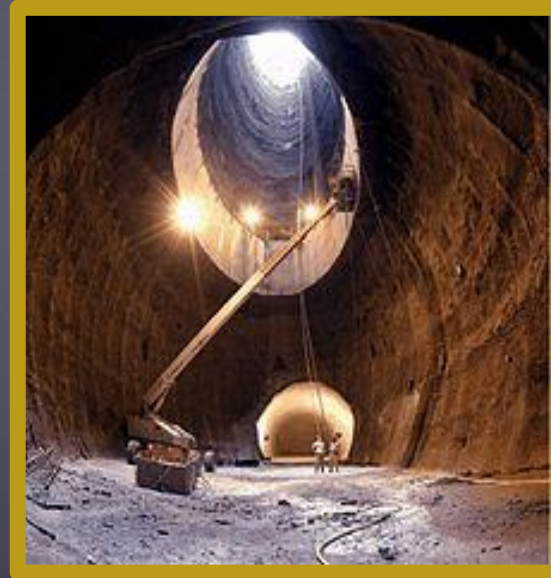
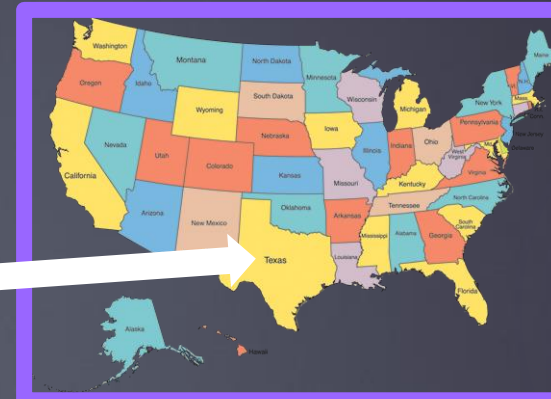
Remember: The short life of SSC (1983-1993)

The American project

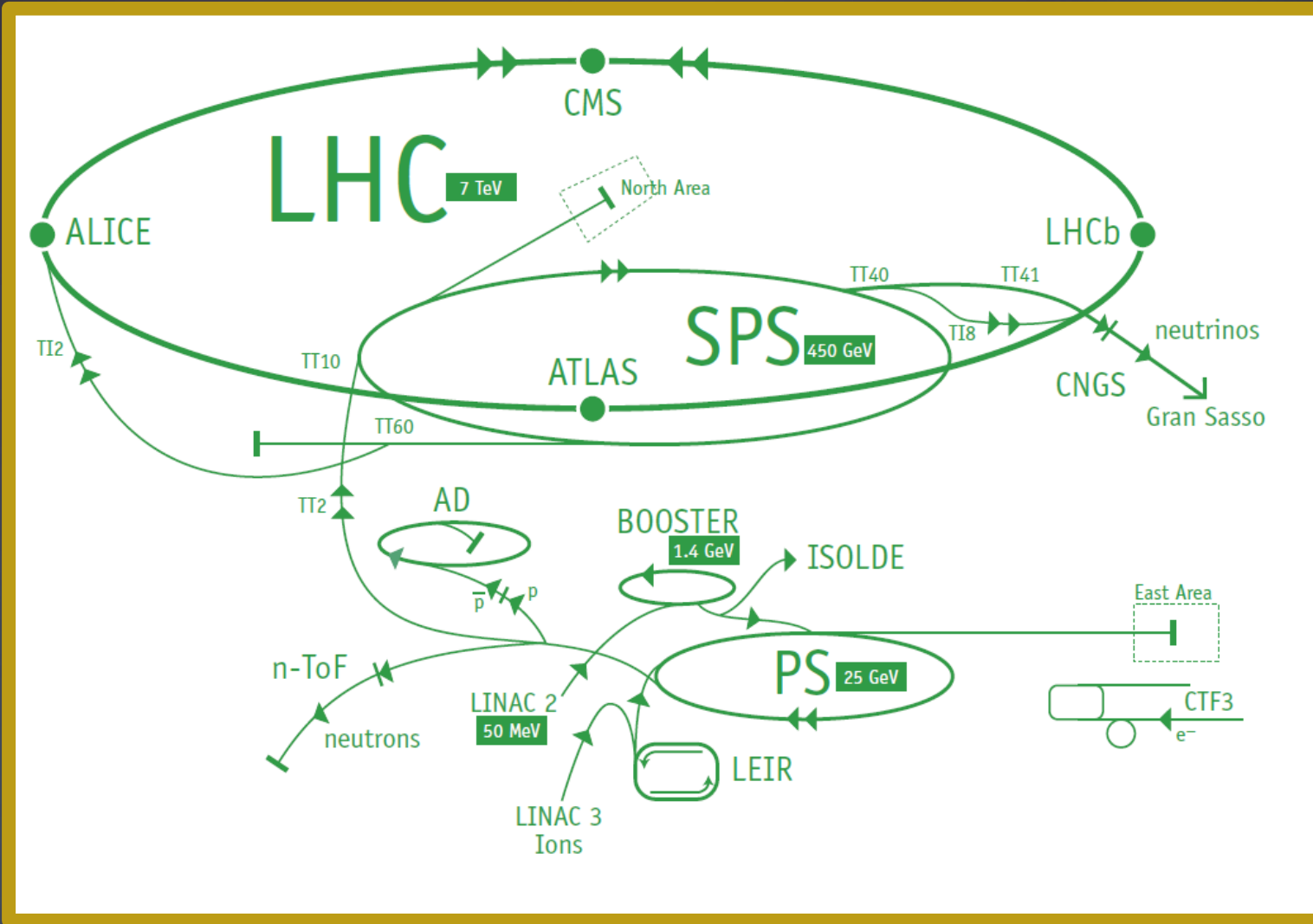
21

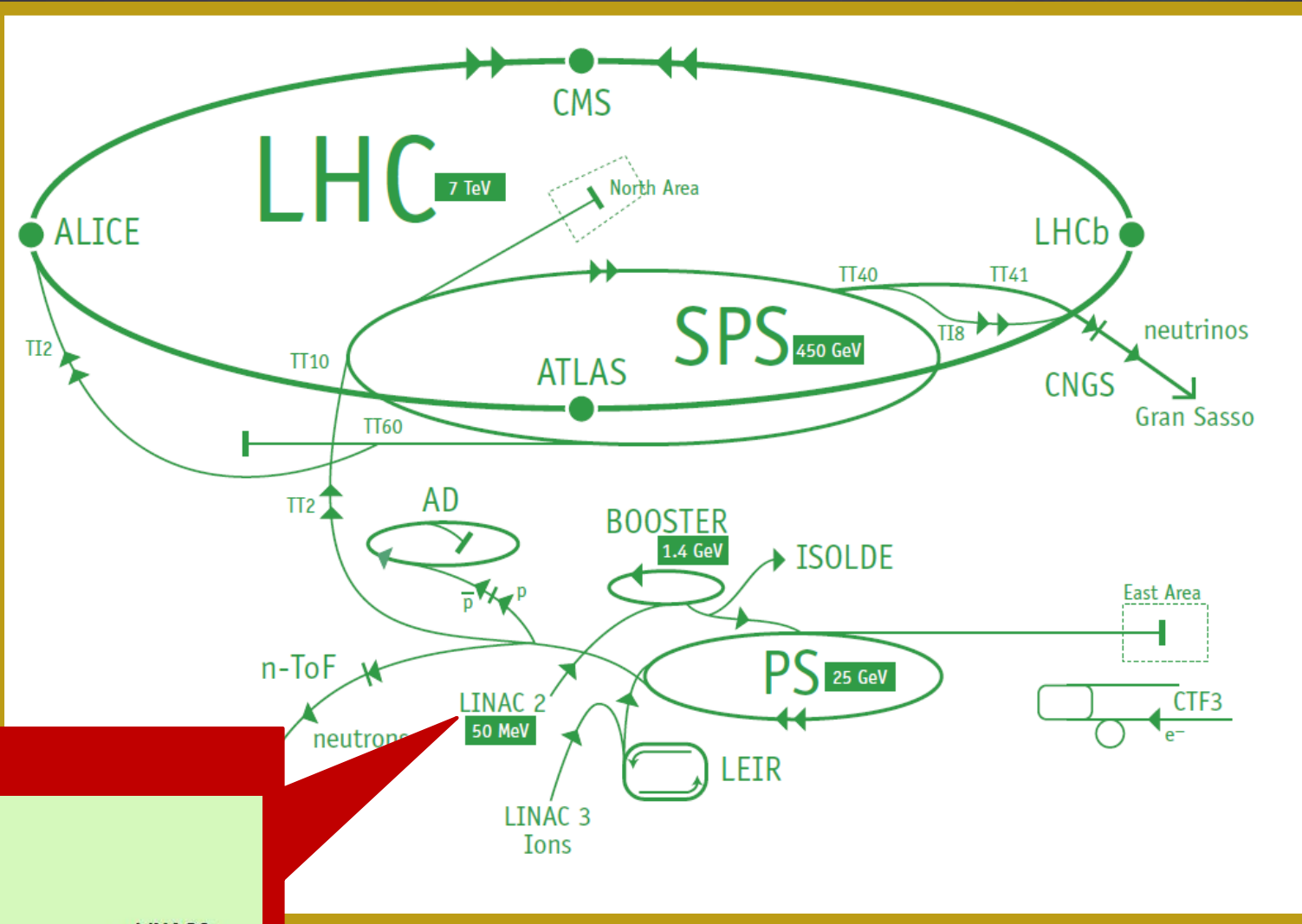
Tunnel with circumference of 87Km, project started in 1983. Foreseen energy 20TeV per beam.

- ▶ Construction began at Waxahachie, Texas in 1990.
- ▶ Excavation of ~20Km of tunnel, construction of magnets, buildings in place, hire physicists.
- ▶ In 1993 the project is abandoned by the US Senat
- ▶ Involved American physicists start to think about joining European project. Positive decision on 1995



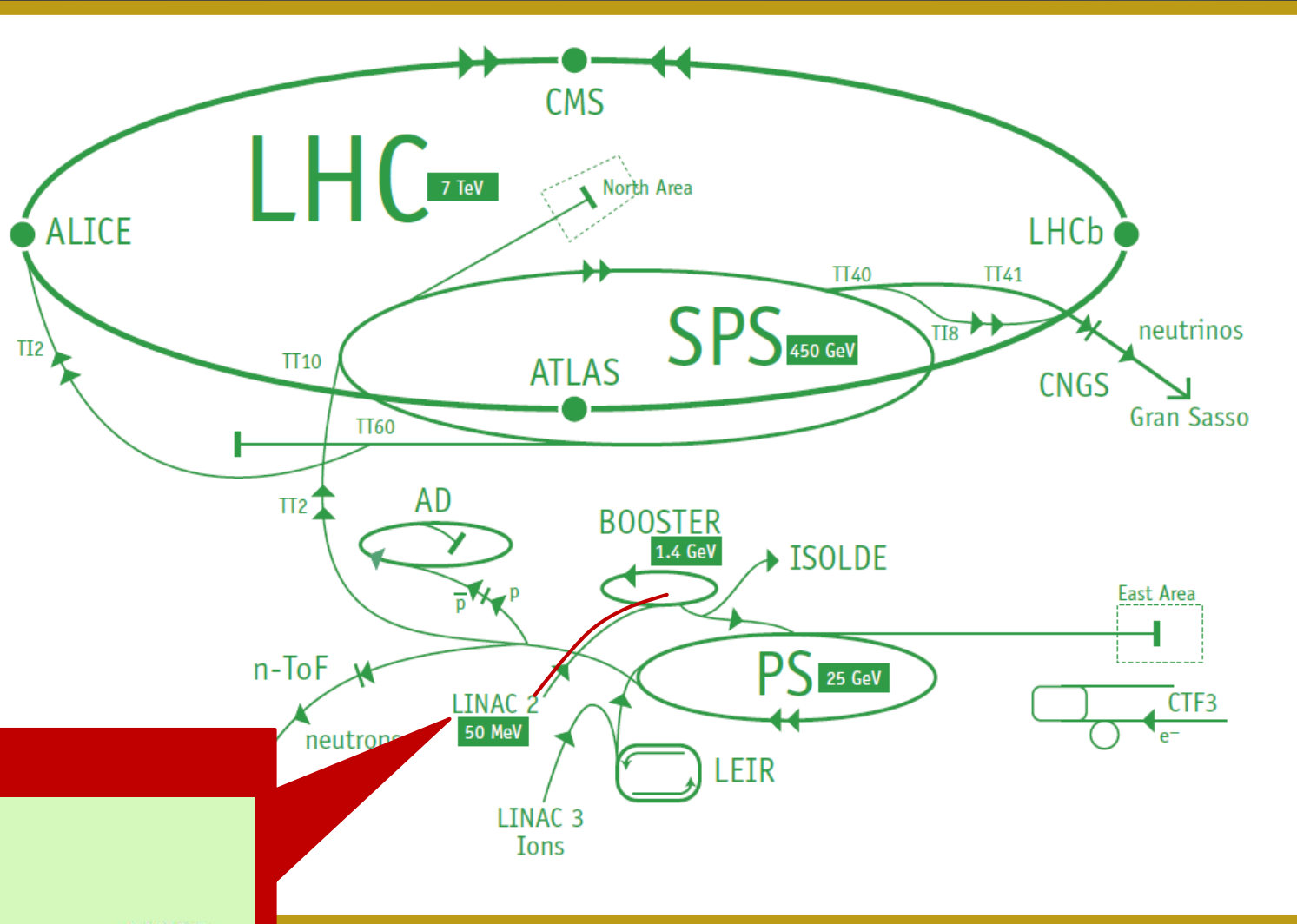
The Lord of the Rings





Proton production

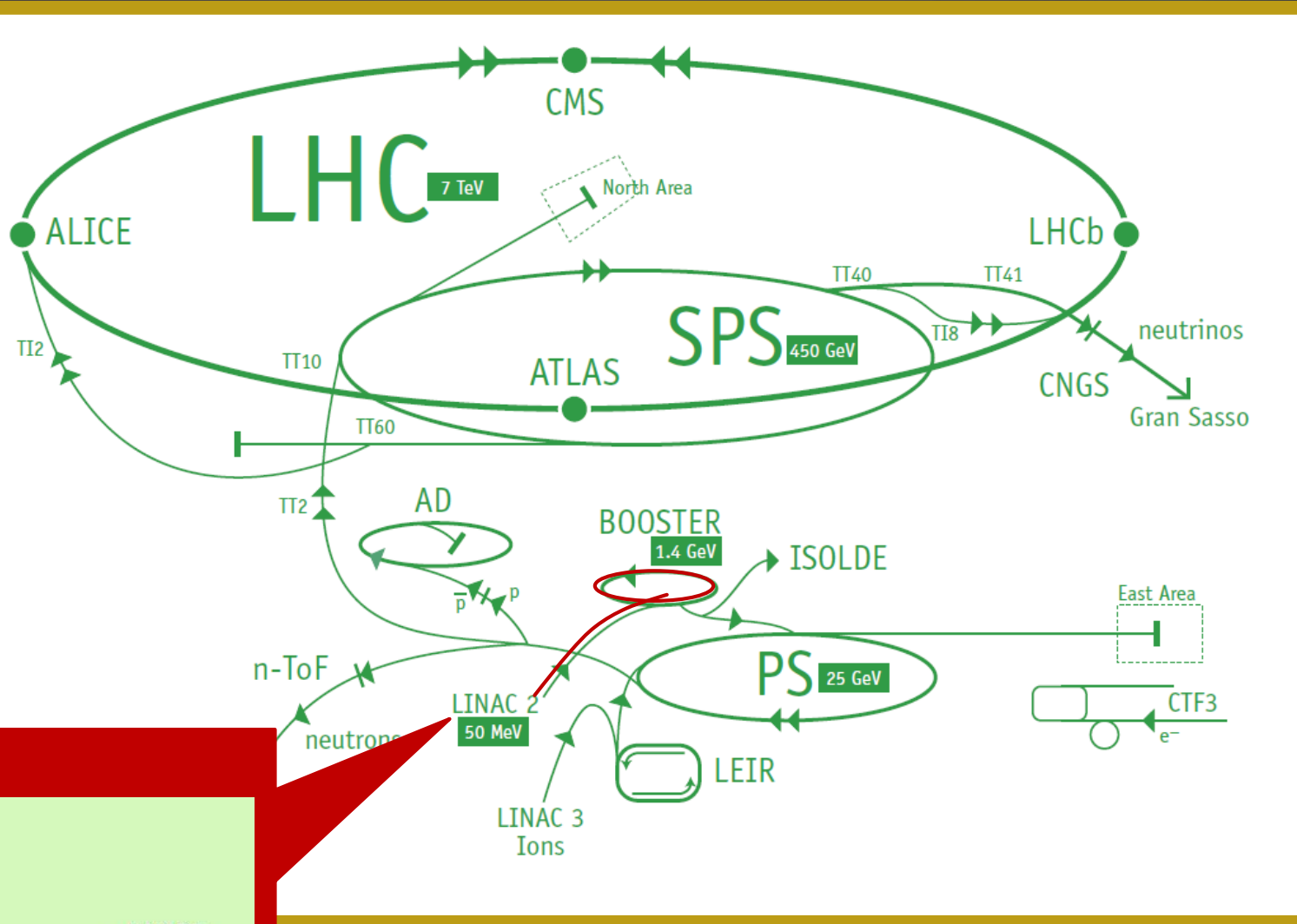




Proton production



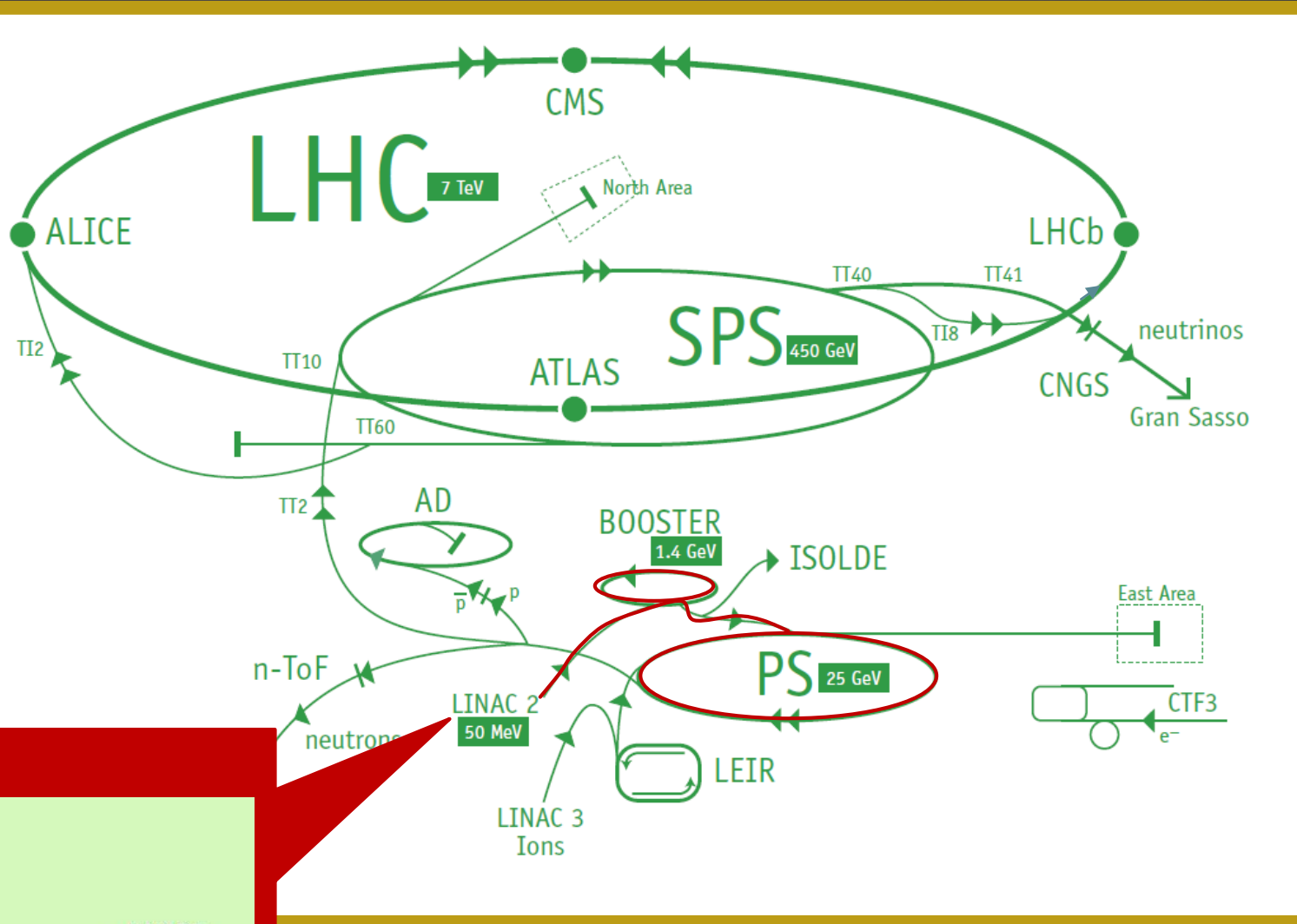
Energy	%c (speed of light)	Machine
50 MeV	31.4	Linac 2



Proton production



Energy	%C (speed of light)	Machine
50 MeV	31.4	Linac 2
1.4 GeV	91.6	Booster PS

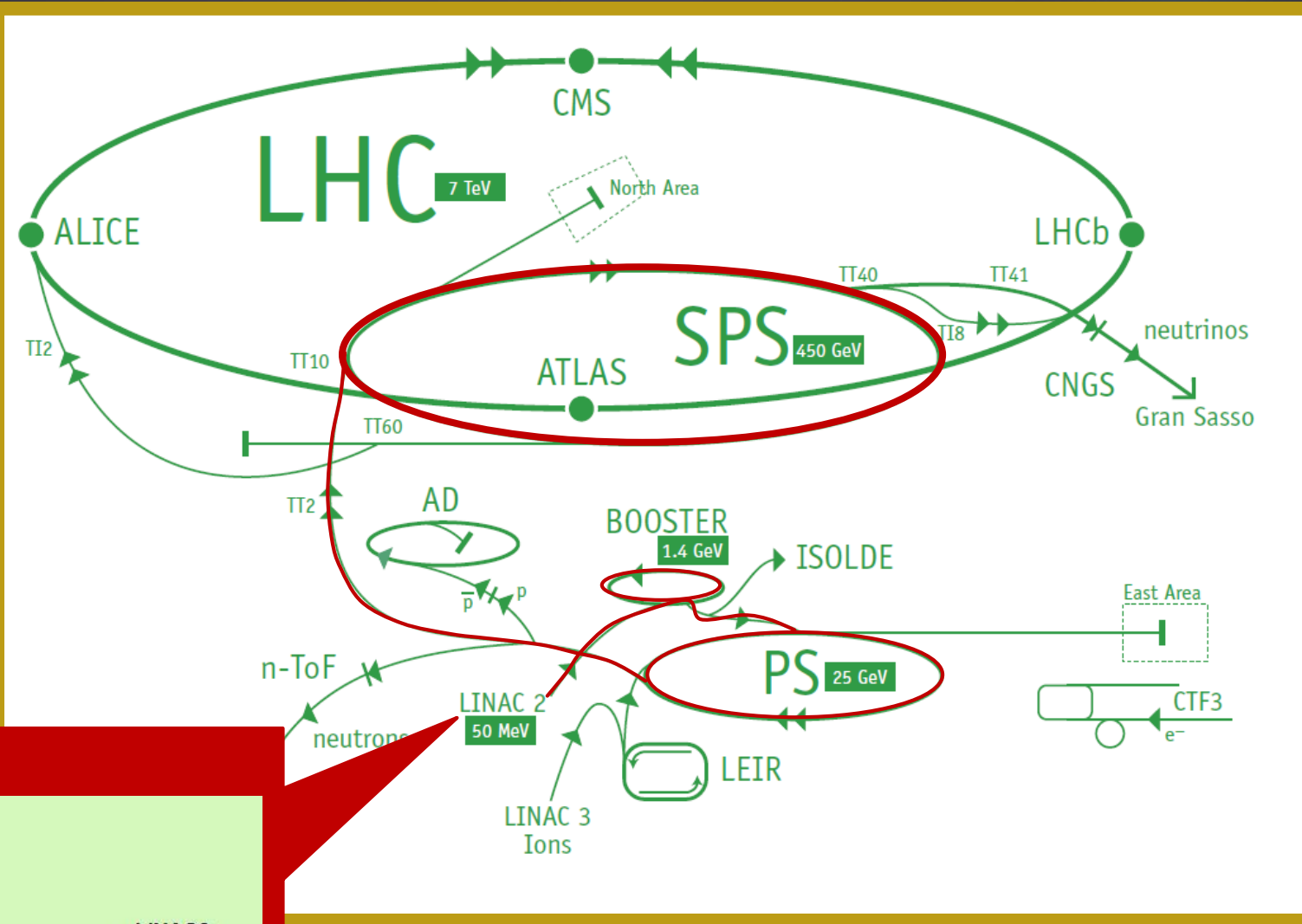


Proton production



Energy	%c (speed of light)	Machine
50 MeV	31.4	Linac 2
1.4 GeV	91.6	Booster PS
25 GeV	99.93	PS

The Lord of the Rings



Proton production

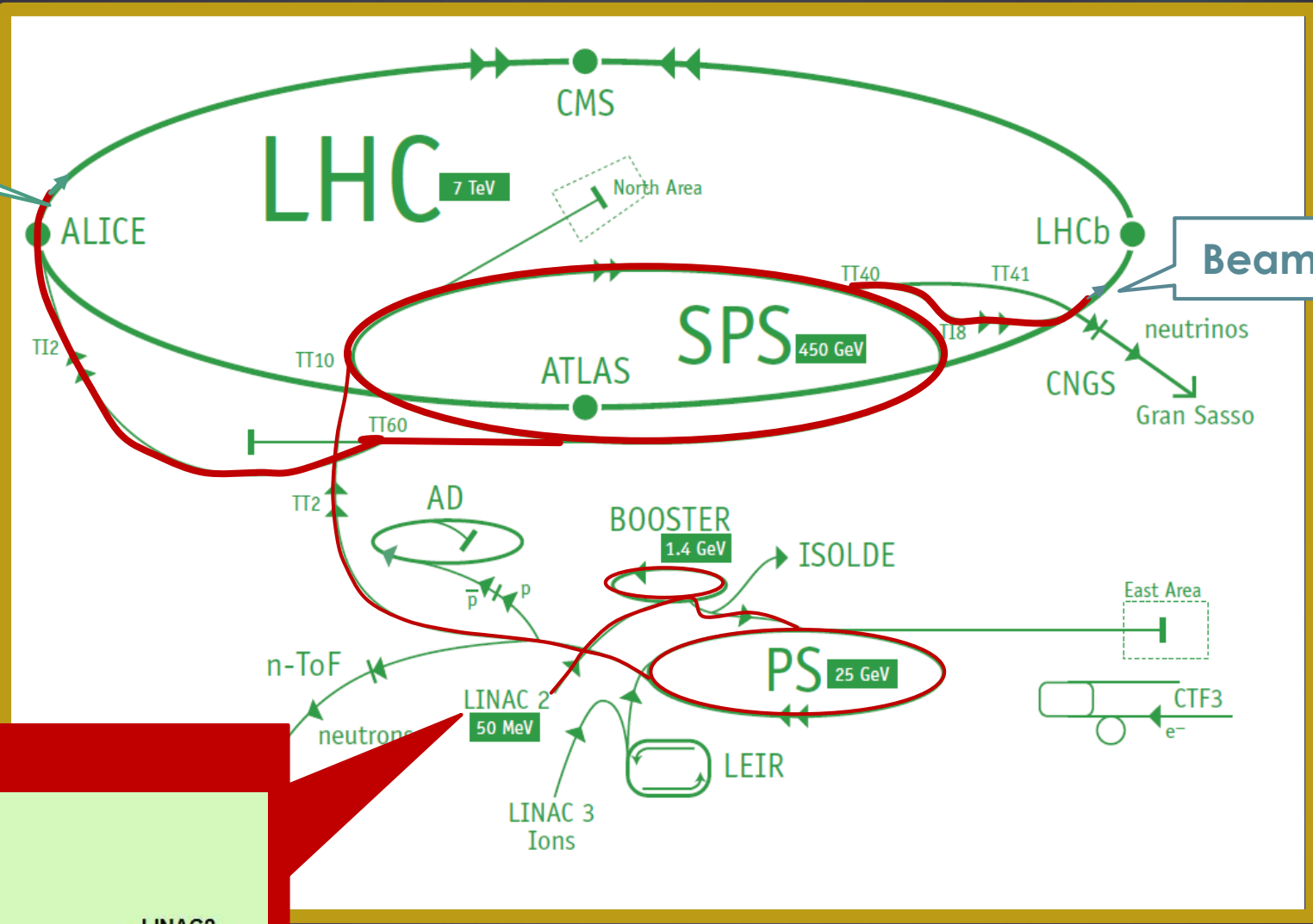


Energy	%C (speed of light)	Machine
50 MeV	31.4	Linac 2
1.4 GeV	91.6	Booster PS
25 GeV	99.93	PS
450 GeV	99.9998	SPS

The Lord of the Rings

Beam 1

Beam 2



Proton production

H₂ → LINAC2 PSB PS SPS → LHC

Energy	%c (speed of light)	Machine
50 MeV	31.4	Linac 2
1.4 GeV	91.6	Booster PS
25 GeV	99.93	PS
450 GeV	99.9998	SPS
7 TeV	99.9999991	LHC

The LHC is made out of:

27 Km ring constructed between the Jura and the Geneva Lake, underground

The LHC is made out of:

30

27 Km ring constructed between the Jura and the Geneva Lake, underground

8 RF cavities accelerating each proton beam
The cavities ensure the high concentration of protons inside bunches.



5 MV/m at 400MHz
superconducting,
operating at 4.5K
Installed in straight
sections

The LHC is made out of:

31

27 Km ring constructed between the Jura and the Geneva Lake, underground

8 RF cavities accelerating each proton beam
The cavities ensure the high concentration of protons inside bunches.

A total of 9593 magnets

Among them :

- 1232 dipole superconducting magnets
- 392 main quadrupoles ; to keep tight beam dimensions
- Higher order multipoles (6-8-10) to correct imperfections
- Insertion magnets



5 MV/m at 400MHz
superconducting,
operating at 4.5K
Installed in straight
sections

The LHC is made out of:

32

27 Km ring constructed between the Jura and the Geneva Lake, underground

8 RF cavities accelerating each proton beam
The cavities ensure the high concentration of protons inside bunches.

A total of 9593 magnets

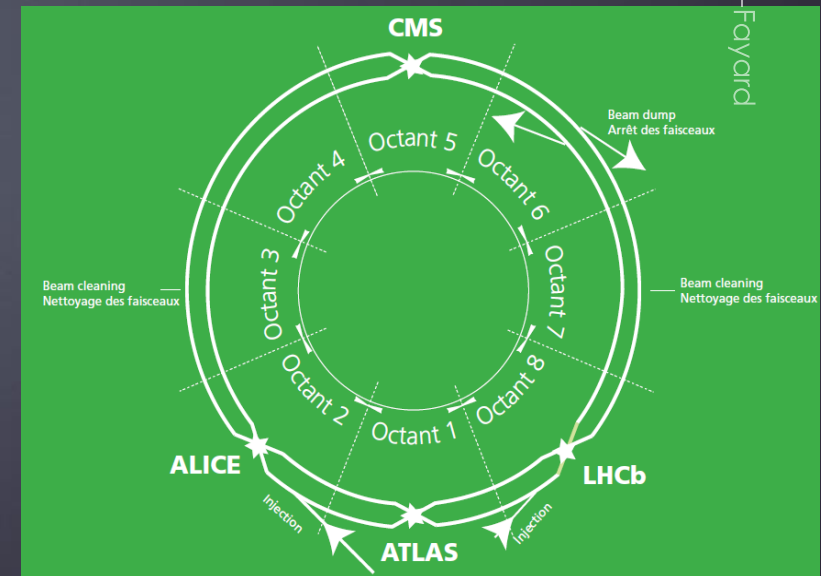
Among them :

- 1232 dipole superconducting magnets
- 392 main quadrupoles ; to keep tight beam dimensions
- Higher order multipoles (6-8-10) to correct imperfections
- Insertion magnets

Working unit of LHC: the octant
8 sectors that are independently furnished and powered.



5 MV/m at 400MHz superconducting, operating at 4.5K
Installed in straight sections

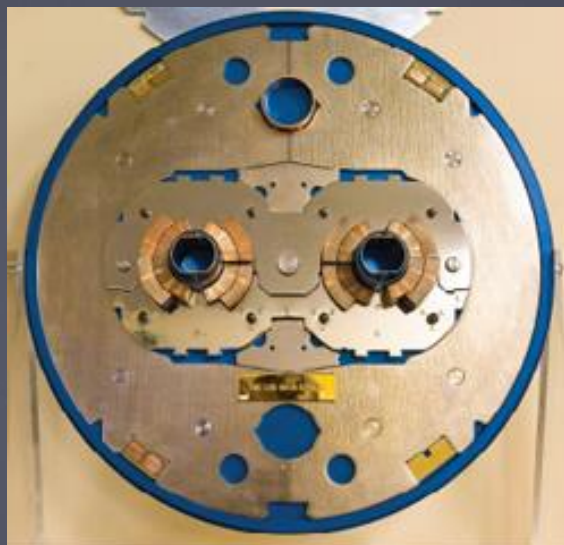


1232 dipole magnets of 15m long to hold the protons within the LHC orbit



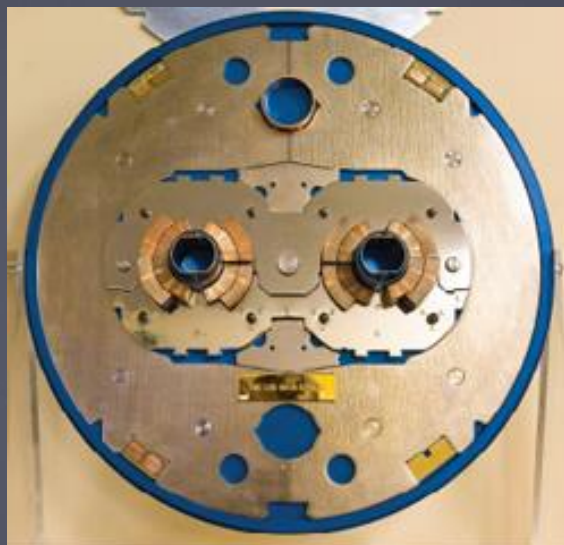
1232 dipole magnets of 15m long to hold the protons within the LHC orbit

Dipole coils operate at 1.9K to flow the 11kA of current necessary to produce the 8 Tesla (for 7 TeV beam) without thermal loss in the superconducting Niobium-Titanium cables

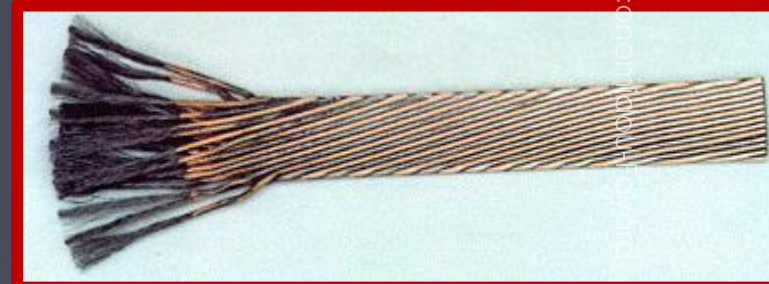


1232 dipole magnets of 15m long to hold the protons within the LHC orbit

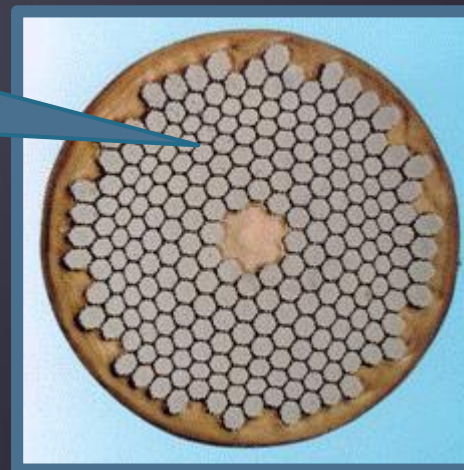
Dipole coils operate at 1.9K to flow the 11kA of current necessary to produce the 8 Tesla (for 7 TeV beam) without thermal loss in the superconducting Niobium-Titanium cables



A cable = 36 twisted 15mm strands

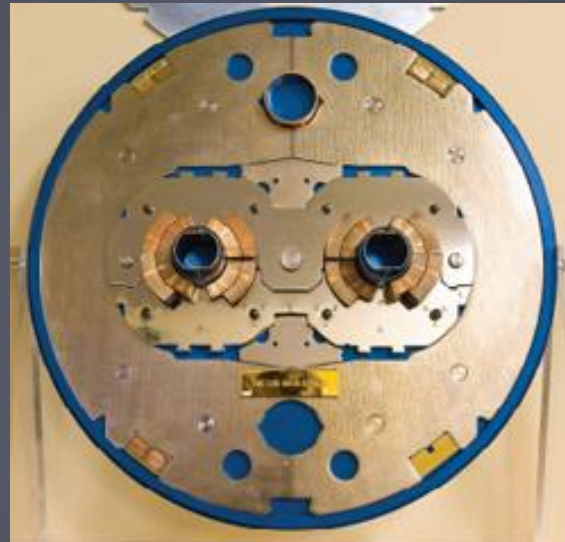


A strand : 6000 – 9000 filaments of 7 μ m NbTi alloy.

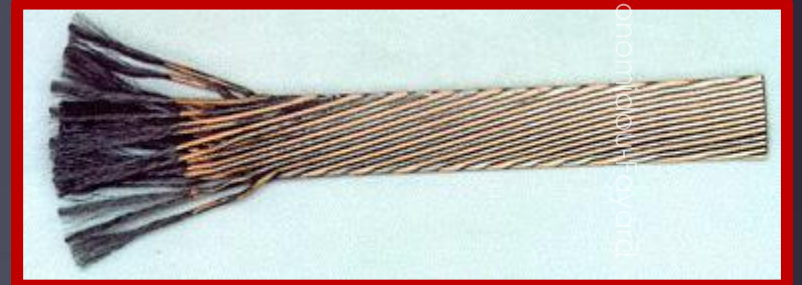


1232 dipole magnets of 15m long to hold the protons within the LHC orbit

Dipole coils operate at 1.9K to flow the 11kA of current necessary to produce the 8 Tesla (for 7 TeV beam) without thermal loss in the superconducting Niobium-Titanium cables

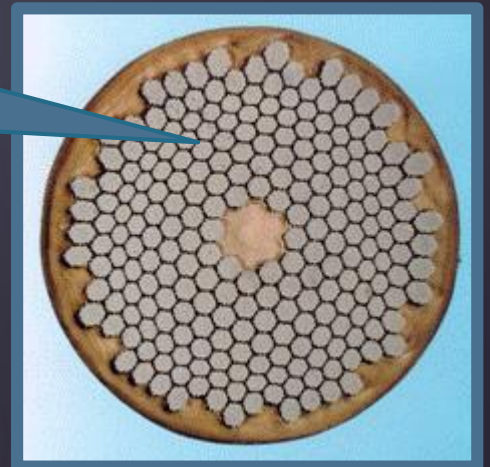


A cable = 36 twisted 15mm strands



A strand : 6000 – 9000 filaments of 7 μ m NbTi alloy.

270000 Km of strands



Train and stock the magnets ready for installation

37

Initially : All magnets trained to reach 8 Tesla

Fully tested for leak tightness, mechanical and electrical integrity, instrumentation, field quality



Train and stock the magnets ready for installation

Initially : All magnets trained to reach 8 Tesla

Fully tested for leak tightness, mechanical and electrical integrity, instrumentation, field quality

Stored in the fields around CERN, waiting for installation in the tunnel



The vacuum in the LHC

39

Three separate vacuum systems

Insulation vacuum for helium distribution
50Km of piping at 10^{-6} mbar

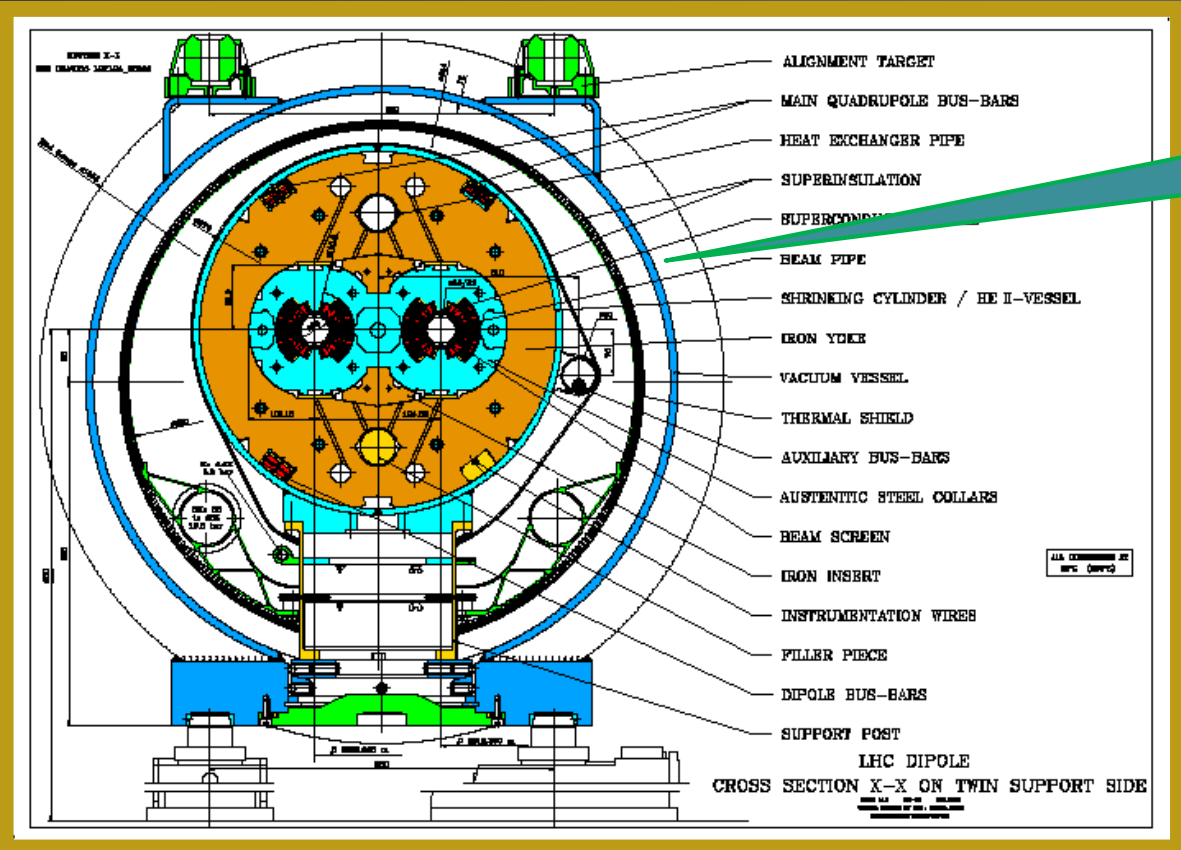
slides 2015, Lydia Iconomidou-Fayard
9/06/2015

The vacuum in the LHC

Three separate vacuum systems

Insulation vacuum for helium distribution
50Km of piping at 10^{-6} mbar

Insulation vacuum for the
cryomagnets



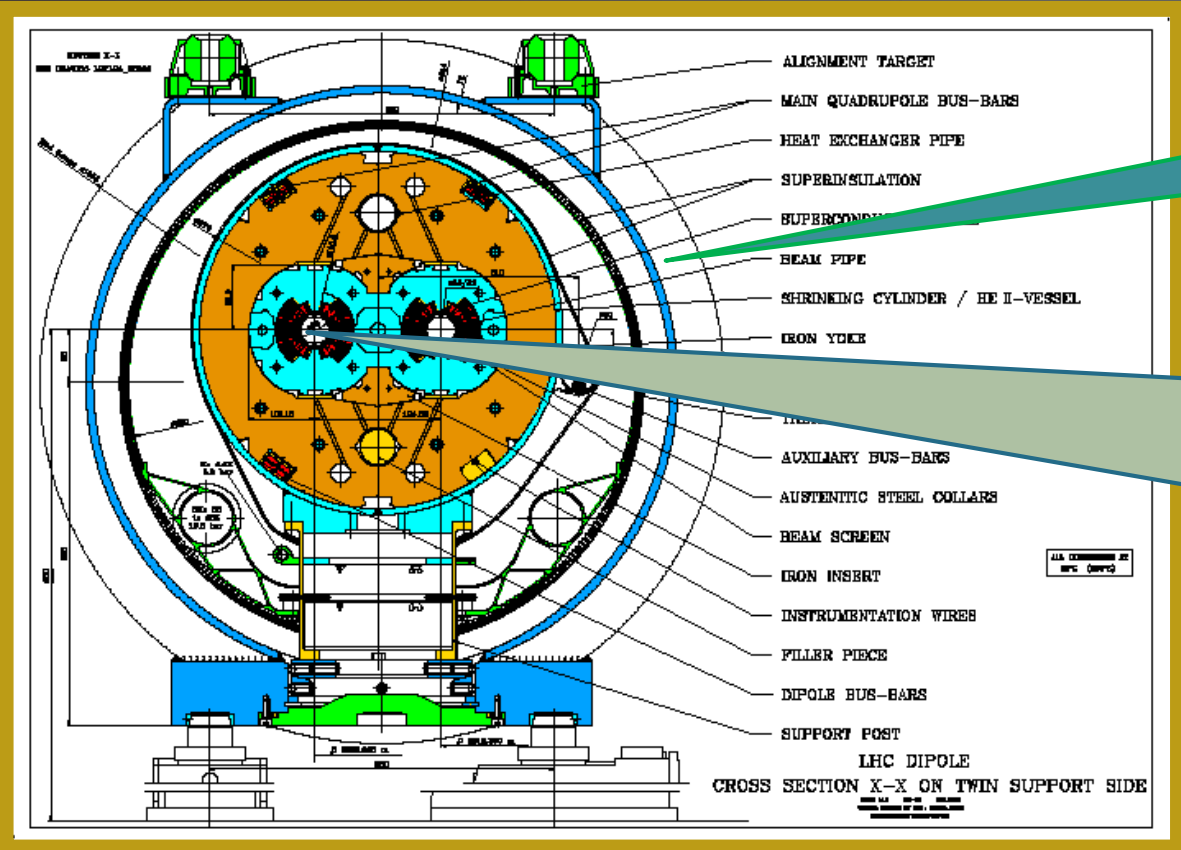
The vacuum in the LHC

Three separate vacuum systems

Insulation vacuum for helium distribution
50Km of piping at 10^{-6} mbar

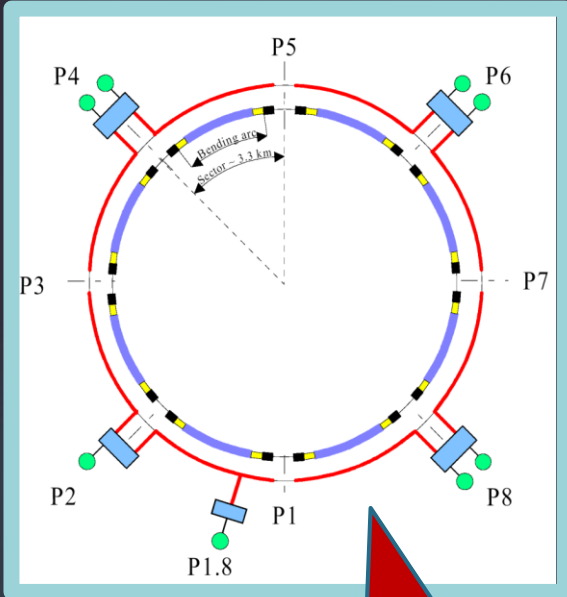
Insulation vacuum for the cryomagnets

Ultra- high vacuum in the beam pipes 48 Km of the arc sections (at 1.9K) and 6 km of straight lines at room temperature)
 10^{-11} mbar



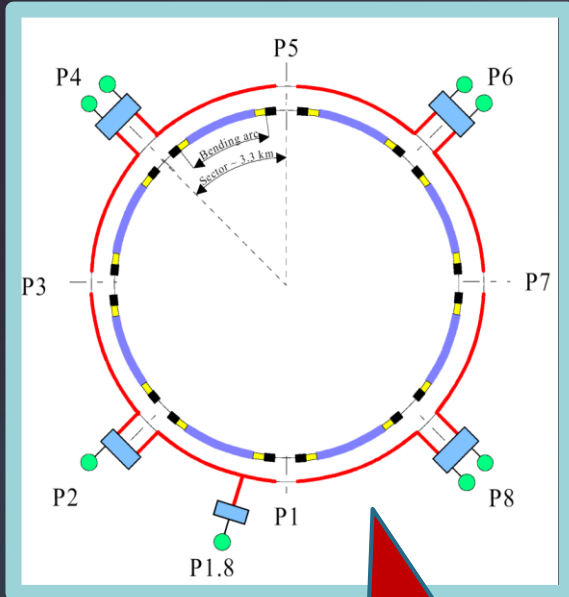
Cooling down the LHC sectors

42



5 cryogenic islands,
8 cryogenic plants
(one per sector)

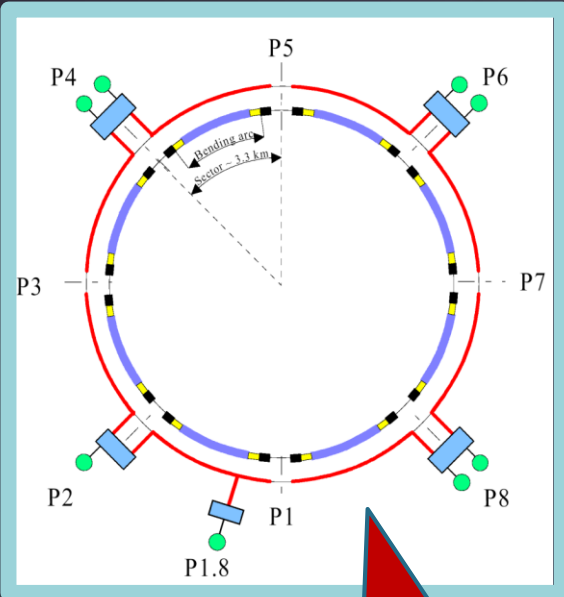
Cooling down the LHC sectors



5 cryogenic islands,
8 cryogenic plants
(one per sector)



Cooling down the LHC sectors



Several weeks to complete!

Done in three steps

→ 10 Ktons of liquid nitrogen to cool down the Helium at 80 K

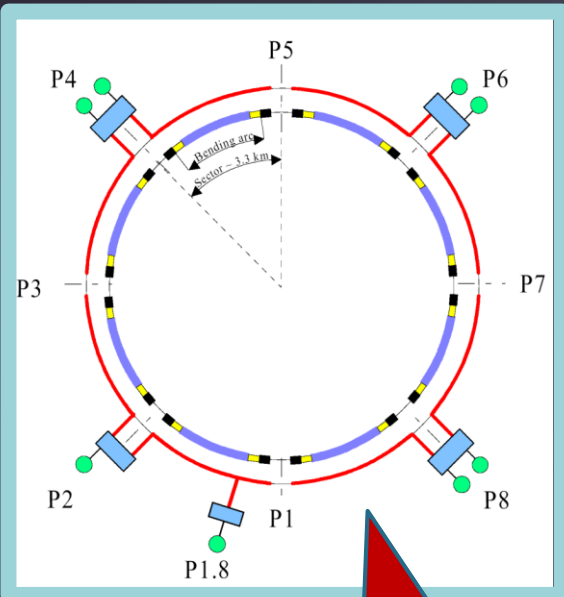
Invisibles 2015, Lydica | 16/06/2015

5 cryogenic islands,
8 cryogenic plants
(one per sector)



Cooling down the LHC sectors

45



Several weeks to complete!

Done in three steps

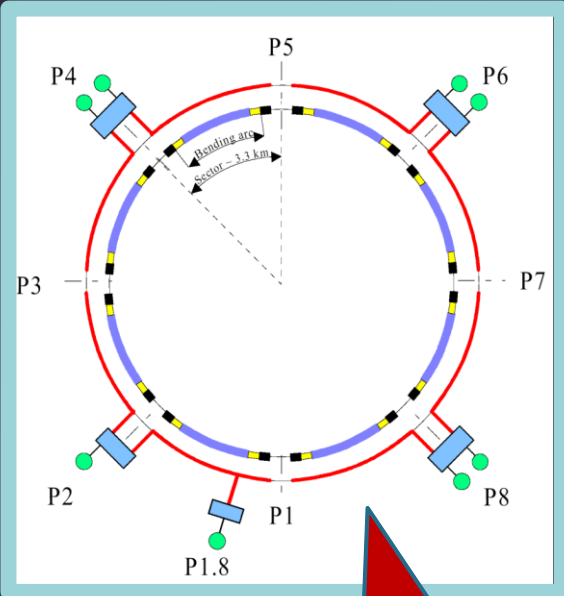
- 10 Ktons of liquid nitrogen to cool down the Helium at 80 K
- The 120 tons of helium are further cooled down to 4.5 K using turbines

Invisibles 2015, Lydia Iconopoulou
16/06/2015

5 cryogenic islands,
8 cryogenic plants
(one per sector)



Cooling down the LHC sectors



Several weeks to complete!

Done in three steps

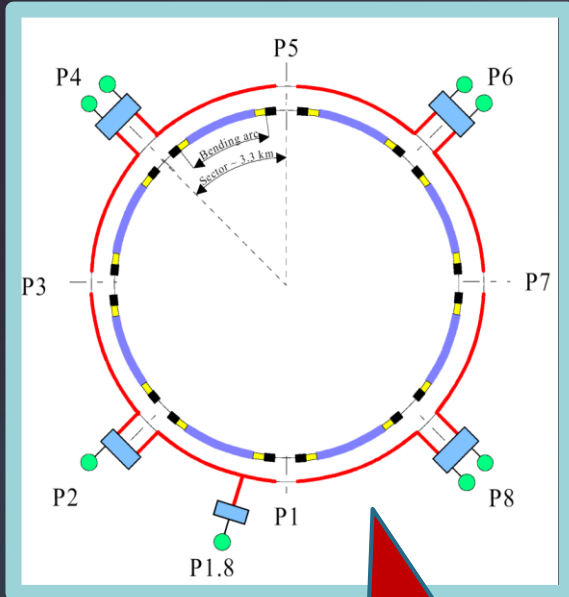
- 10 Ktons of liquid nitrogen to cool down the Helium at 80 K
- The 120 tons of helium are further cooled down to 4.5 K using turbines
- The liquid helium at 4.5 K is injected in the cold masses of LHC. The magnetic coils become superconducting.

Invisibles 2015, Lydia Iconopoulou, 16/06/2015

5 cryogenic islands,
8 cryogenic plants
(one per sector)



Cooling down the LHC sectors



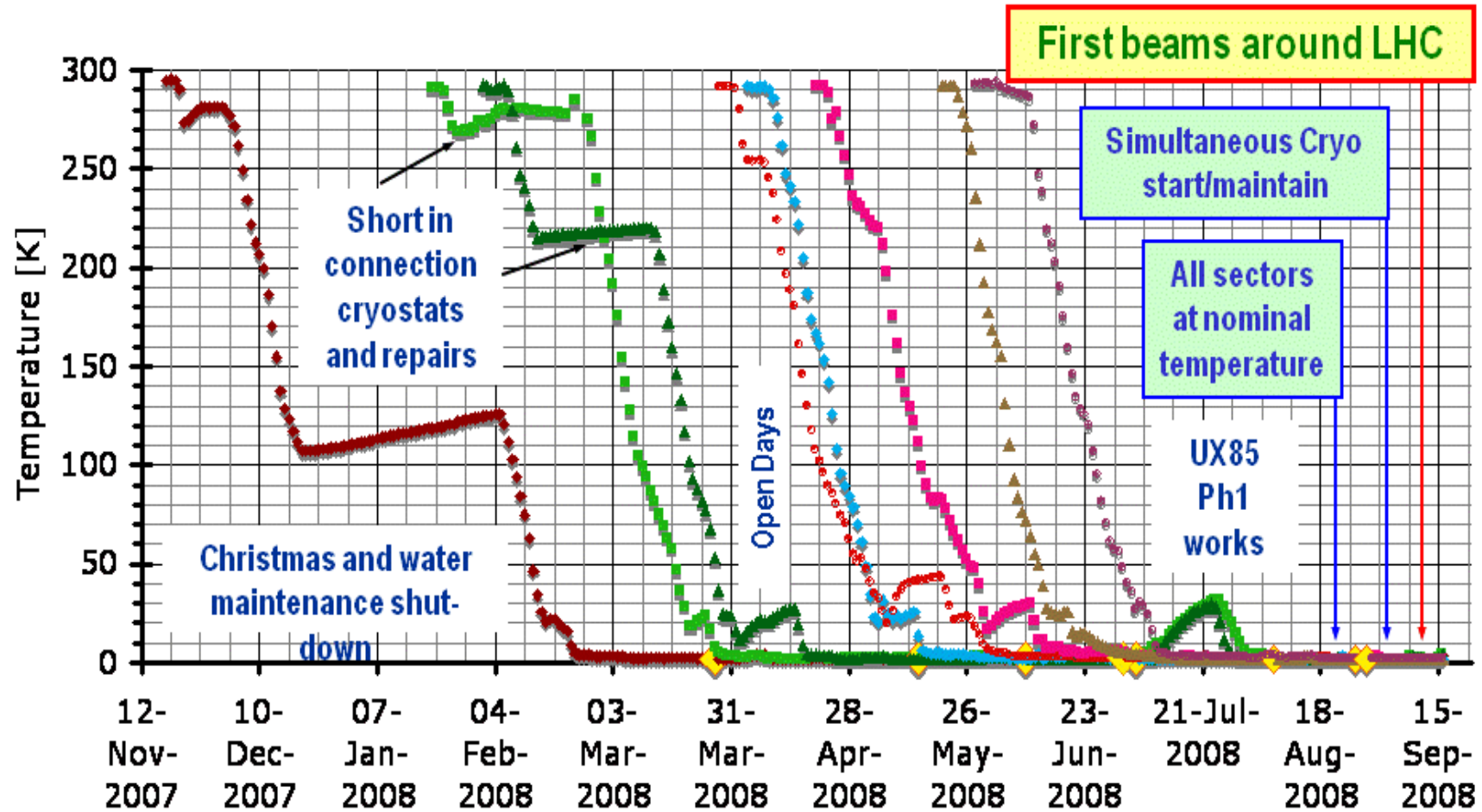
Several weeks to complete!

Done in three steps

- 10 Ktons of liquid nitrogen to cool down the Helium at 80 K
- The 120 tons of helium are further cooled down to 4.5 K using turbines
- The liquid helium at 4.5 K is injected in the cold masses of LHC. The magnetic coils become superconducting.
- The helium is then refrigerated down to 1.9 K where it is superfluid. In that temperature, NbTi cables have the best capacity to keep high currents for 8Tesla field.

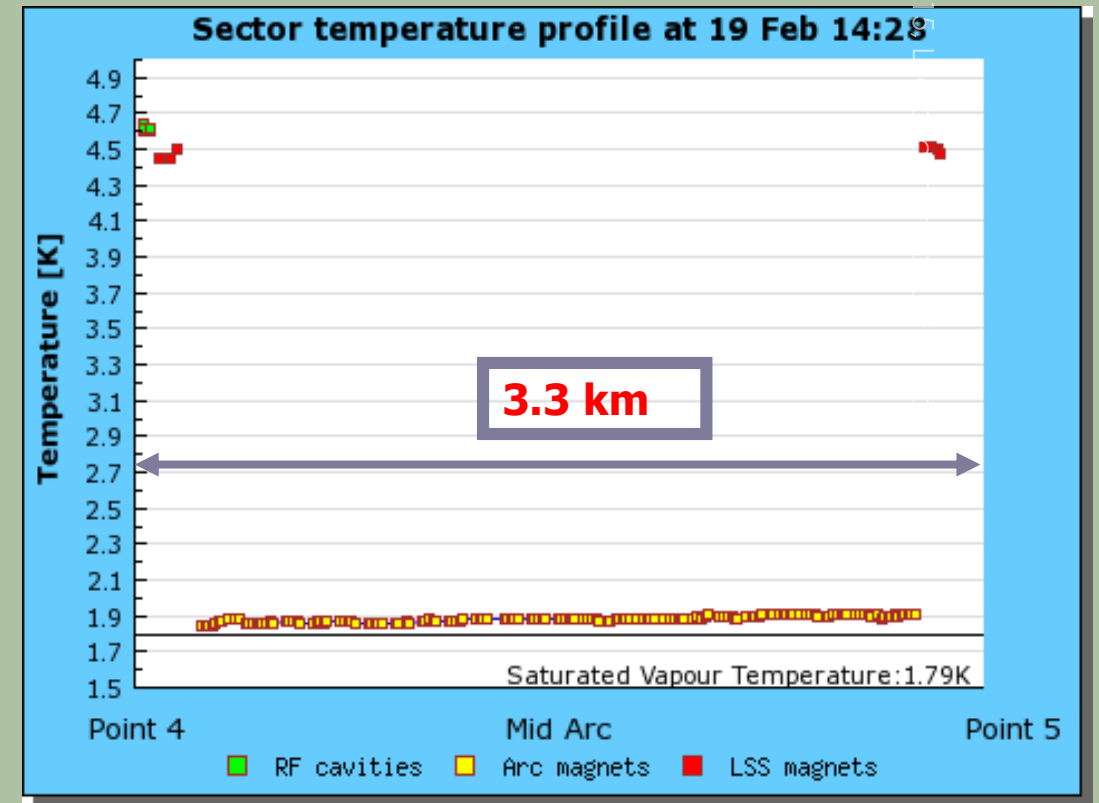
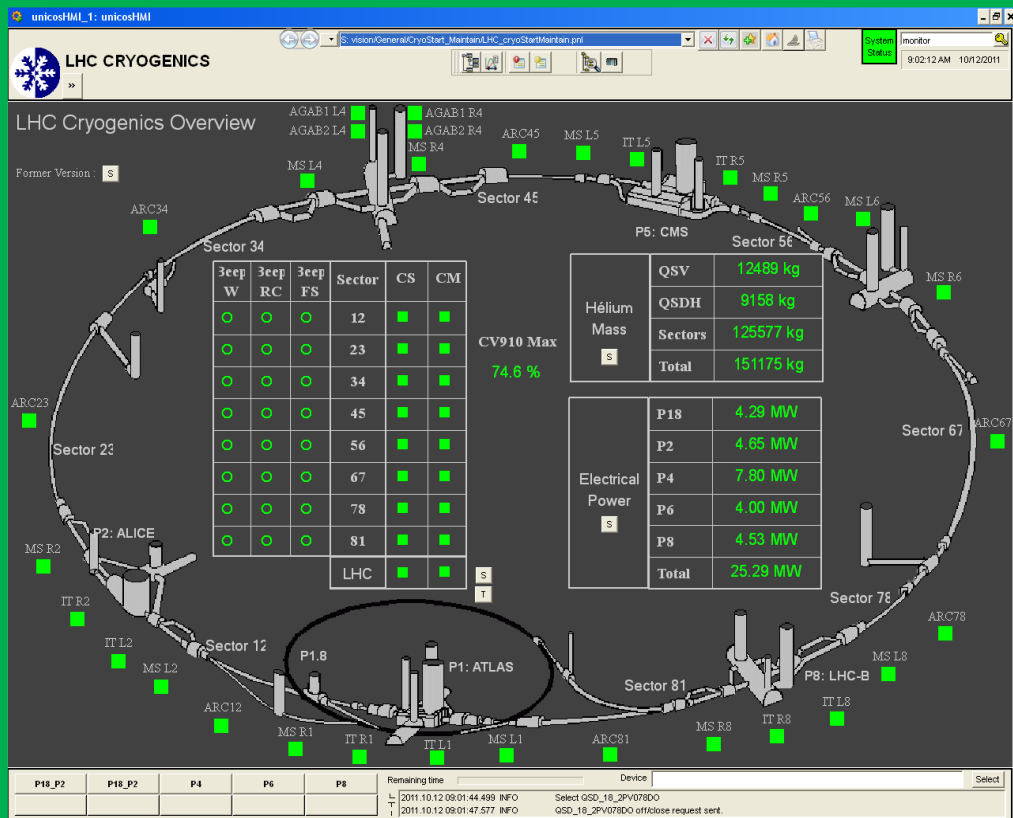
5 cryogenic islands,
8 cryogenic plants
(one per sector)

First cool-down the LHC sectors



Long learning period : finally one sector / month

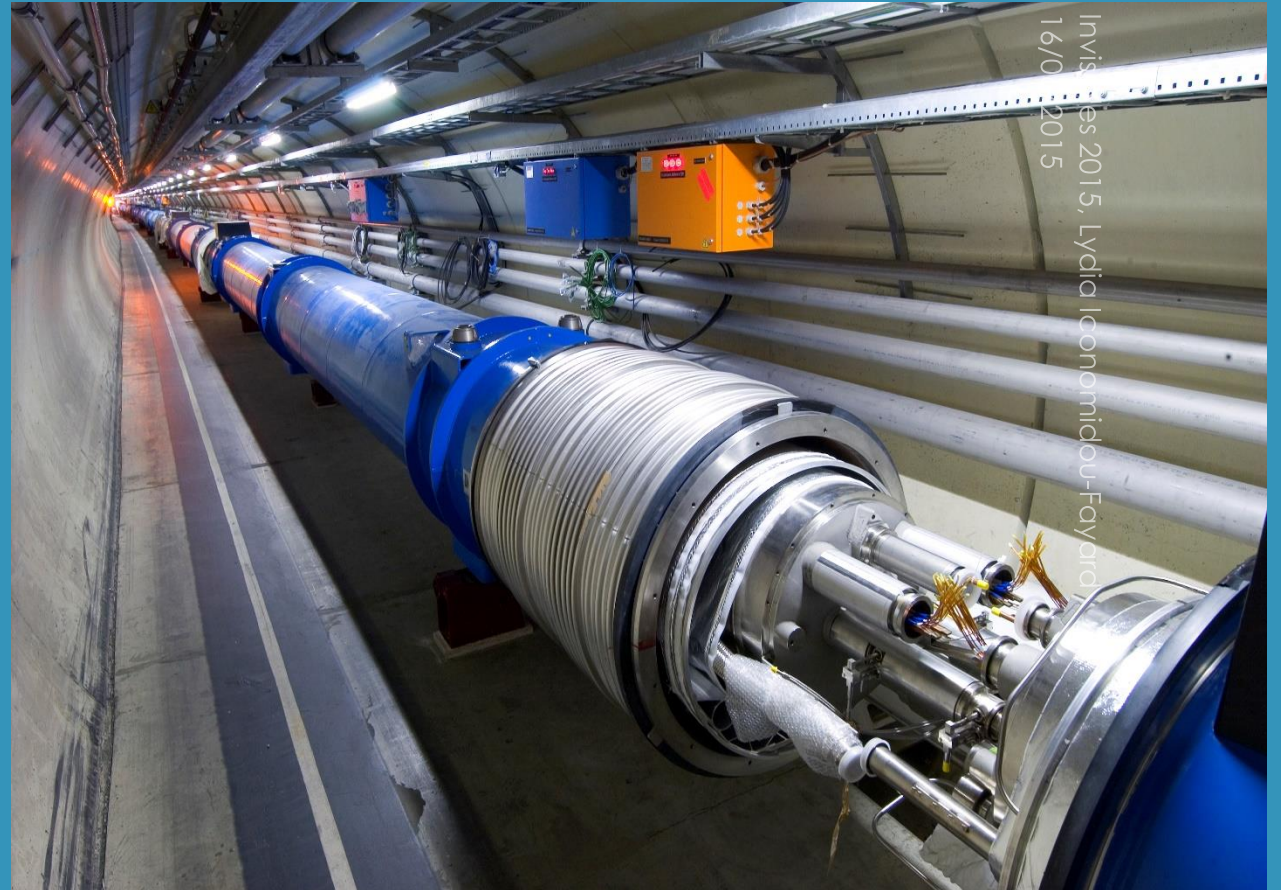
Strict monitoring of the LHC cryogenic systems



Building-up the LHC

50

A titanic achievement



Invisibles 2015, Lydia Iconomidou-Fayard
16/01/2015

Building-up the LHC

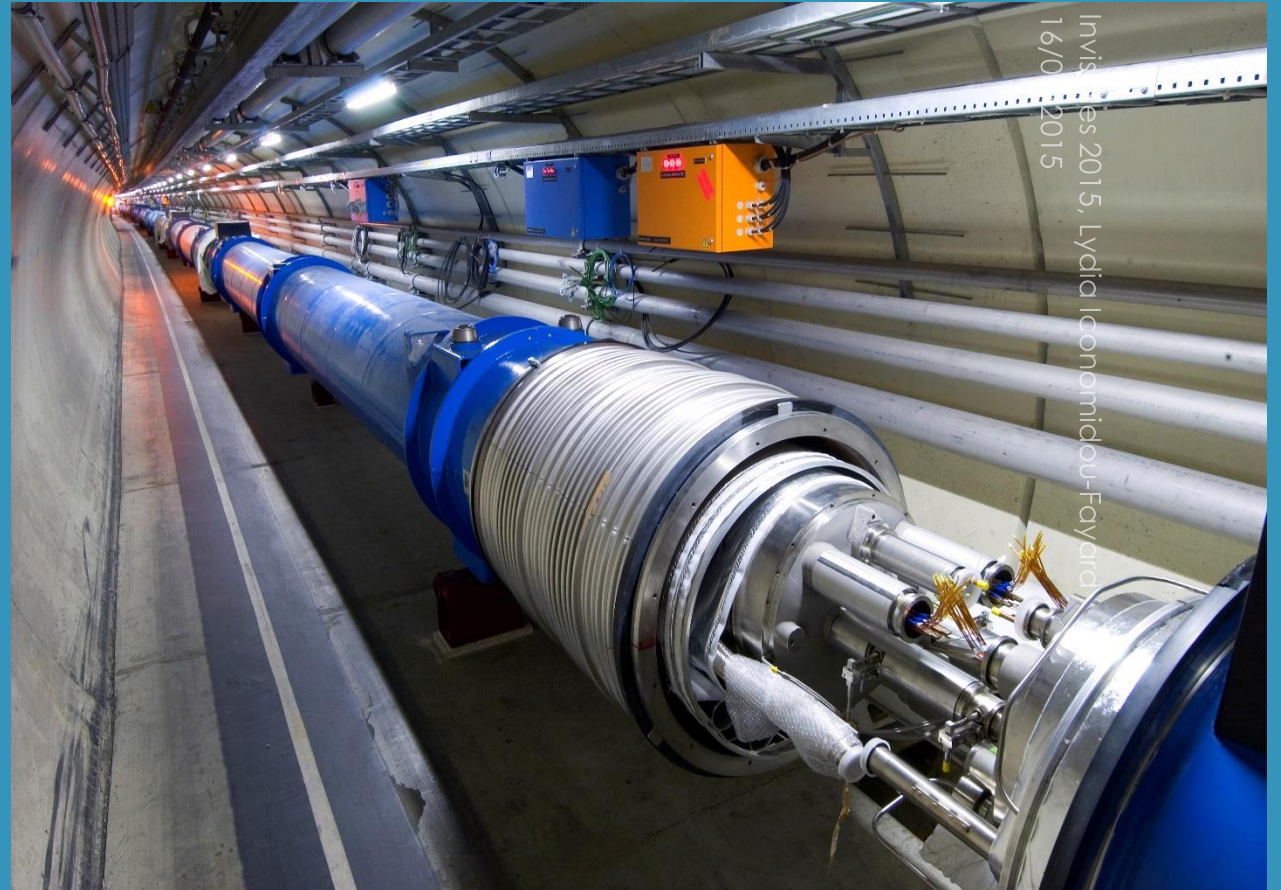
51

A titanic achievement

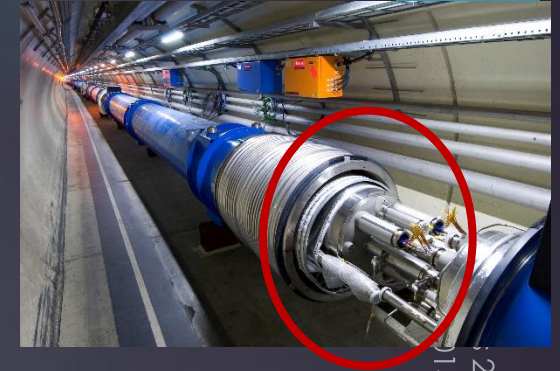
Went through several bad surprises and numerous crises

Delays, failures, accidents, UFO, SEE...

Few examples of encountered issues in some of the next slides

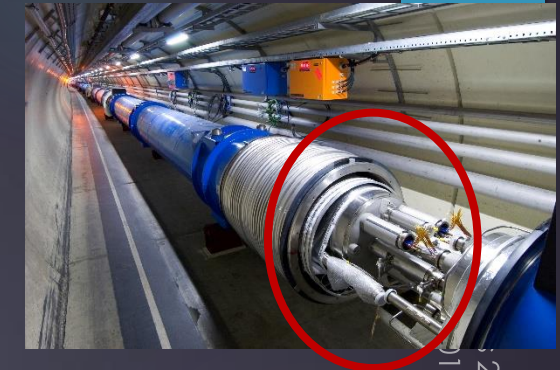


The dipole interconnection: a delicate place to be

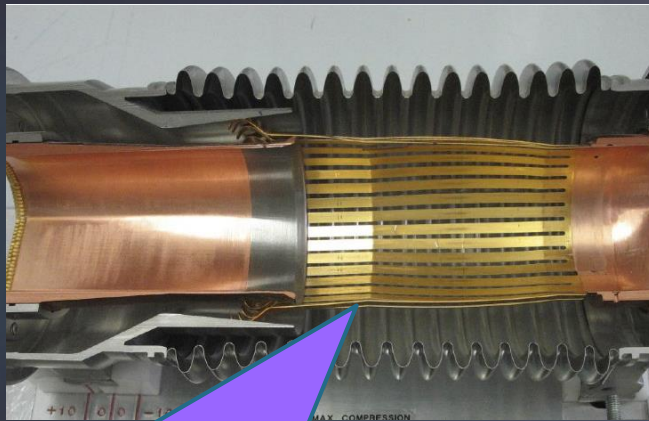


Beam vacuum chambers interconnects
The bellows crisis and repair

The dipole interconnection: a delicate place to be

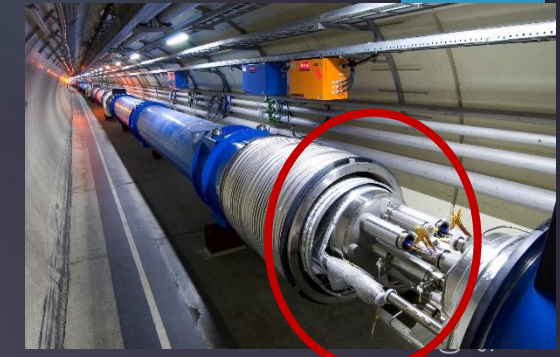


Beam vacuum chambers interconnects
The bellows crisis and repair

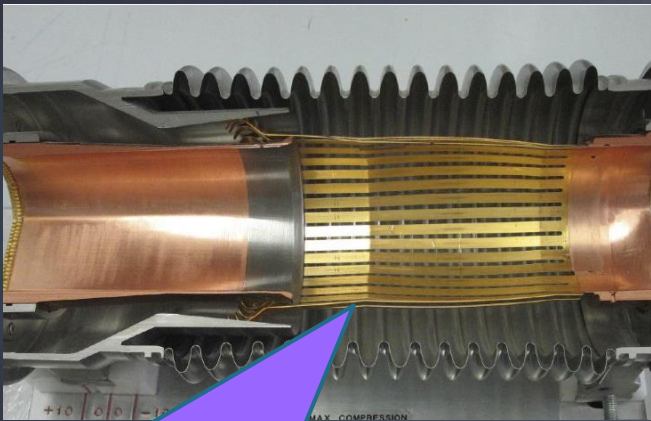


To mitigate the thermal shrink-expansion movements during cooldown-warmup operations

The dipole interconnection: a delicate place to be



Beam vacuum chambers interconnects
The bellows crisis and repair

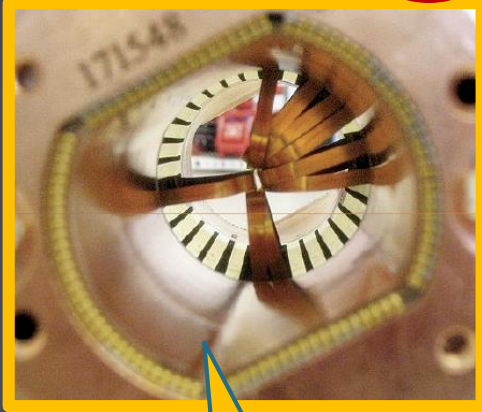


To mitigate the thermal shrink-expansion movements during cooldown-warmup operations

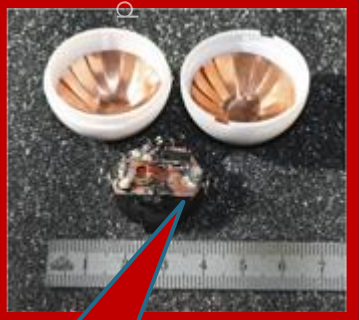
QQBI.26R7 V1 bending angles out of tolerance

Approved manufacturing drawing

P.Strubin CERN TE departement



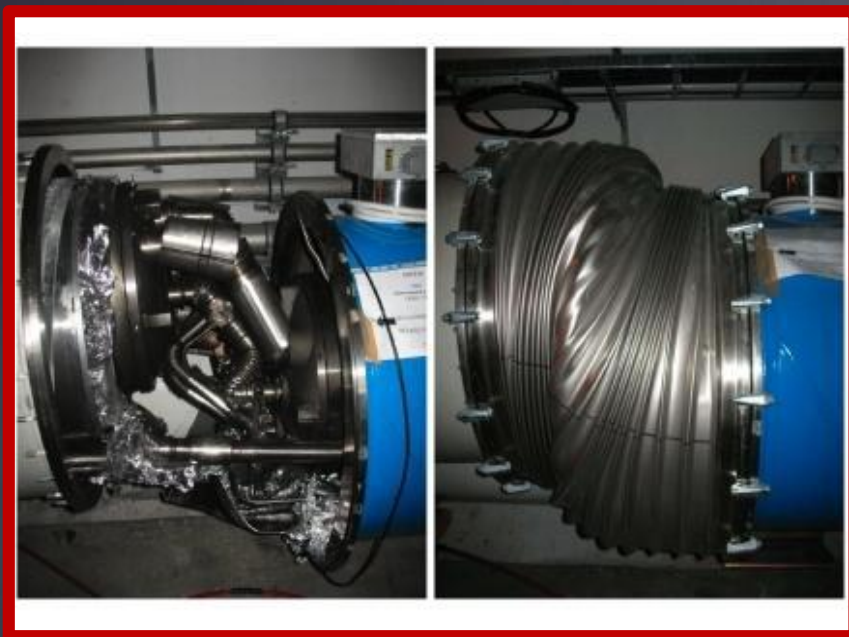
Damaged bellow



Detection ball

2015, Lydia Iconomidou-Fayard

The 1695 dipole interconnections: a delicate place to be



19/09/2008 : **The dark day**

- Violent warm-up at few interconnections in Sector 3-4.
- 660 MJ flew in the magnets, explosion
- Damages along 700m

The 1695 dipole interconnections: a delicate place to be

57

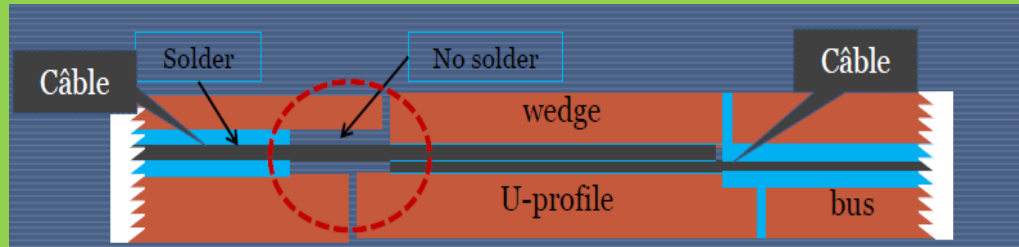
Invisib
16/06/



19/09/2008 : The dark day

- Violent warm-up at few interconnections in Sector 3-4.
- 660 MJ flew in the magnets, explosion
- Damages along 700m

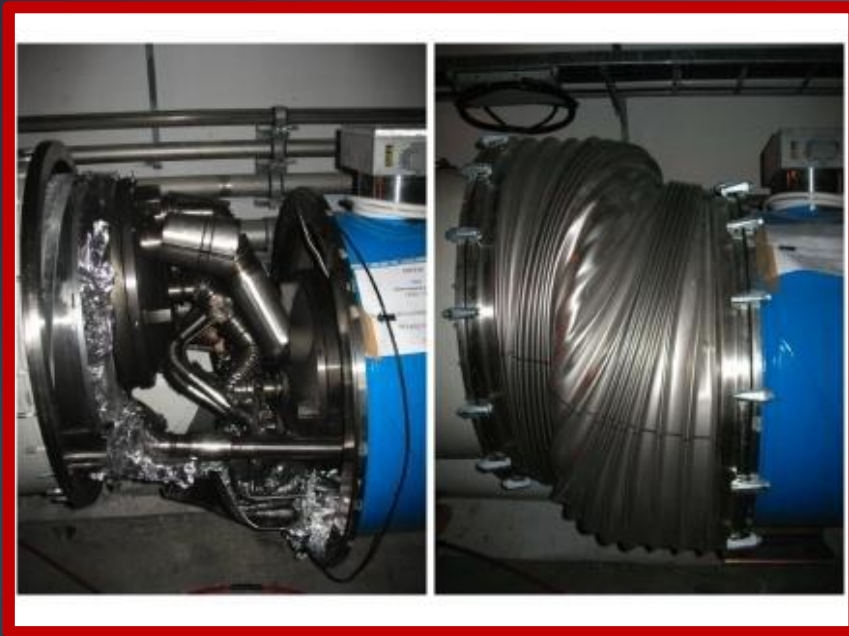
dou-Fayard



The 1695 dipole interconnections: a delicate place to be

58

Invisib
16/06/



19/09/2008 : The dark day

- Violent warm-up at few interconnections in Sector 3-4.
- 660 MJ flew in the magnets, explosion
- Damages along 700m

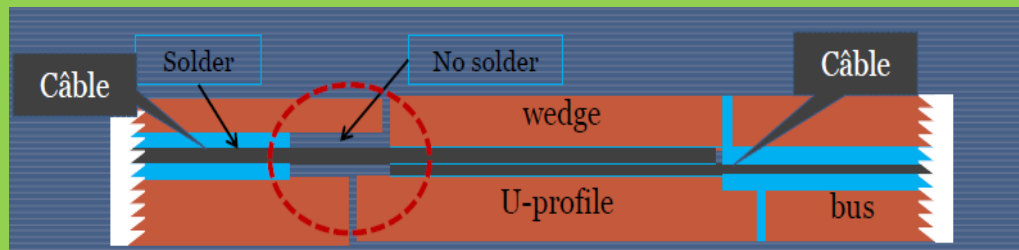
dou-Fayard

→ Warm-up sectors

→ 39 Dipoles and 14 quadripoles repaired or exchanged

→ Consolidation of the busbars along the LHC ring, Installation of additional safety procedures

→ 18 months delay in LHC operations



LHC beams: few important numbers

59

4mn20 to fill one beam with 1380 (in 2012) proton bunches from SPS, separated by 50 ns (7m)

20 mn to achieve 7TeV /beam

Invisible 2015, Lydia Iconomidou-Fayard
16/06/2015

LHC beams: few important numbers

60

4mn20 to fill one beam with 1380 (in 2012) proton bunches from SPS, separated by 50 ns (7m)

Each bunch contains 1.7×10^{11} (in 2012) protons
Bunch dimensions vary along the LHC ring

20 mn to achieve 7TeV /beam

Invisible 2015, Lydia Iconomidou-Fayard
16/06/2015

LHC beams: few important numbers

61

4mn20 to fill one beam with 1380 (in 2012) proton bunches from SPS, separated by 50 ns (7m)

20 mn to achieve 7TeV /beam

Each bunch contains 1.7×10^{11} (in 2012) protons
Bunch dimensions vary along the LHC ring

Instantaneous luminosity $L =$

$$\frac{(\text{Nb of Protons/bunch})^2 \times \text{Nb of Bunches} \times \text{Nb of turns/second}}{4 \times \pi \times \sigma^x \times \sigma^y}$$

$$4 \times \pi \times \sigma^x \times \sigma^y$$

LHC beams: few important numbers

62

4mn20 to fill one beam with 1380 (in 2012) proton bunches from SPS, separated by 50 ns (7m)

Each bunch contains 1.7×10^{11} (in 2012) protons
Bunch dimensions vary along the LHC ring

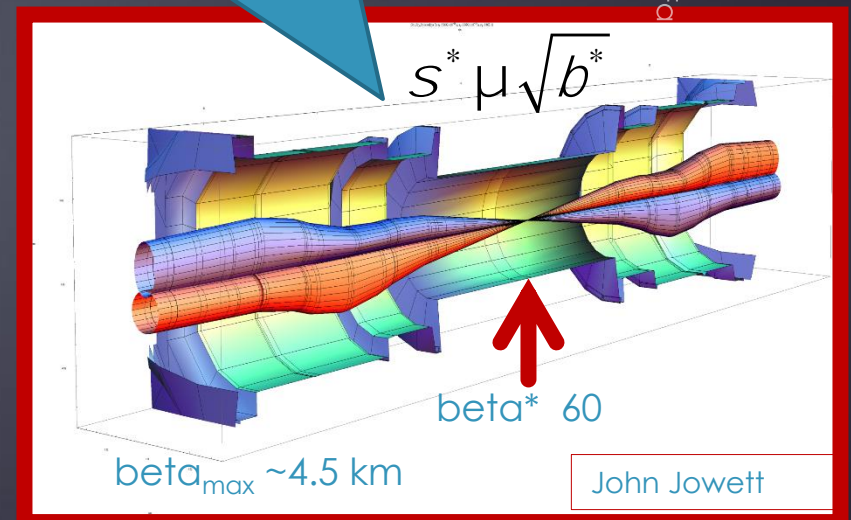
Instantaneous luminosity $L =$

$(\text{Nb of Protons/bunch})^2 \times \text{Nb of Bunches} \times \text{Nb of turns/second}$

$$4 \times \pi \times \sigma^x \times \sigma^y$$

20 mn to achieve 7TeV /beam

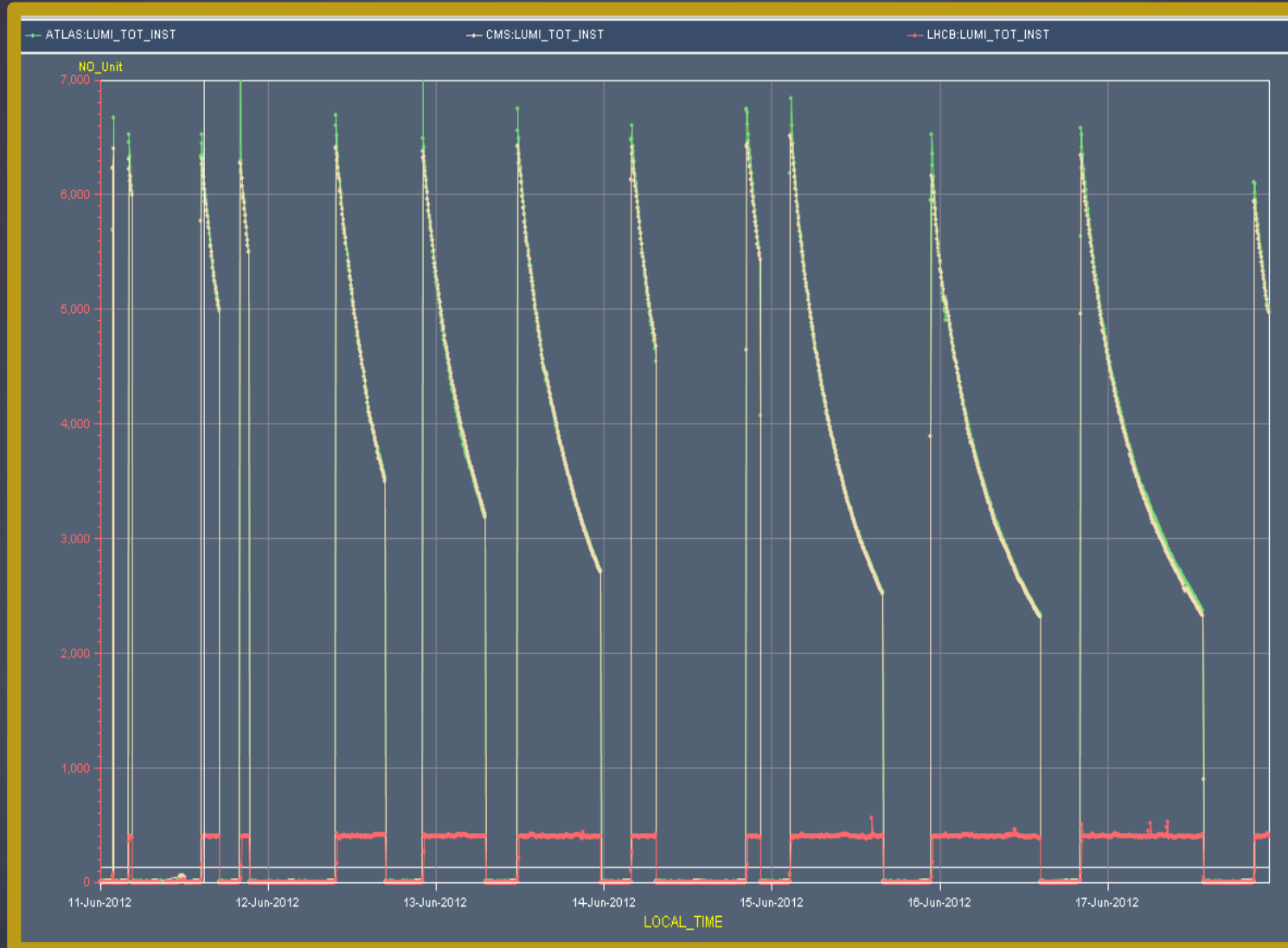
Beam size adjusted along the LHC rings. Squeezed-down close to interaction points



Invisible 2015, Lydi
16/06/2015
DU-FO

Challenges for the beam lifetime

63



Challenges for the beam lifetime: **Collimation**

- ▶ Without clean beam, immediate magnet quench in injection.

Challenges for the beam lifetime: **Collimation**

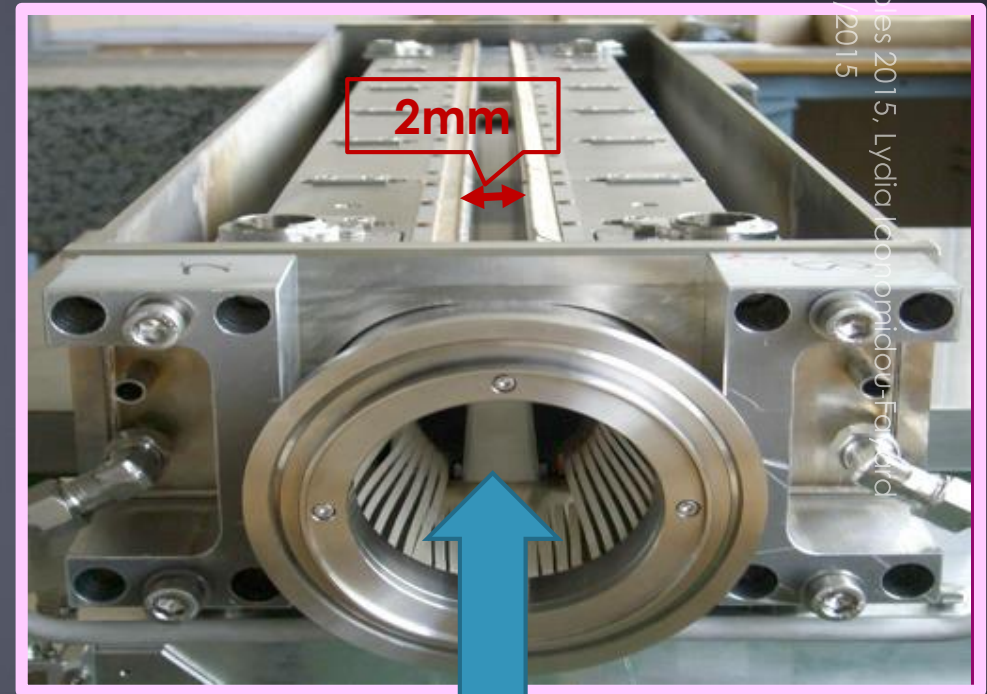
65

- ▶ Without clean beam, immediate magnet quench in injection.
- ▶ ~100 collimators along the LHC, symmetrically placed around the beam to clean it from primary and scattered particles

Challenges for the beam lifetime: Collimation

66

- ▶ Without clean beam, immediate magnet quench in injection.
- ▶ ~100 collimators along the LHC, symmetrically placed around the beam to clean it from primary and scattered particles
- ▶ Their alignment is a key parameter (collimator 2 mm wide !)

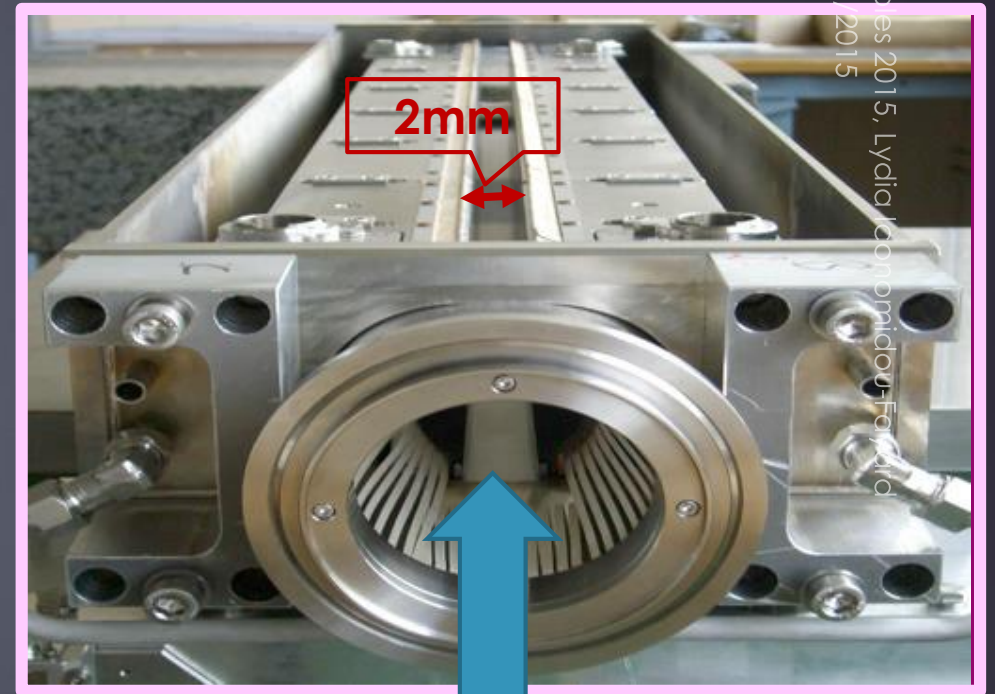


Invisibles 2015, Lydia Jorandou-Fordio
16/06/2015

Challenges for the beam lifetime: Collimation

67

- ▶ Without clean beam, immediate magnet quench in injection.
- ▶ ~100 collimators along the LHC, symmetrically placed around the beam to clean it from primary and scattered particles
- ▶ Their alignment is a key parameter (collimator 2 mm wide !)
- ▶ Very satisfying functioning during Run1



Invisibles 2015, Lydia Jorrandou-Ford
16/06/2015

Challenges for the beam lifetime: the electron cloud

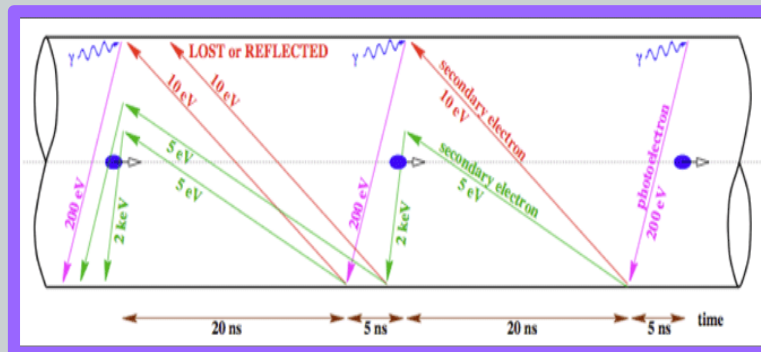


Electrons from ionized outgassed molecules released from the beam pipe.

Challenges for the beam lifetime: the electron cloud

Electrons from ionized outgassed molecules released from the beam pipe.

Building-up an electron cloud interacting with the protons and the pipe walls



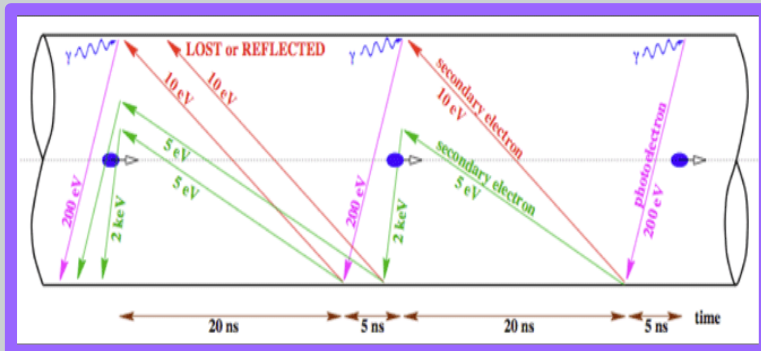
Challenges for the beam lifetime: the electron cloud

70

Electrons from ionized outgassed molecules released from the beam pipe.

Building-up an electron cloud interacting with the protons and the pipe walls

→ Instabilities, beam emittance and vacuum deteriorated, lifetime shortened

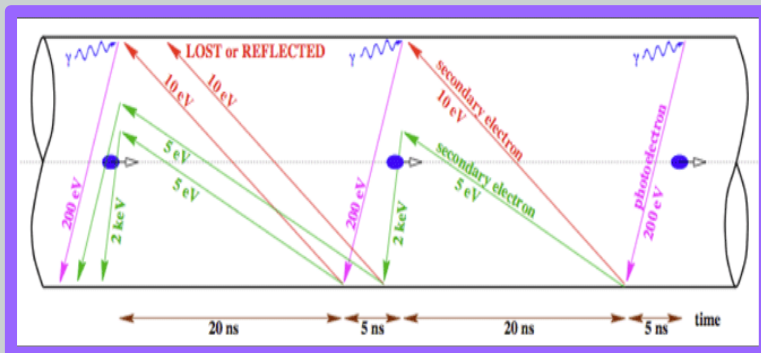


Challenges for the beam lifetime: the electron cloud

Electrons from ionized outgassed molecules released from the beam pipe.

Building-up an electron cloud interacting with the protons and the pipe walls

→ Instabilities, beam emittance and vacuum deteriorated, lifetime shortened



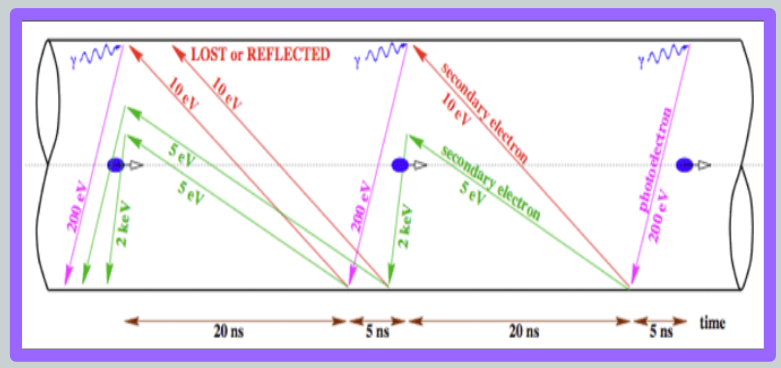
Cure : periods of “Scrubbing “ with intense beams at 450GeV.

Challenges for the beam lifetime: the electron cloud

Electrons from ionized outgassed molecules released from the beam pipe.

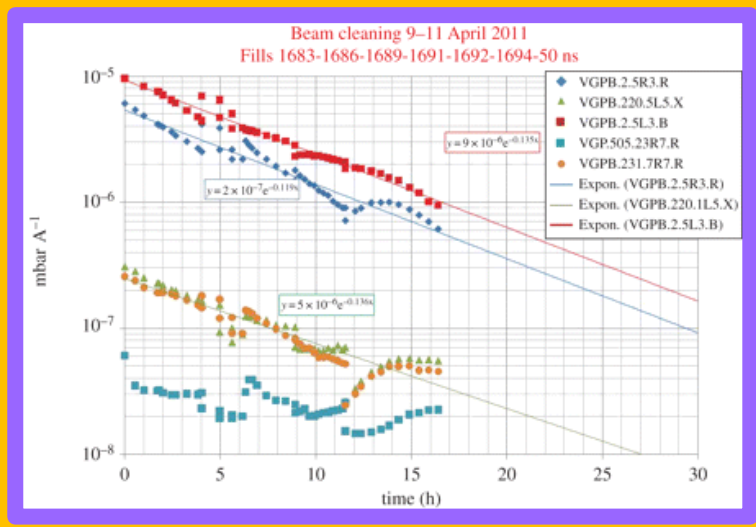
Building-up an electron cloud interacting with the protons and the pipe walls

→ Instabilities, beam emittance and vacuum deteriorated, lifetime shortened



Cure : periods of “Scrubbing “ with intense beams at 450GeV.

Clean the pipe walls and pump the dust. → Impressive improvement!



Challenges for the beam lifetime: **SEE and UFOs**



Challenges for the beam lifetime: **SEE and UFOs**



SEE : Single Event Effects

beam induced radiation can impact electronics in the tunnel and cause beam losses.

Challenges for the beam lifetime: **SEE and UFOs**



SEE : Single Event Effects

beam induced radiation can impact electronics in the tunnel and cause beam losses.

Solution: Relocation and shielding of the sensitive material

Rate improved from $\sim 12/\text{fb}^{-1}$ to $\sim 3/\text{fb}^{-1}$

Challenges for the beam lifetime

76

SEE and UFOs



SEE : Single Event Effects

beam induced radiation can impact electronics in the tunnel and cause beam losses.

Solution: Relocation and shielding of the sensitive material

Rate improved from $\sim 12/\text{fb}^{-1}$ to $\sim 3/\text{fb}^{-1}$

UFOs : Unidentified Falling Objects

→ Likely dust particles

→ Located often close to Main injection Kickers.

→ Beam loss within $\sim \text{ms}$

16/06/2015

Invisibles 2015, Lydia Iconomidou-Fayard

Challenges for the beam lifetime

SEE and UFOs



77

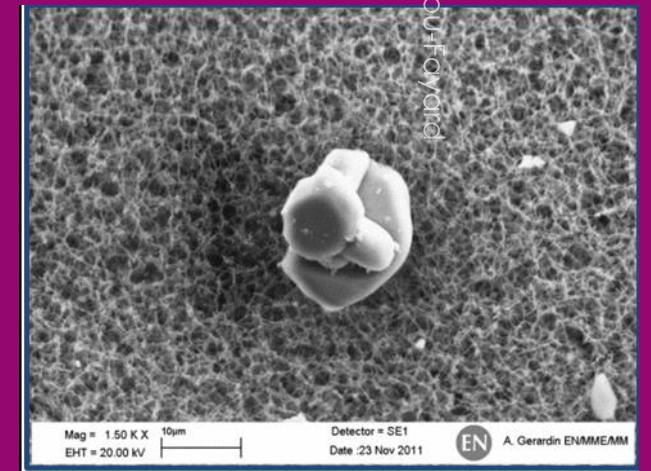
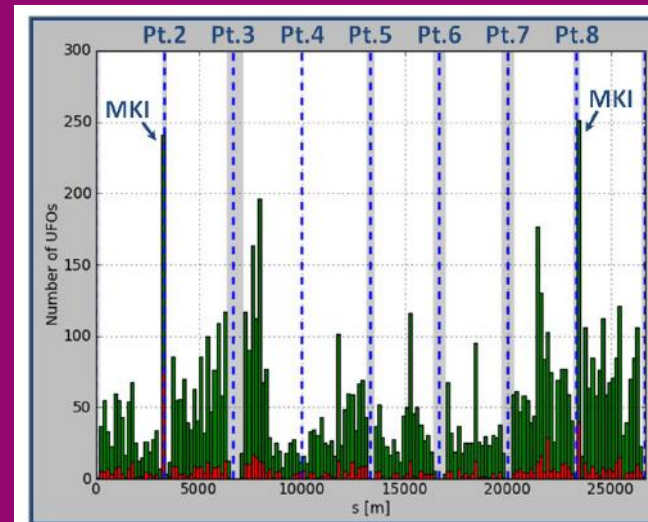
SEE : Single Event Effects

beam induced radiation can impact electronics in the tunnel and cause beam losses.

Solution: Relocation and shielding of the sensitive material
Rate improved from $\sim 12/\text{fb}^{-1}$ to $\sim 3/\text{fb}^{-1}$

UFOs : Unidentified Falling Objects

- Likely dust particles
- Located often close to Main injection Kickers.
- Beam loss within $\sim \text{ms}$



The end point of the LHC beams

78

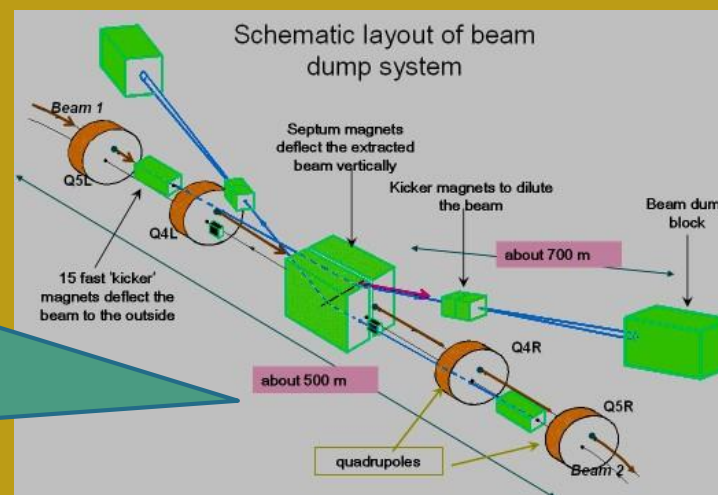
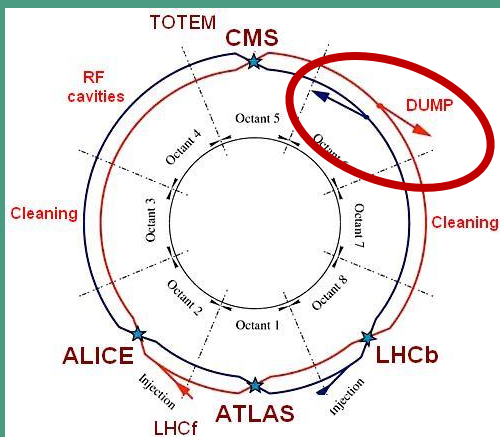
Want to dump the beams when

- 1) The beam quality has been deteriorated
- 2) the Beam loss monitors (BLM) installed along the machine detect activity beyond the safety threshold

The end point of the LHC beams

Want to dump the beams when

- 1) The beam quality has been deteriorated
- 2) the Beam loss monitors (BLM) installed along the machine detect activity beyond the safety threshold



PROTON PHYSICS: BEAM DUMP

Energy:	3502 GeV	I(B1):	2.48e+09	I(B2):	9.43e+08
---------	----------	--------	----------	--------	----------

BTVDD.689339.B1 Updated: 17:10:36

BTVDD.629339.B2 Updated: 17:10:37

Comments 30-10-2011 17:12:49 :	BIS status and SMP flags	B1	B2
Dumped the last proton physics fill of the 2011 Preparing MD: ATS dry-run.	Link Status of Beam Permits	true	true
	Global Beam Permit	false	false
	Setup Beam	false	false
	Beam Presence	false	false
	Moveable Devices Allowed In Stable Beams	false	false

The lessons from LHC operation in Run 1

80

- ▶ Huge technological achievements in 3 years, with payoff a unique discovery!



The lessons from LHC operation in Run 1

81

- ▶ Huge technological achievements in 3 years, with payoff a unique discovery!
- ▶ Demonstration of capability for prompt reaction, analysis of problems, design of solutions and organization of repair.



The lessons from LHC operation in Run 1

82

- ▶ Huge technological achievements in 3 years, with payoff a unique discovery!
- ▶ Demonstration of capability for prompt reaction, analysis of problems, design of solutions and organization of repair.
- ▶ Proved the control of beam stability injecting bursts with 150% higher density than foreseen, at 50ns spacing.



The lessons from LHC operation in Run 1

84

- ▶ Huge technological achievements in 3 years, with payoff a unique discovery!
- ▶ Demonstration of capability for prompt reaction, analysis of problems, design of solutions and organization of repair.
- ▶ Proved the control of beam stability injecting bursts with 150% higher density than foreseen, at 50ns spacing.
- ▶ Excellent control of beam dimensions at interaction regions, achieving low β^* . Zero quench from losses
- ▶ Development of performant monitoring and complex control tool at all levels



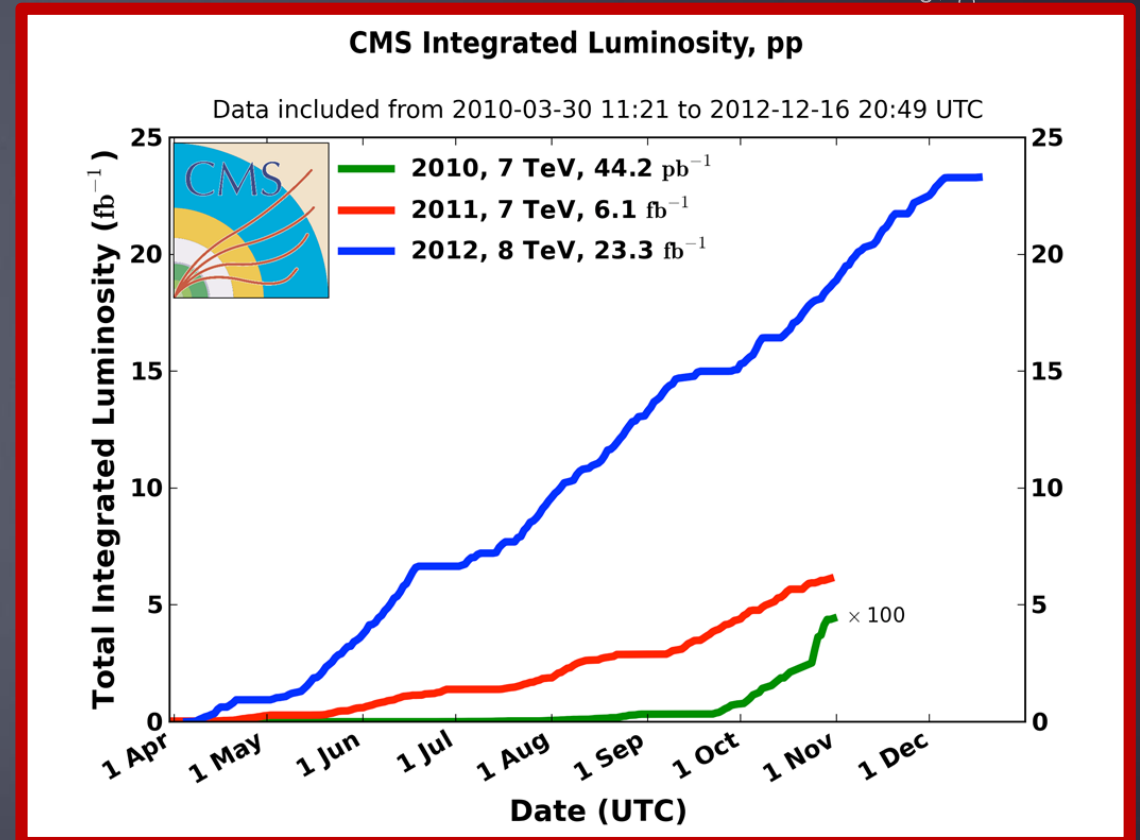
The lessons from LHC operation in Run 1

85

- ▶ Huge technological achievements in 3 years, with payoff a unique discovery!
- ▶ Demonstration of capability for prompt reaction, analysis of problems, design of solutions and organization of repair.
- ▶ Proved the control of beam stability injecting bursts with 150% higher density than foreseen, at 50ns spacing.
- ▶ Excellent control of beam dimensions at interaction regions, achieving low β^* . Zero quench from losses
- ▶ Development of performant monitoring and complex control tool at all levels



Invisite
16/06



The secret: the excellence of expert and technical teams working on a prototype machine of unprecedented hi-tech



SMACC project : Closure of the last interconnection – 18.06.2014
Activity led by A Musso (TE-MS)



The main 2013-14 LHC consolidations

1695 Openings and final reclosures of the interconnections



Complete reconstruction of 1500 of these splices



Consolidation of the 10170 13kA splices, installing 27 000 shunts



Installation of 5000 consolidated electrical insulation systems



300 000 electrical resistance measurements



10170 orbital welding of stainless steel lines



18 000 electrical Quality Assurance tests



10170 leak tightness tests



4 quadrupole magnets to be replaced



15 dipole magnets to be replaced



Installation of 612 pressure relief devices to bring the total to 1344



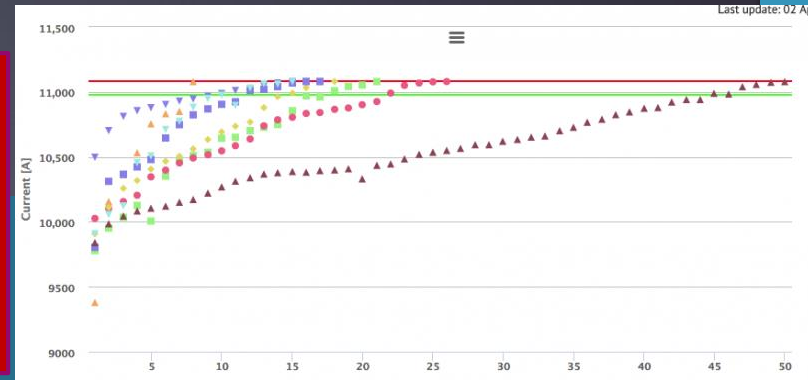
Consolidation of the 13 kA circuits in the 16 main electrical feed-boxes

We are experiencing Run 2

88

- ▶ All magnets trained at 7TeV
- ▶ Working energy for 2015 : 6.5TeV

Current



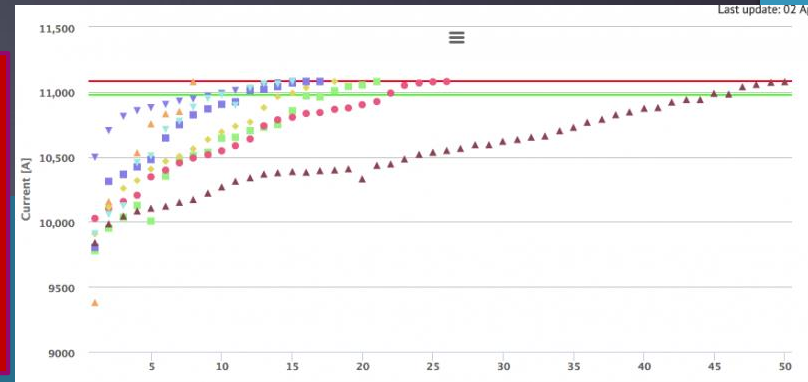
Nb of days

We are experiencing Run 2

89

- ▶ All magnets trained at 7TeV
- ▶ Working energy for 2015 : 6.5TeV
- ▶ Acquired experience of great help

Current



Nb of days

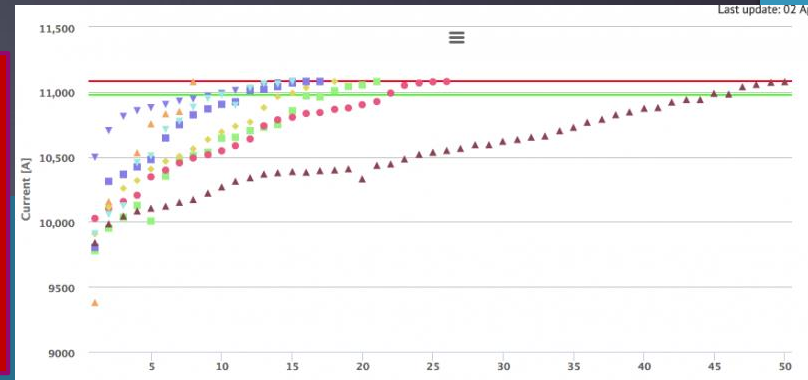
Invisibles 2015, Lydia
omidou-Fayard

We are experiencing Run 2

90

- ▶ All magnets trained at 7TeV
- ▶ Working energy for 2015 : 6.5TeV
- ▶ Acquired experience of great help
- ▶ However stay tuned:
- ▶ Want to increase the instantaneous luminosity x 2 → Double the nb of bunches (with 1.15×10^{11} ppb instead of 1.6×10^{11} ppb)

Current



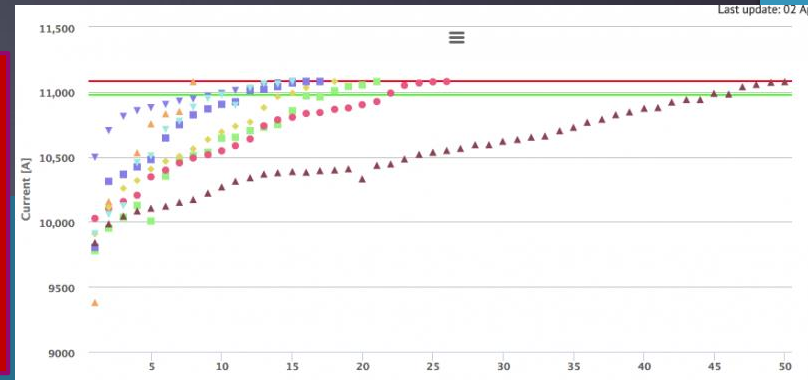
Nb of days

We are experiencing Run 2

91

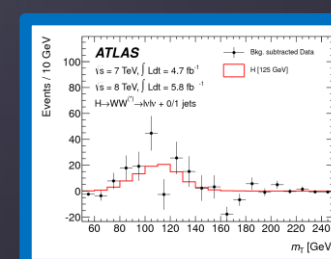
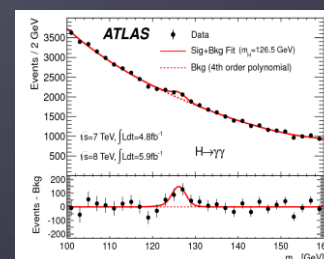
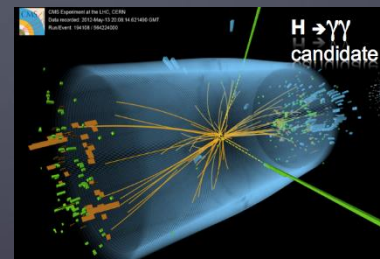
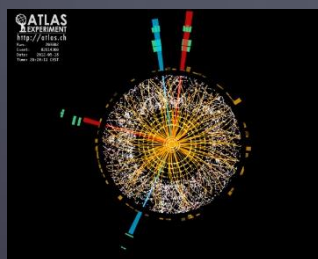
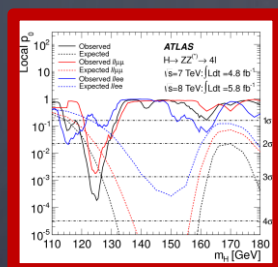
- ▶ All magnets trained at 7TeV
- ▶ Working energy for 2015 : 6.5TeV
- ▶ Acquired experience of great help
- ▶ However stay tuned:
- ▶ Want to increase the instantaneous luminosity x 2 → Double the nb of bunches (with 1.15×10^{11} ppb instead of 1.6×10^{11} ppb)
- ▶ Starting with 50ns (as in 2011 and 2012) and then go down to 25ns bunch to bunch spacing to keep the pileup lower. Warnings:
 - possible beam-beam interactions and electron cloud issues
 - higher UFO rate

Current



Nb of days

The LHC detectors or how to take Higgs pictures



Observing particles emerging in HE collisions

- ▶ Electrons, photons, muons, taus, tops, neutrinos, parton jets..
- ▶ Detectors must be able to trigger, reconstruct and identify them

Observing particles emerging in HE collisions

- ▶ Electrons, photons, muons, taus, tops, neutrinos, parton jets..
- ▶ Detectors must be able to trigger, reconstruct and identify them
- ▶ **LHC's prime goal was (is) the Scalar Boson discovery (SuSY).**
 - ▶ Same candles : e, μ , γ , ν , jets, missing energy ...

Observing particles emerging in HE collisions

- ▶ Electrons, photons, muons, taus, tops, neutrinos, parton jets..
- ▶ Detectors must be able to trigger, reconstruct and identify them
- ▶ **LHC's prime goal was (is) the Scalar Boson discovery (SuSY).**
 - ▶ Same candles : e , μ , γ , ν , jets, missing energy ...
 - ▶ At LHC's energies, the parton density is such that a lot of gluons are radiated as ISR/FSR on top of the main hard scattering. **Huge background to the interesting processes.**

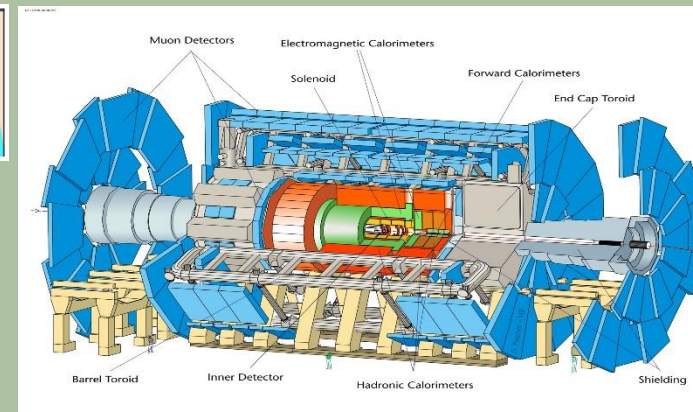
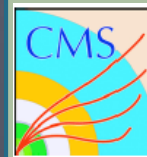
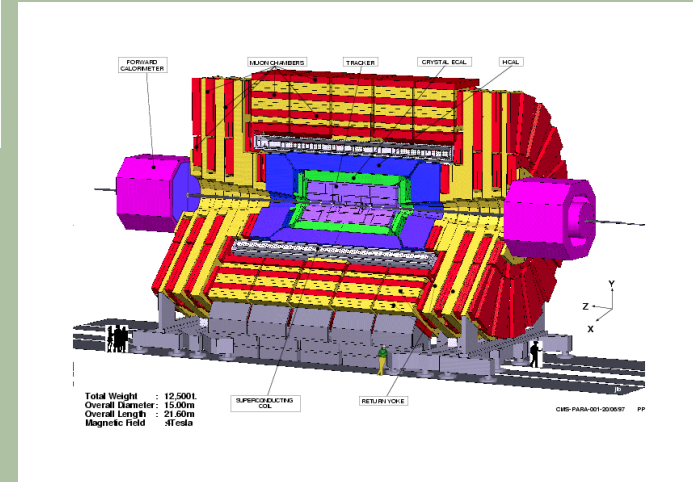
Observing particles emerging in HE collisions

- ▶ Electrons, photons, muons, taus, tops, neutrinos, parton jets..
- ▶ Detectors must be able to trigger, reconstruct and identify them
- ▶ **LHC's prime goal was (is) the Scalar Boson discovery (SuSY).**
 - ▶ Same candles : e , μ , γ , ν , jets, missing energy ...
 - ▶ At LHC's energies, the parton density is such that a lot of gluons are radiated as ISR/FSR on top of the main hard scattering. **Huge background to the interesting processes.**
 - ▶ Detectors must identify efficiently the hunted signatures and highly discriminate the background.
 - ▶ Unexplored kinematical regime → Guarantee the observation of the unexpected..

Constraints for a LHC detector

97

→ Be as hermetic as possible



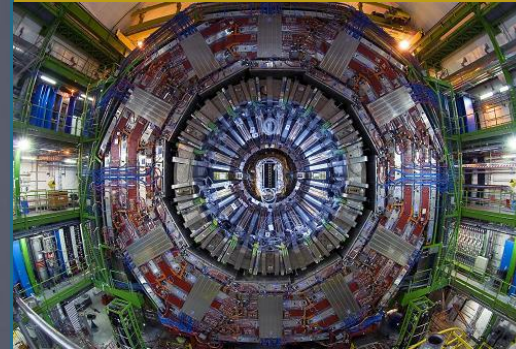
Invisibles 2015, Lydia Iconomidou-Foyard
16/06/2015

Constraints for a LHC detector

98

- Be as hermetic as possible
- Be stable with time

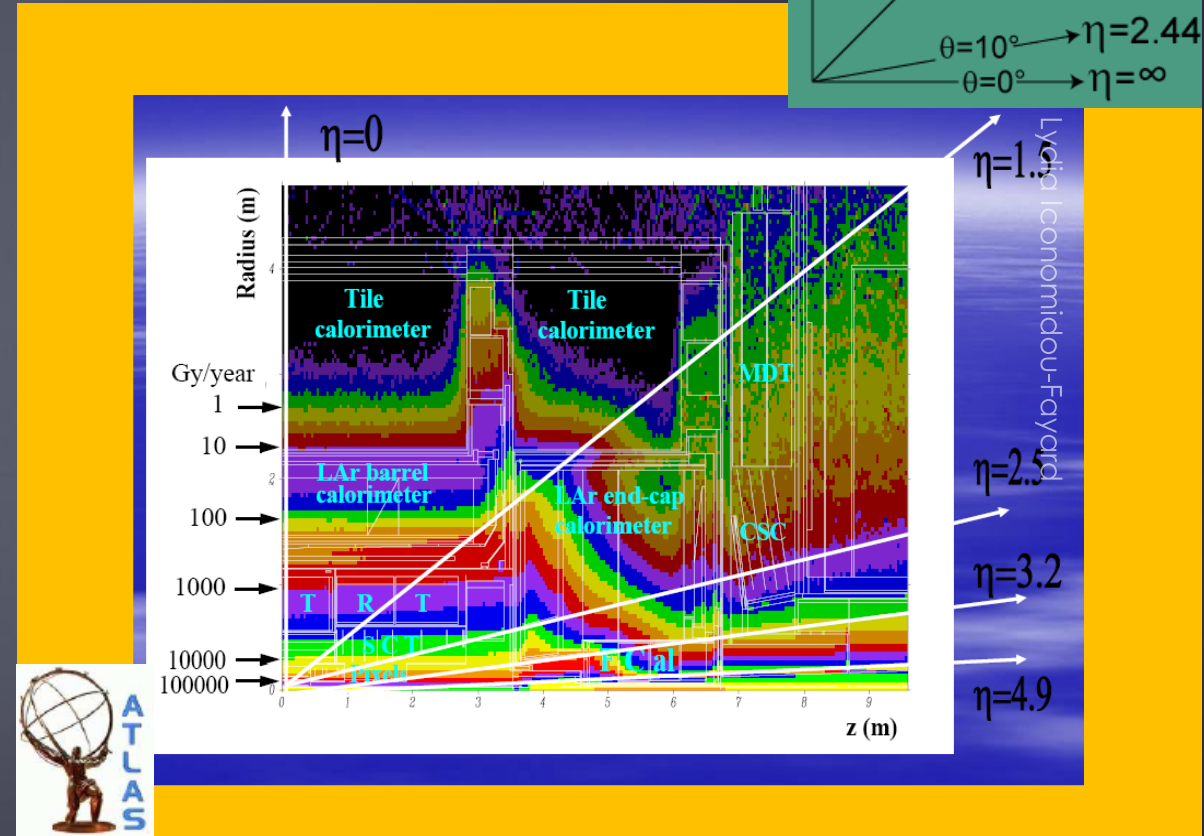
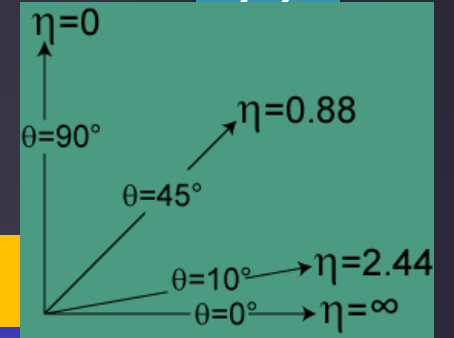
- Long run periods
- Huge detectors with imbricated elements involving poor accessibility



Invisibles 2015, Lydia Iconomidou-Foyard
16/06/2015

Constraints for a LHC detector

- Be as hermetic as possible
- Be stable with time
- Be as hard as possible to radiations



Constraints for a LHC detector

100

Invisibles 2015, Lydia Icor
16/06/2015

- Be as hermetic as possible
- Be stable with time
- Be as hard as possible to radiations
- Stand the high event rates

Use pipelined-multilayer deadtimeless triggers

- Decrease the 40 MHz initial rate down to few 100 Hz. First level synchronous, next ones asynchronous
- Keep only the interesting signatures for the physics analyses

Constraints for a LHC detector

101

- Be as hermetic as possible
- Be stable with time
- Be as hard as possible to radiations
- Stand the high event rates
- Ensure precise energy and momentum measurements in a large dynamic range

The interesting physics processes give particles with P_T from few GeV to few hundreds of GeV

Constraints for a LHC detector

102

- Be as hermetic as possible
- Be stable with time
- Be as hard as possible to radiations
- Stand the high event rates
- Ensure precise energy and momentum measurements in a large dynamic range
- Provide high background rejection

Detector design must be optimized such to allow the discrimination between signal and background signatures.

Particles going through matter

103

Invisibles 2015, Lydia Iconomidou-Fayard
16/06/2015

- ▶ Need to identify the interaction point, the trajectory and the energy of the particle.

Particles going through matter

104

Invisibles 2015, Lydia Iconomidou-Fayard
16/06/2015

- ▶ Need to identify the interaction point, the trajectory and the energy of the particle.
- ▶ Charged particles interact with atoms kicking-out electrons. This process can be used to sign charged particle's trajectory.
- ▶ Magnetic fields allow the measurement of charged particle's momenta

Particles going through matter

105

Invisibles 2015, Lydia Iconomidou-Fayard
16/06/2015

- ▶ Need to identify the interaction point, the trajectory and the energy of the particle.
- ▶ Charged particles interact with atoms kicking-out electrons. This process can be used to sign charged particle's trajectory.
- ▶ Magnetic fields allow the measurement of charged particle's momenta
- ▶ Neutral elm particles interact with matter through bremsstrahlung and pair creation and their energy is released till full absorption. Calorimetry,

Particles going through matter

106

Invisibles 2015, Lydia Iconomidou-Fayard
16/06/2015

- ▶ Need to identify the interaction point, the trajectory and the energy of the particle.
- ▶ Charged particles interact with atoms kicking-out electrons. This process can be used to sign charged particle's trajectory.
- ▶ Magnetic fields allow the measurement of charged particle's momenta
- ▶ Neutral elm particles interact with matter through bremsstrahlung and pair creation and their energy is released till full absorption. Calorimetry,
- ▶ Muons are bent and very slightly interacting

Particles going through matter

107

Invisibles 2015, Lydia Iconomidou-Fayard
16/06/2015

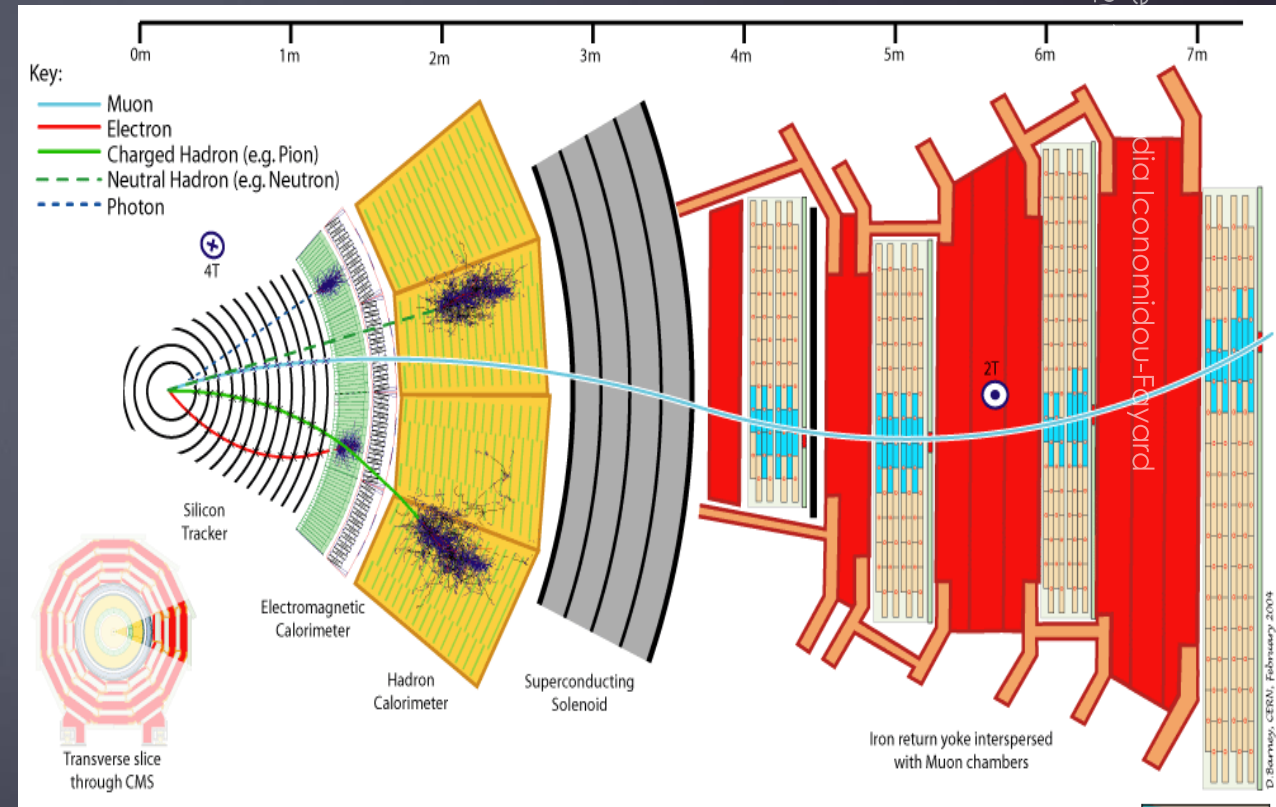
- ▶ Need to identify the interaction point, the trajectory and the energy of the particle.
- ▶ Charged particles interact with atoms kicking-out electrons. This process can be used to sign charged particle's trajectory.
- ▶ Magnetic fields allow the measurement of charged particle's momenta
- ▶ Neutral elm particles interact with matter through bremsstrahlung and pair creation and their energy is released till full absorption. Calorimetry,
- ▶ Muons are bent and very slightly interacting
- ▶ Neutrinos are seen as "missing energy"

Particles going through matter

108

Invisible
16/06/12

- ▶ Need to identify the interaction point, the trajectory and the energy of the particle.
- ▶ Charged particles interact with atoms kicking-out electrons. This process can be used to sign charged particle's trajectory.
- ▶ Magnetic fields allow the measurement of charged particle's momenta
- ▶ Neutral elm particles interact with matter through bremsstrahlung and pair creation and their energy is released till full absorption. Calorimetry,
- ▶ Muons are bent and very slightly interacting
- ▶ Neutrinos are seen as "missing energy"



Calorimeters for the Higgs

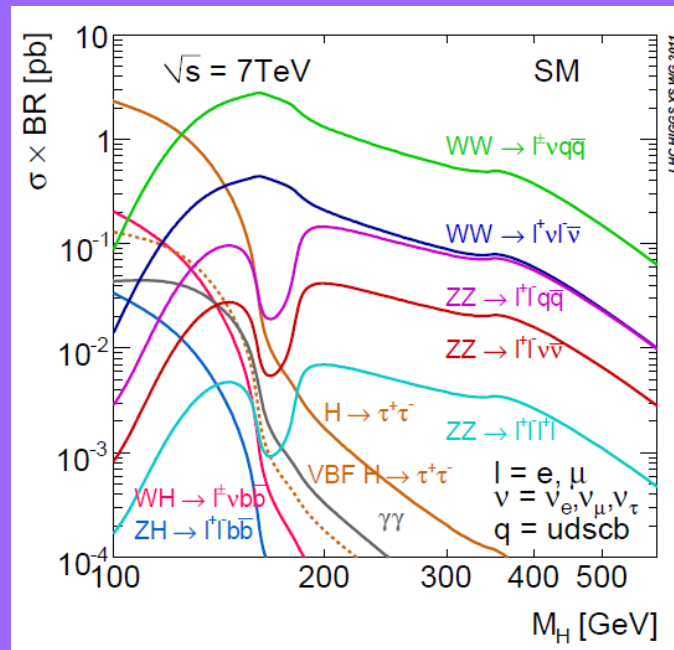
109

- ▶ Designed to achieve **the best possible performances for the measurement of photons**, to be prepared for the case of **low mass Higgs**. Region known to be difficult but privileged by Susy

Calorimeters for the Higgs

110

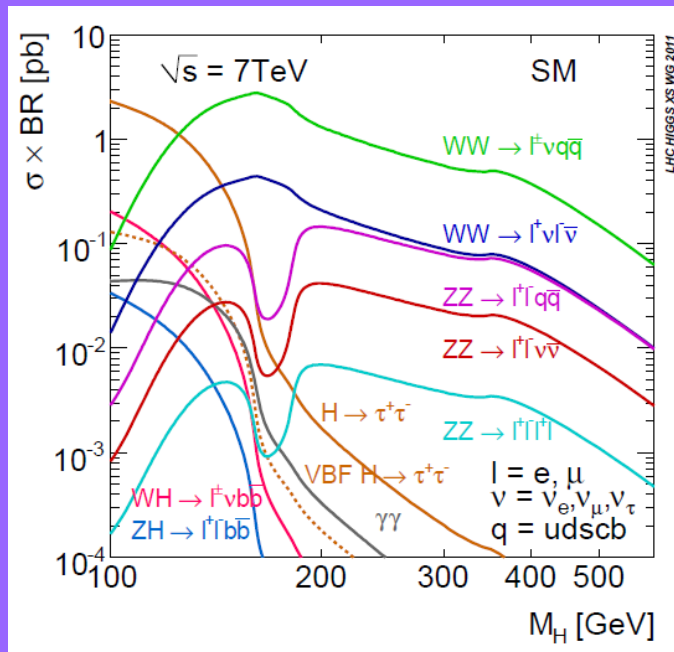
- ▶ Designed to achieve **the best possible performances for the measurement of photons**, to be prepared for the case of **low mass Higgs**. Region known to be difficult but privileged by Susy and ELW precision fits



Calorimeters for the Higgs

- ▶ Designed to achieve **the best possible performances for the measurement of photons**, to be prepared for the case of **low mass Higgs**. Region known to be difficult but privileged by Susy and ELW precision fits

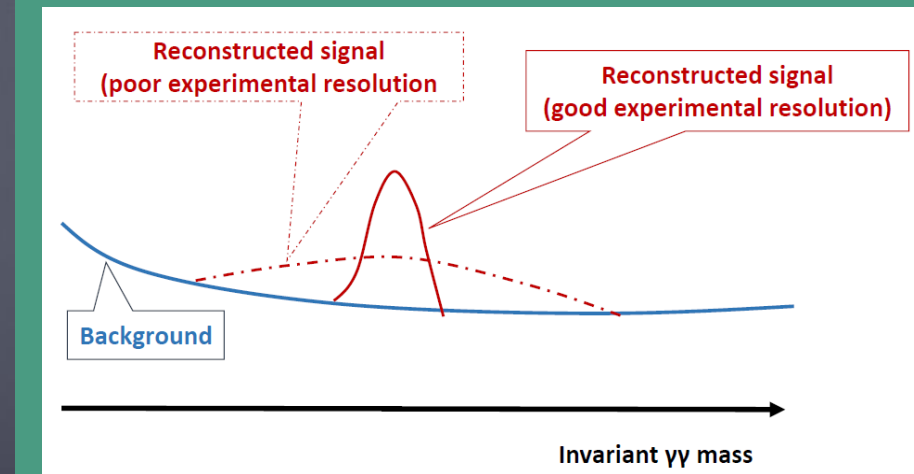
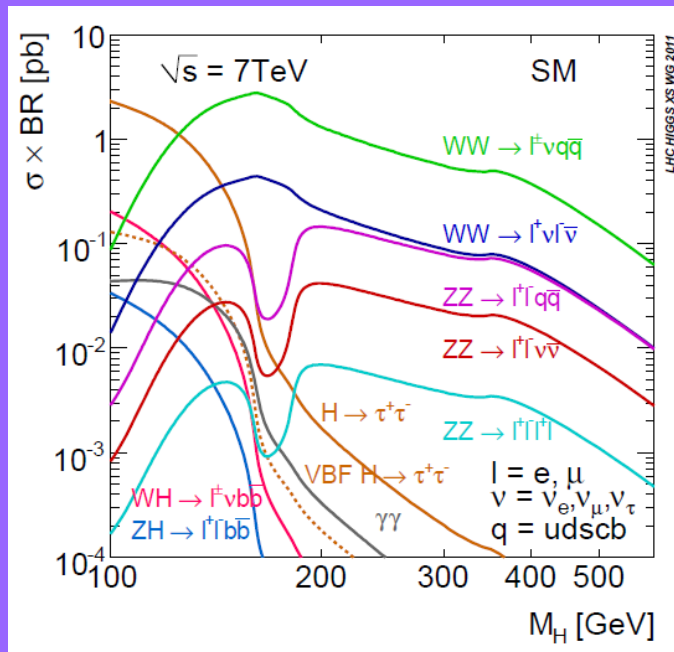
H- $\gamma\gamma$: Very challenging channel, but clear signature if photon energies measured with very good resolution
(natural Higgs width at $\sim 130\text{GeV}$ is few MeV)



Calorimeters for the Higgs

- Designed to achieve **the best possible performances for the measurement of photons**, to be prepared for the case of **low mass Higgs**. Region known to be difficult but privileged by Susy and ELW precision fits

H- $\gamma\gamma$: Very challenging channel, but clear signature if photon energies measured with very good resolution
(natural Higgs width at $\sim 130\text{GeV}$ is few MeV)



The CMS electromagnetic Calorimeter

113

Crystals of lead Tungstate
Collect the scintillation light with APD photodiodes

61200 Crystals ($2.2 \times 2.2 \times 23 \text{ cm}^3$) in barrel (67 t)

14648 Crystals ($2.6 \times 2.6 \times 22 \text{ cm}^3$) in EndCaps (23 t)

The CMS electromagnetic Calorimeter

114

Crystals of lead Tungstate
Collect the scintillation light with APD photodiodes

61200 Crystals ($2.2 \times 2.2 \times 23 \text{ cm}^3$) in barrel (67 t)

14648 Crystals ($2.6 \times 2.6 \times 22 \text{ cm}^3$) in EndCaps (23 t)



© 2015, Eydiol, Iconomicoq-Foyard

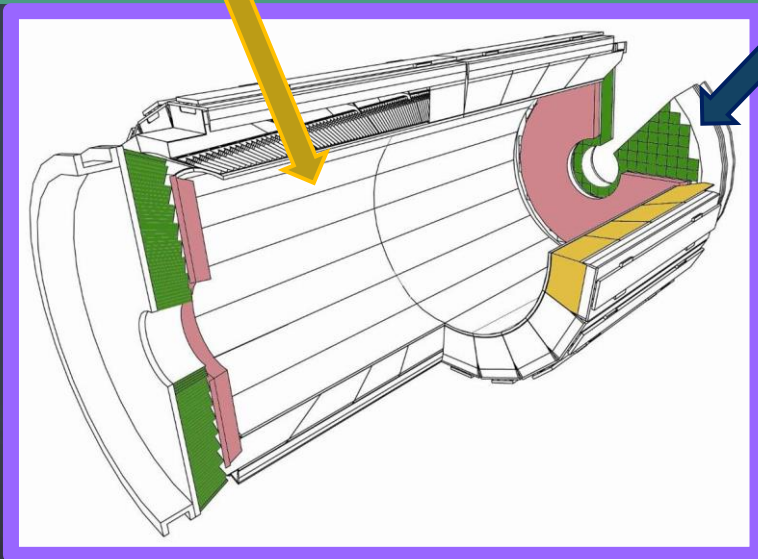
The CMS electromagnetic Calorimeter

115

Crystals of lead Tungstate
Collect the scintillation light with APD photodiodes

61200 Crystals ($2.2 \times 2.2 \times 23 \text{ cm}^3$) in barrel (67 t)

14648 Crystals ($2.6 \times 2.6 \times 22 \text{ cm}^3$) in EndCaps (23 t)



© 2015, Eyrol, L'conomique-Fayard

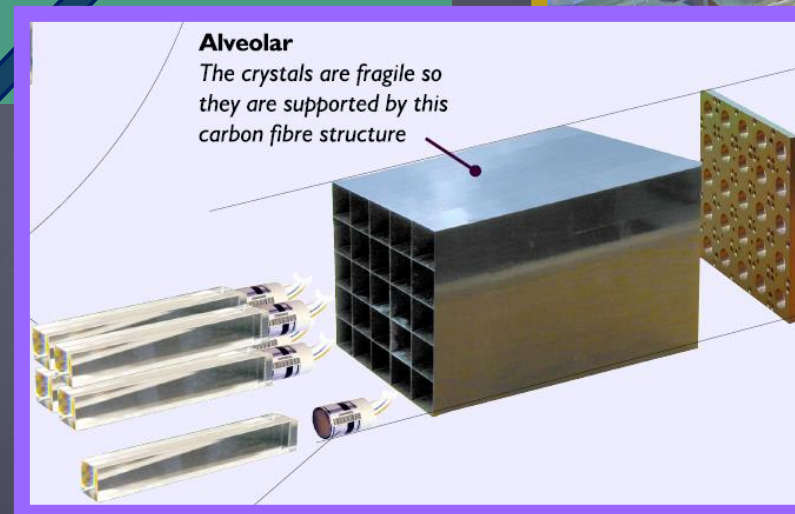
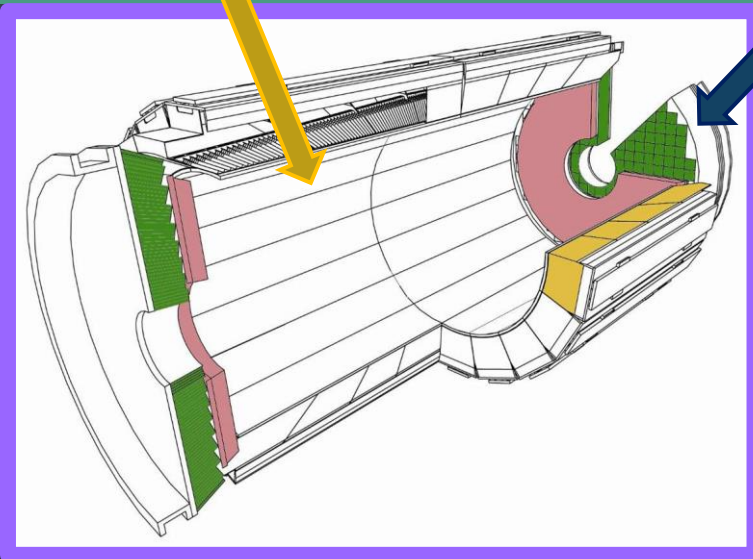
The CMS electromagnetic Calorimeter

Crystals of lead Tungstate
Collect the scintillation light with APD photodiodes

61200 Crystals (2.2 x 2.2 x 23 cm³) in barrel (67 t)
14648 Crystals (2.6 x 2.6 x 22 cm³) in EndCaps (23 t)



© 2015, Eyrol, Iconominicom-Fayard



$$\frac{\sigma(E)}{E} = \frac{2.4\%}{\sqrt{E}} \oplus \frac{142 \text{ MeV}}{E} \oplus 0.44\%$$

The CMS electromagnetic Calorimeter

117

▶ Lead tungstate properties

→ Short X_0 : 0.89cm Dense: $R_M = 2.1$ cm

The CMS electromagnetic Calorimeter

118

► Lead tungstate properties

→ Short X_0 : 0.89cm Dense: $R_M = 2.1\text{cm}$

Radiation length X_0

$$X_0 = \frac{716.4 \text{ A}}{Z(Z+1)\log(287/\sqrt{Z})}$$

The traversed distance after what the electron loses $1/e$ of his energy

The CMS electromagnetic Calorimeter

119

► Lead tungstate properties

→ Short X_0 : 0.89cm Dense: $R_M = 2.1$ cm

Moliere radius R_M

$$R_M = 0.0265 X_0 (Z+1.2)$$

The radius of the cylinder that contains 90% of the released energy around the electron

The CMS electromagnetic Calorimeter

120

▶ Lead tungstate properties

- Short X_0 : 0.89cm Dense: $R_M = 2.1$ cm
- Fast light emission : almost 80% in 25ns
- Temperature dependent 2.2%/ C, requires T stabilization down to <0.1C
- Has low light yield → needs amplification
- Intrinsic excellent resolution

The CMS electromagnetic Calorimeter

121

▶ Lead tungstate properties

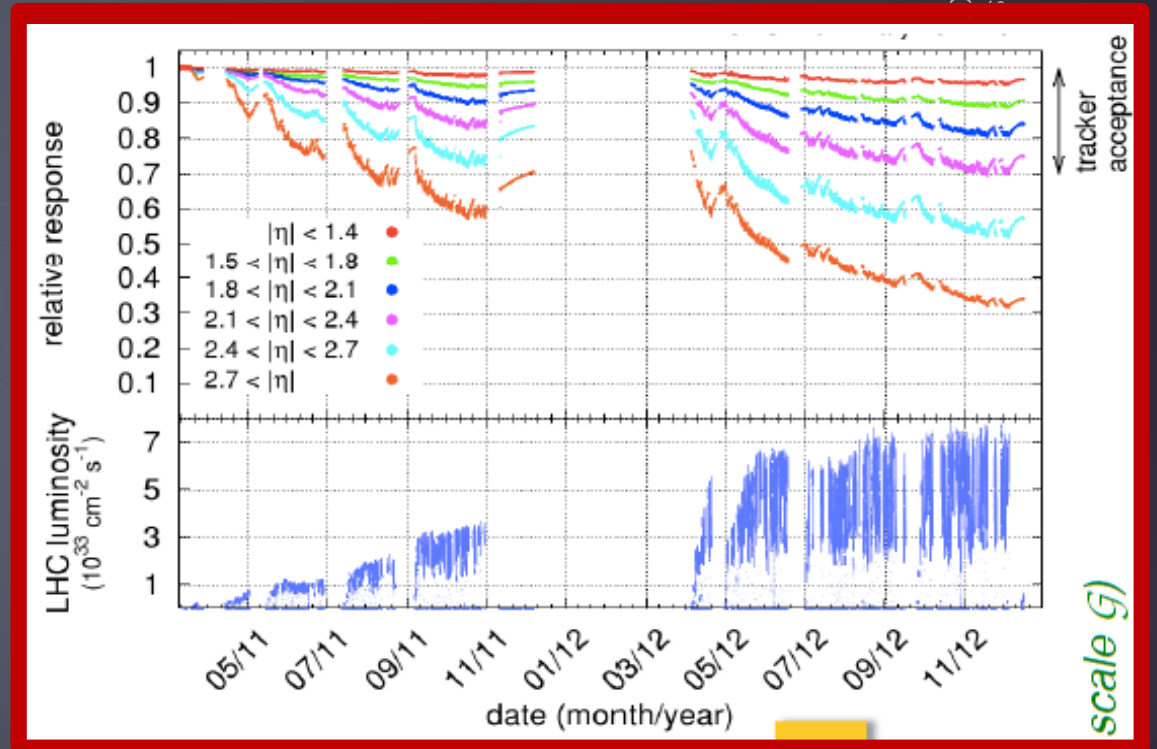
- Short X_0 : 0.89cm Dense: $R_M = 2.1$ cm
- Fast light emission : almost 80% in 25ns
- Temperature dependent 2.2%/ C, requires T stabilization down to <0.1C
- Has low light yield → needs amplification
- Intrinsic excellent resolution
- Light response sensitive to irradiation → Laser monitoring

The CMS electromagnetic Calorimeter

122

▶ Lead tungstate properties

- Short X_0 : 0.89cm Dense: $R_M = 2.1$ cm
- Fast light emission : almost 80% in 25ns
- Temperature dependent 2.2%/ C, requires T stabilization down to <0.1C
- Has low light yield → needs amplification
- Intrinsic excellent resolution
- Light response sensitive to irradiation → Laser monitoring

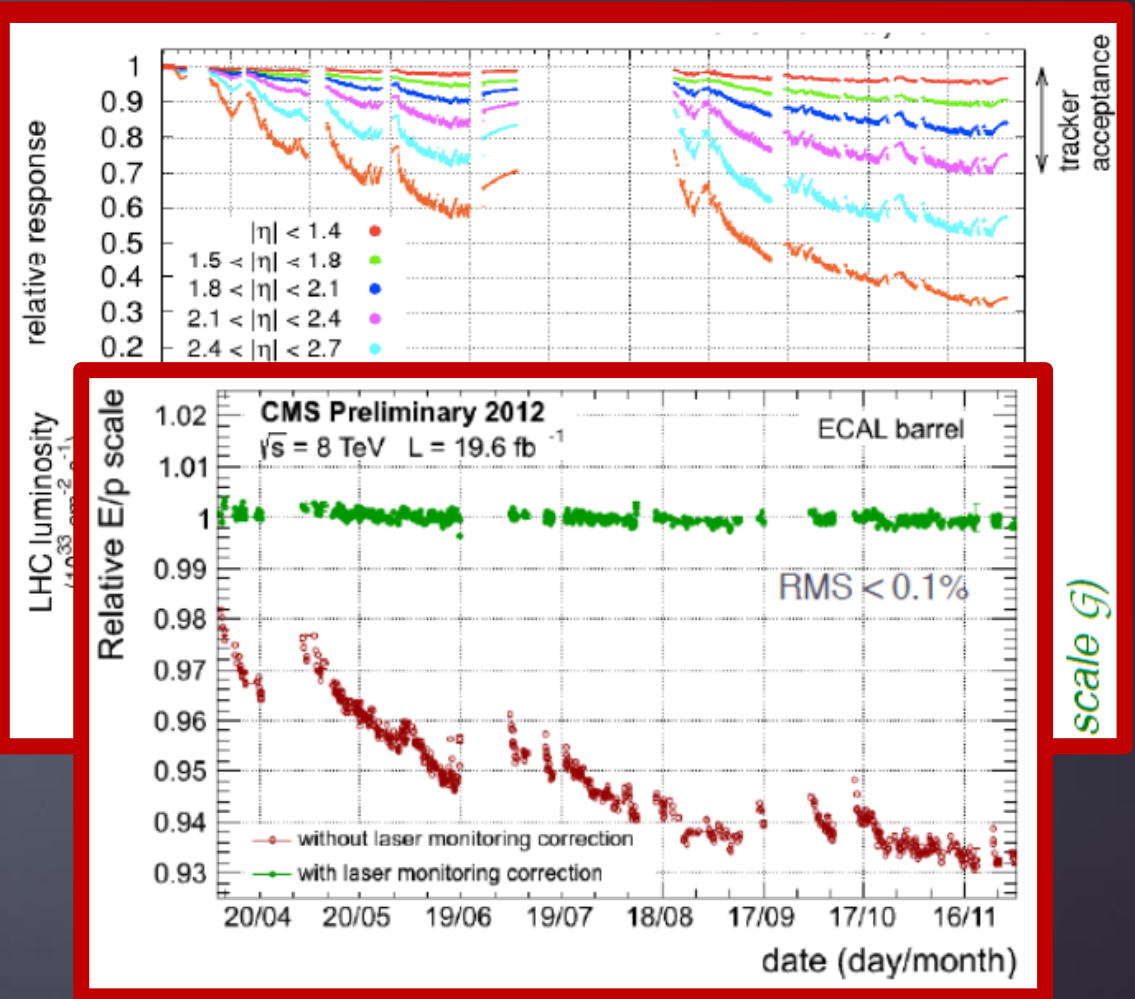


The CMS electromagnetic Calorimeter

123

► Lead tungstate properties

- Short X_0 : 0.89cm Dense: $R_M = 2.1$ cm
- Fast light emission : almost 80% in 25ns
- Temperature dependent 2.2%/ C, requires T stabilization down to <0.1C
- Has low light yield → needs amplification
- Intrinsic excellent resolution
- Light response sensitive to irradiation → Laser monitoring



The ATLAS electromagnetic Calorimeter

→ Lead-Liquid Argon calorimeter

$X_0 = 2\text{cm}$ $R_M = 4\text{cm}$

→ Stable, radiation hard, fast, uniform

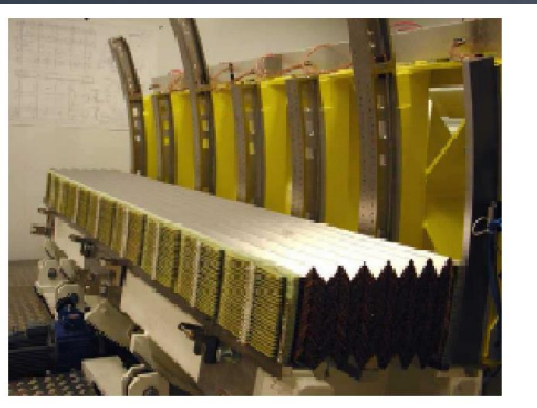
The ATLAS electromagnetic Calorimeter

125

→ Lead-Liquid Argon calorimeter

$X_0 = 2\text{cm}$ $R_M = 4\text{cm}$

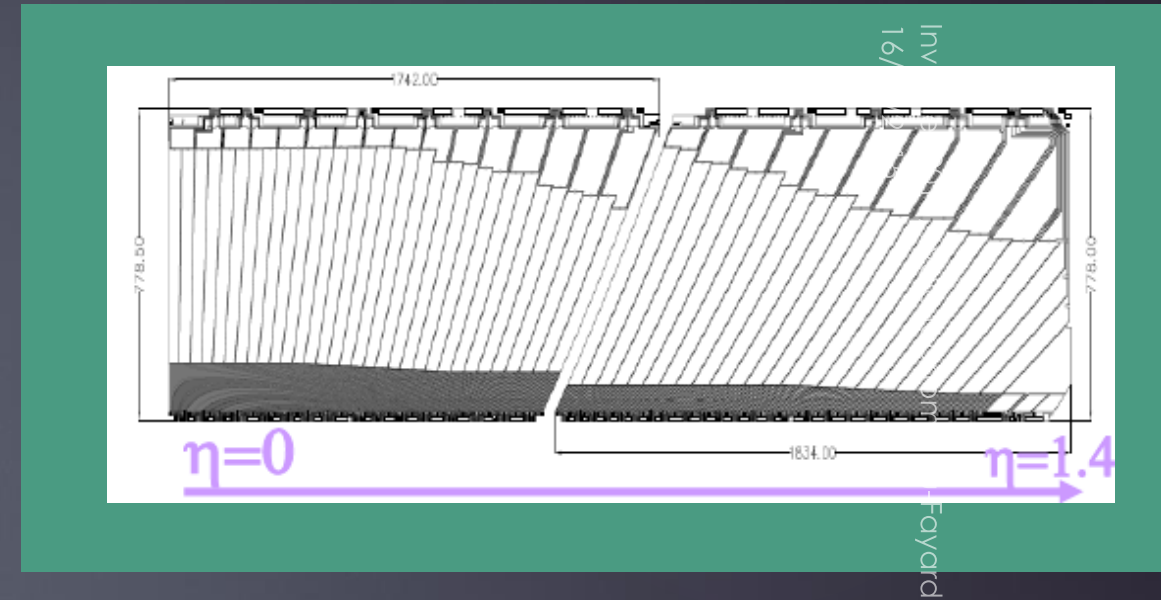
→ Stable, radiation hard, fast, uniform



The ATLAS electromagnetic Calorimeter

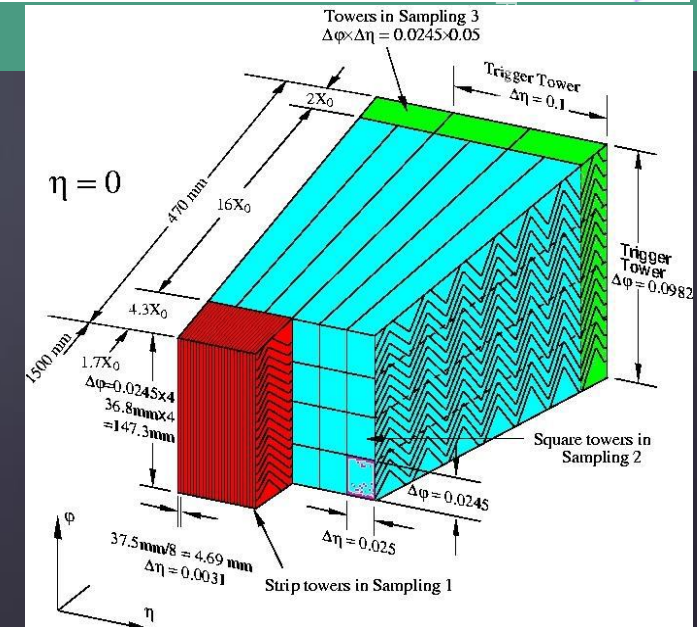
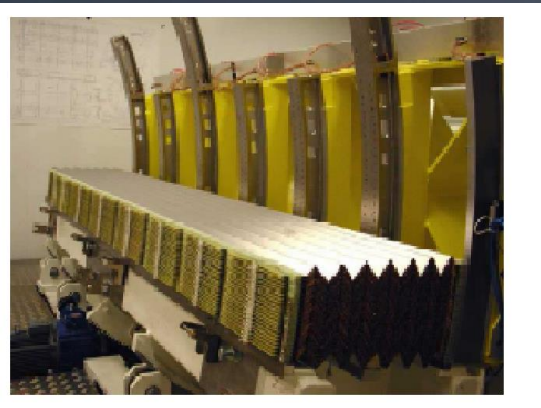
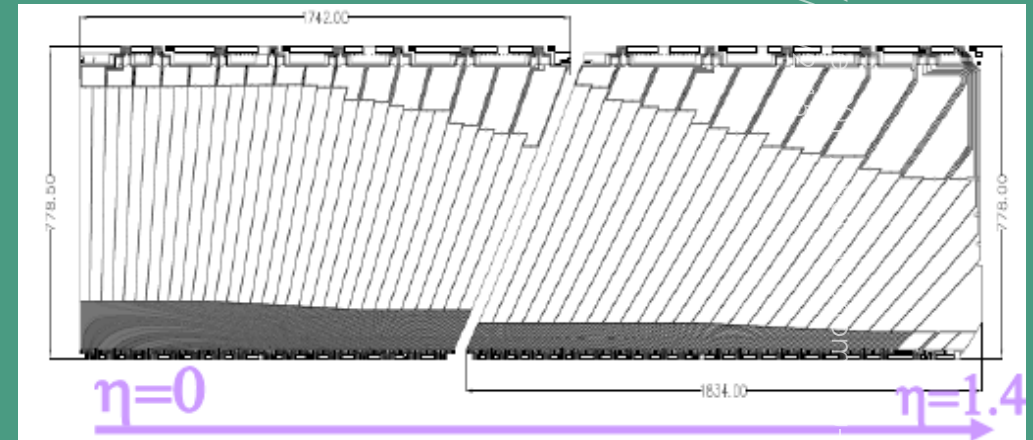
126

- Lead-Liquid Argon calorimeter
 $X_0 = 2\text{cm}$ $R_M = 4\text{cm}$
- Stable, radiation hard, fast, uniform
- Longitudinally segmented in 3 layers:
Front (3-5 X_0), middle (17 X_0), back (5-15 X_0)



The ATLAS electromagnetic Calorimeter

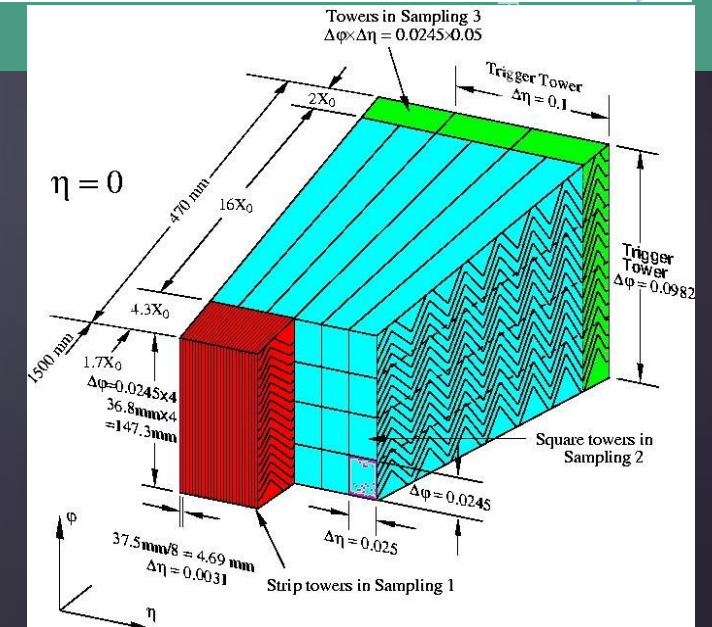
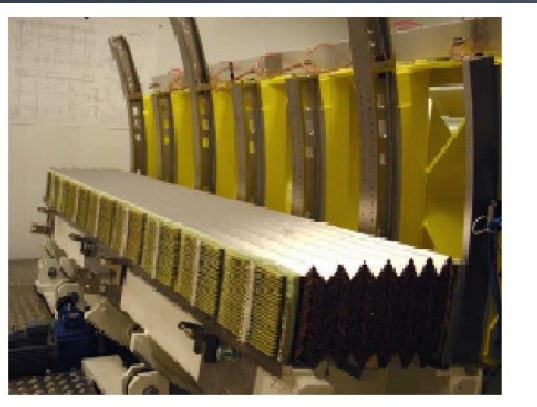
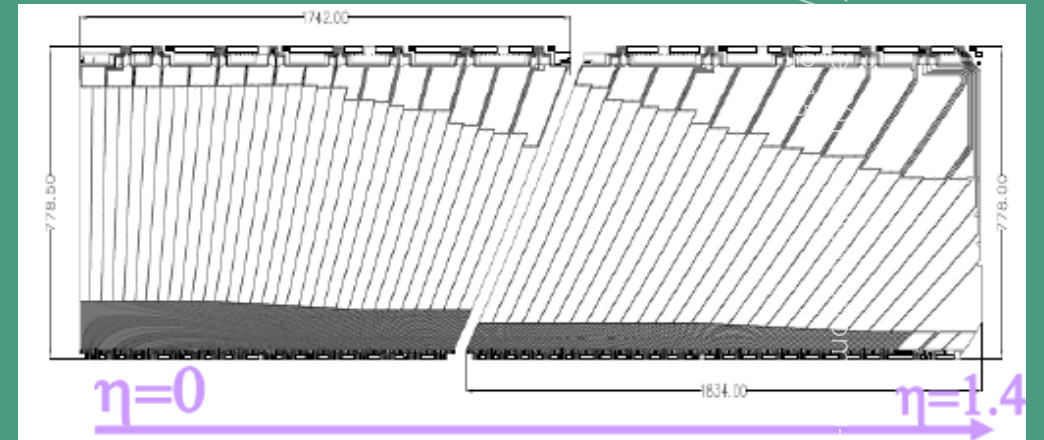
- Lead-Liquid Argon calorimeter
- $X_0 = 2\text{cm}$ $R_M = 4\text{cm}$
- Stable, radiation hard, fast, uniform
- Longitudinally segmented in 3 layers: Front (3-5 X_0), middle (17 X_0), back (5-15 X_0)



The ATLAS electromagnetic Calorimeter

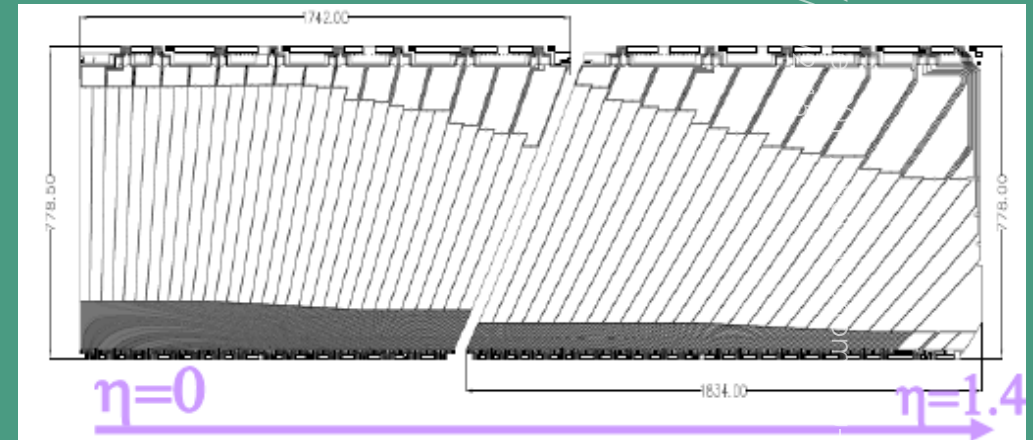
128

- Lead-Liquid Argon calorimeter
- $X_0 = 2\text{cm}$ $R_M = 4\text{cm}$
- Stable, radiation hard, fast, uniform
- Longitudinally segmented in 3 layers:
Front ($3-5 X_0$), middle ($17 X_0$), back ($5-15 X_0$)
- Mounted in 3 pieces, barrel and 2 EndCaps, placed in 3 different cryostats
- A total ~ 180000 channels

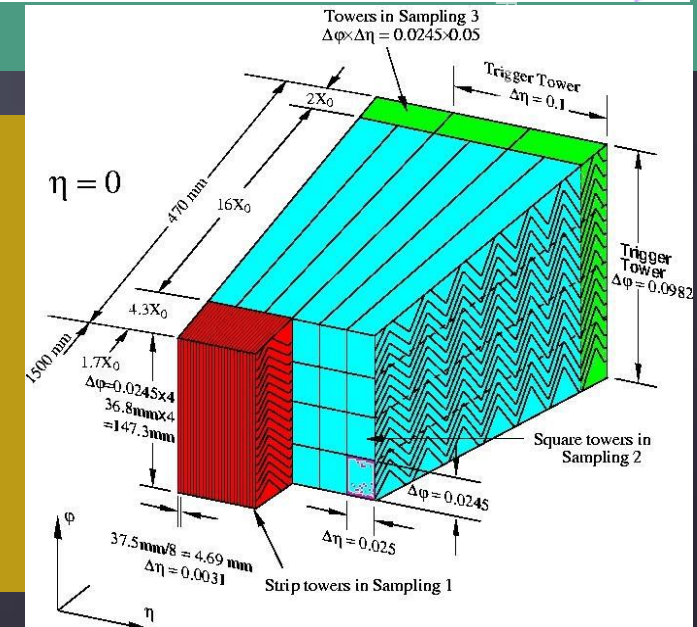
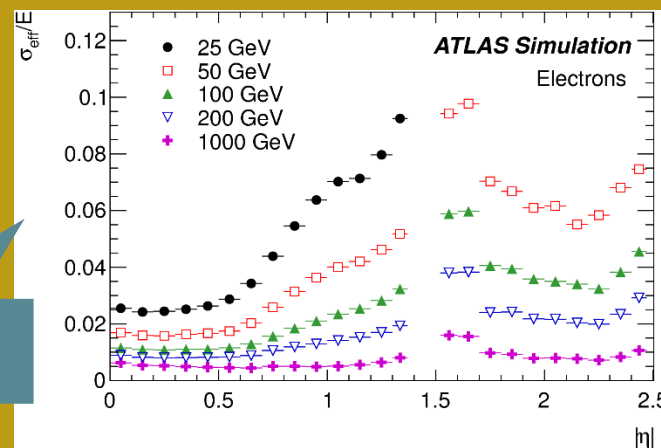


The ATLAS electromagnetic Calorimeter

- Lead-Liquid Argon calorimeter
- $X_0 = 2\text{cm}$ $R_M = 4\text{cm}$
- Stable, radiation hard, fast, uniform
- Longitudinally segmented in 3 layers: Front (3-5 X_0), middle (17 X_0), back (5-15 X_0)
- Mounted in 3 pieces, barrel and 2 EndCaps, placed in 3 different cryostats
- A total ~180000 channels

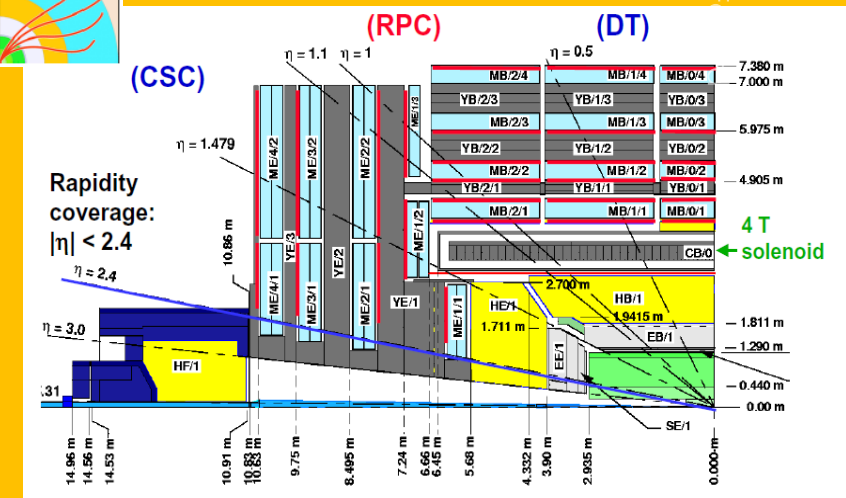
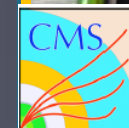


$\sigma(E)/E$

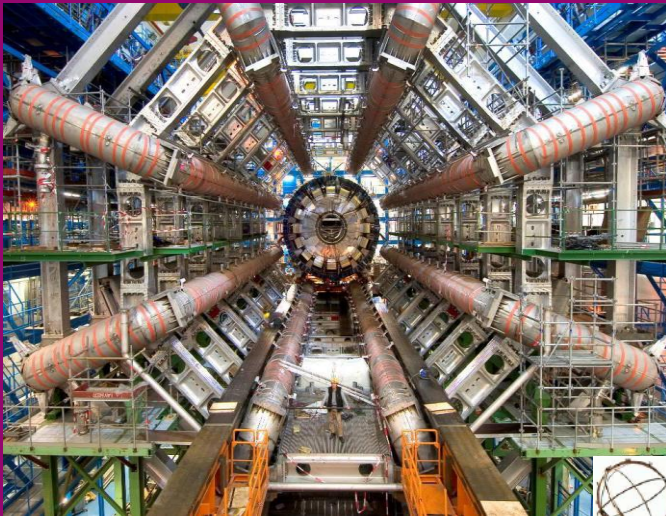


Muon systems in ATLAS and CMS

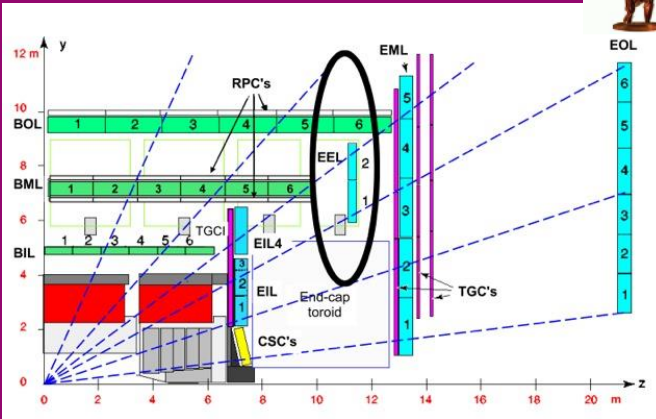
Solenoid supraconducting magnet with a 4 Tesla field
4 stations of chambers interleaved between the iron yoke.



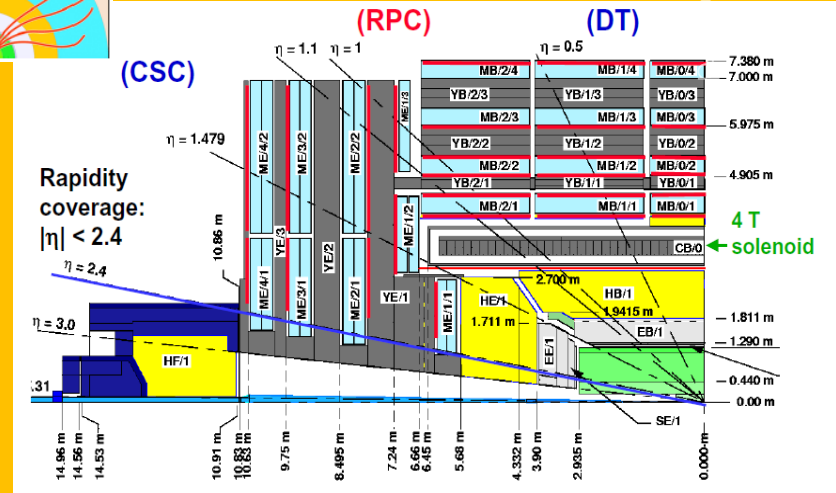
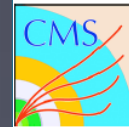
Muon systems in ATLAS and CMS



Solenoid supraconducting magnet with a 4 Tesla field
4 stations of chambers interleaved between the iron yoke.



8 toroidal supraconducting coils (0.5-1 Tesla)
3 Stations of chambers
Muons measured in the InnerDetector and in the Muon System



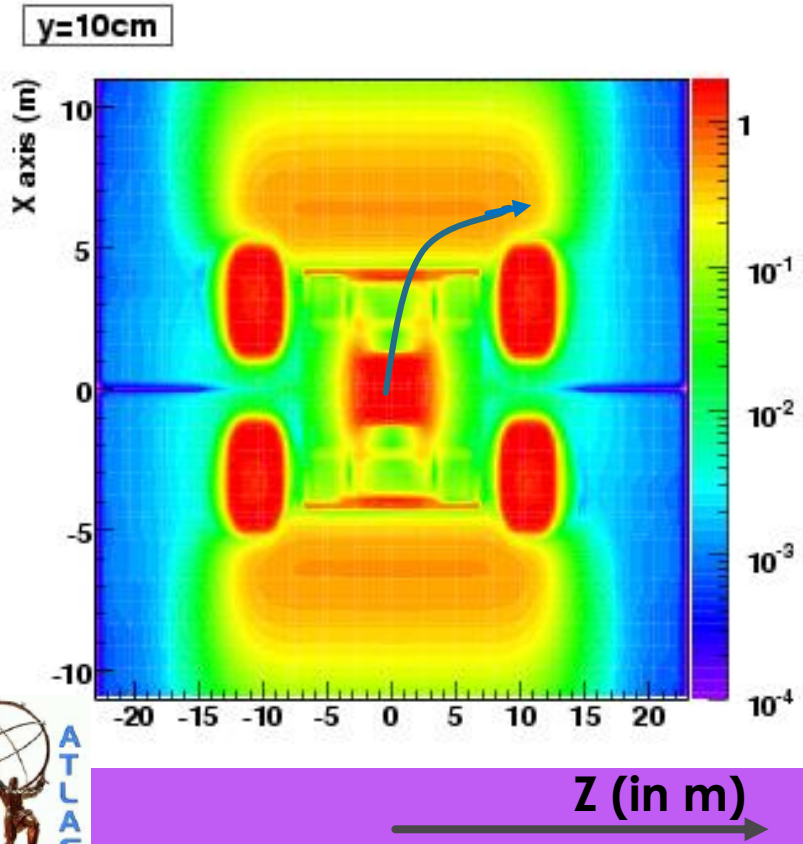
Magnetic fields in ATLAS and CMS

132

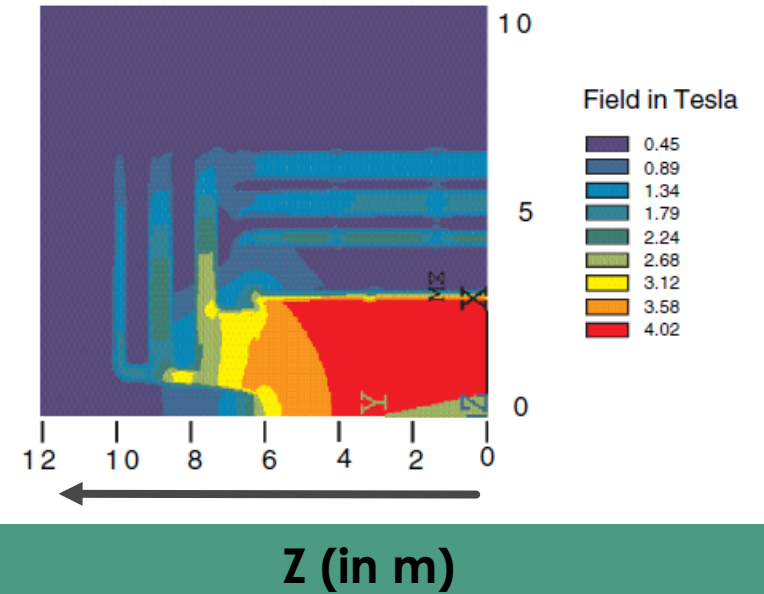
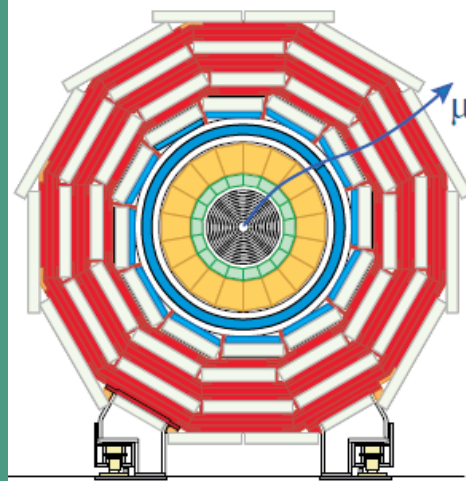
Invisibles 2015, Lydic
16/06/2015



Bending in ϕ and in Z



Bending in ϕ

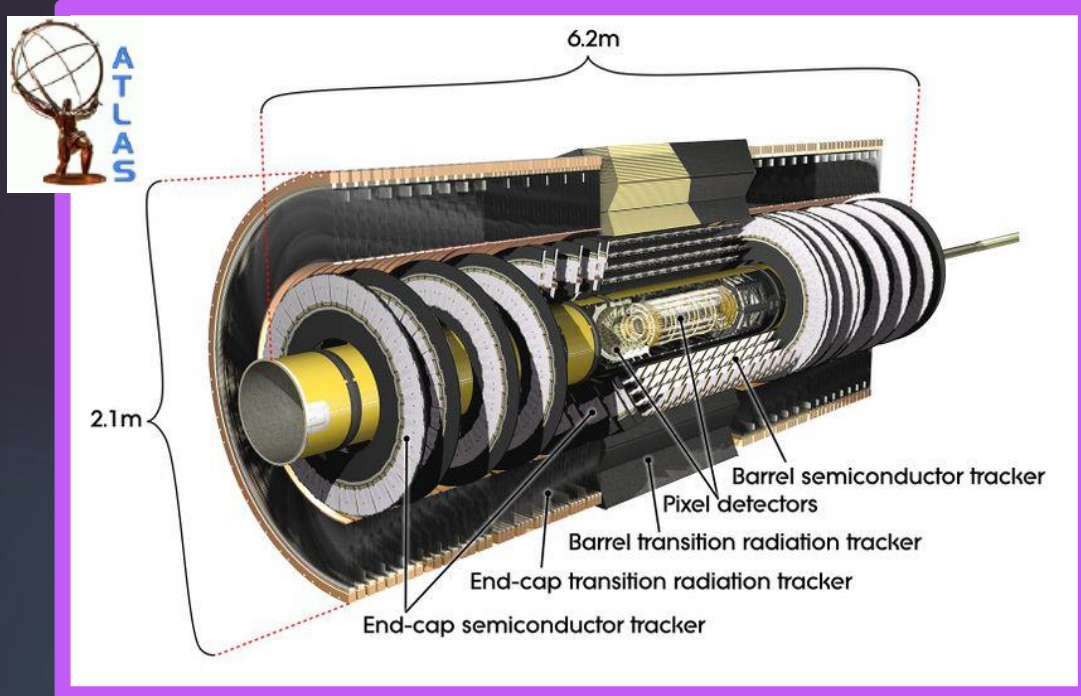


The Challenges

- 1) Reconstruct the interaction points and the tracks of charged particles with high precision
- 2) High multiplicity environment requires fine granularity of the sensitive detectors to achieve efficient separation
- 3) Need to go as close as possible to the beam axis and to have sufficient lever arm
- 4) Amount of tracking detector material has to be kept low before the calorimeters

The tracking systems of ATLAS & CMS

134



1) Semiconductor detectors

- Three layers of high granularity pixels (starting at 4cm from the Interaction Point)
- Four layers of silicon microstrips

2) Transition radiation detector (electron-pion discrimination)

Silicon detectors

- 1) Three layers of pixels at 4.4, 7.3 and 10.2cm from the interaction point
- 2) 10 layers of microstrip detectors

Elementary particle reconstruction



Electrons and photons

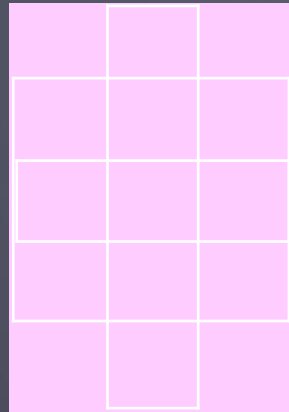


An « electron candidate » in ATLAS

137

Definition : « A **track** in the inner detector pointing to a **cluster** found in the electromagnetic calorimeter. »

Sliding -window looks for energy deposits $>2.5\text{GeV}$ in 3×5 frame $3\times(0.025\times 0.025)$ in (η, ϕ)



Energy seed in $3\times 5 E_t > 2.5 \text{ GeV}$

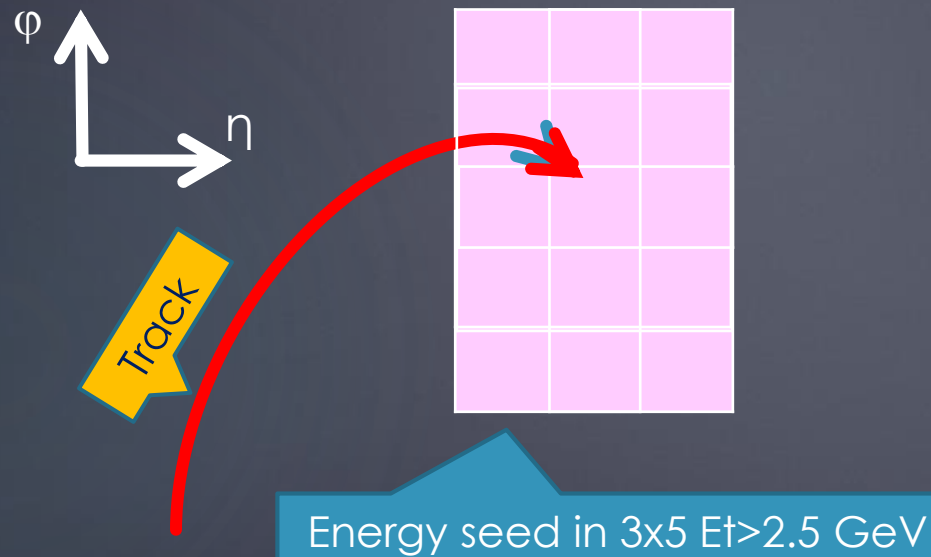
An « electron candidate » in ATLAS

138

Definition : « A **track** in the inner detector pointing to **a cluster** found in the electromagnetic calorimeter. »

Sliding -window looks for energy deposits $>2.5\text{GeV}$ in 3×5 frame $3\times (0.025\times 0.025)$ in (η, ϕ)

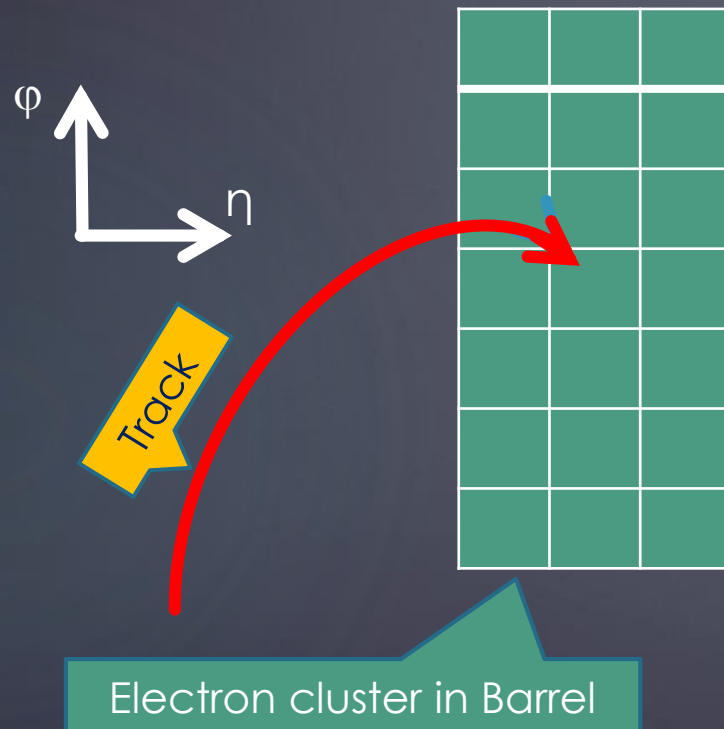
If a track matches the cluster..



An « electron candidate » in ATLAS

139

Definition : « A **track** in the inner detector pointing to **a cluster** found in the electromagnetic calorimeter. »



Sliding -window looks for energy deposits $>2.5\text{GeV}$ in 3×5 frame $3 \times (0.025 \times 0.025)$ in (η, ϕ)

If a track matches the cluster..

An electron is reconstructed in a 3×7 window in the Barrel and 5×5 in EndCaps

An « electron candidate » in ATLAS

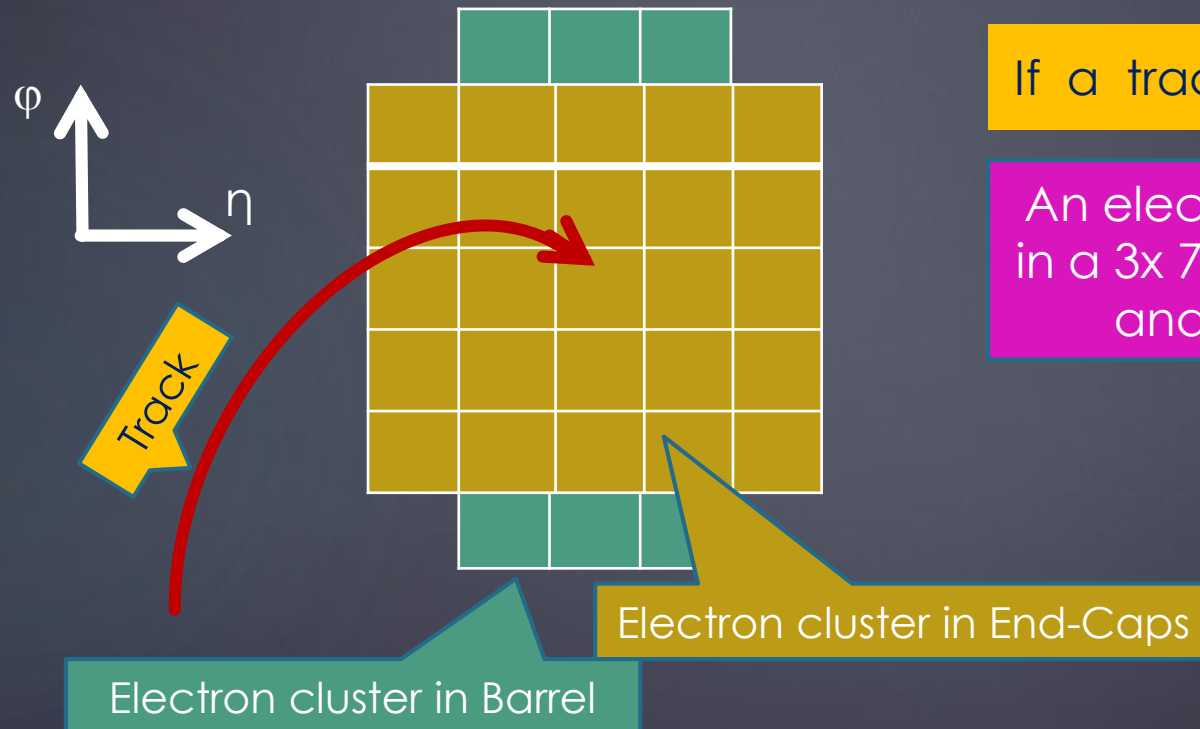
140

Definition : « A **track** in the inner detector pointing to **a cluster** found in the electromagnetic calorimeter. »

Sliding -window looks for energy deposits $>2.5\text{GeV}$ in 3×5 frame $3 \times (0.025 \times 0.025)$ in (η, ϕ)

If a track matches the cluster..

An electron is reconstructed in a 3×7 window in the Barrel and 5×5 in EndCaps



An « electron candidate » in ATLAS

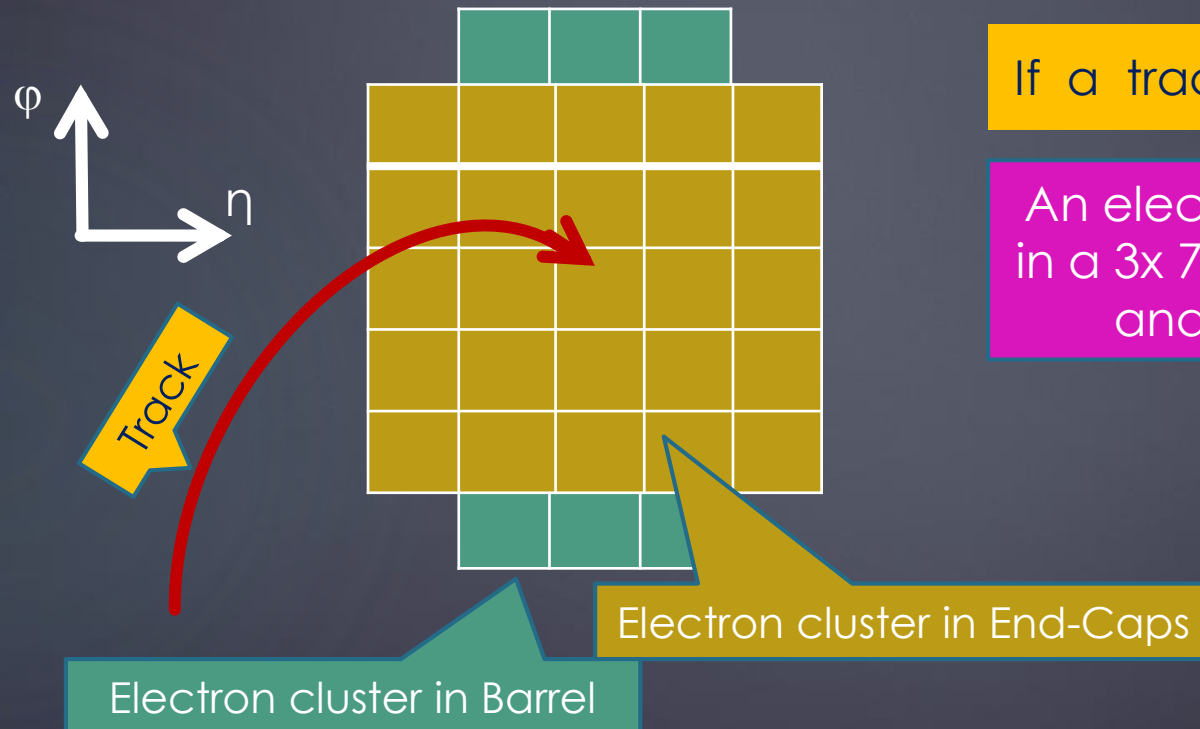
Definition : « A **track** in the inner detector pointing to a **cluster** found in the electromagnetic calorimeter. »

Sliding -window looks for energy deposits $>2.5\text{GeV}$ in 3×5 frame $3 \times (0.025 \times 0.025)$ in (η, ϕ)

If a track matches the cluster..

An electron is reconstructed in a 3×7 window in the Barrel and 5×5 in EndCaps

Electron energy from:
**Deposits in the 3 layers
**Signal in preshower
**Estimated lateral and longitudinal leakage
Electron direction from Track



Bremsstrahlung (1)

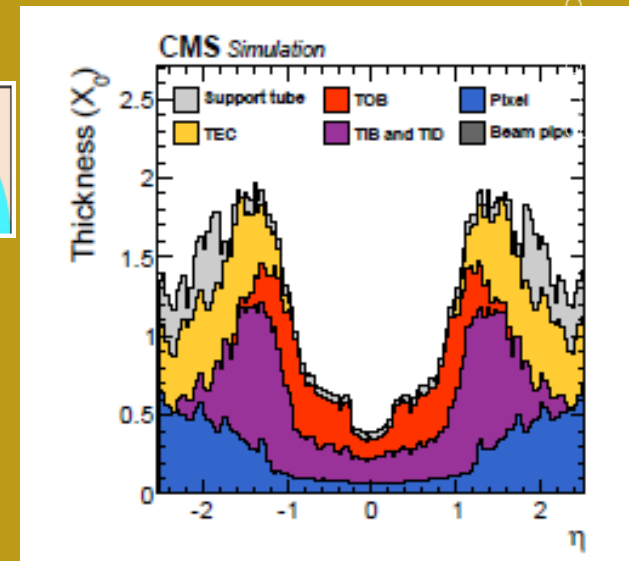
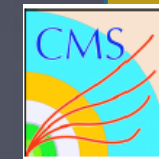
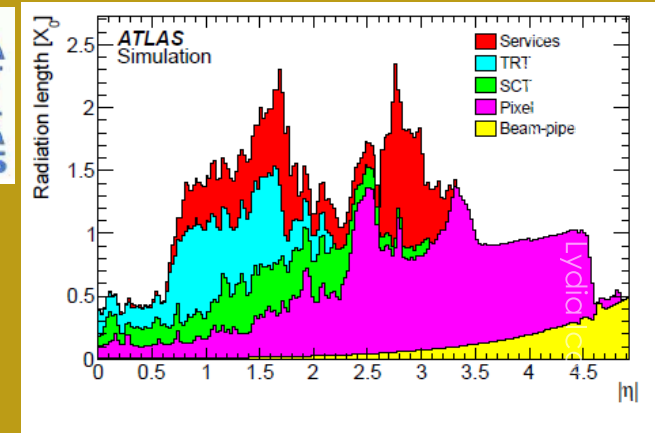
142

An electron radiates
photons +-energetic.
Consequences:

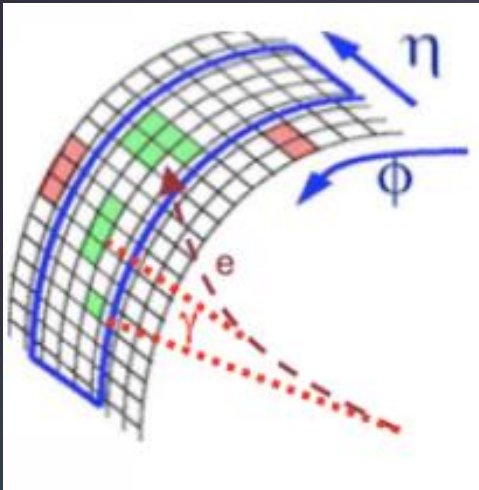
Bremsstrahlung (1)

An electron radiates photons +-energetic.
Consequences:

Energy loss,
depending on the
amount of
traversed material



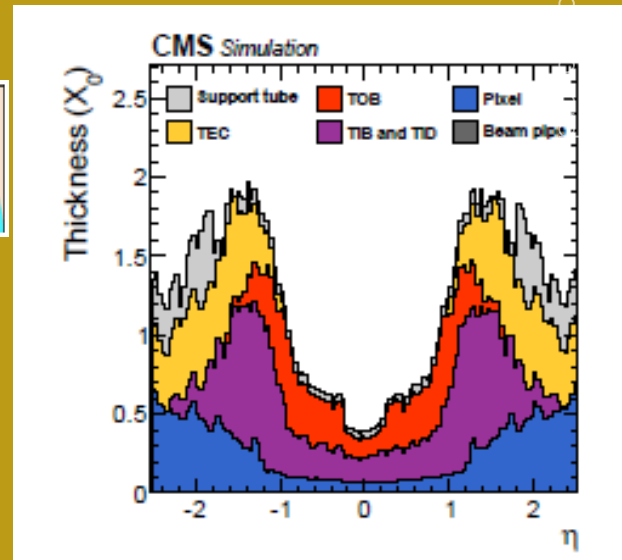
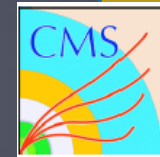
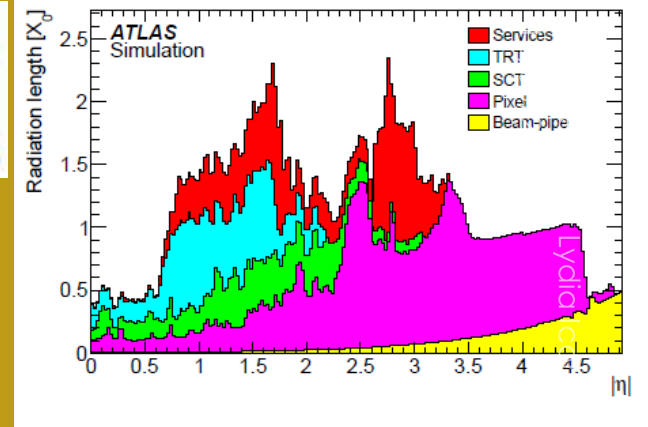
Bremsstrahlung (1)



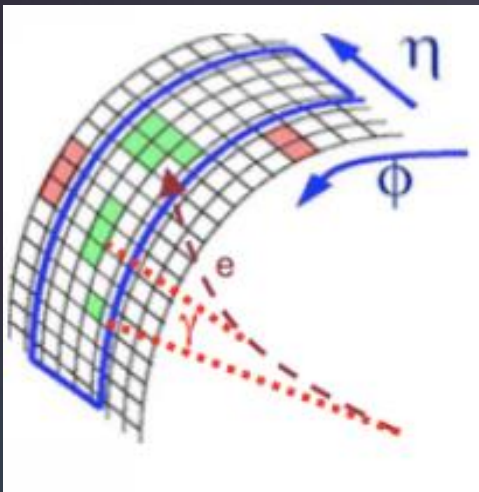
An electron radiates photons +-energetic. Consequences:

Energy loss, depending on the amount of traversed material

Modification of the bent track path. It must be considered in the reconstruction to avoid inefficiencies



Bremsstrahlung (1)



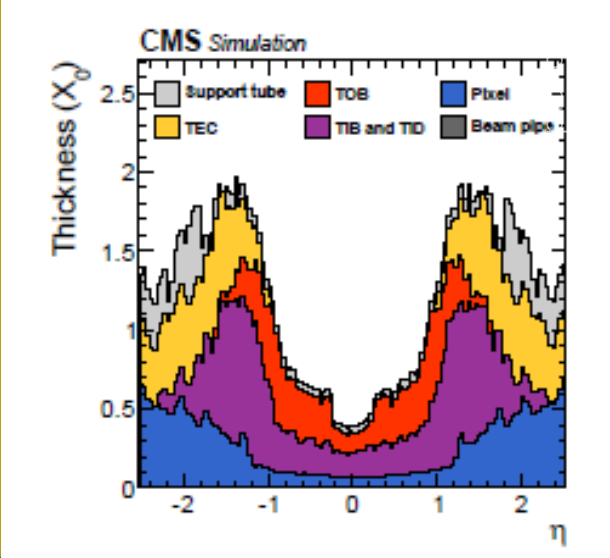
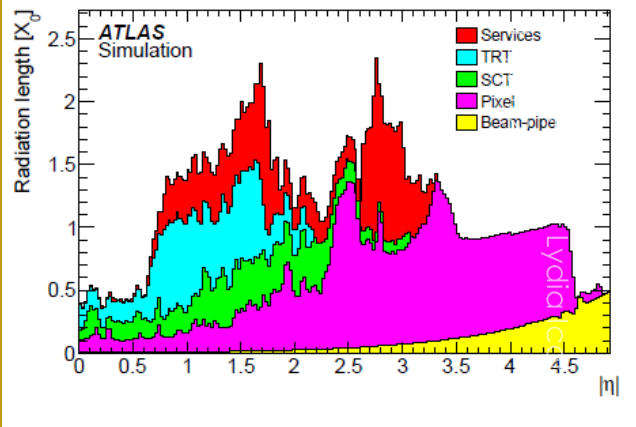
An electron radiates photons +-energetic.
Consequences:

Energy loss, depending on the amount of traversed material

Modification of the bent track path. It must be considered in the reconstruction to avoid inefficiencies

In case of strong magnetic field in the Inner Detector, the initial electron can lead to multiple clusters in the calorimeter

Experiment	Field
CMS	4 Tesla
ATLAS	2 Tesla



Bremsstrahlung (2)

146

CMS : 33% (85%) of electron energy radiated before the barrel (EndCap) calorimeter.

→ Strong field bends the electron far from photons

→ “SuperCluster algorithm” to collect the full energy and improve the resolution.

→ Specific track reconstruction to take into account the brem.

Bremsstrahlung (2)

147

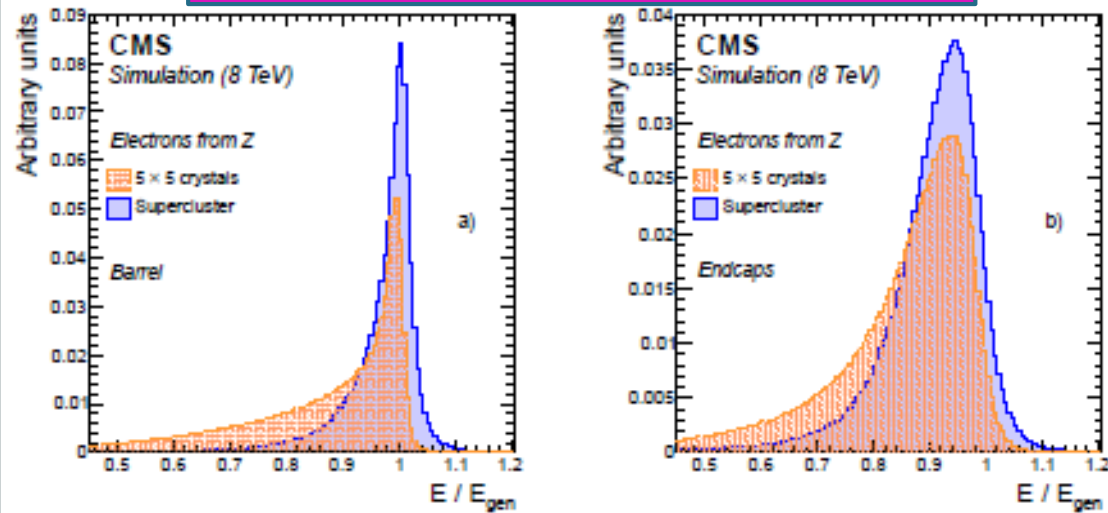
CMS : 33% (85%) of electron energy radiated before the barrel (EndCap) calorimeter.

→ Strong field bends the electron far from photons

→ “SuperCluster algorithm” to collect the full energy and improve the resolution.

→ Specific track reconstruction to take into account the brems.

CMS : Emeas/Egen with 5x5 and with SuperCluster

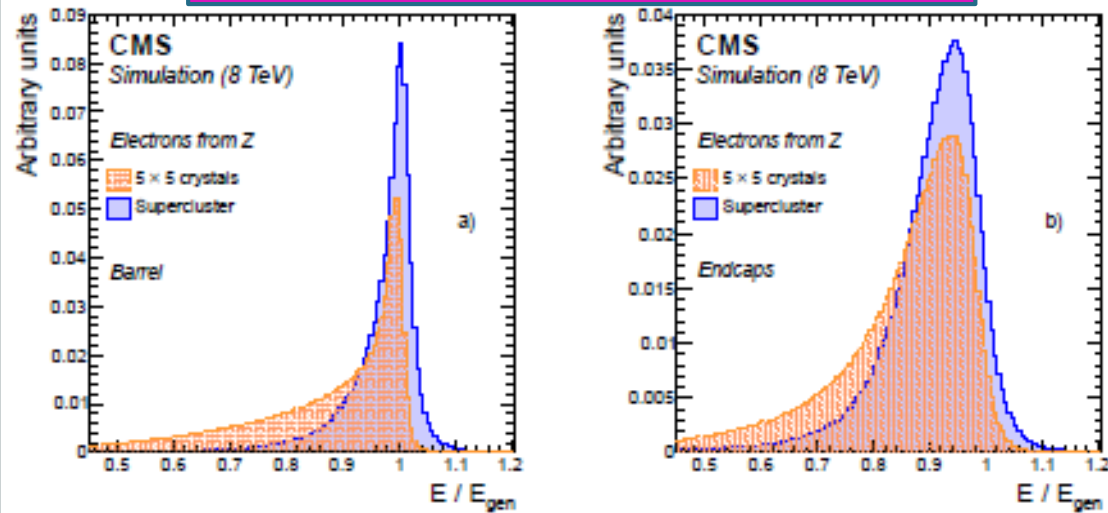


Bremsstrahlung (2)

CMS : 33% (85%) of electron energy radiated before the barrel (EndCap) calorimeter.
→ Strong field bends the electron far from photons
→ “SuperCluster algorithm” to collect the full energy and improve the resolution.
→ Specific track reconstruction to take into account the brems.

ATLAS: weaker field.
In general radiated photons belong to cluster window
→ From 2012 on, specific track reconstruction to take into account the brems .
→ Especially important for low ET

CMS : Emeas/Egen with 5x5 and with SuperCluster



Bremsstrahlung (2)

CMS : 33% (85%) of electron energy radiated before the barrel (EndCap) calorimeter.

→ Strong field bends the electron far from photons

→ “SuperCluster algorithm” to collect the full energy and improve the resolution.

→ Specific track reconstruction to take into account the brems.

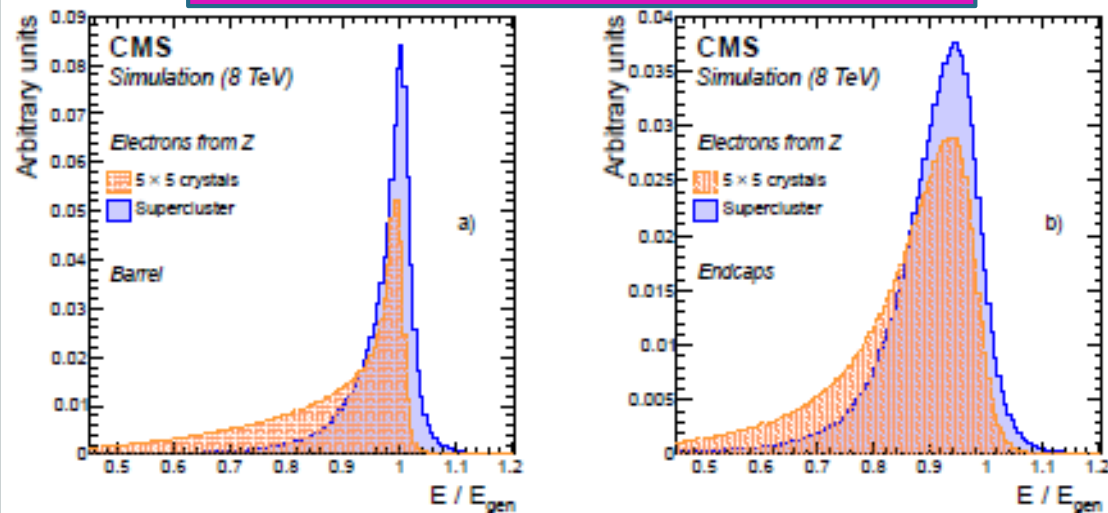
ATLAS: weaker field.

In general radiated photons belong to cluster window

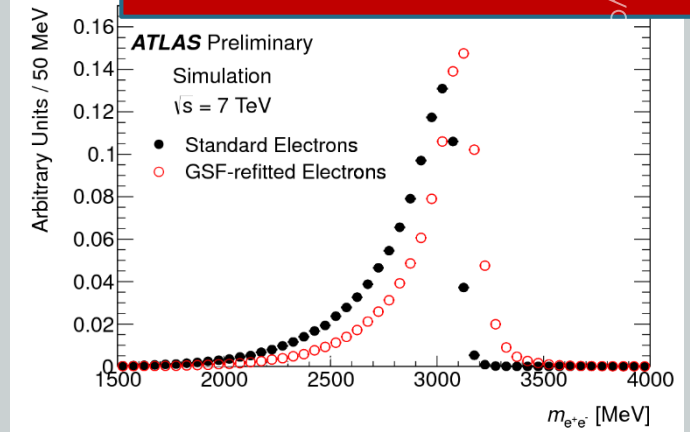
→ From 2012 on, specific track reconstruction to take into account the brems .

→ Especially important for low ET

CMS : Emeas/Egen with 5x5 and with SuperCluster



ATLAS : J/Ψ mass computed from tracks



Photons and their conversions

150

A photon can convert when going through the material in front of the calorimeter

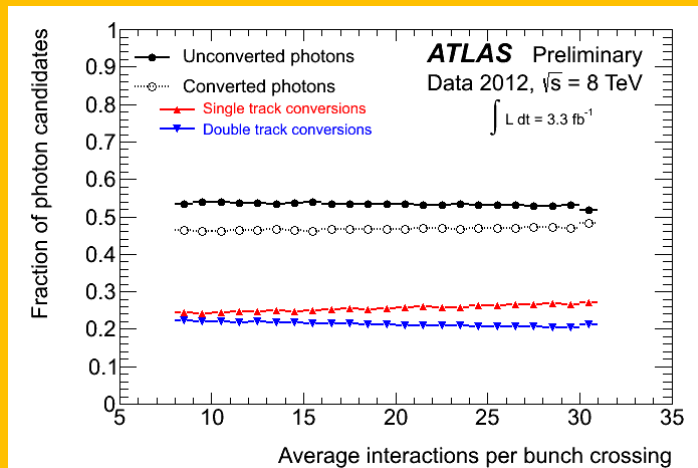
ATLAS : ~47% of photons are converted

Photons and their conversions

151

Invisibles 2015, Lydia Iconomidou-Fayard
16/06/2015

A photon can convert when going through the material in front of the calorimeter
ATLAS : ~47% of photons are converted



Photons and their conversions

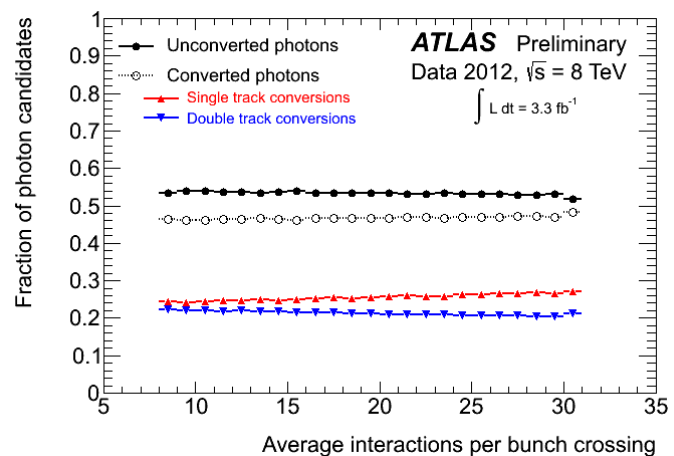
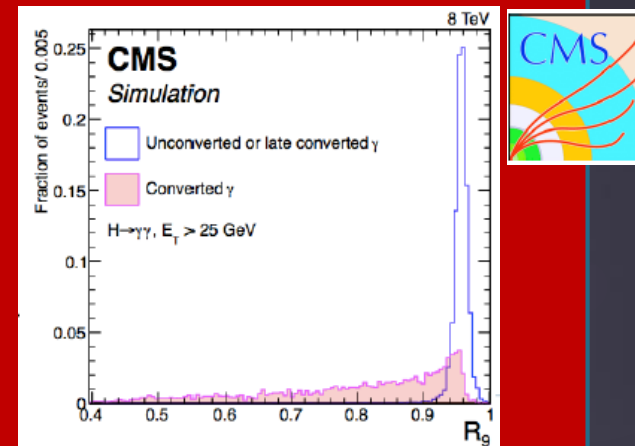
152

Invisibles 2015, Lydia Iconomidou-Fayard
16/06/2015

A photon can convert when going through the material in front of the calorimeter

ATLAS : ~47% of photons are converted

Single or double track conversions
Require careful handling for the reconstruction
to recover good performances

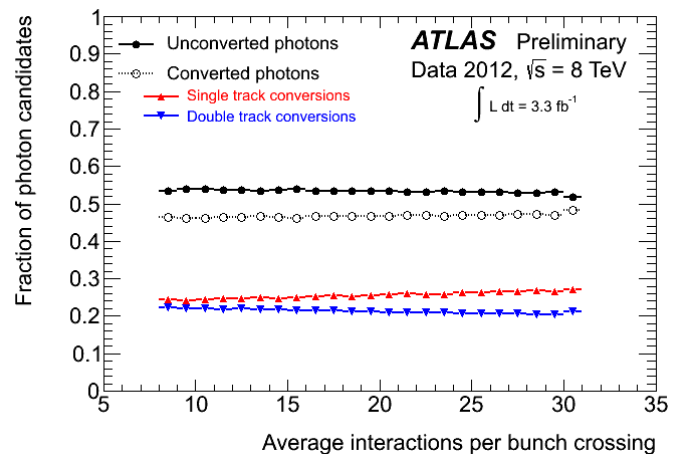
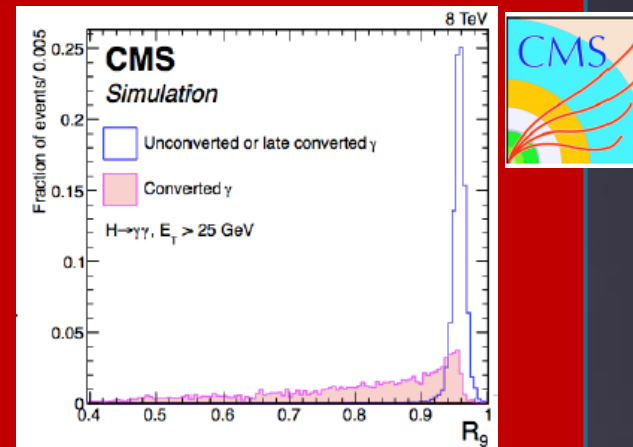


Photons and their conversions

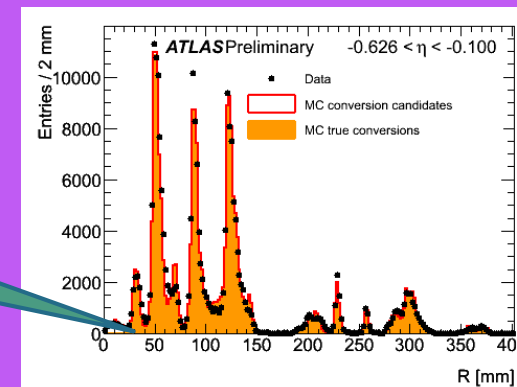
A photon can convert when going through the material in front of the calorimeter

ATLAS : ~47% of photons are converted

Single or double track conversions
Require careful handling for the reconstruction
to recover good performances



Photon conversions: An estimator of material distribution



The necessary steps before using electrons and photons in ATLAS (1)

154

Invisibles 2015, Lydia Iconomidou-Fayard
16/06/2015

The necessary steps before using electrons and photons in ATLAS (1)

→ .. We need Absolute Energy calibration

The necessary steps before using electrons and photons in ATLAS (1)

156

→ .. We need Absolute Energy calibration

Determined with electrons from standard candle resonances

Z- \rightarrow ee, J/ ψ - \rightarrow ee and W- \rightarrow e ν

The necessary steps before using electrons and photons in ATLAS (1)

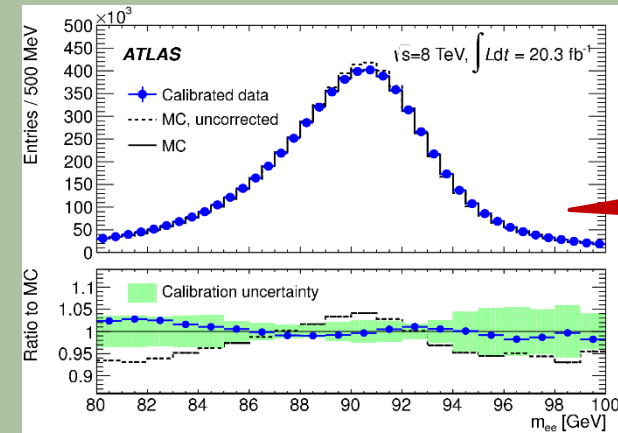
157

→ .. We need Absolute Energy calibration

Determined with electrons from standard candle resonances

Z- \rightarrow ee, J/ ψ - \rightarrow ee and W- \rightarrow ev

→ Z- \rightarrow ee mass compared with the MC in bins of pseudorapidity : **scale of the calorimeter response**



Z- \rightarrow ee

The necessary steps before using electrons and photons in ATLAS (1)

158

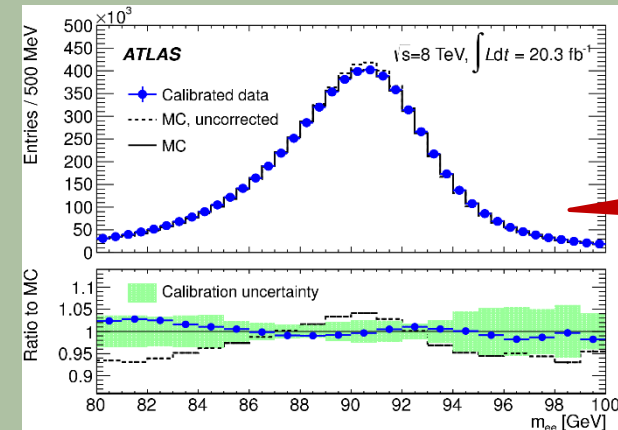
→ .. We need Absolute Energy calibration

Determined with electrons from standard candle resonances

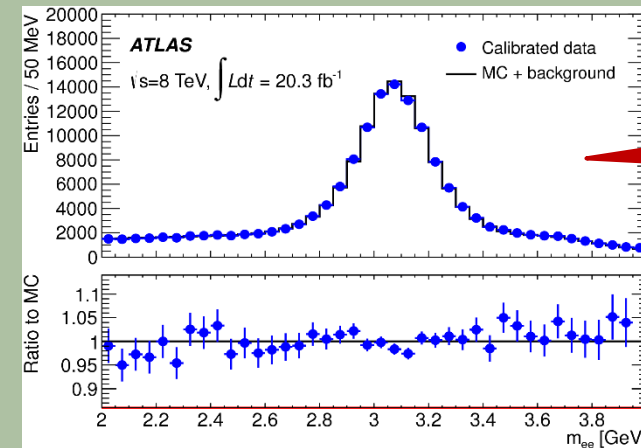
Z->ee, J/ψ->ee and W->eν

→ Z->ee mass compared with the MC in bins of pseudorapidity : **scale of the calorimeter response**

→ J/psi allows to test linearity for electrons with low Et



Z->ee



J/ψ->ee

16/0
Invisibles 2015, L
Tomidou-Fayard

The necessary steps before using electrons and photons in ATLAS (1)

159

→ .. We need Absolute Energy calibration

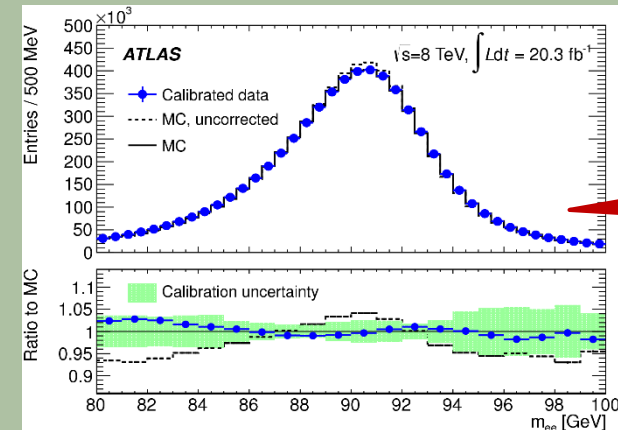
Determined with electrons from standard candle resonances

Z->ee, J/ψ->ee and W->ev

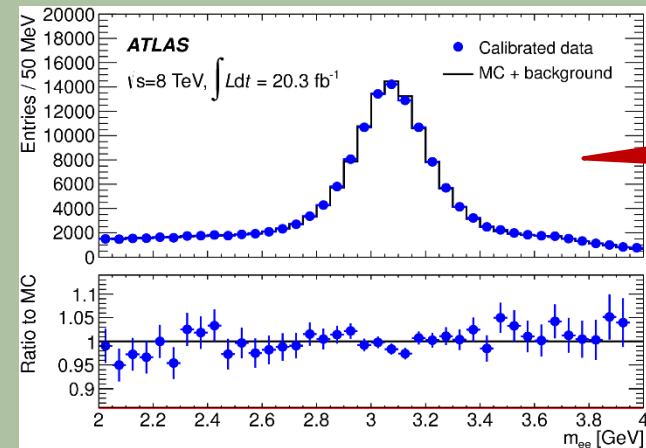
→ Z->ee mass compared with the MC in bins of pseudorapidity : **scale of the calorimeter response**

→ J/psi allows to test **linearity** for electrons with low Et

→ W->ev used for E/p tests and also to check the **uniformity**.



Z->ee



J/ψ->ee

The necessary steps before using electrons in ATLAS

160

Invisibles 2015, Lydia Iconomidou-Fayard
16/06/2015

Need **discrimination against jets** faking electrons

The necessary steps before using electrons in ATLAS

161

Invisibles 2015, Lydia Iconomidou-Fayard
16/06/2015

Need **discrimination against jets** faking electrons

Define identification criteria for few efficiency-VS-rejection pairs

The necessary steps before using electrons in ATLAS

162

Invisibles 2015, Lydia Iconomidou-Fayard
16/06/2015

Need **discrimination against jets** faking electrons

Define identification criteria for few efficiency-VS-rejection pairs

Criteria based on:

- Quality of the track
- Track-Cluster matching
- Longitudinal and lateral shower development in the LiqArgon Calo

The necessary steps before using electrons in ATLAS

163

Invisibles 2015, Lydia Iconomidou-Fayard
16/06/2015

Need **discrimination against jets** faking electrons

Need to know the **efficiency** of electron reconstruction and identification

Define identification criteria for few efficiency-VS-rejection pairs

Criteria based on:

- Quality of the track
- Track-Cluster matching
- Longitudinal and lateral shower development in the LiqArgon Calo

The necessary steps before using electrons in ATLAS

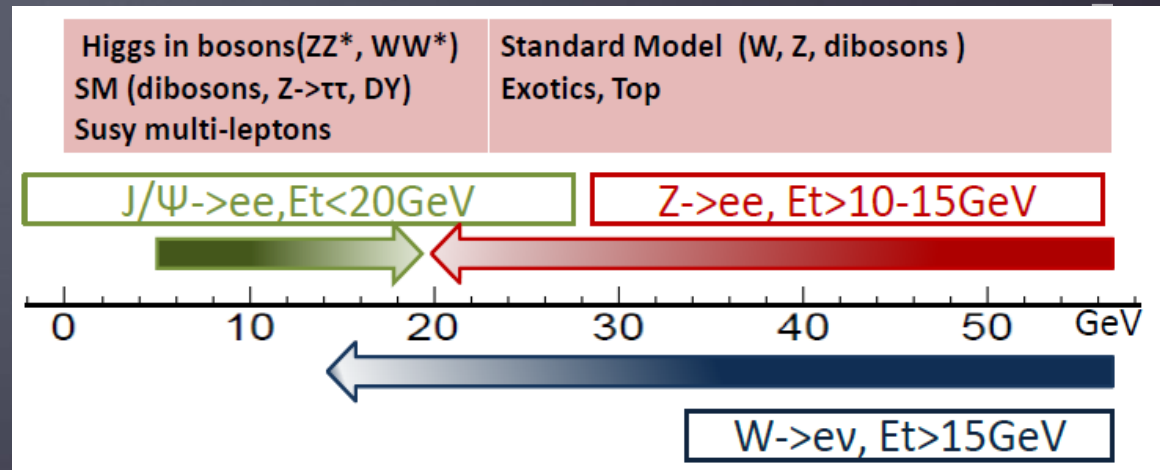
Need **discrimination against jets** faking electrons

Define identification criteria for few efficiency-VS-rejection pairs

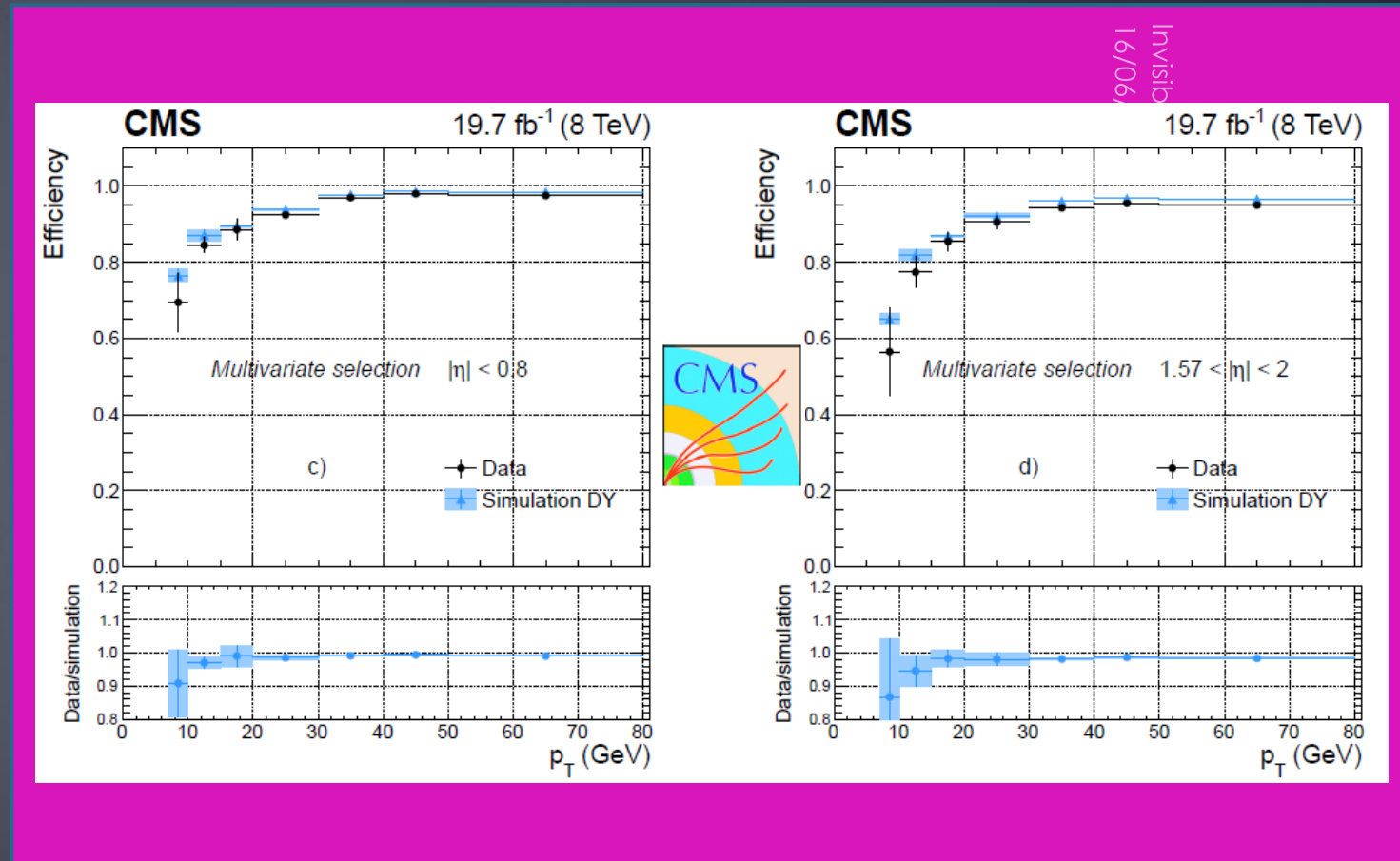
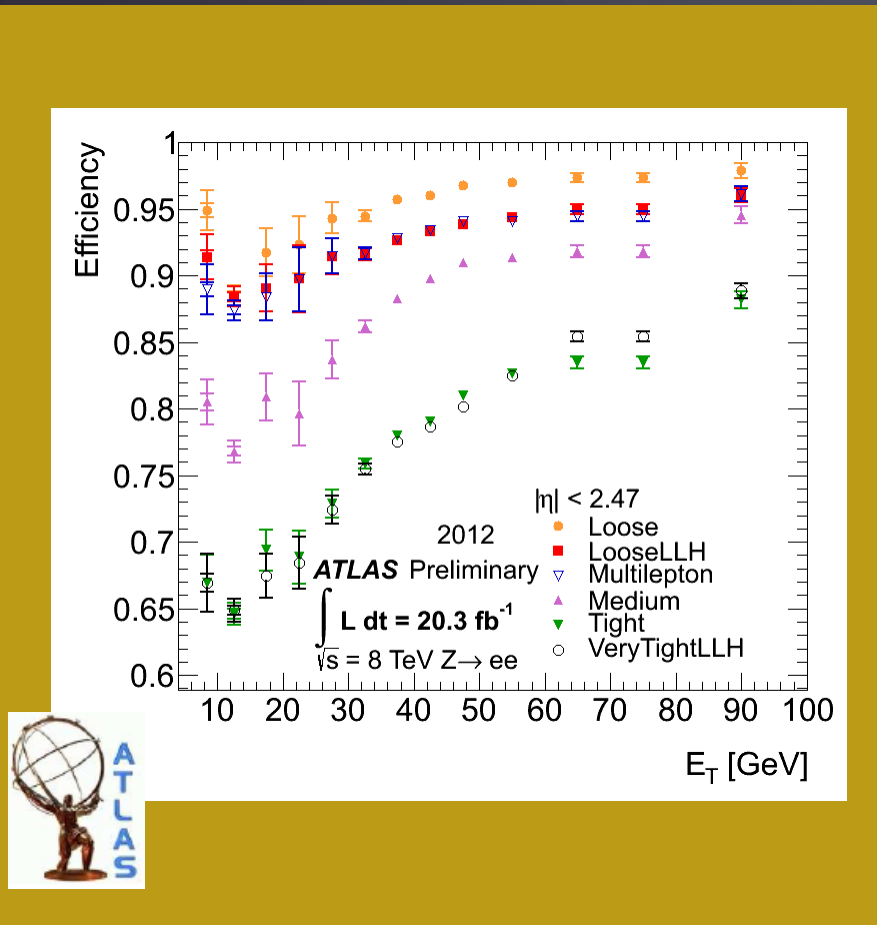
Criteria based on:
→ Quality of the track
→ Track-Cluster matching
→ Longitudinal and lateral shower development in the LiqArgon Calo

Need to know the **efficiency** of electron reconstruction and identification

Apply Tag-and-Probe methods in $Z \rightarrow ee$, $J/\psi \rightarrow ee$ and $W \rightarrow ev$ samples



Examples of efficiencies to electrons



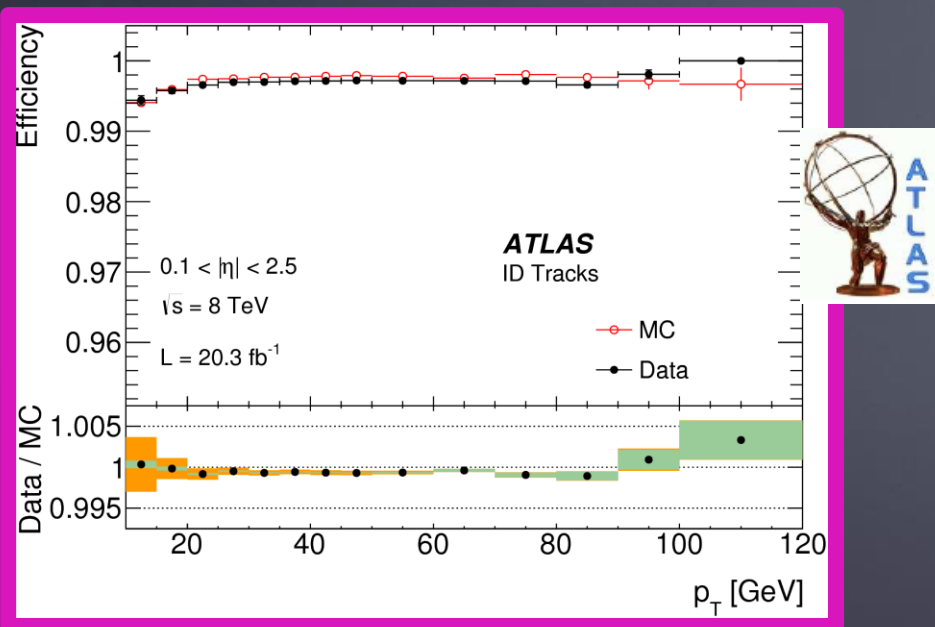
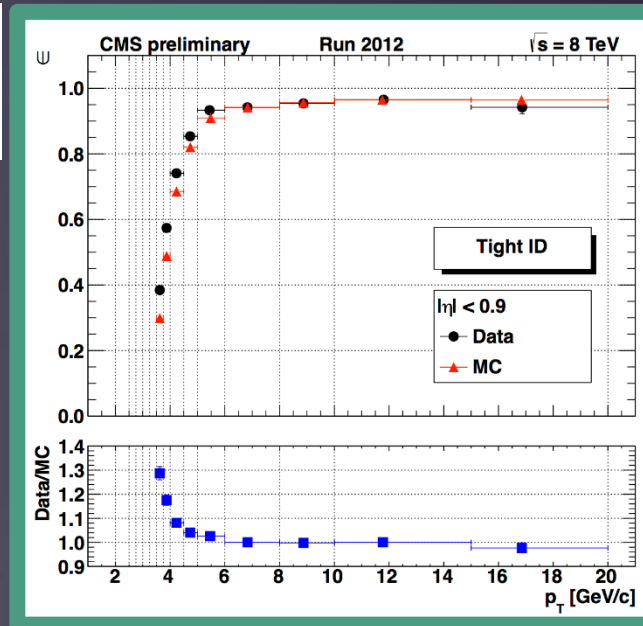
Several Identification menus with increasing rejection

Muons



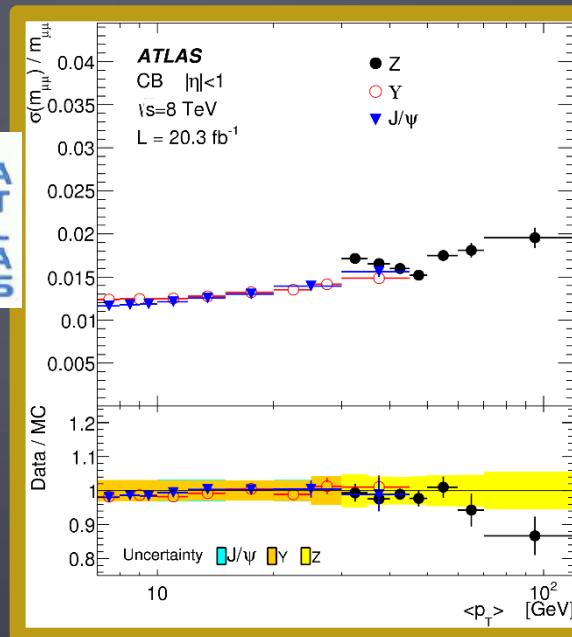
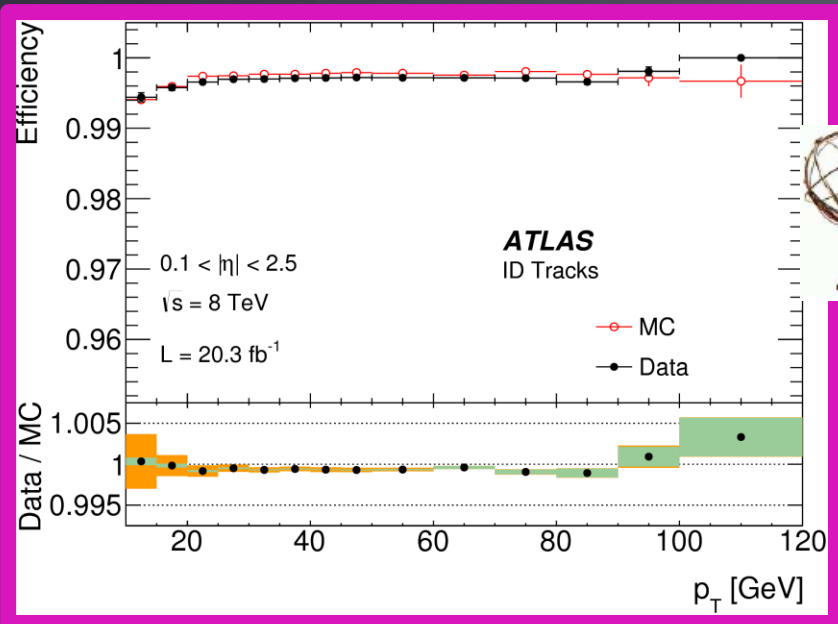
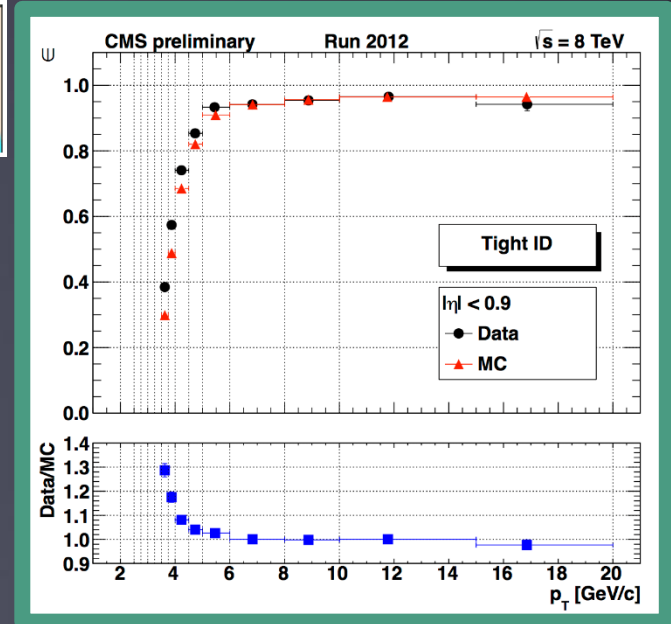
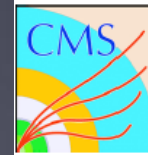
Efficiencies and resolutions

Muons trajectories reconstructed from both muon spectrometer and inner detectors
Very high efficiency(99%)



Efficiencies and resolutions

Muons trajectories reconstructed from both muon spectrometer and inner detectors
Very high efficiency(99%)

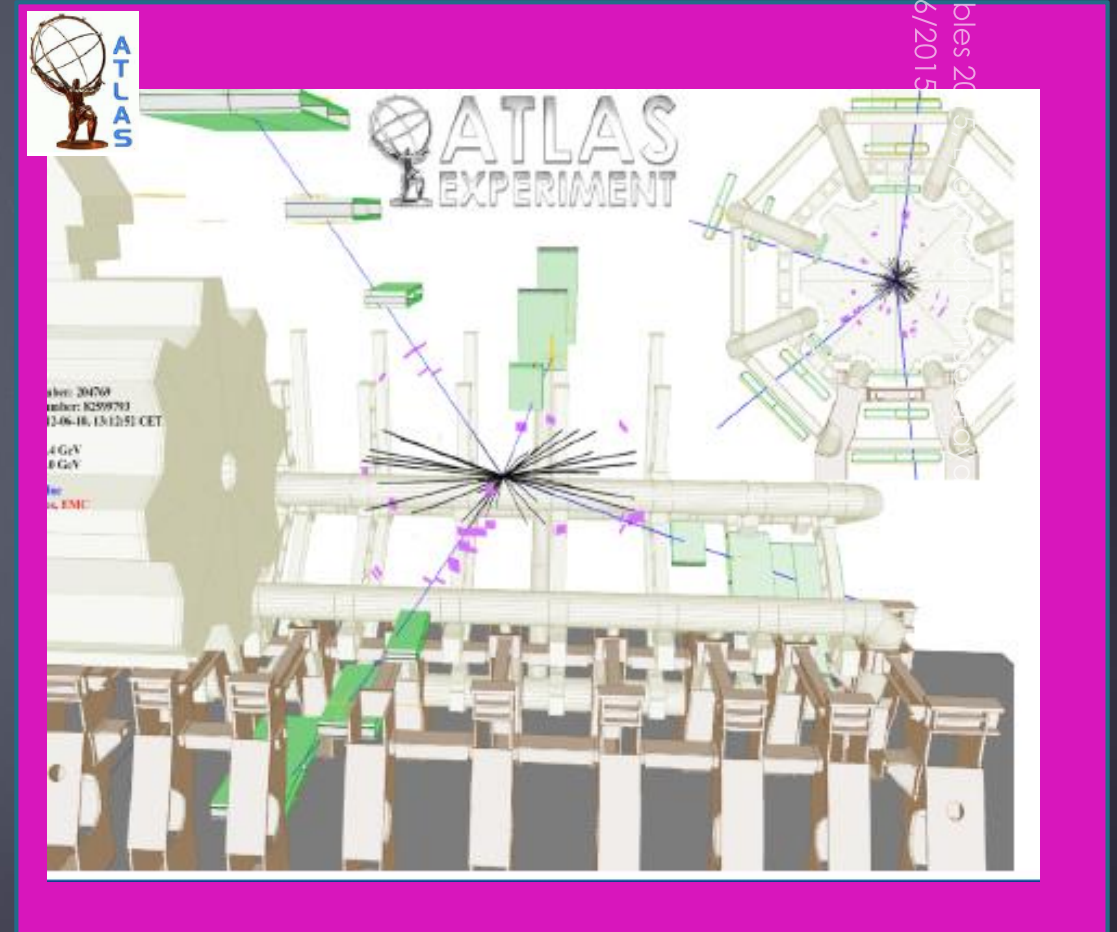
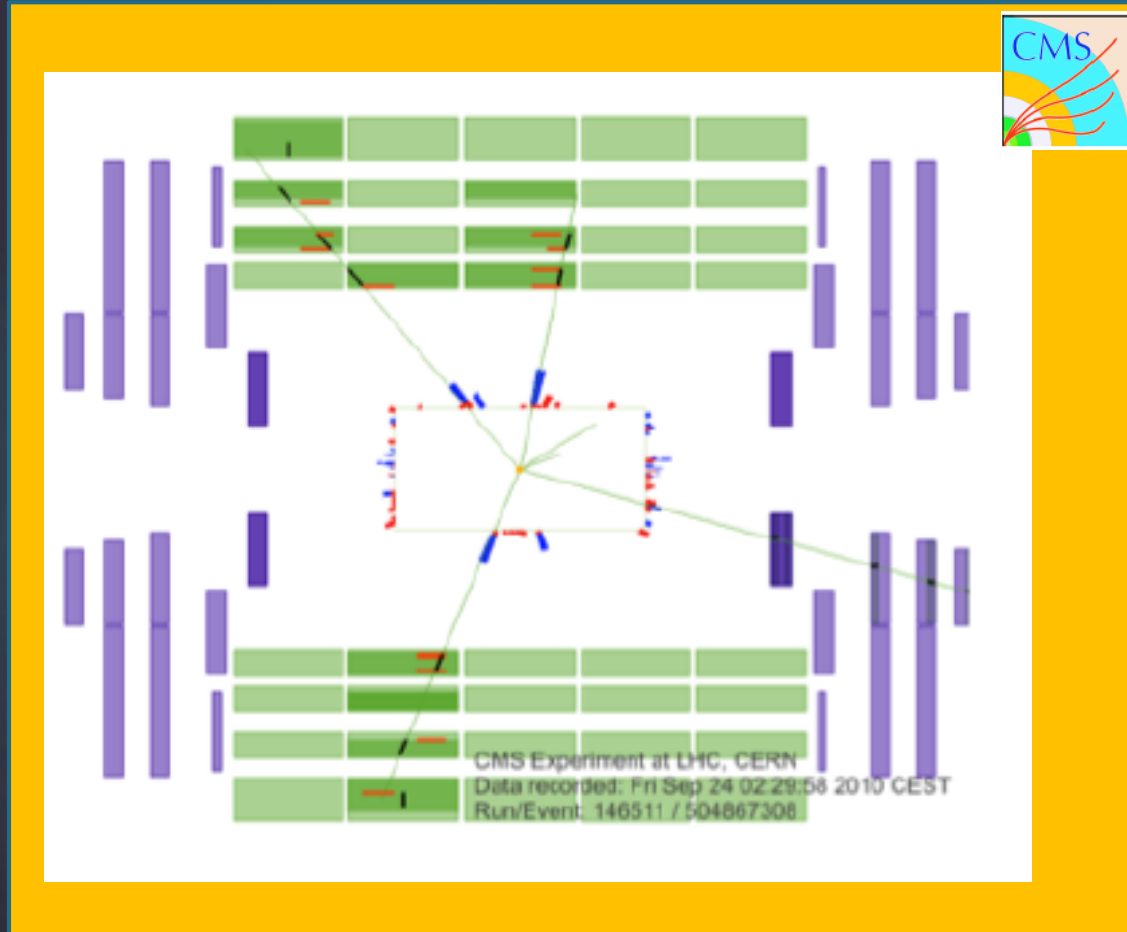


Momentum resolution

ATLAS : $\sim < 2\%$ at 50 GeV
CMS: $\sim 1\%$ at 50 GeV

Higgs \rightarrow $ZZ^* \rightarrow$ 4muon candidates

169



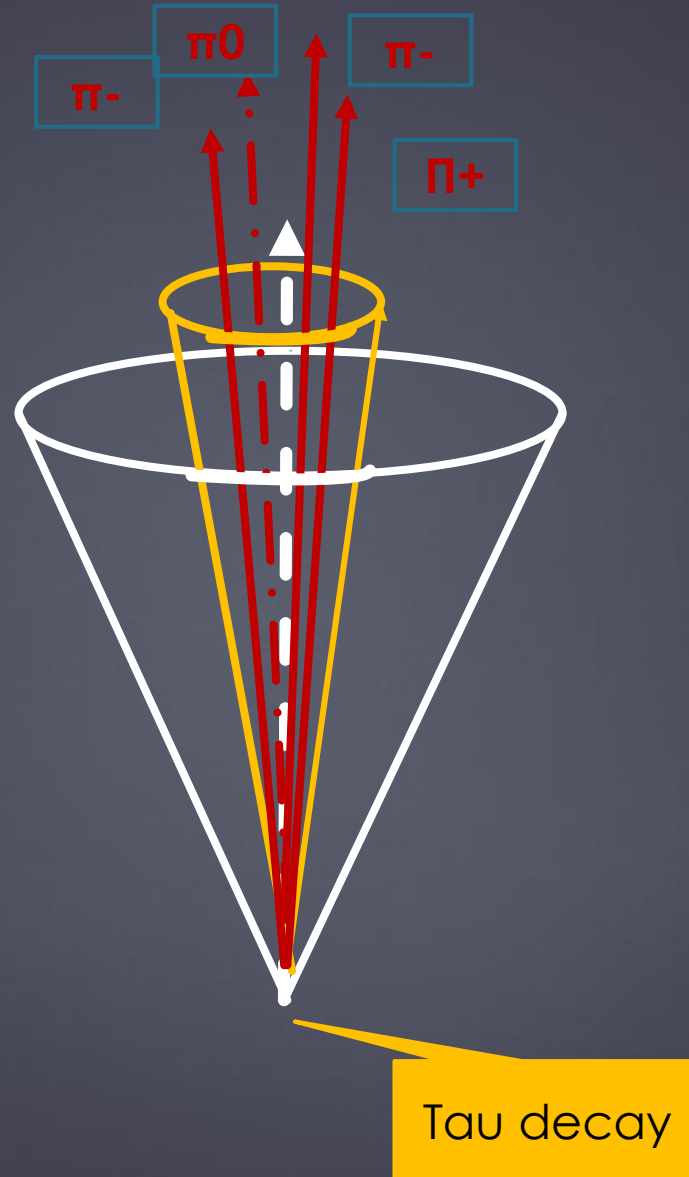
Invisibles 2011
16/06/2015

Taus



Taus

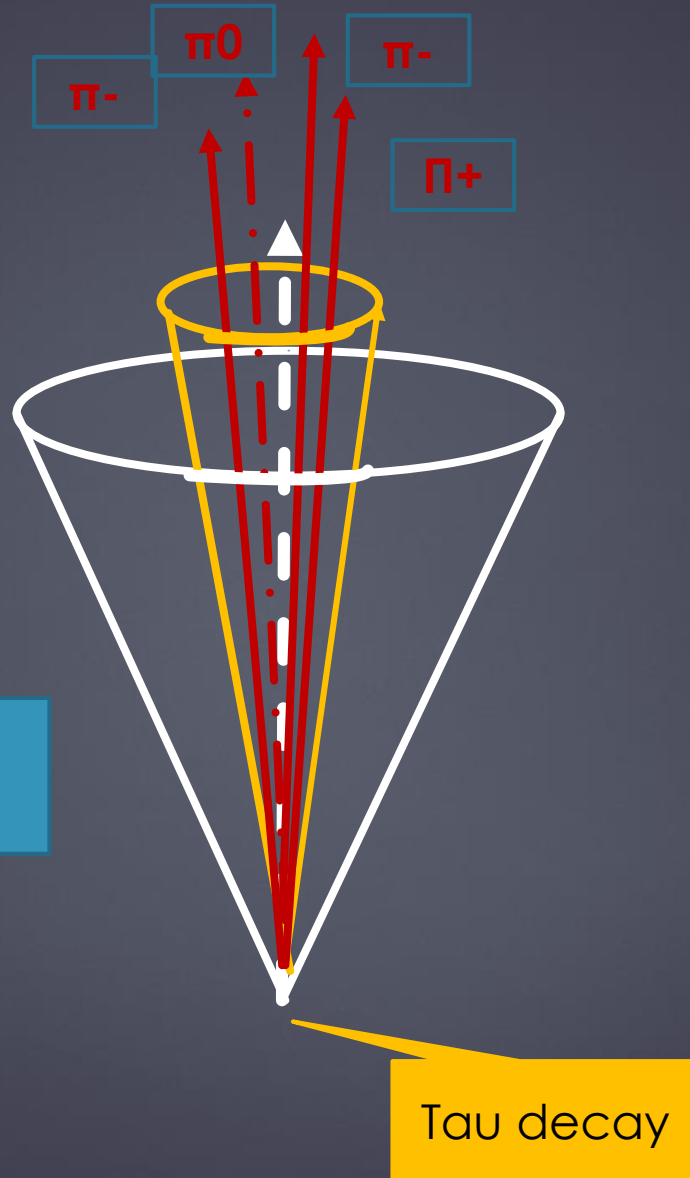
Tau Decays	Leptonic decays	Hadronic decays
	35.2%	
1-prong		46.7%
3-prong		13.9%



Taus

Tau Decays	Leptonic decays	Hadronic decays
	35.2%	
1-prong		46.7%
3-prong		13.9%

Very short flight path (87 μ m)
Only hadronic decays considered

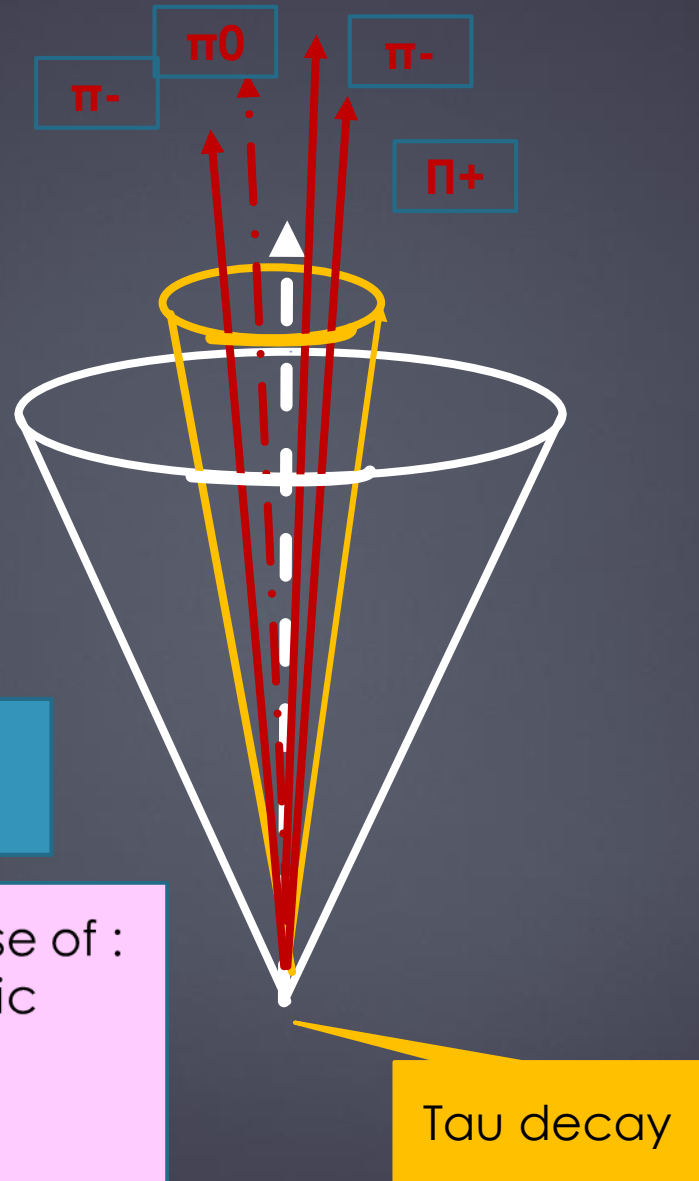


Taus

Tau Decays	Leptonic decays	Hadronic decays
	35.2%	
1-prong		46.7%
3-prong		13.9%

Very short flight path (87 μ m)
Only hadronic decays considered

For reconstructing the taus, make use of :
→ compact core of the tau hadronic decays
→ Small number of charged tracks
→ Isolation of the compact core

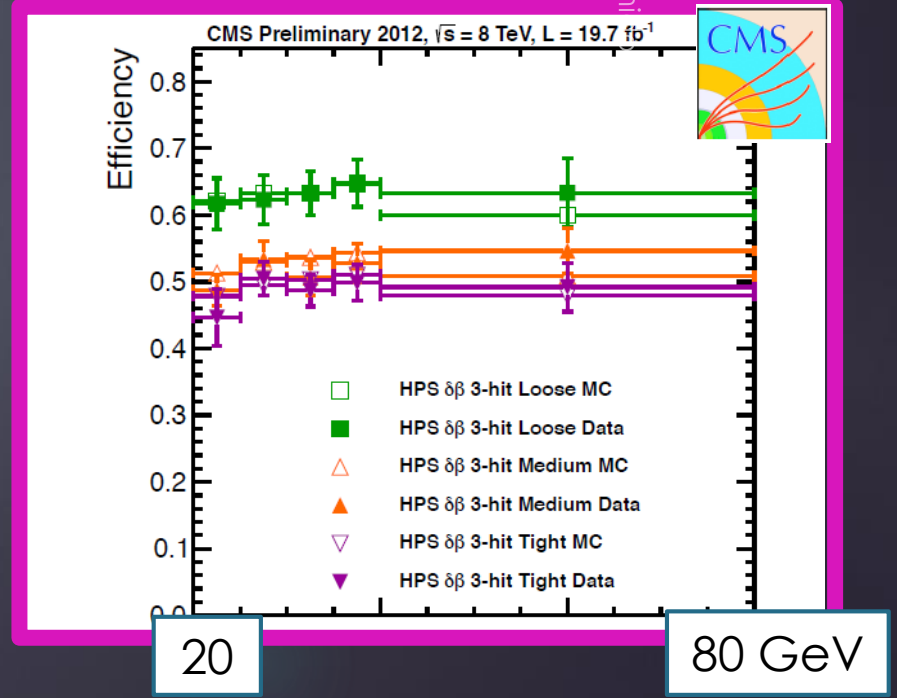
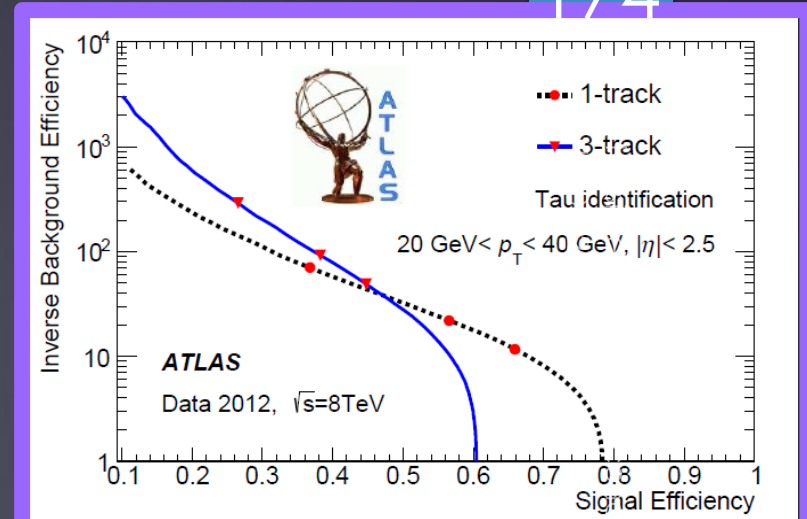
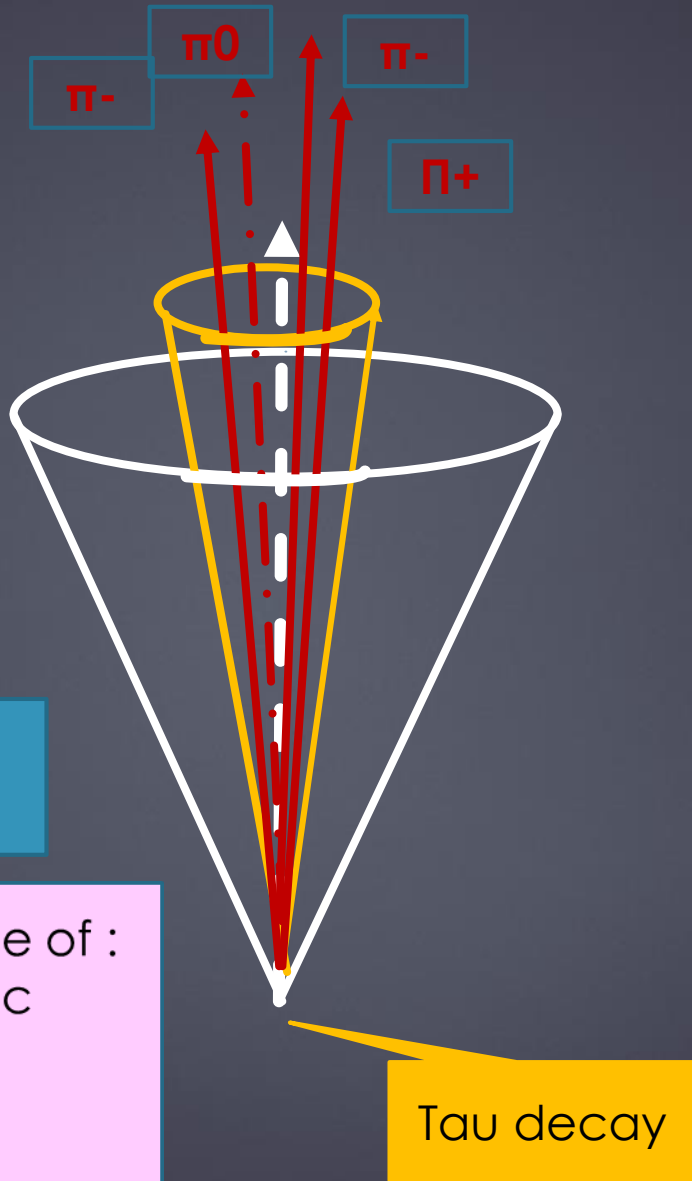


Taus

Tau Decays	Leptonic decays	Hadronic decays
	35.2%	
1-prong		46.7%
3-prong		13.9%

Very short flight path (87 μ m)
Only hadronic decays considered

For reconstructing the taus, make use of :
 → compact core of the tau hadronic decays
 → Small number of charged tracks
 → Isolation of the compact core



Parton Jets



Parton (u,d,b,c,s,g) jets (1)

176

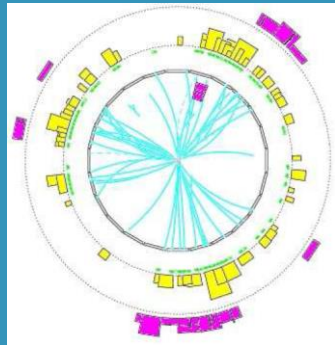
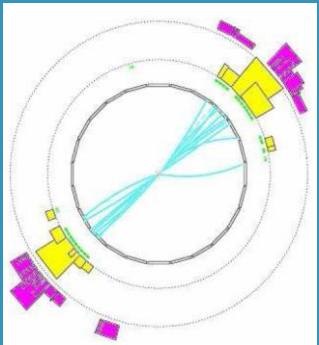
High energy partons undergo hadronization and appear in detectors as a spray of particles

Parton (u,d,b,c,s,g) jets (1)

177

High energy partons undergo hadronization and appear in detectors as a spray of particles

Counting of jets is not always a trivial task

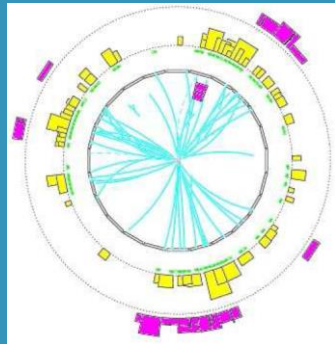
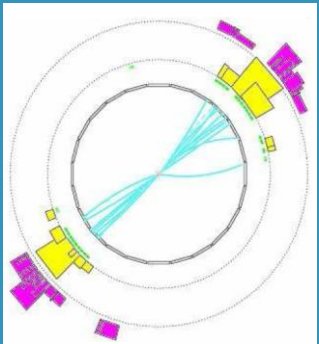


Parton (u,d,b,c,s,g) jets (1)

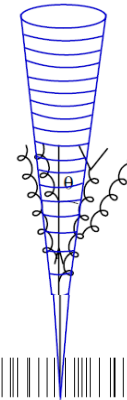
High energy partons undergo hadronization and appear in detectors as a spray of particles

Measure the energy released **within a cone.**

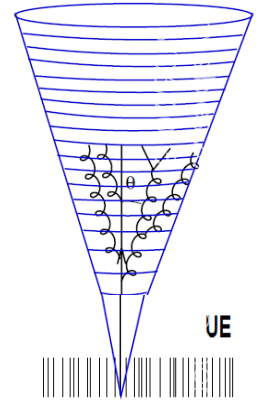
Counting of jets is not always a trivial task



Small jet radius



Large jet radius



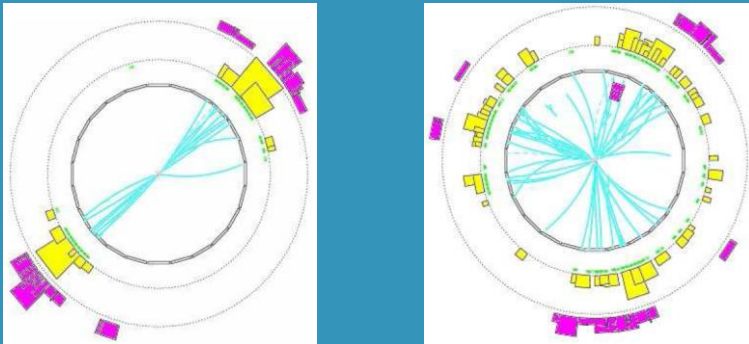
dou-Foyard

Parton (u,d,b,c,s,g) jets (1)

High energy partons undergo hadronization and appear in detectors as a spray of particles

Measure the energy released **within a cone.**

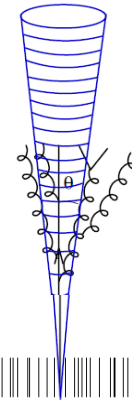
Counting of jets is not always a trivial task



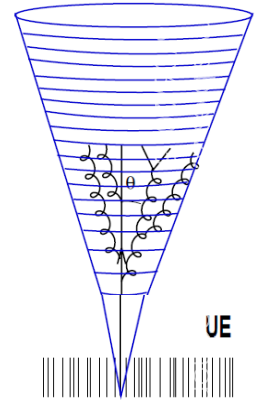
What size of cone?

Large size:
→ better for energy containment
→ Bad for pileup, noise and jet separation

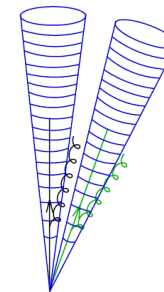
Small jet radius



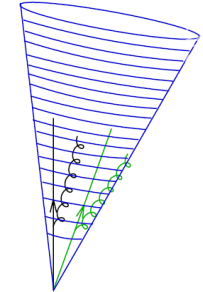
Large jet radius



Small jet radius



Large jet radius



Parton (u,d,b,c,s,g) jets (2)

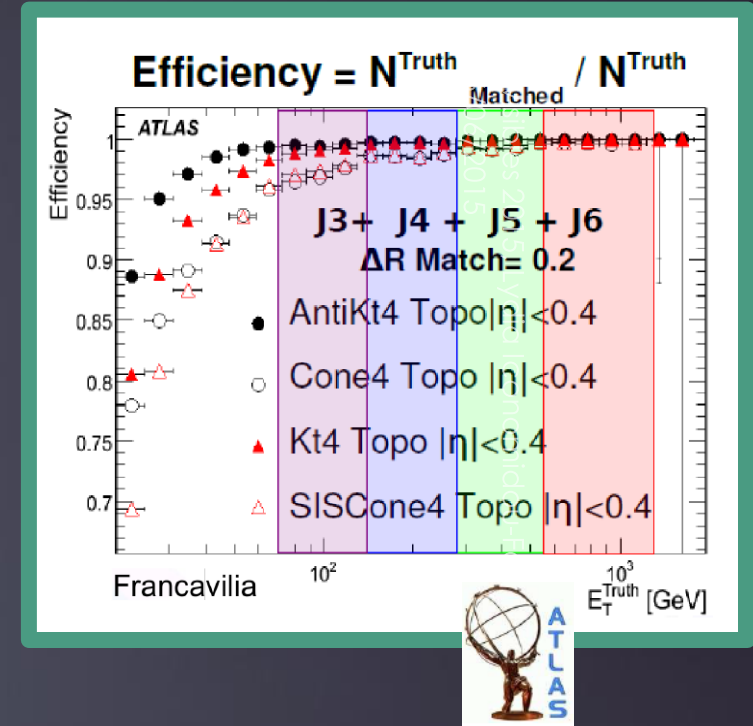
180

The so-called “anti-Kt” algorithm is used in LHC to reconstruct jets.
Uses the P_T of the tracks and the distance between clusters

Parton (u,d,b,c,s,g) jets (2)

The so-called “anti-Kt” algorithm is used in LHC to reconstruct jets.
Uses the P_T of the tracks and the distance between clusters

Various cones used”
 $R=0.4,0.5,0.6,0.8$
Anti-Kt provides **efficiency Improvement** especially at low P_T .



Parton (u,d,b,c,s,g) jets (2)

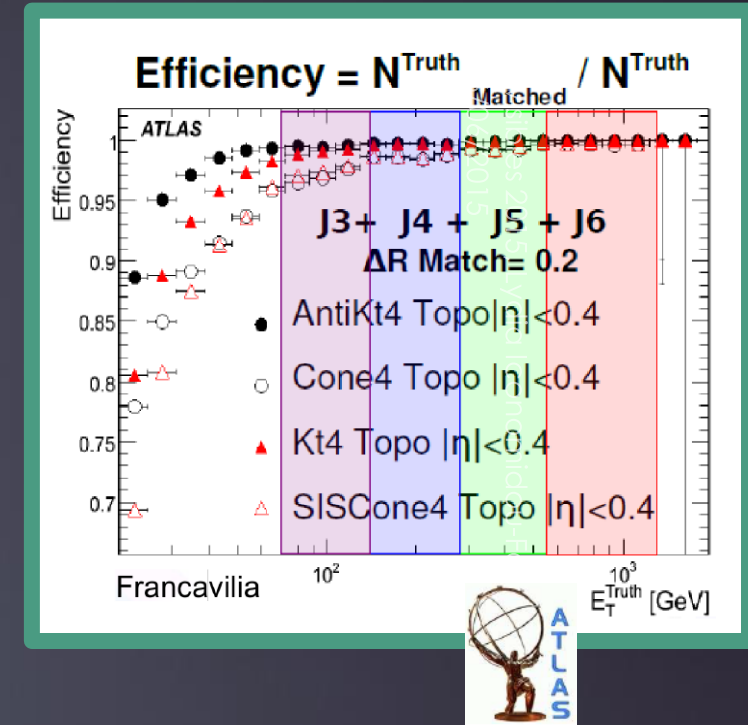
182

The so-called “anti-Kt” algorithm is used in LHC to reconstruct jets.
Uses the P_T of the tracks and the distance between clusters

Various cones used”
 $R=0.4,0.5,0.6,0.8$
Anti-Kt provides **efficiency Improvement** especially at low P_T .

Jet Energy calibration and resolution :
a challenging task

Information from inner detector, and energies from electromagnetic and hadronic calorimeters.
Using γ +jet, Z+jets, dijets events



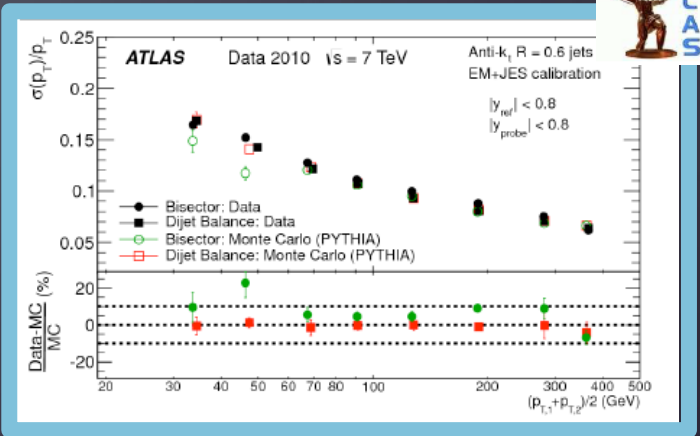
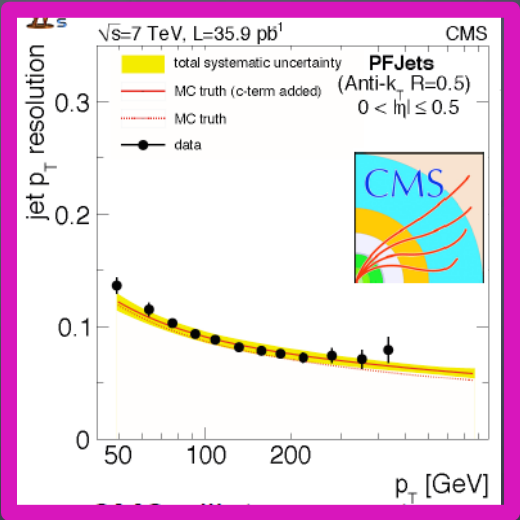
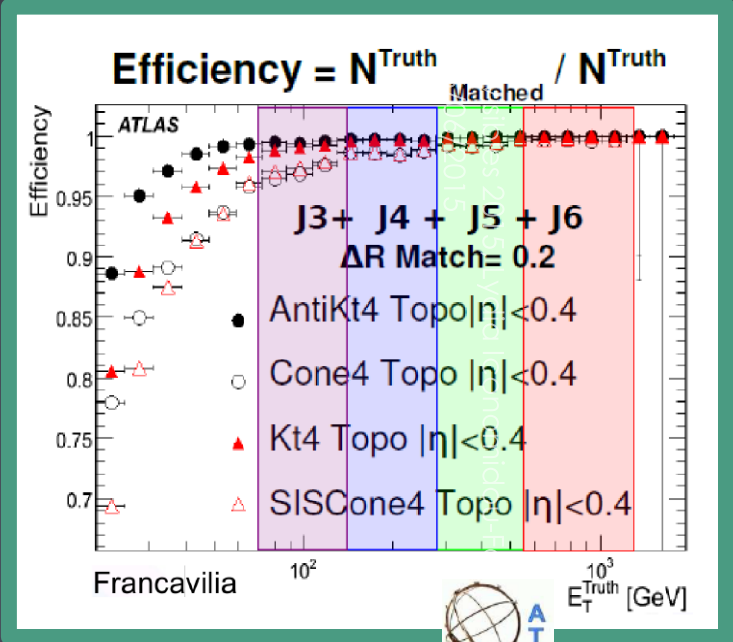
Parton (u,d,b,c,s,g) jets (2)

The so-called “anti-Kt” algorithm is used in LHC to reconstruct jets.
 Uses the P_T of the tracks and the distance between clusters

Various cones used”
 $R=0.4,0.5,0.6,0.8$
 Anti-Kt provides **efficiency Improvement** especially at low P_T .

Jet Energy calibration and resolution :
a challenging task

Information from inner detector, and energies from electromagnetic and hadronic calorimeters.
 Using γ +jet, Z+jets, dijets events



Looking for neutrinos and other ghost particles



Missing transverse energy E_T^{miss}

185

Missing (unseen) energy:
Signature of neutrinos and
of new Physics

Missing transverse energy E_T^{miss}

186

Missing (unseen) energy:
Signature of neutrinos and
of new Physics

It can be measured only in
the transverse detector
plane, the acceptance
following eta being restricted.

Missing transverse energy E_T^{miss}

187

Missing (unseen) energy:
Signature of neutrinos and
of new Physics

It can be measured only in
the transverse detector
plane, the acceptance
following eta being restricted.

$$E_{x(y)}^{\text{miss}} = E_{x(y)}^{\text{miss,HardTerm}} + E_{x(y)}^{\text{miss,SoftTerm}} = - \sum_{\text{hard objects}} p_{x(y)} - \sum_{\text{soft signals}} p_{x(y)}$$

$$E_T^{\text{miss}} = |\mathbf{E}_T^{\text{miss}}| = \sqrt{(E_x^{\text{miss}})^2 + (E_y^{\text{miss}})^2}$$

In ATLAS: E_T^{miss} from Calorimeters
In CMS : From Particle-Flow technics

Missing transverse energy E_T^{miss}

188

Missing (unseen) energy:
Signature of neutrinos and
of new Physics

It can be measured only in
the transverse detector
plane, the acceptance
following eta being restricted.

$$E_{x(y)}^{\text{miss}} = E_{x(y)}^{\text{miss,HardTerm}} + E_{x(y)}^{\text{miss,SoftTerm}} = - \sum_{\text{hard objects}} p_{x(y)} - \sum_{\text{soft signals}} p_{x(y)}$$

$$E_T^{\text{miss}} = |\mathbf{E}_T^{\text{miss}}| = \sqrt{(E_x^{\text{miss}})^2 + (E_y^{\text{miss}})^2}$$

In ATLAS: E_T^{miss} from Calorimeters
In CMS : From Particle-Flow technics

Warning: contributions to E_T^{miss} from lack of
transverse hermiticity, from detection
inefficiencies, noise, etc

Missing transverse energy E_T^{miss}

Missing (unseen) energy:
Signature of neutrinos and
of new Physics

It can be measured only in
the transverse detector
plane, the acceptance
following eta being restricted.

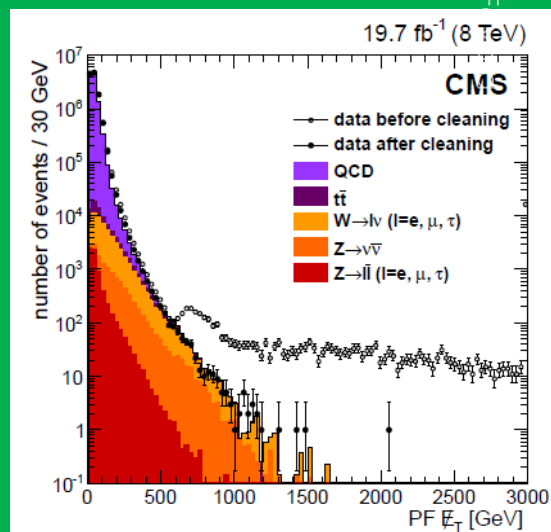
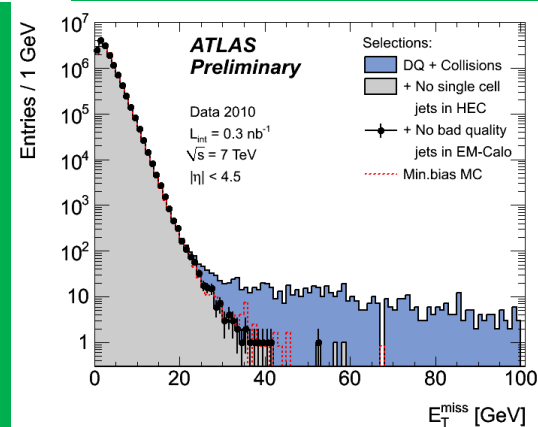
$$E_{x(y)}^{\text{miss}} = E_{x(y)}^{\text{miss,HardTerm}} + E_{x(y)}^{\text{miss,SoftTerm}} = - \sum_{\text{hard objects}} p_{x(y)} - \sum_{\text{soft signals}} p_{x(y)}$$

$$E_T^{\text{miss}} = |\mathbf{E}_T^{\text{miss}}| = \sqrt{(E_x^{\text{miss}})^2 + (E_y^{\text{miss}})^2}$$

In ATLAS: E_T^{miss} from Calorimeters
In CMS : From Particle-Flow technics

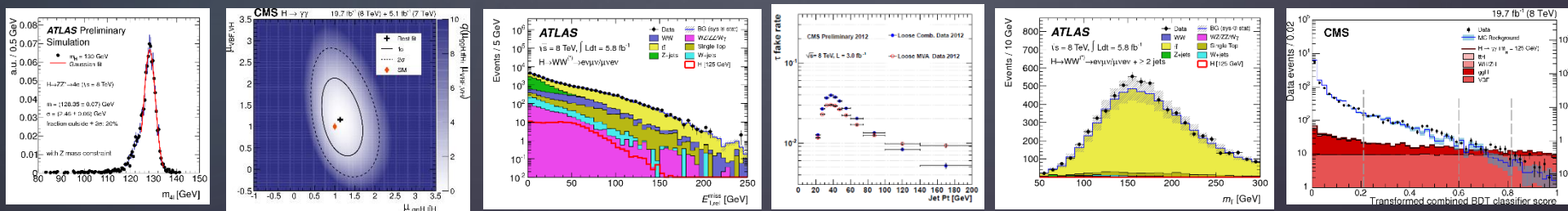
Warning: contributions to E_T^{miss} from lack of
transverse hermiticity, from detection
inefficiencies, noise, etc

Require perfect
“cleaning” of the events

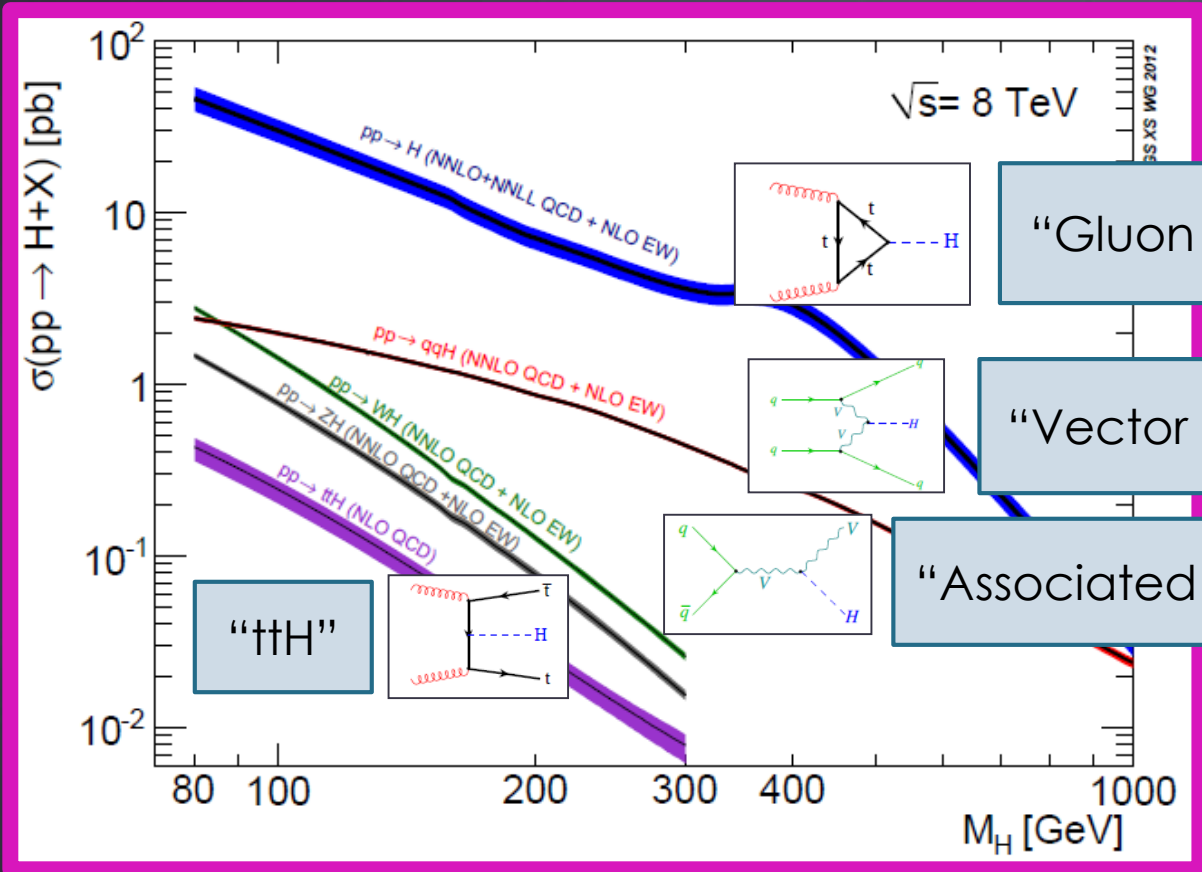


Invisibles 2015, Lydia Iconomidou-F

The analyses to identify the Higgs decays and properties



The production channels of the Scalar Boson



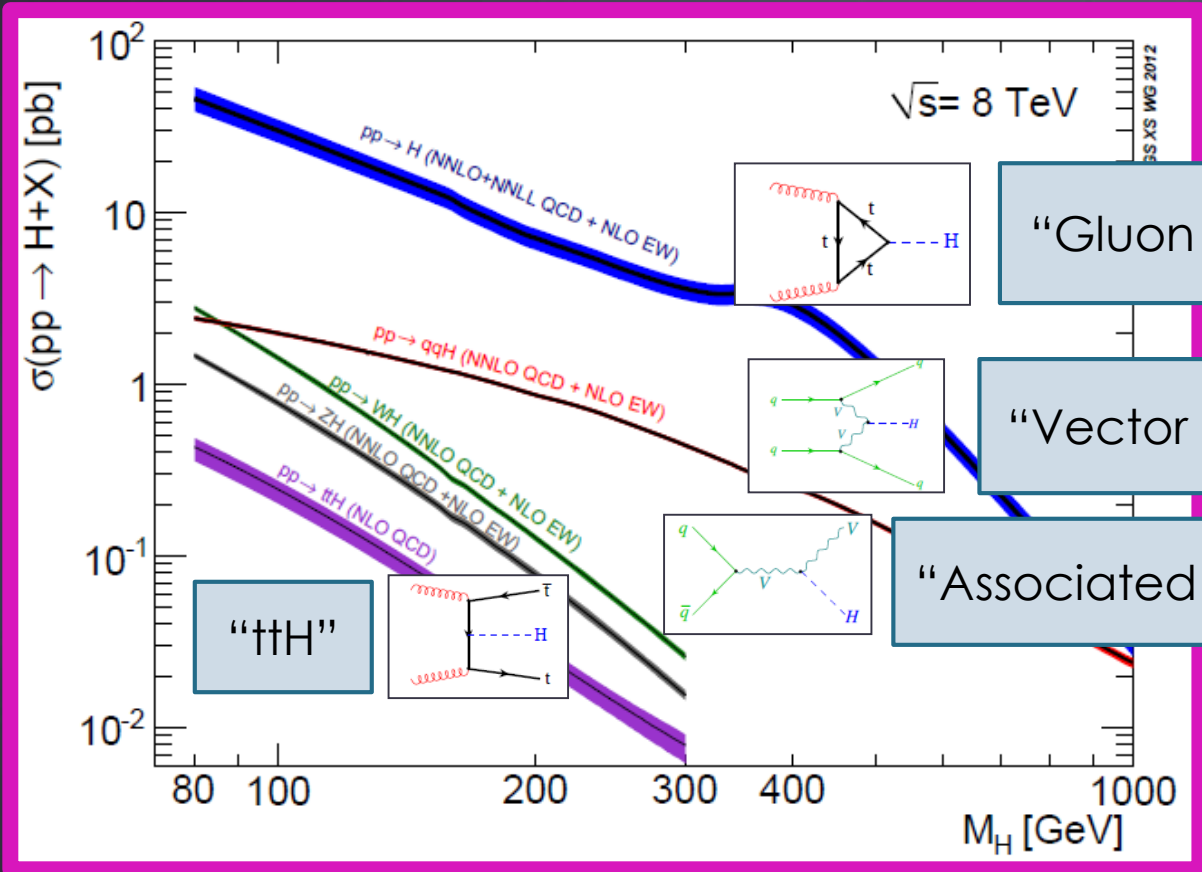
"Gluon fusion"

"Vector boson fusion"

"Associated production"

For $M_H = 125 \text{ GeV}$	
8 TeV	13 TeV
VBF/ggF $\sim 1/12$	ggF $\sim \times 2.3$
VH/ggF $\sim 1/17$	VBF $\sim \times 2.4$
ttH/ggF $\sim 1/150$	VH $\sim \times 2.0$
	ttH $\sim \times 3.9$

The production channels of the Scalar Boson

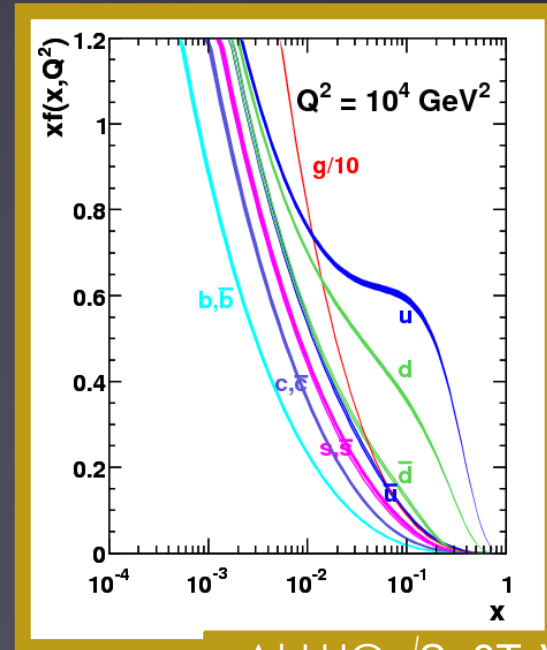


“Gluon fusion”

“Vector boson fusion”

“Associated production”

“ttH”



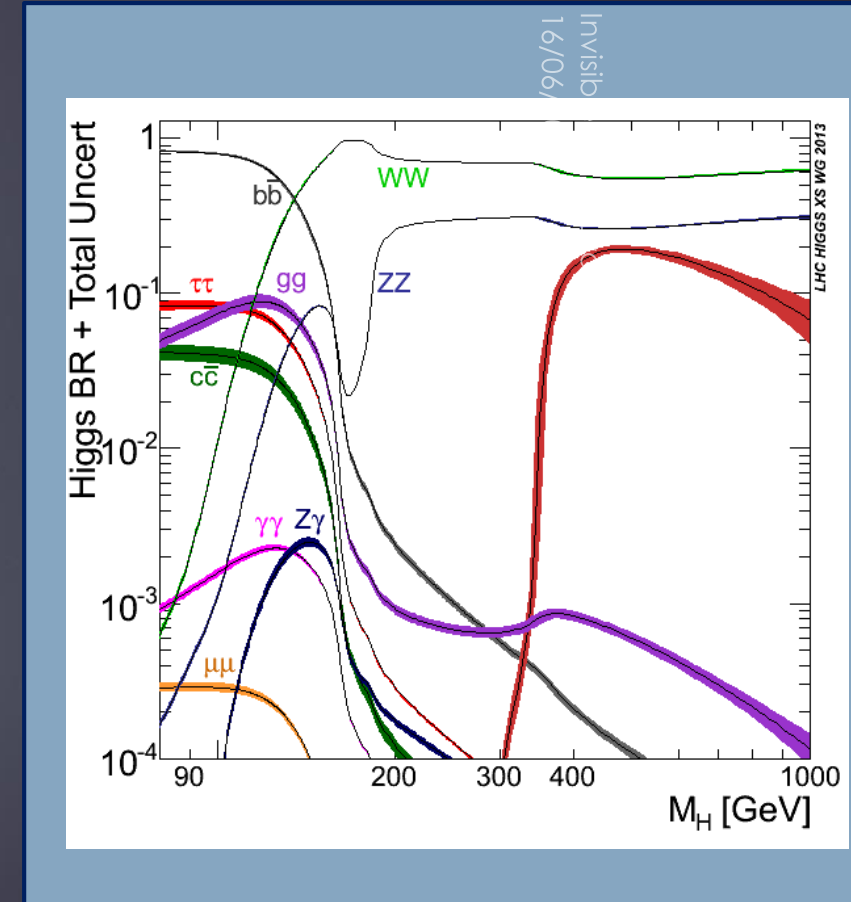
At LHC $\sqrt{s} \sim 8 \text{ TeV}$
 For $M \sim 100 \text{ GeV}$
 $x \approx M/\sqrt{s} = 0.01$

For $M_H = 125 \text{ GeV}$

8 TeV	13 TeV
VBF/ggF $\sim 1/12$	ggF $\sim \times 2.3$
VH/ggF $\sim 1/17$	VBF $\sim \times 2.4$
ttH/ggF $\sim 1/150$	VH $\sim \times 2.0$
	ttH $\sim \times 3.9$

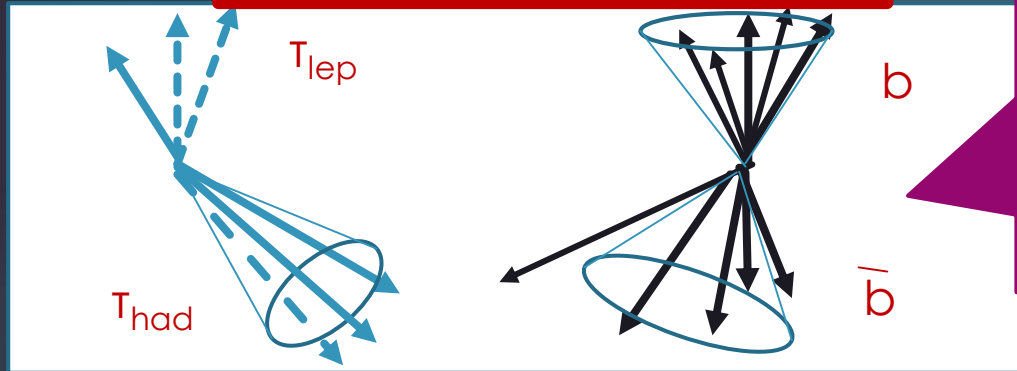
The decay channels of the Scalar Boson

193

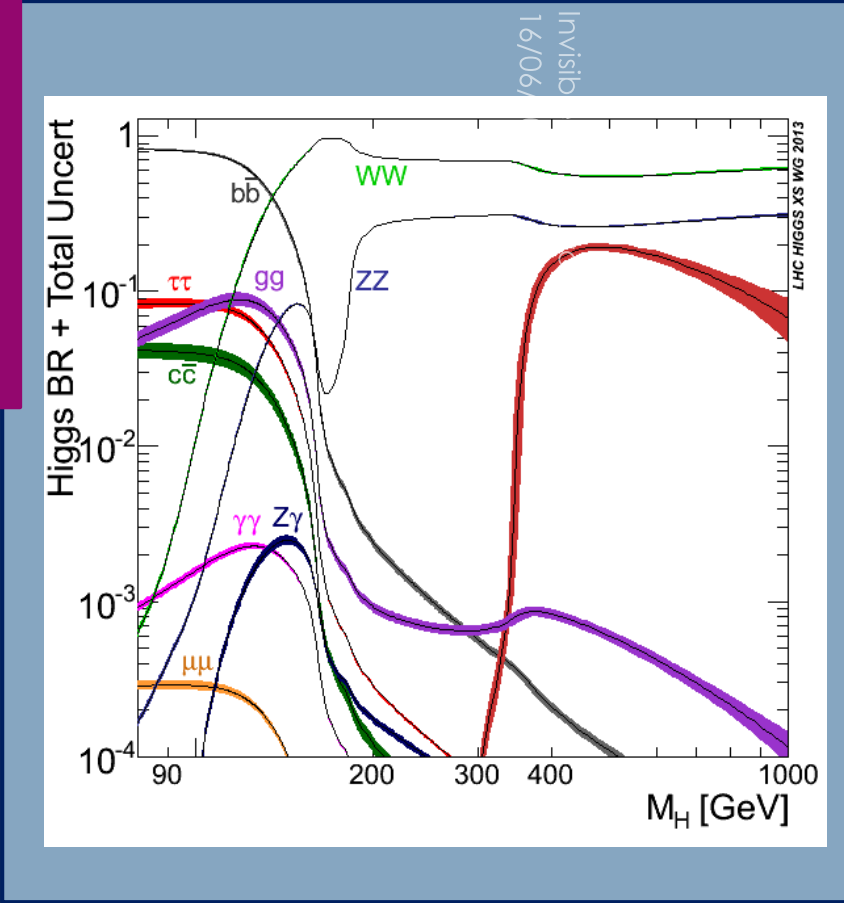


The decay channels of the Scalar Boson

The "abundant" channels

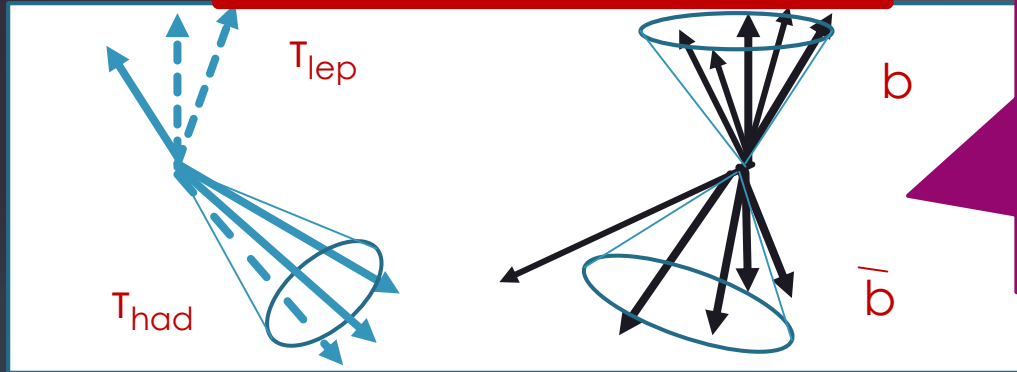


H->bb, H->τ τ :
 The highest couplings to the Scalar Boson at ~125GeV
 BUT signed by "jets"
Difficult to disentangle from the overflowing QCD background



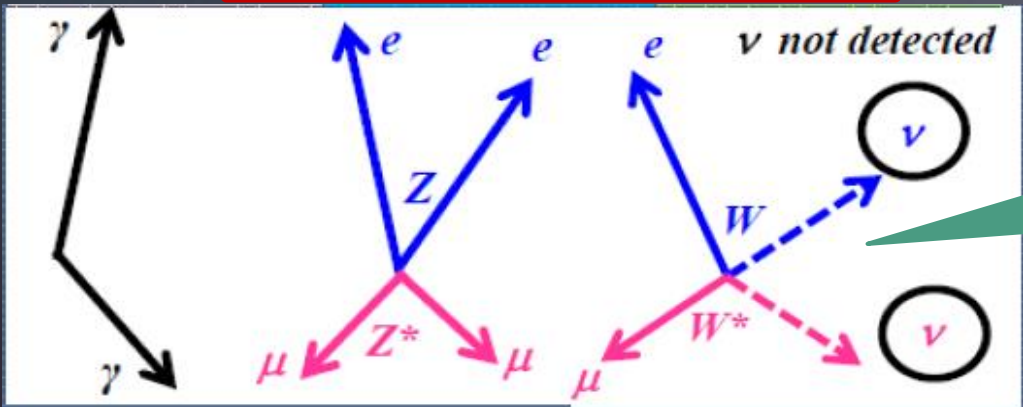
The decay channels of the Scalar Boson

The "abundant" channels

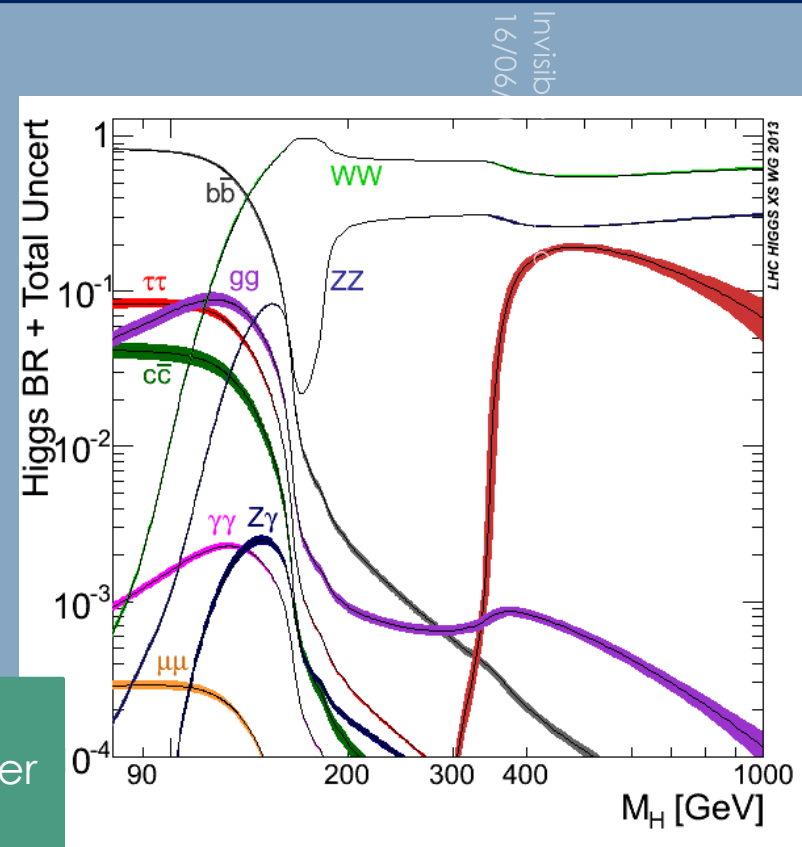


H->bb, H->τ τ :
 The highest couplings to the Scalar Boson at ~125GeV
 BUT signed by "jets"
Difficult to disentangle from the overflowing QCD background

The "easier" channels

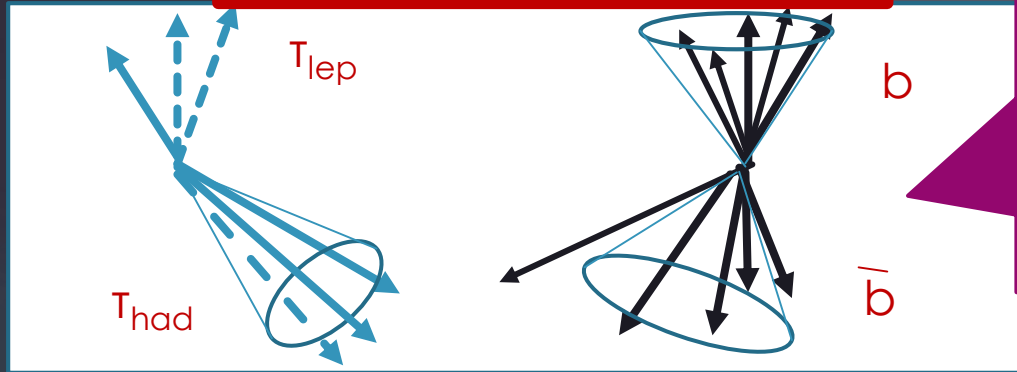


H->γγ, H->ZZ, H->WW
 Leptonic final states, lower rates BUT
"Easy" to distinguish



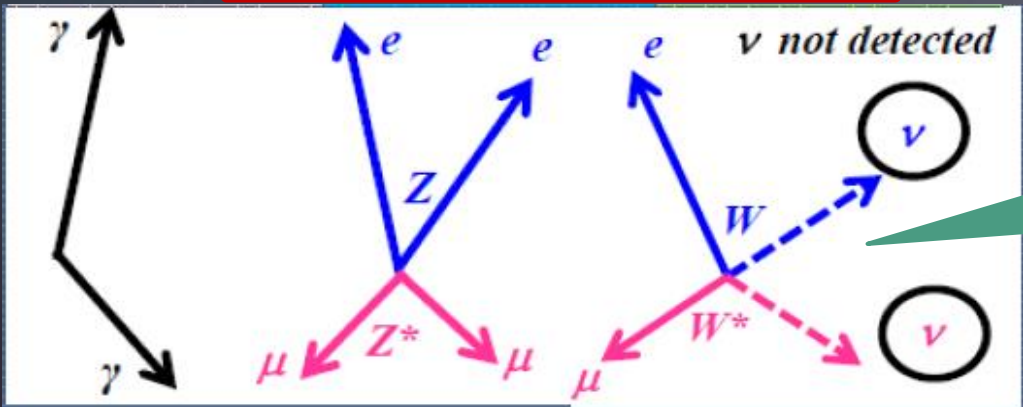
The decay channels of the Scalar Boson

The "abundant" channels



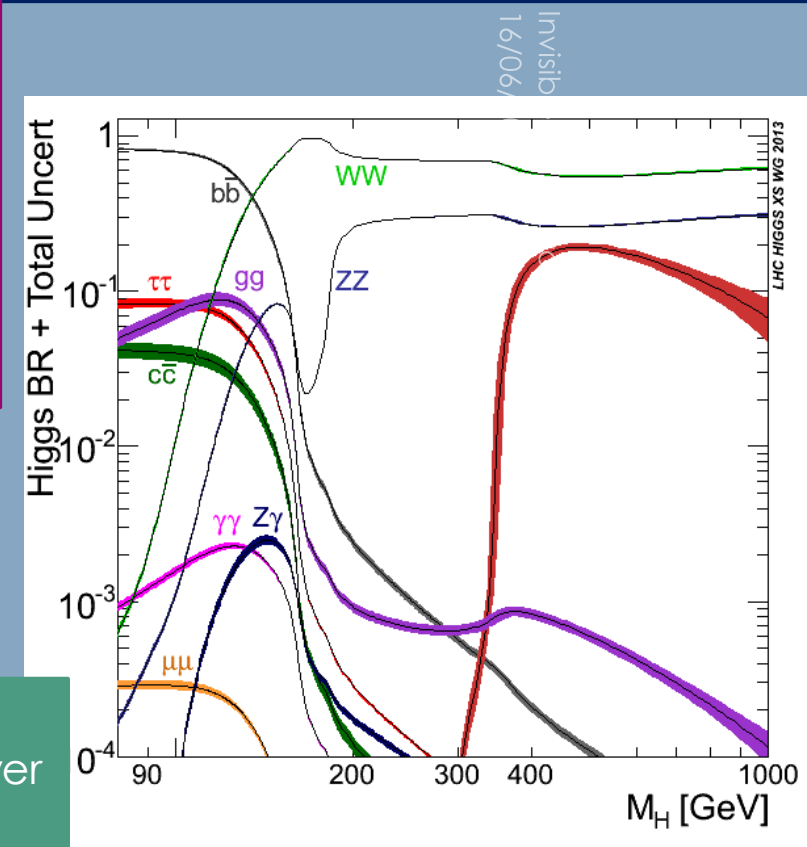
H->bb, H->τ τ :
 The highest couplings to the Scalar Boson at ~125GeV
 BUT signed by "jets"
Difficult to disentangle from the overflowing QCD background

The "easier" channels



H->γγ, H->ZZ, H->WW
 Leptonic final states, lower rates BUT
"Easy" to distinguish

Allow precise mass determination if final state is fully contained



Discussed points

197

In the following we give the description of the main analysis tips for:

- ▶ The main decay channels (observation or-and evidence)
- ▶ The Scalar boson mass measurement
- ▶ The Scalar boson couplings
- ▶ The Scalar boson properties

H- \rightarrow $\gamma\gamma$: the historical channel

198

- Clean signature: 2 isolated high P_T photons.
- $P_{T1} > 40\text{GeV}$ $P_{T2} > 30\text{GeV}$
- **Look for a bump in the diphoton mass spectrum**
- Small S/B ~ 0.03

H \rightarrow $\gamma\gamma$: the historical channel

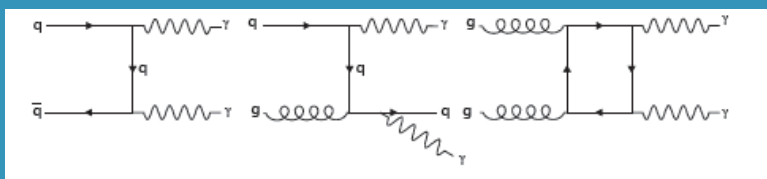
→ Clean signature: 2 isolated high P_T photons.

→ $P_{T1} > 40\text{GeV}$ $P_{T2} > 30\text{GeV}$

→ **Look for a bump in the diphoton mass spectrum**

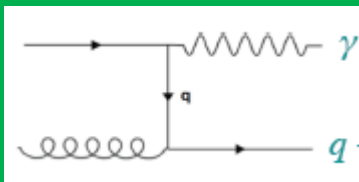
→ Small S/B ~ 0.03

→ Irreducible background:



Non resonant in $M_{\gamma\gamma}$

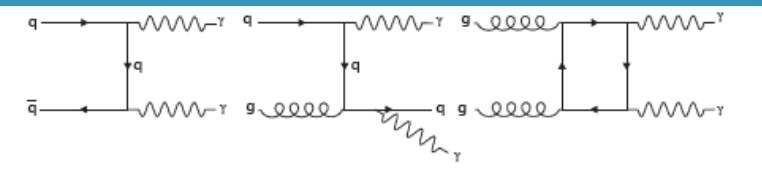
→ Reducible:
 $\gamma + \text{Jet} (\pi^0)$,
 $\text{Jet}(\pi^0) + \text{Jet}(\pi^0)$



H \rightarrow $\gamma\gamma$: the historical channel

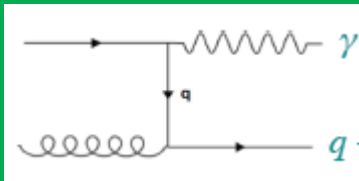
- \rightarrow Clean signature: 2 isolated high P_T photons.
- $\rightarrow P_{T1} > 40\text{GeV}$ $P_{T2} > 30\text{GeV}$
- \rightarrow Look for a bump in the diphoton mass spectrum
- \rightarrow Small S/B ~ 0.03

\rightarrow Irreducible background:



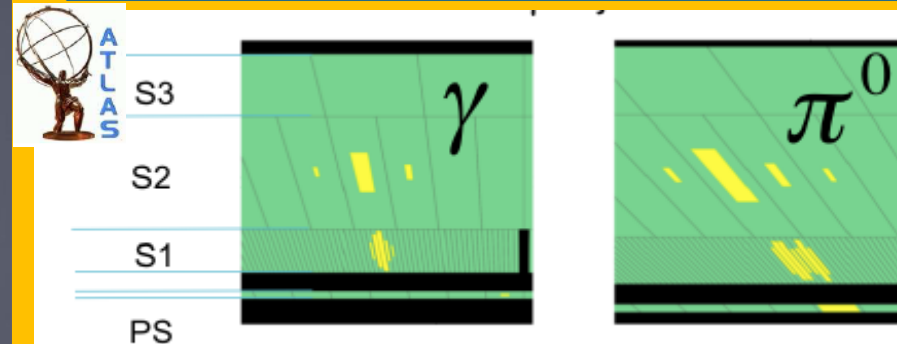
Non resonant in $M_{\gamma\gamma}$

\rightarrow Reducible:
 γ +Jet (π^0),
 Jet(π^0)+Jet(π^0)



ATLAS

Make use of the fine granularity of the first calorimetric layer.

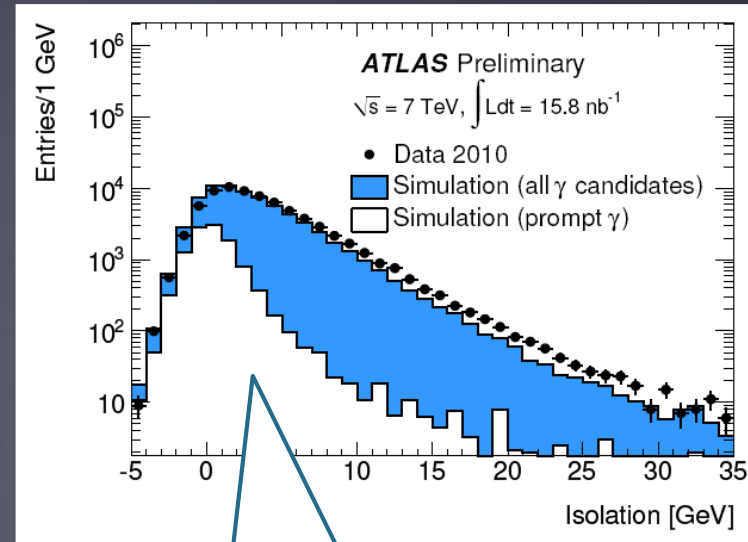


Opening angle of the two photons of a π^0 of $P_T=40\text{GeV}$ is ≥ 0.007 , to be compared with strip size= 0.003

H- $\rightarrow\gamma\gamma$: Measure the Reducible background

A fake photon (mis-identified jet or photon in jet) is surrounded by energy.

→ Use “isolation” to disentangle genuine from fake photons



Genuine photons
Well isolated

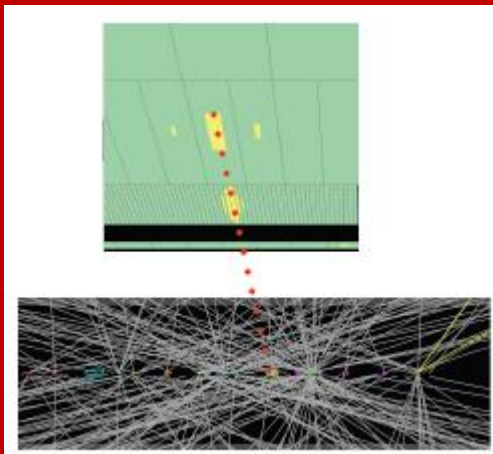
Data driven technic
Use isolation to count and identify the background pollution in regions without signal

H- $\rightarrow\gamma\gamma$: The Di-Photon mass spectrum

$$M^2_{\gamma\gamma} = 2 E_1 E_2 (1 - \cos\theta)$$

→ Energies from Calo

→ Photon direction from likelihood including the Calo pointing (thanks to the 3-layer segmentation)



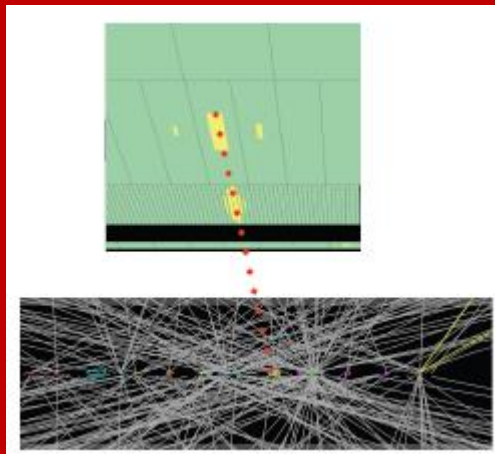
Vertex resolution $\sim 1.5\text{cm}$

H- \rightarrow $\gamma\gamma$: The Di-Photon mass spectrum

$$M^2_{\gamma\gamma} = 2 E_1 E_2 (1 - \cos\Theta)$$

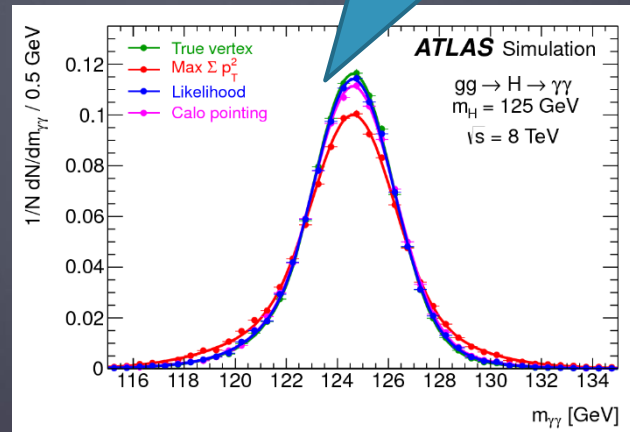
\rightarrow Energies from Calo

\rightarrow Photon direction from likelihood including the Calo pointing (thanks to the 3-layer segmentation)



Vertex resolution $\sim 1.5\text{cm}$

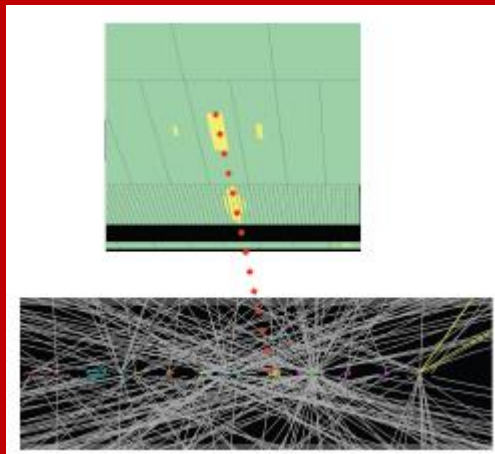
Calo pointing very close to truth.
Likelihood improves further the agreement



H- \rightarrow $\gamma\gamma$: The Di-Photon mass spectrum

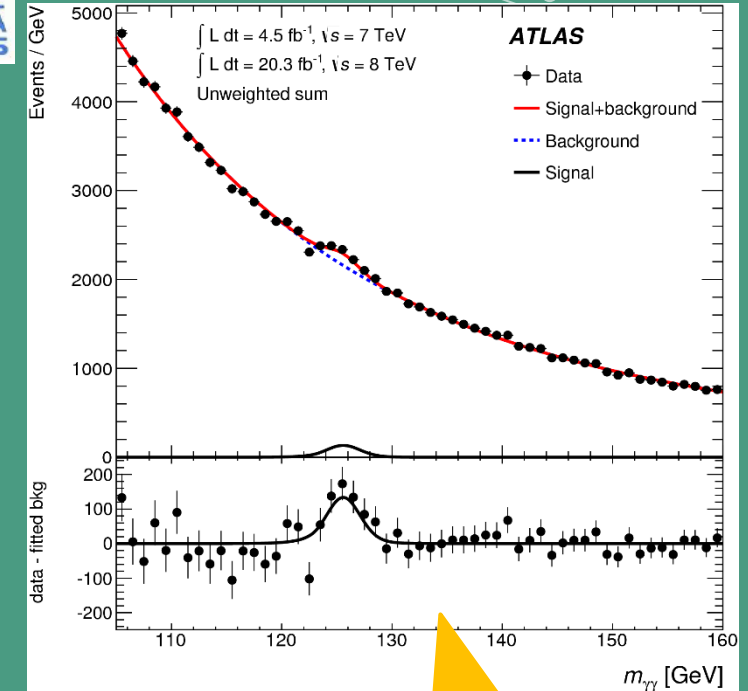
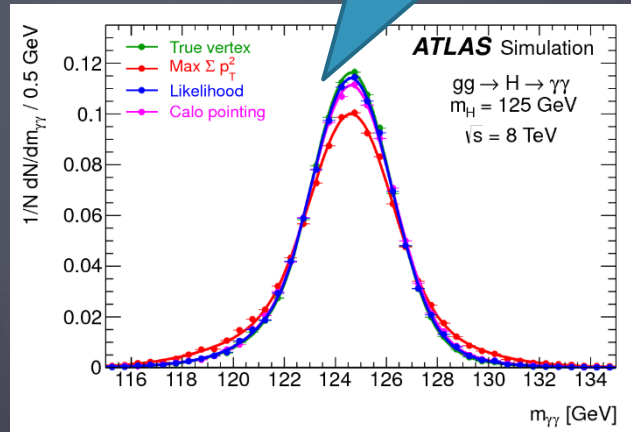
$$M^2_{\gamma\gamma} = 2 E_1 E_2 (1 - \cos\Theta)$$

- Energies from Calo
- Photon direction from likelihood including the Calo pointing (thanks to the 3-layer segmentation)



Vertex resolution \sim 1.5cm

Calo pointing very close to truth. Likelihood improves further the agreement



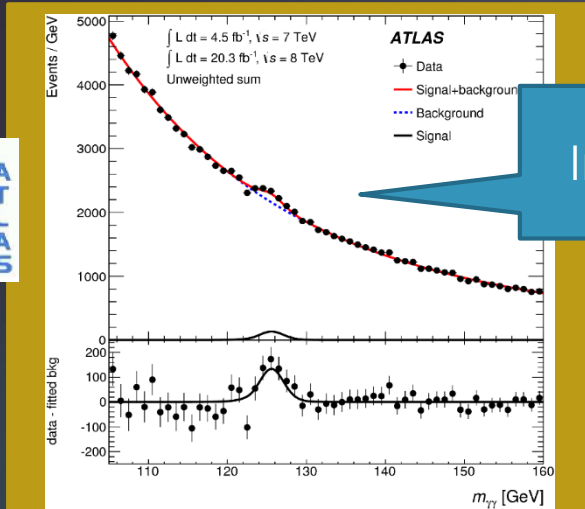
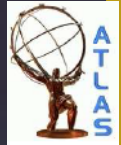
Final state contained Nice mass peak!

Invisib 16/06/

How to extract the “most significant” result from the data?

205

Invisibles 2015, Lydia Iconomidou-Fayard
16/06/2015



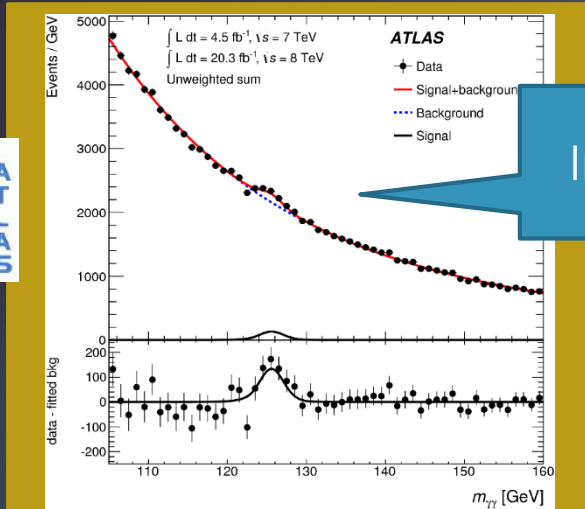
Inclusive plot

Detector resolution, systematic effects and background yields vary with some kinematical photon variables:
PT, η , conversion status etc..

How to extract the “most significant” result from the data?

206

Invisibles 2015, Lydia Iconomidou-Fayard
16/06/2015

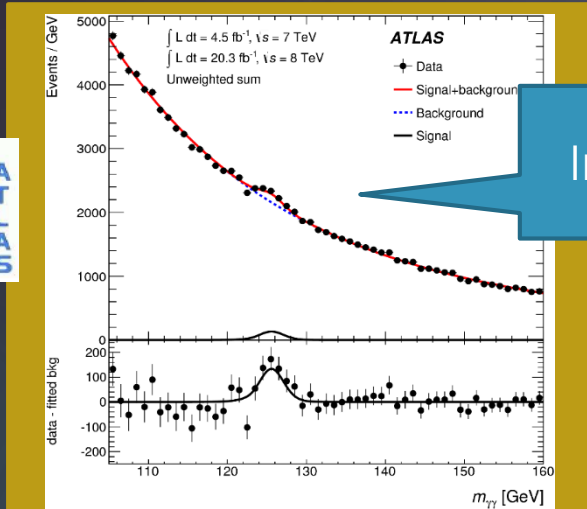
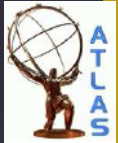


Inclusive plot

Detector resolution, systematic effects and background yields vary with some kinematical photon variables:
PT, η , conversion status etc..

Split the data in exclusive appropriate categories to optimize the S/B ratios

How to extract the “most significant” result from the data?



Inclusive plot

Detector resolution, systematic effects and background yields vary with some kinematical photon variables: p_T , η , conversion status etc..

Split the data in exclusive appropriate categories to optimize the S/B ratios

Category	n_{sig}	FWHM [GeV]	b in $\pm\sigma_{FWHM}$	s/b [%]
Inclusive	402.	3.69	10670	3.39
Unconv. central low p_T	59.3	3.13	801	6.66
Unconv. central high p_T	7.1	2.81	26.0	24.6
Unconv. rest low p_T	96.2	3.49	2624	3.30
Unconv. rest high p_T	10.4	3.11	93.9	9.95
Unconv. transition	26.0	4.24	910	2.57
Conv. central low p_T	37.2	3.47	589	5.69
Conv. central high p_T	4.5	3.07	20.9	19.4
Conv. rest low p_T	107.2	4.23	3834	2.52
Conv. rest high p_T	11.9	3.71	144.2	7.44
Conv. transition	42.1	5.31	1177	1.92

Nb of signal events

Resolution

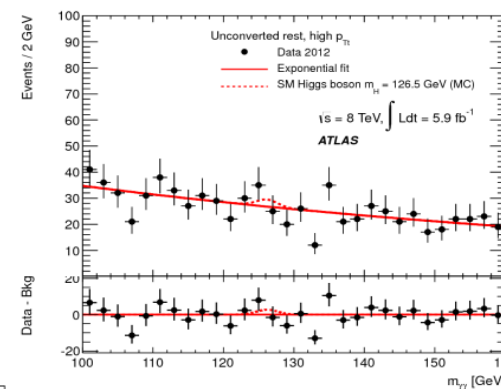
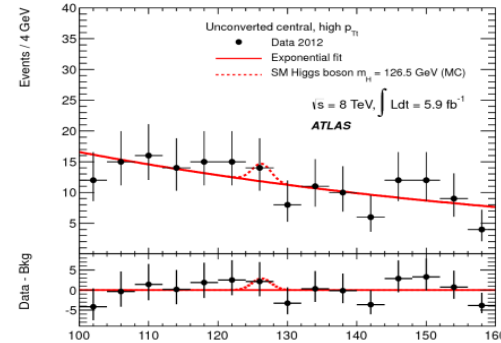
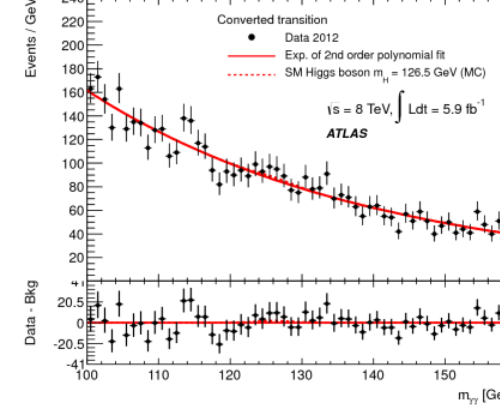
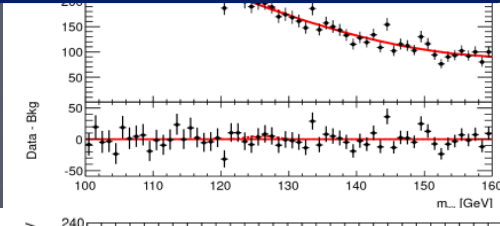
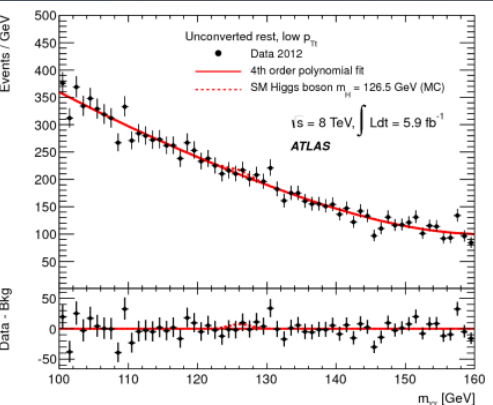
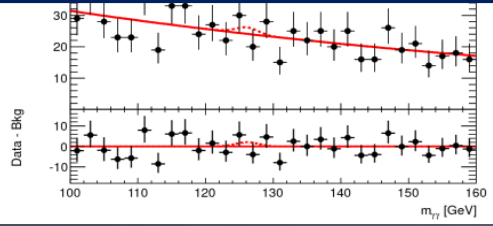
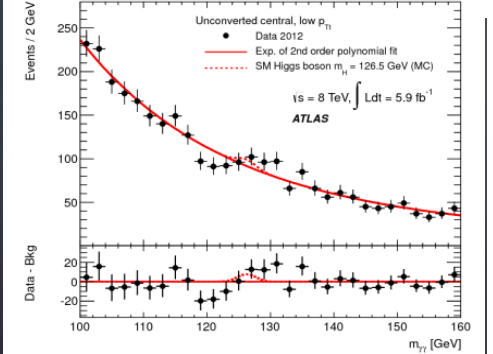
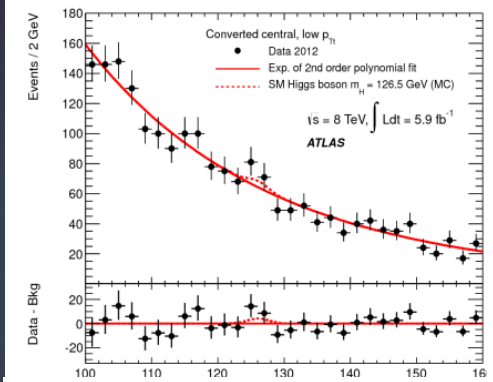
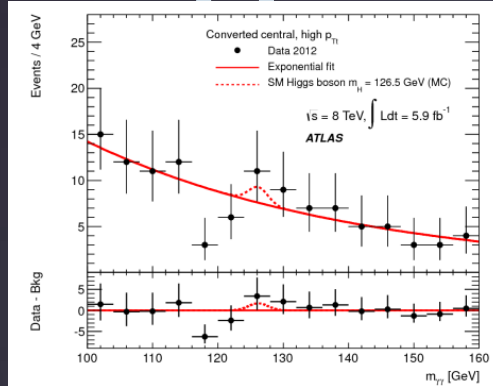
Nb of backg. events

S/B ratio

H \rightarrow $\gamma\gamma$: Diphoton mass spectra

In each Category:

Fit of the signal :
 Use a Crystal-Ball function for the bulk of events and a wider Gaussian for tails.
 Function parameters depend on the category and are extracted from MC

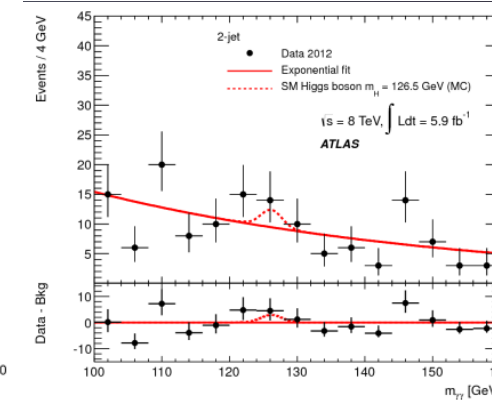
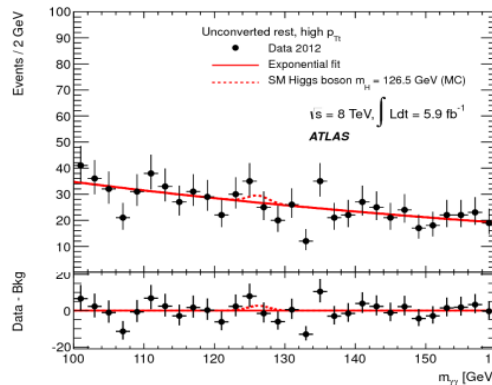
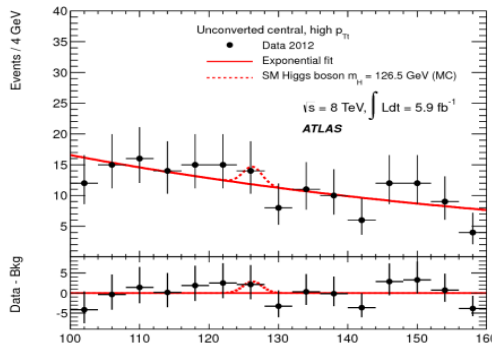
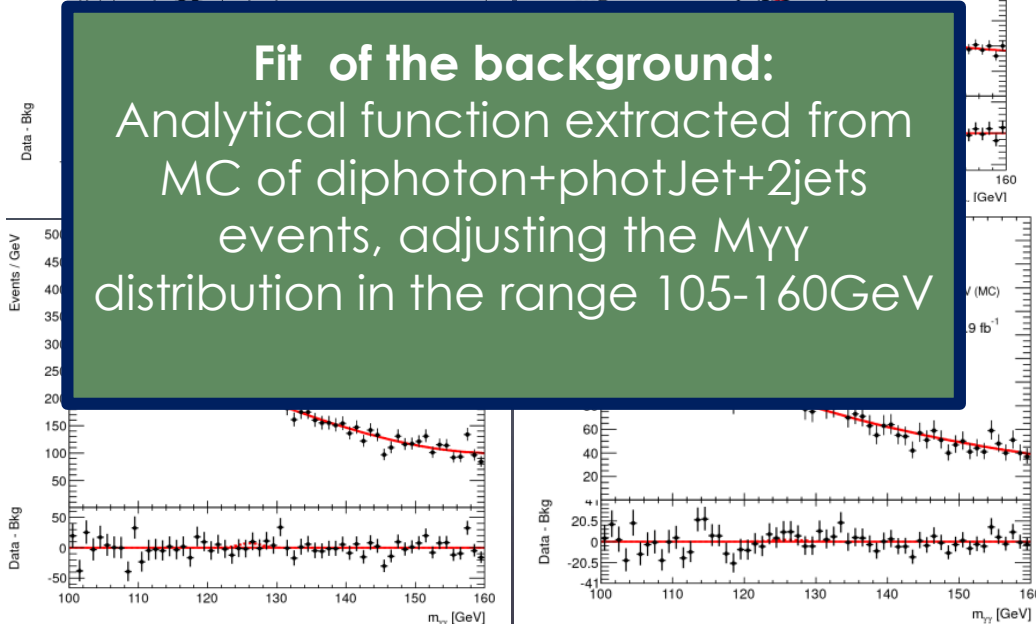
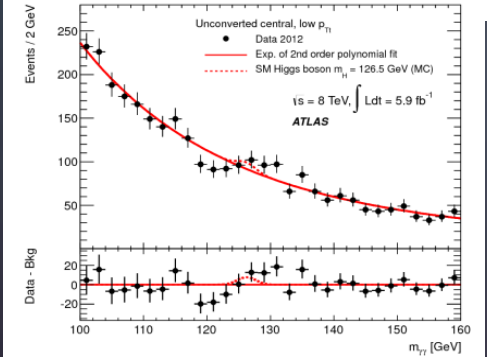
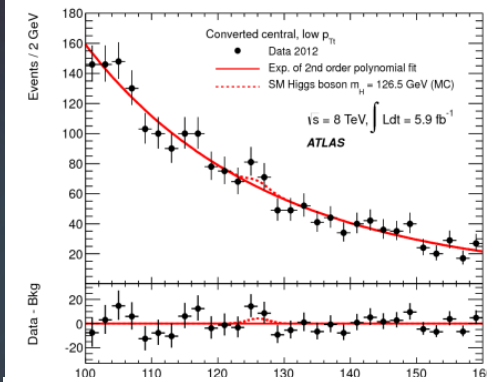
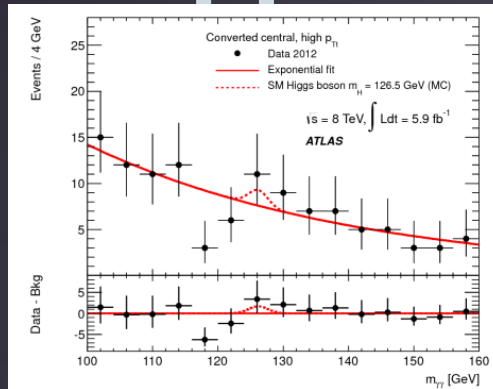


H → $\gamma\gamma$: Diphoton mass spectra

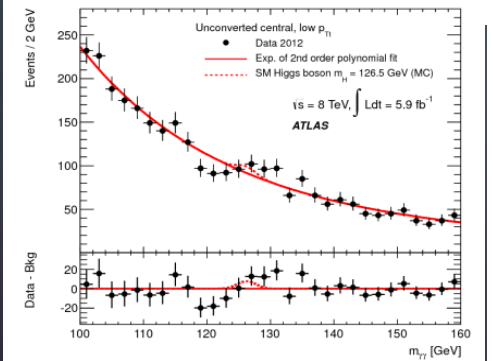
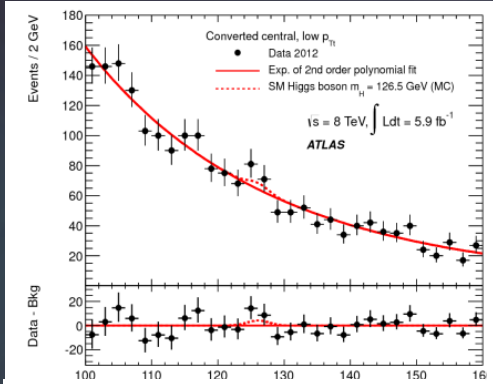
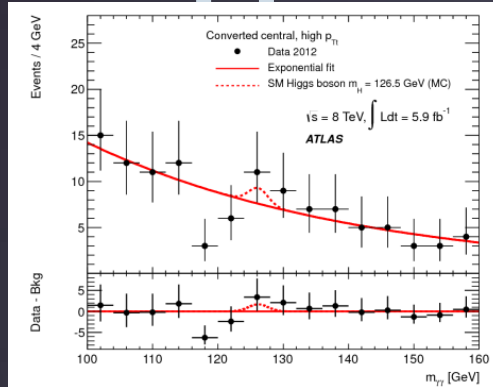
In each Category:

Fit of the signal :
 Use a Crystal-Ball function for the bulk of events and a wider Gaussian for tails.

Fit of the background:
 Analytical function extracted from MC of diphoton+photJet+2jets events, adjusting the $M_{\gamma\gamma}$ distribution in the range 105-160GeV



H → $\gamma\gamma$: Diphoton mass spectra

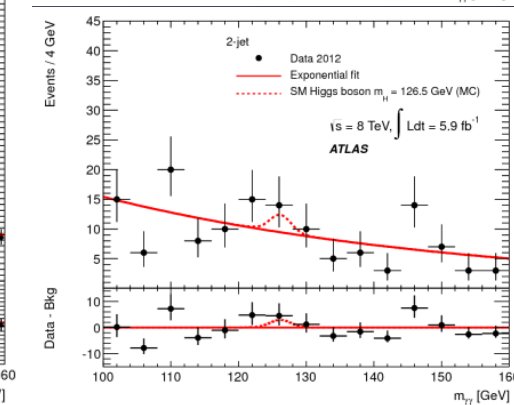
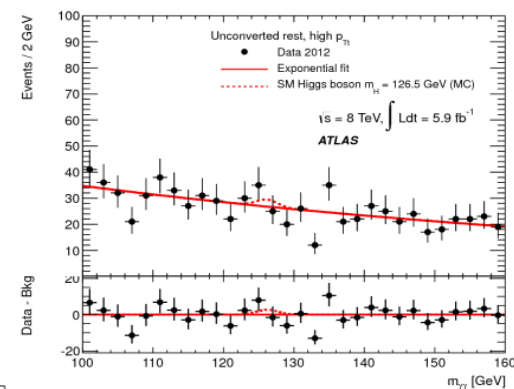
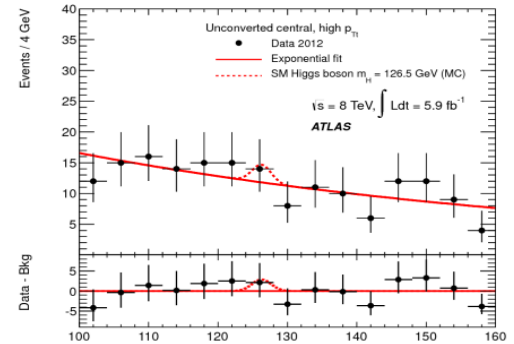


In each Category:

Fit of the signal :
 Use a Crystal-Ball function for the bulk of events and a wider Gaussian for tails.
 Function parameters depend on the category and are extracted from MC

Fit of the background:
 Analytical function extracted from MC of diphoton+photJet+2jets events, adjusting the $M_{\gamma\gamma}$ distribution in the range 105-160GeV

Final mass: simultaneous maximum likelihood fit of all 10 categories



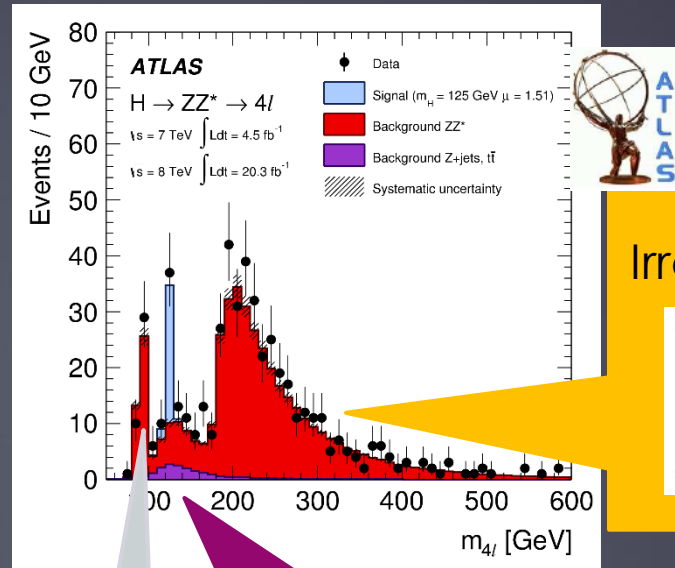
$H \rightarrow ZZ^* \rightarrow 4l (\mu, e)$: the golden mode

211

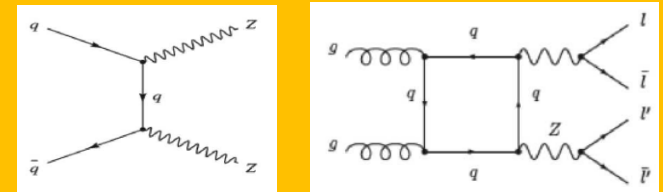
Very suppressed at low H mass.
 $\sigma \times \text{Br} = 2.9 \text{ fb}^{-1}$
But low background ! S/B ~ 1.5

H \rightarrow ZZ* \rightarrow 4l (μ, e) : the golden mode

Very suppressed at low H mass.
 $\sigma \times Br = 2.9 \text{ fb}^{-1}$
 But low background ! S/B ~ 1.5

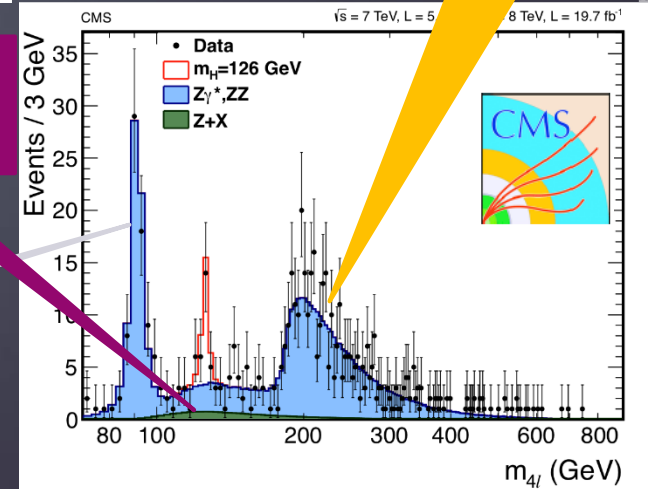
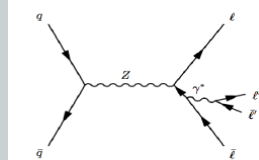


Irreducible ZZ opens-up at $\sim 2M_Z$



Small reducible from Z+jets, ttbar,

Z \rightarrow 4leptons



H \rightarrow ZZ* \rightarrow 4l (μ, e) : the golden mode

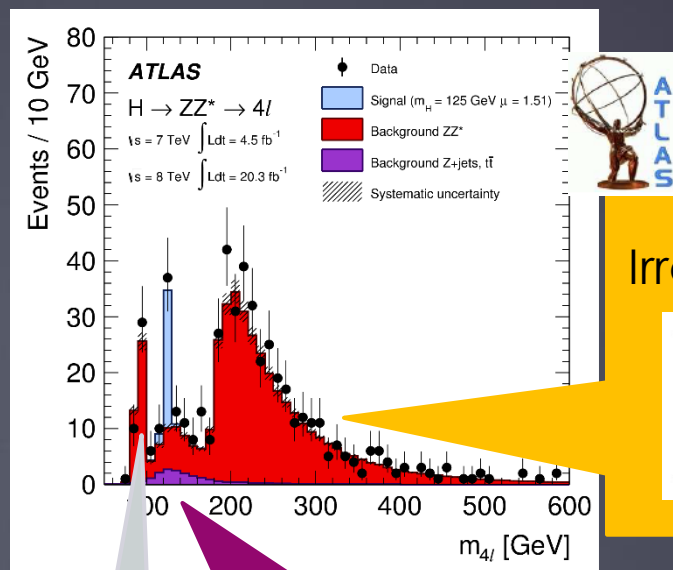
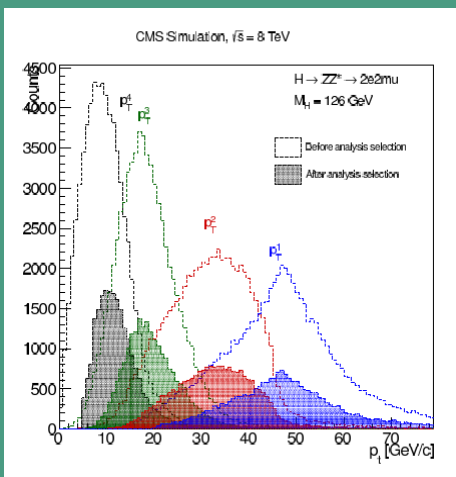
Very suppressed at low H mass.
 $\sigma \times Br = 2.9 \text{ fb}^{-1}$
 But low background ! S/B ~ 1.5

To optimize the detection:

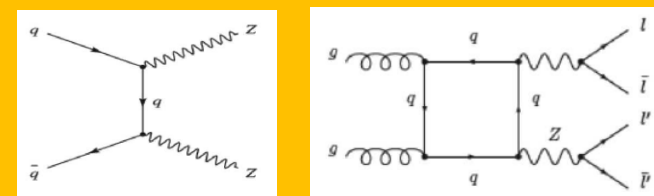
\rightarrow The highest reconstruction and identification efficiencies are required for electrons and muons.

\rightarrow The low Higgs mass implies at least 1 virtual Z decaying into low Et leptons.

\rightarrow Start efficient detection from $P_T = 6(7) \text{ GeV}$, a challenge..

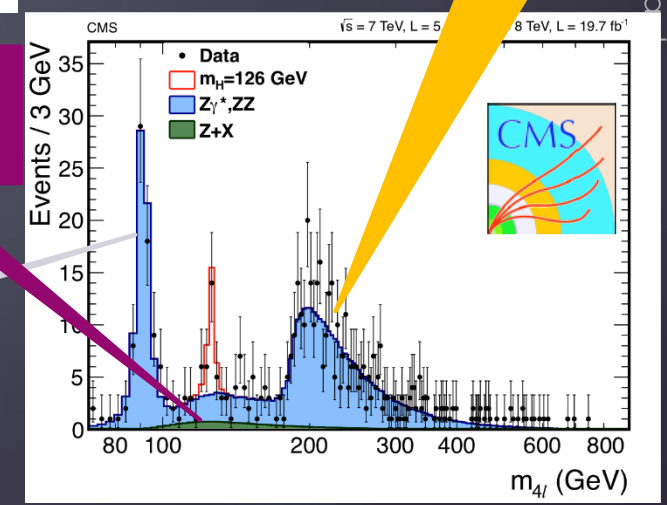
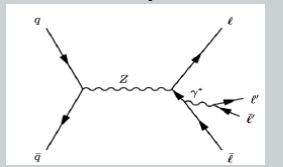


Irreducible ZZ opens-up at $\sim 2M_Z$



Small reducible from Z+jets, ttbar,

Z \rightarrow 4leptons



Invisibles 2
16/06/2011

H \rightarrow ZZ* \rightarrow 4l : Signal and background

214

Final states: 4e, 4 μ , 2e2 μ , 2 μ 2e
Pt > 20, 15, 10, 7 (6)

“Loose” Identification criteria

The closest to Z mass = M_{12} (50-106 GeV)

The second pair M_{34}

H \rightarrow ZZ* \rightarrow 4l : Signal and background

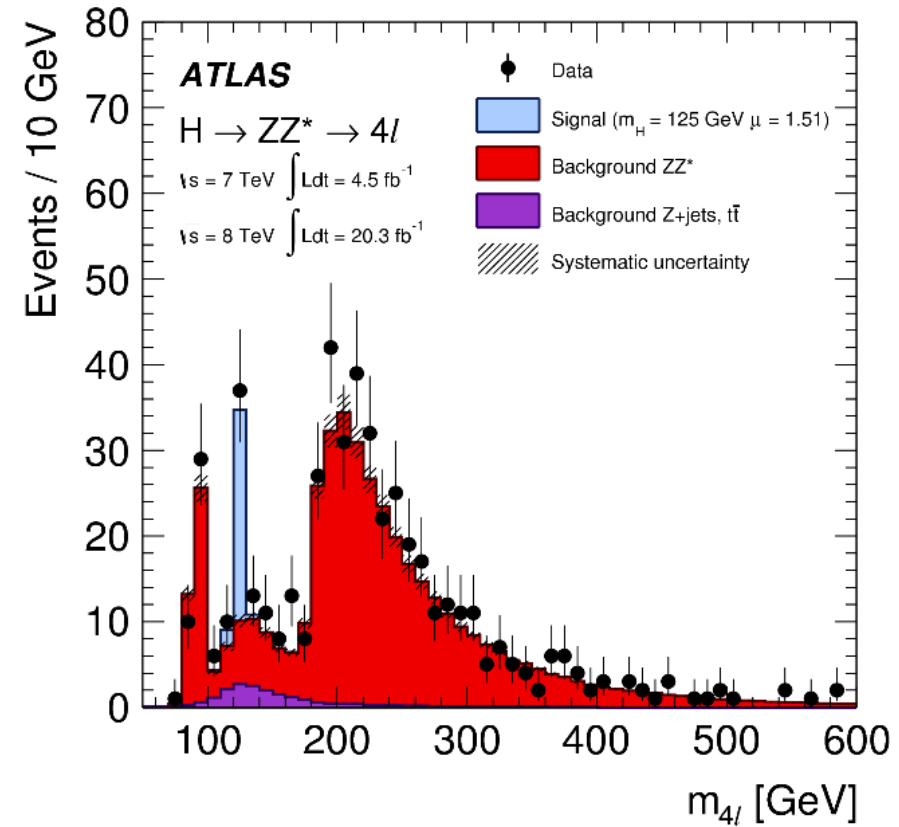
215

Final states: 4e, 4 μ , 2e2 μ , 2 μ 2e
Pt > 20, 15, 10, 7 (6)

“Loose” Identification criteria

The closest to Z mass = M_{12} (50-106 GeV)

The second pair M_{34}



H \rightarrow ZZ* \rightarrow 4l : Signal and background

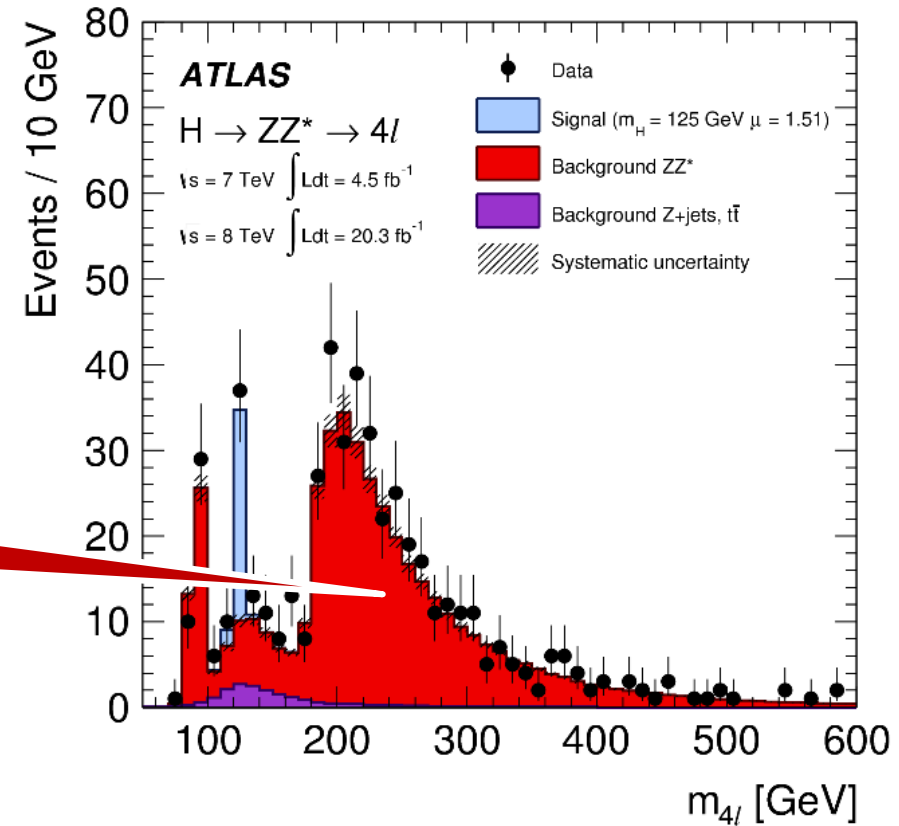
216

Final states: 4e, 4 μ , 2e2 μ , 2 μ 2e
Pt > 20, 15, 10, 7 (6)

“Loose” Identification criteria

The closest to Z mass = M_{12} (50-106 GeV)
The second pair M_{34}

Irreducible : pp \rightarrow ZZ*
Shape from MC simulation
Scaled to luminosity
Non resonant spectrum



H \rightarrow ZZ* \rightarrow 4l : Signal and background

217

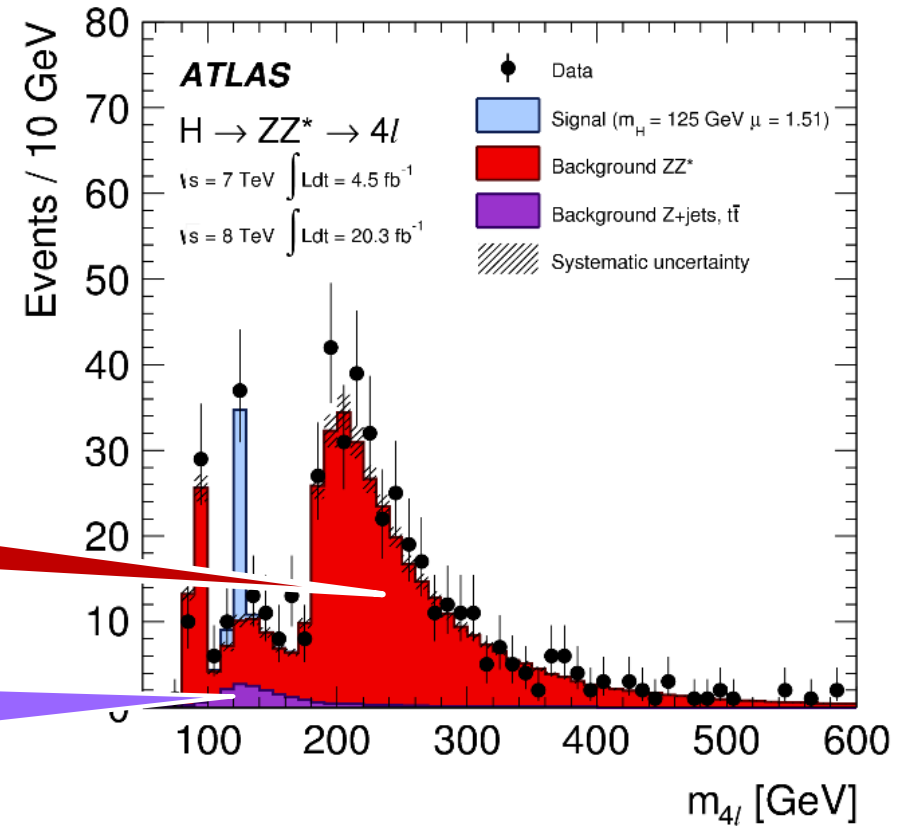
Final states: 4e, 4 μ , 2e2 μ , 2 μ 2e
Pt > 20, 15, 10, 7 (6)

“Loose” Identification criteria

The closest to Z mass = M_{12} (50-106 GeV)
The second pair M_{34}

Irreducible : pp \rightarrow ZZ*
Shape from MC simulation
Scaled to luminosity
Non resonant spectrum

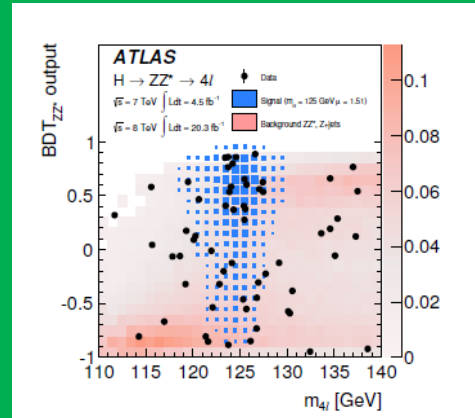
Reducible : Z+jets, ttbar \rightarrow 4l
Sizeable at low 4l invariant mass
Reduced by isolation and
impact parameter criteria



Reducible background depends on the subleading lepton pair flavor.
Data driven measurement in enriched control regions

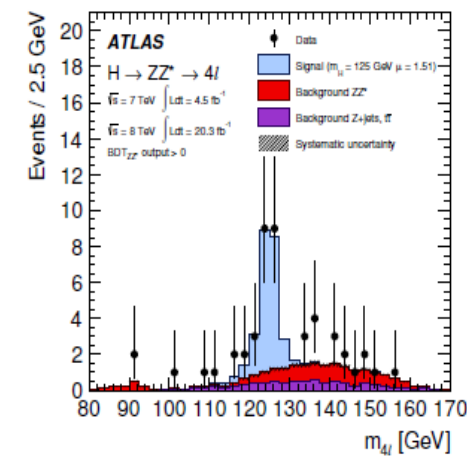
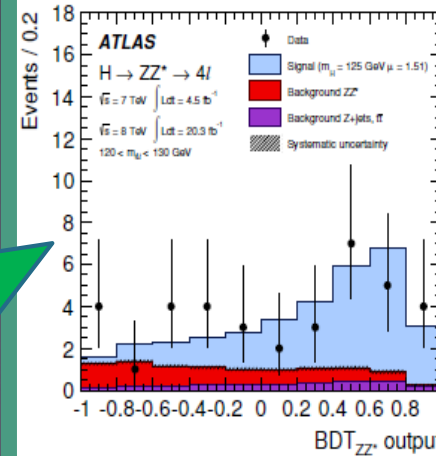
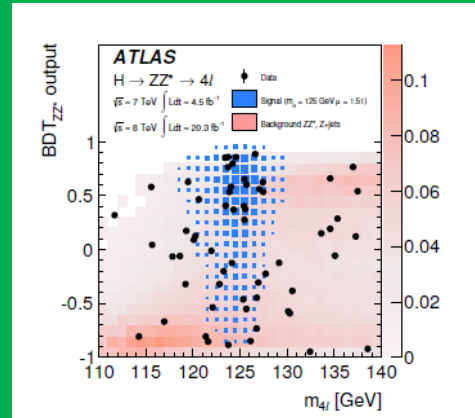
H \rightarrow ZZ* \rightarrow 4l :

A BoostedDecisionTree
to **better discriminate**
H \rightarrow ZZ* from ZZ*:
Uses P_T^{4l} , the 4l
pseudorapidity η^{4l} and
the Matrix Elements



H \rightarrow ZZ* \rightarrow 4l :

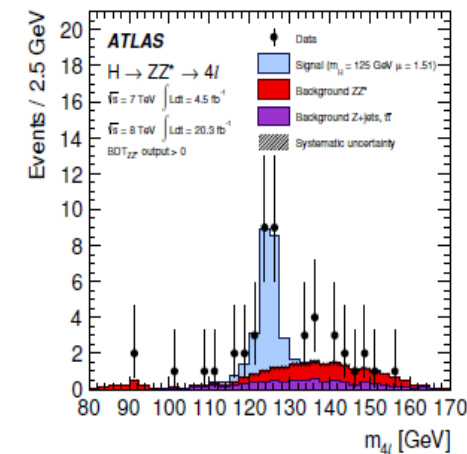
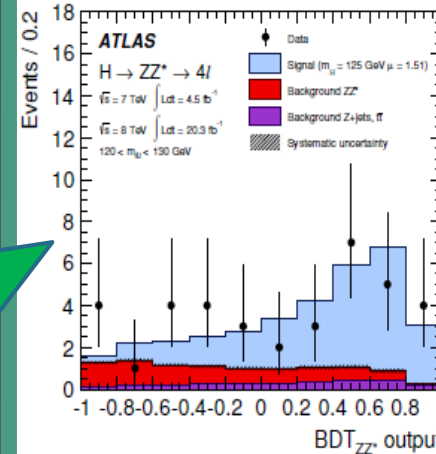
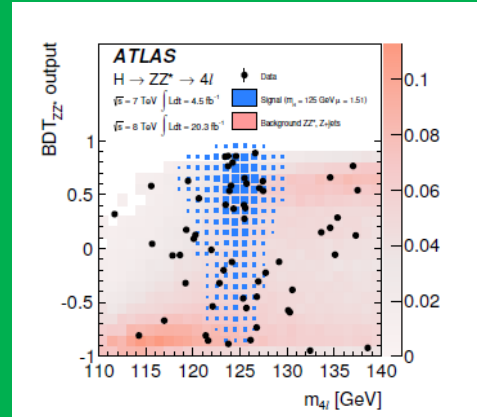
A BoostedDecisionTree
to better discriminate
H \rightarrow ZZ* from ZZ*:
Uses P_{\uparrow}^{4l} , the 4l
pseudorapidity η^{4l} and
the Matrix Elements



H → ZZ* → 4l :



A BoostedDecisionTree to better discriminate H → ZZ* from ZZ*:
 Uses P_{\top}^{4l} , the 4l pseudorapidity η^{4l} and the Matrix Elements



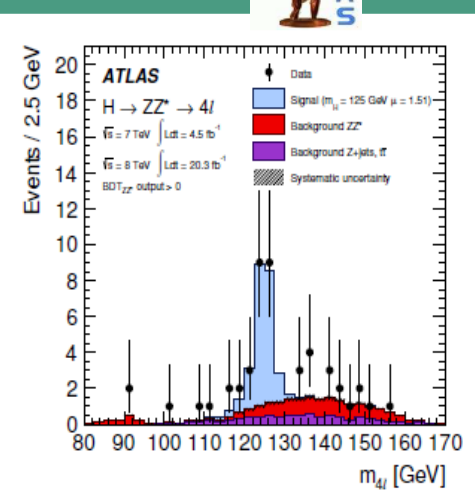
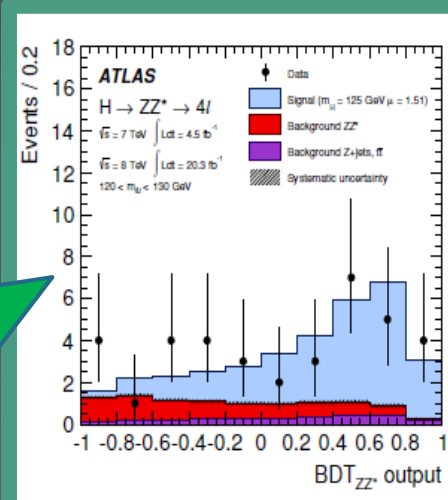
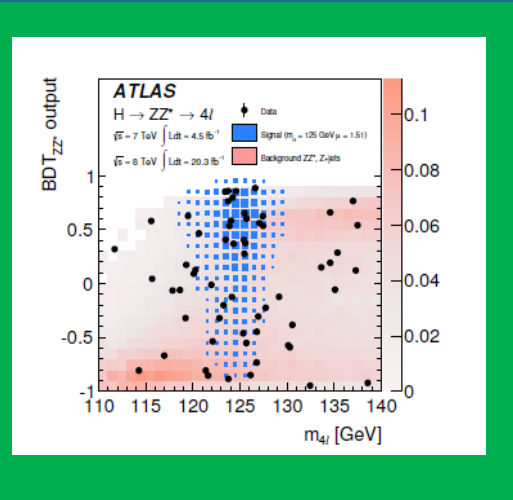
Final state	Signal full mass range	Signal	ZZ*	Z + jets, tt	S/B	Expected	Observed
$\sqrt{s} = 7 \text{ TeV}$ and $\sqrt{s} = 8 \text{ TeV}$							
4 μ	6.80 ± 0.67	6.20 ± 0.61	2.82 ± 0.14	0.79 ± 0.13	1.7	9.81 ± 0.64	14
2e2 μ	4.58 ± 0.45	4.04 ± 0.40	1.99 ± 0.10	0.69 ± 0.11	1.5	6.72 ± 0.42	9
2 μ 2e	3.56 ± 0.36	3.15 ± 0.32	1.38 ± 0.08	0.72 ± 0.12	1.5	5.24 ± 0.35	6
4e	3.25 ± 0.34	2.77 ± 0.29	1.22 ± 0.08	0.76 ± 0.11	1.4	4.75 ± 0.32	8
Total	18.2 ± 1.8	16.2 ± 1.6	7.41 ± 0.40	2.95 ± 0.33	1.6	26.5 ± 1.7	37

← In mass range 120-130 GeV →

H → ZZ* → 4l :

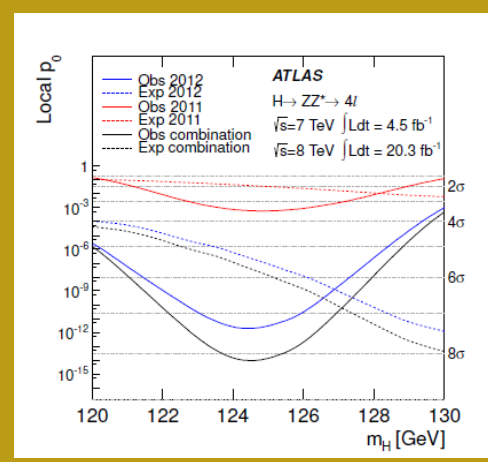


A BoostedDecisionTree to better discriminate H → ZZ* from ZZ*:
 Uses P_{\top}^{4l} , the 4l pseudorapidity η^{4l} and the Matrix Elements



Final state	Signal full mass range	Signal	ZZ*	Z + jets, tt	S/B	Expected	Observed
$\sqrt{s} = 7 \text{ TeV and } \sqrt{s} = 8 \text{ TeV}$							
4 μ	6.80 ± 0.67	6.20 ± 0.61	2.82 ± 0.14	0.79 ± 0.13	1.7	9.81 ± 0.64	14
2e2 μ	4.58 ± 0.45	4.04 ± 0.40	1.99 ± 0.10	0.69 ± 0.11	1.5	6.72 ± 0.42	9
2 μ 2e	3.56 ± 0.36	3.15 ± 0.32	1.38 ± 0.08	0.72 ± 0.12	1.5	5.24 ± 0.35	6
4e	3.25 ± 0.34	2.77 ± 0.29	1.22 ± 0.08	0.76 ± 0.11	1.4	4.75 ± 0.32	8
Total	18.2 ± 1.8	16.2 ± 1.6	7.41 ± 0.40	2.95 ± 0.33	1.6	26.5 ± 1.7	37

In mass range 120-130 GeV



Local $P_0 = 8.2 \sigma$ ($m = 124.51 \text{ GeV}$)

H- \rightarrow WW*: the abundant

222

H- \rightarrow WW* : 22% of the decays at $M_H=125\text{GeV}$.

Keep the most sensitive
experimental channels:
leptonic decays, W- \rightarrow ev, W- \rightarrow $\mu\nu$

H- \rightarrow WW*: the abundant

223

H- \rightarrow WW* : 22% of the decays at $M_H=125\text{GeV}$.

Keep the most sensitive
experimental channels:
leptonic decays, W- \rightarrow ev, W- \rightarrow $\mu\nu$

H- \rightarrow WW* has overwhelming backgrounds
The Drell-Yan ($ee, \mu\mu$), WW, W γ , ZZ- \rightarrow llvv,
ttbar, tW, multijets ...

H- \rightarrow WW*: the abundant

224

H- \rightarrow WW* : 22% of the decays at $M_H=125\text{GeV}$.

Keep the most sensitive
experimental channels:
leptonic decays, W- \rightarrow ev, W- \rightarrow $\mu\nu$

H- \rightarrow WW* has overwhelming backgrounds
The Drell-Yan (ee, $\mu\mu$), WW, W γ , ZZ- \rightarrow llvv,
ttbar, tW, multijets ...

Here, an overview of the selection (in
practice much more complexe!)

- \rightarrow Two well identified leptons with opposite sign and $P_T > 10\text{GeV}$
- \rightarrow Well isolated in the tracker and the Calorimeter (to suppress jets)
- \rightarrow $M_{ll} > 10\text{ GeV}$ (suppress the DY)
- \rightarrow $|m_{ll} - M_Z| > 15\text{GeV}$ (suppress the Z)
- \rightarrow Require high E_T^{miss} and P_T^{miss} (to sign the neutrinos)
- \rightarrow Count the nb of Jets
- \rightarrow $M_{ll} < 50\text{ GeV}$ and $\Delta\phi_{ll} < 1.8$ (Assuming Scalar Higgs)

H- \rightarrow WW*: the abundant

225

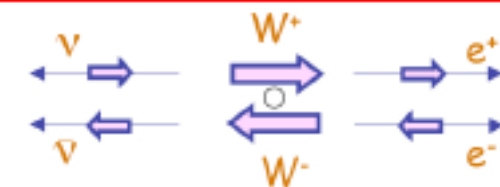
H- \rightarrow WW* : 22% of the decays at $M_H=125\text{GeV}$.

Keep the most sensitive
experimental channels:
leptonic decays, W- \rightarrow ev, W- \rightarrow μ \nu

H- \rightarrow WW* has overwhelming backgrounds
The Drell-Yan (ee, $\mu\mu$), WW, W γ , ZZ- \rightarrow llvv,
ttbar, tW, multijets ...

Here, an overview of the selection (in
practice much more complexe!)

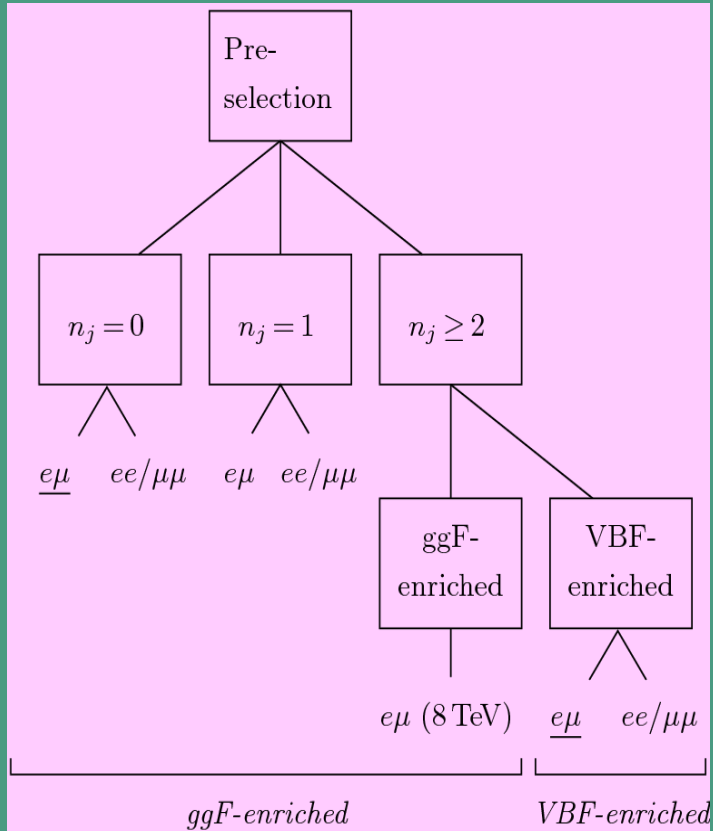
- \rightarrow Two well identified leptons with opposite sign and $P_T > 10\text{GeV}$
- \rightarrow Well isolated in the tracker and the Calorimeter (to suppress jets)
- \rightarrow $M_{ll} > 10\text{ GeV}$ (suppress the DY)
- \rightarrow $|m_{ll} - M_Z| > 15\text{GeV}$ (suppress the Z)
- \rightarrow Require high E_T^{miss} and P_T^{miss} (to sign the neutrinos)
- \rightarrow Count the nb of Jets
- \rightarrow $M_{ll} < 50\text{ GeV}$ and $\Delta\phi_{ll} < 1.8$ (Assuming Scalar Higgs)



H- \rightarrow WW* \rightarrow lvlv : Categories

226

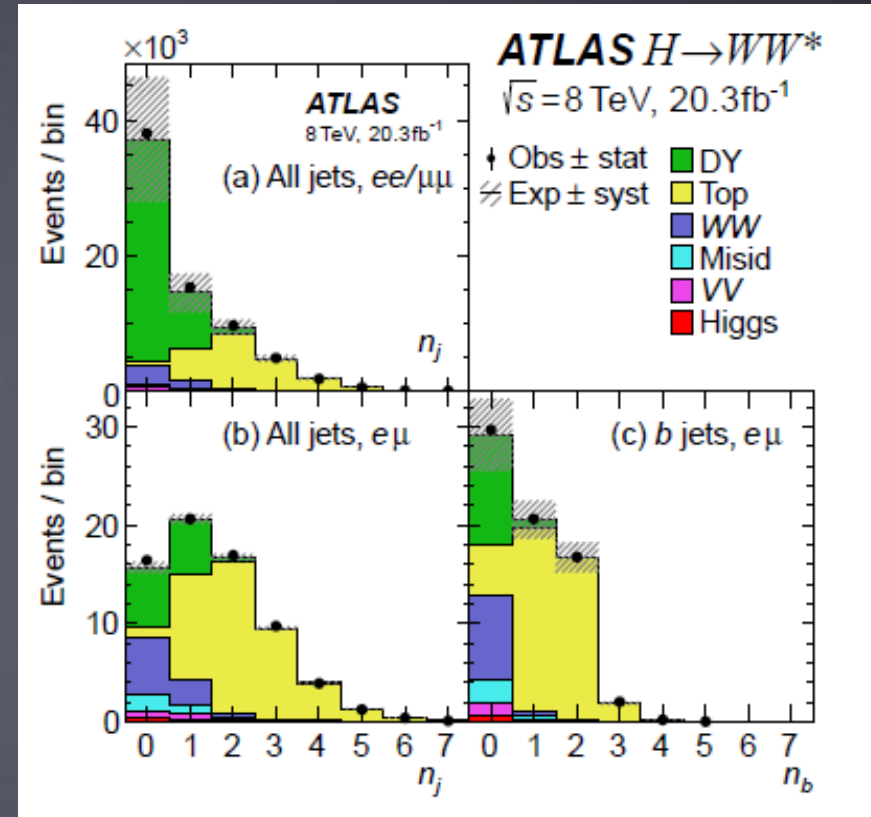
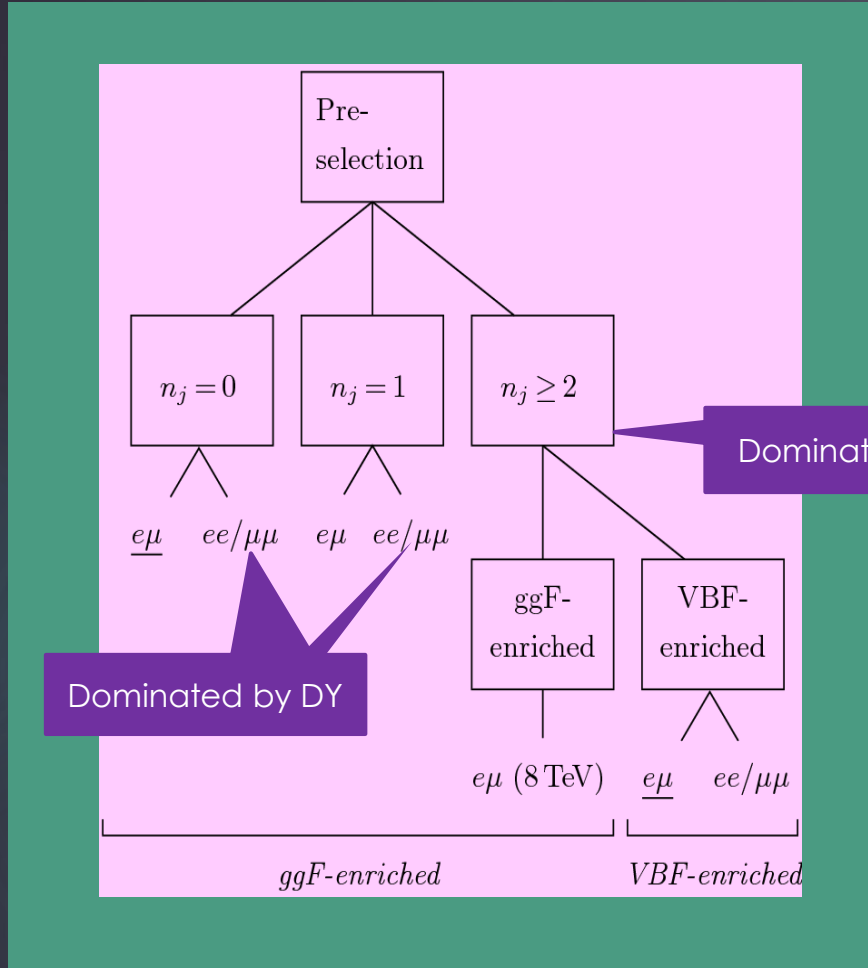
Invisibles 2015, Lydia Iconomidou-Fayard
16/06/2015



Principle :

Adapt the cuts to optimize the suppression of the backgrounds = $f(\text{category})$

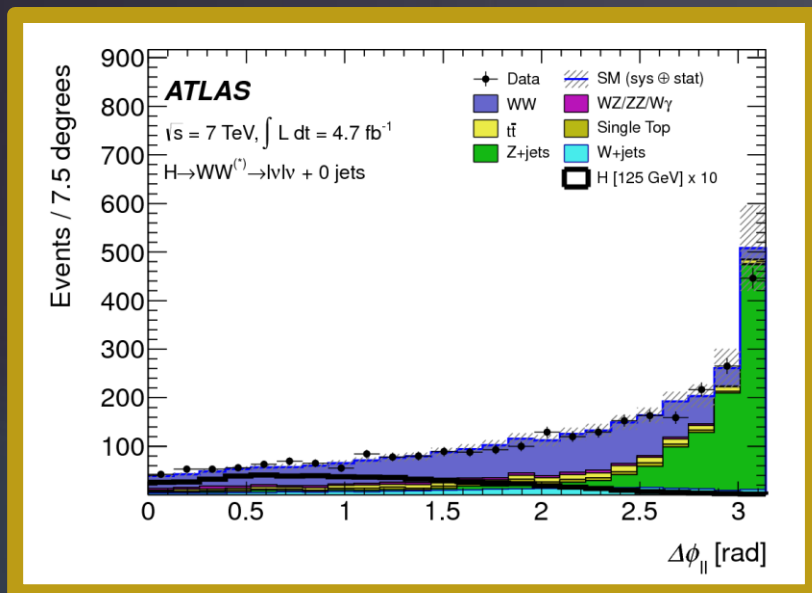
H- \rightarrow WW* \rightarrow lvlv : Categories



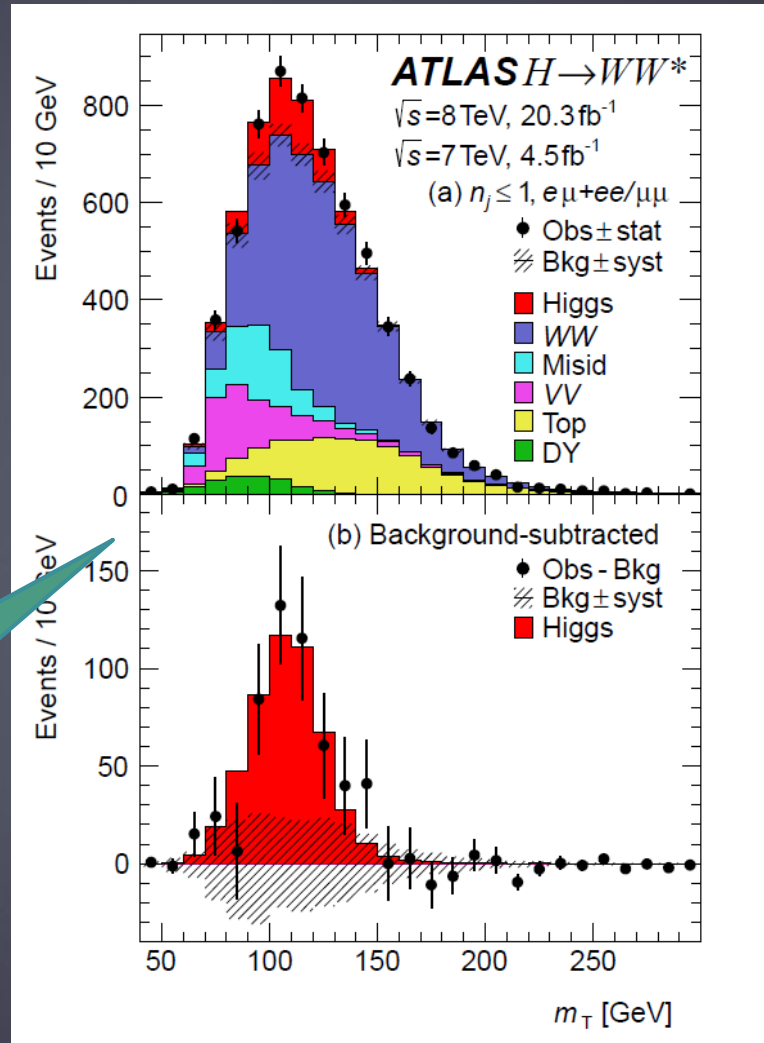
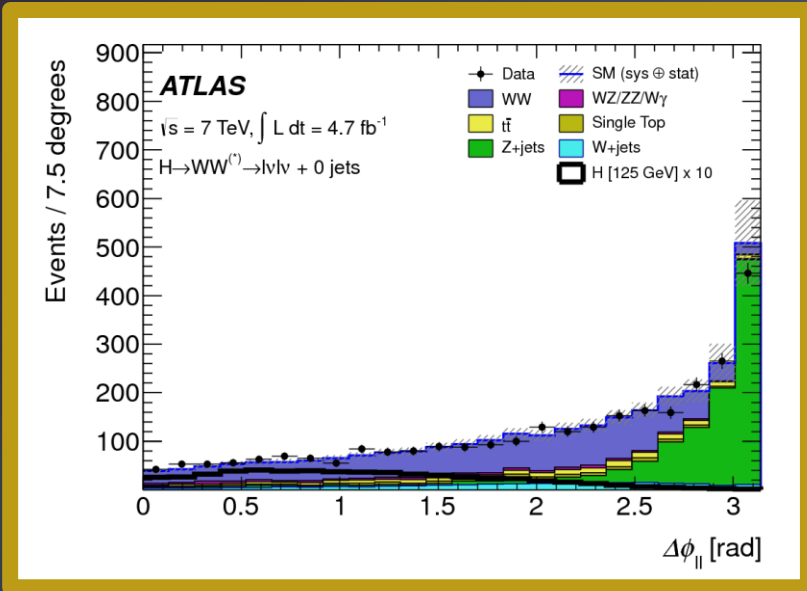
Principle :
 Adapt the cuts to optimize the suppression of the backgrounds = f(category)

H \rightarrow WW* \rightarrow l ν l ν

228

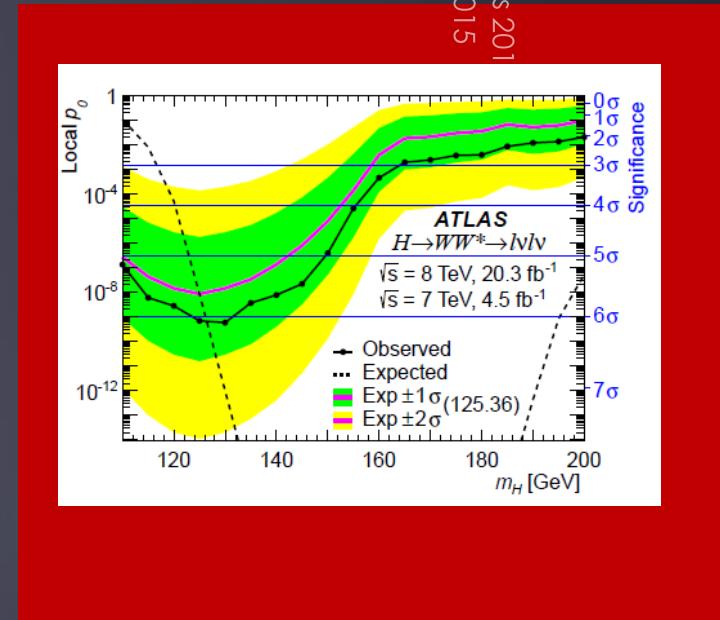


H → WW* → lνlν



$$m_T = \sqrt{(E_T^{\ell\ell} + p_T^{\nu\nu})^2 - |\mathbf{p}_T^{\ell\ell} + \mathbf{p}_T^{\nu\nu}|^2},$$

The final discrimination



$P_0 = 6.5 \sigma$ (5.9 expected)

Invisibles 2011
 16/06/2015

H- \rightarrow τ τ channel

Crucial decay to test H coupling to fermions
BR H- \rightarrow $\tau\tau$ = 6% at 125 GeV
S/B ratio \sim 2%

Use all tau decay types

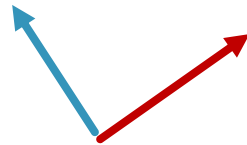
H \rightarrow τ τ channel

231

Crucial decay to test H coupling to fermions
BR H \rightarrow $\tau\tau$ = 6% at 125 GeV
S/B ratio \sim 2%

Use all tau decay types

Tau1 \rightarrow leptonic
Tau2 \rightarrow leptonic



Ask for 2 isolated and well identified leptons with OS

Bckg: Z \rightarrow $\tau^+\tau^-$, Z \rightarrow l^+l^- , $t\bar{t}$
Suppressed using E_T , m_{vis}^{\parallel} and $\Delta\phi^{\parallel}$
and rejecting jets if b-tagged

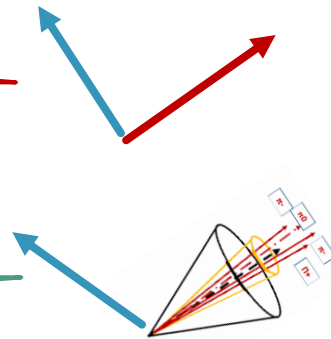
H \rightarrow $\tau\tau$ channel

Crucial decay to test H coupling to fermions
BR H \rightarrow $\tau\tau$ = 6% at 125 GeV
S/B ratio \sim 2%

Use all tau decay types

Tau1 \rightarrow leptonic
Tau2 \rightarrow leptonic

Tau1 \rightarrow leptonic
Tau2 \rightarrow Hadronic



Ask for 2 isolated and well identified leptons with OS

Bckg: Z \rightarrow $\tau\tau$ -, Z \rightarrow $l+l$ -, $t\bar{t}$ bar
Suppressed using E_T , m_{vis}^{\parallel} and $\Delta\phi^{\parallel}$
and rejecting jets if b-tagged

Ask for 1 lepton and one tau-jet with OS.

Bckg: W+jets, $t\bar{t}$ bar
Suppressed using M_T and rejecting jets if b-tagged

H \rightarrow $\tau\tau$ channel

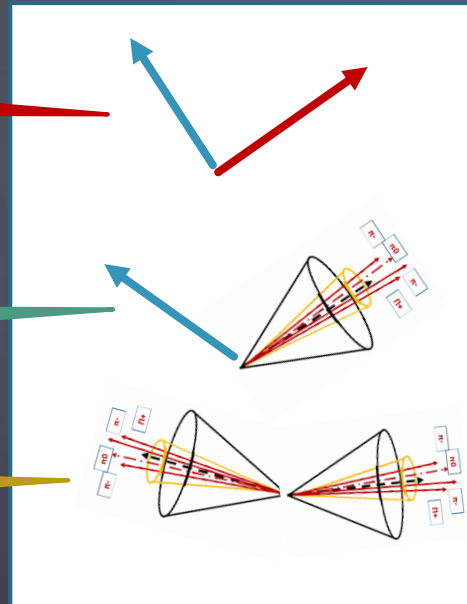
Crucial decay to test H coupling to fermions
BR H \rightarrow $\tau\tau$ = 6% at 125 GeV
S/B ratio \sim 2%

Use all tau decay types

Tau1 \rightarrow leptonic
Tau2 \rightarrow leptonic

Tau1 \rightarrow leptonic
Tau2 \rightarrow Hadronic

Tau1 \rightarrow hadronic
Tau2 \rightarrow hadronic



Ask for 2 isolated and well identified leptons with OS

Bckg: Z \rightarrow $\tau\tau$ -, Z \rightarrow $l+l$ -, $t\bar{t}$ bar
Suppressed using E_T , m_{vis}^{\parallel} and $\Delta\phi^{\parallel}$ and rejecting jets if b-tagged

Ask for 1 lepton and one tau-jet with OS.

Bckg: W+jets, $t\bar{t}$ bar
Suppressed using M_T and rejecting jets if b-tagged

Ask for 2 tau-jets with OS

Bckg : multi jets events
Suppressed by tighter Id and kinematical separation in pseudorapidity

H- \rightarrow T T : reconstructing the invariant mass

234

Final state not fully contained
because of neutrinos

Apply the “**Missing Mass Calculator**”
using all available event info.

→ Solution in 99% of cases

→ Resolution ; ~12-20%

H \rightarrow $\tau\tau$: reconstructing the invariant mass

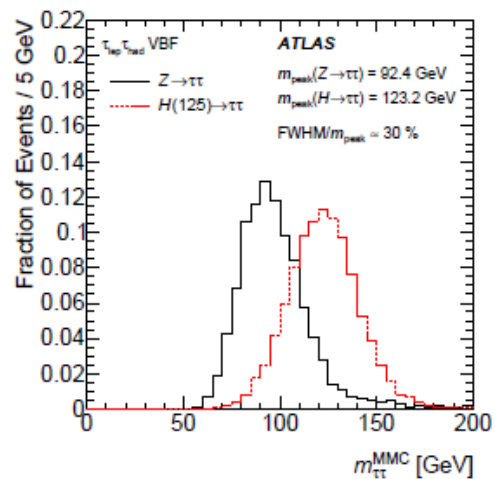
235

Final state not fully contained because of neutrinos

Apply the “**Missing Mass Calculator**” using all available event info.

→ Solution in 99% of cases

→ Resolution ; ~12-20%



H- \rightarrow T T : reconstructing the invariant mass and categorizing

Final state not fully contained
because of neutrinos

Apply the “**Missing Mass Calculator**”
using all available event info.

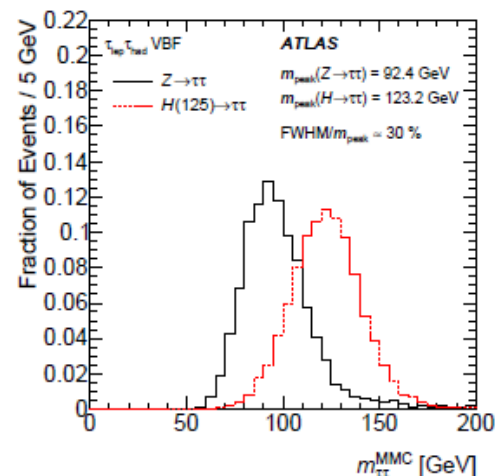
→ Solution in 99% of cases

→ Resolution ; ~12-20%

The 3 decay categories are split further:

--- **VBF** : + 2 high-pt jets with large
separation in pseudorapidity

--- **Boosted Higgs**: no VBF but $P_T^H > 100$ GeV



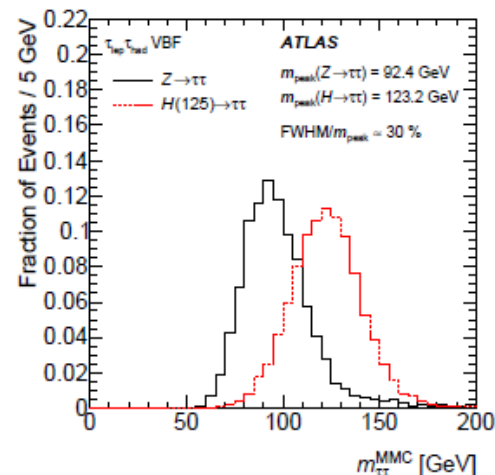
H \rightarrow $\tau\tau$: reconstructing the invariant mass and categorizing

Final state not fully contained because of neutrinos

Apply the “**Missing Mass Calculator**” using all available event info.

→ Solution in 99% of cases

→ Resolution ; ~12-20%



The 3 decay categories are split further:

--- **VBF** : + 2 high-pt jets with large separation in pseudorapidity

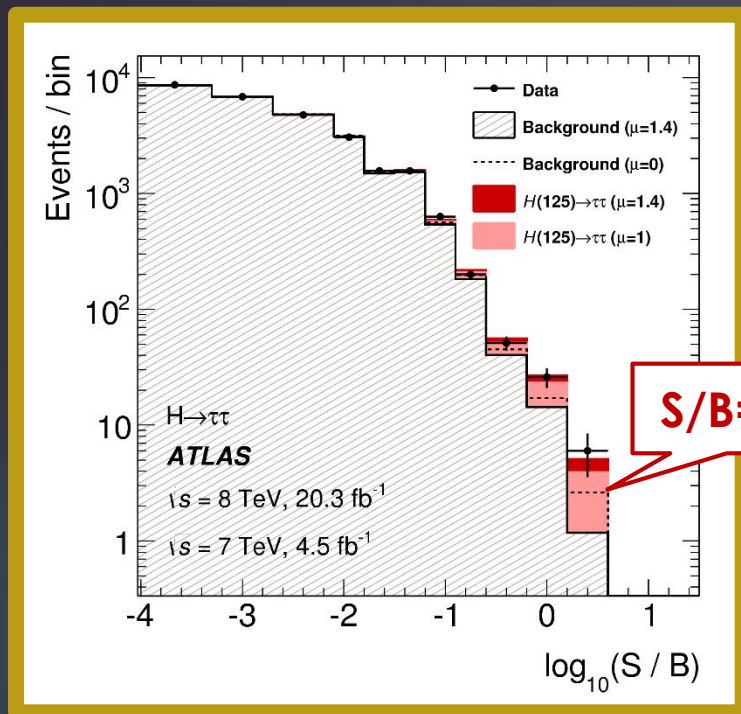
--- **Boosted Higgs**: no VBF but $P_T^H > 100 \text{ GeV}$

Background checked in specific data control regions

Final discriminant is a Boosted Decision Tree ran for all 6 categories

H \rightarrow $\tau\tau$: the ATLAS final result

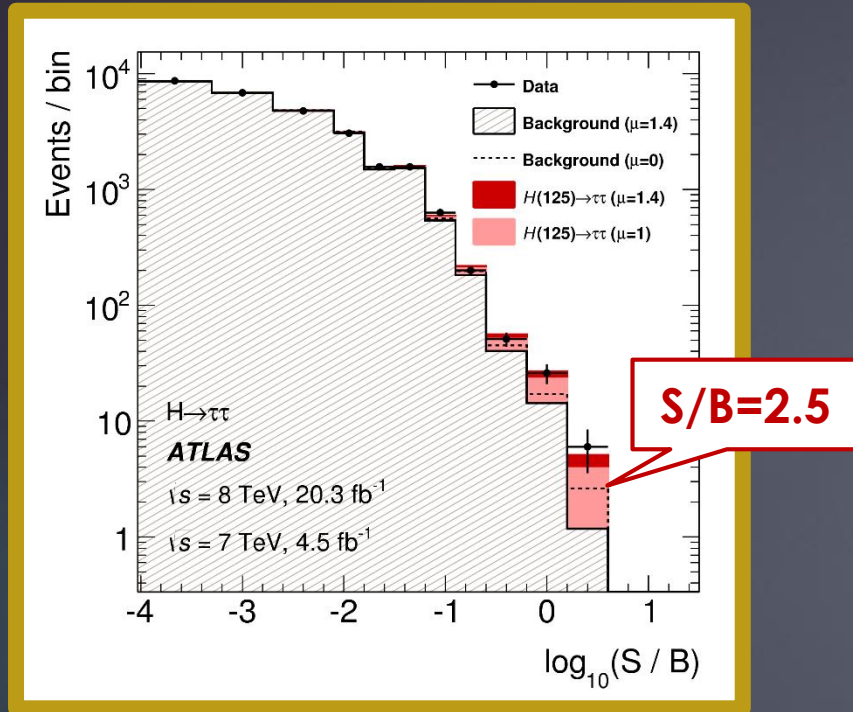
238



H → $\tau\tau$: the ATLAS final result

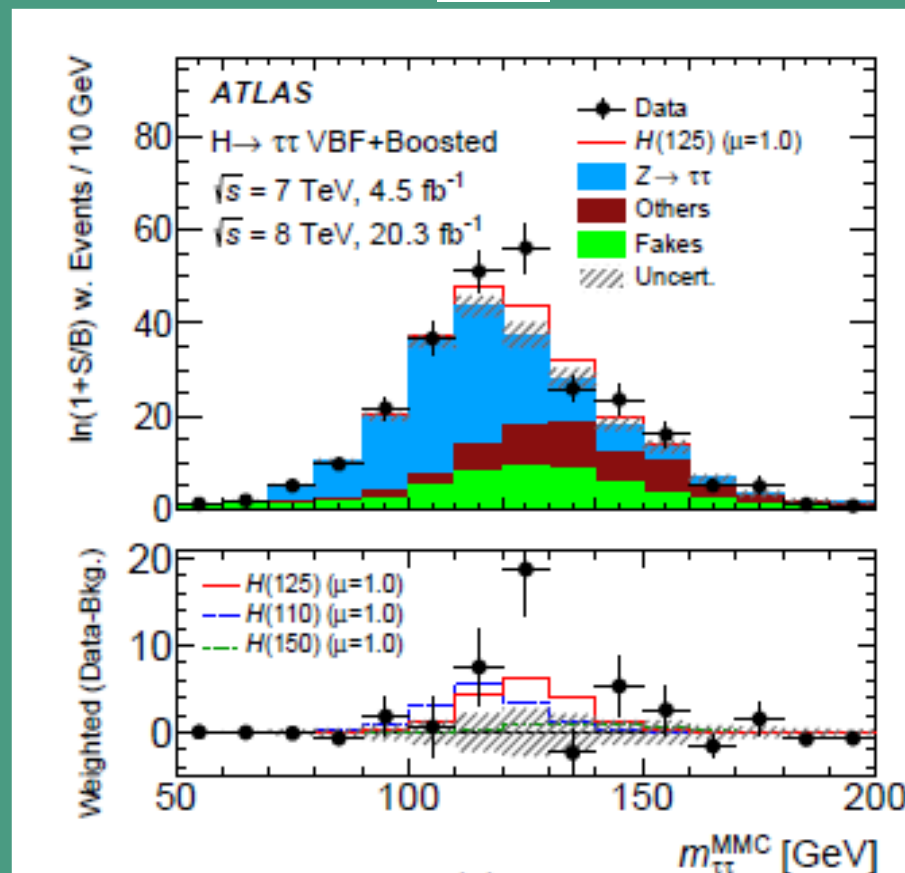
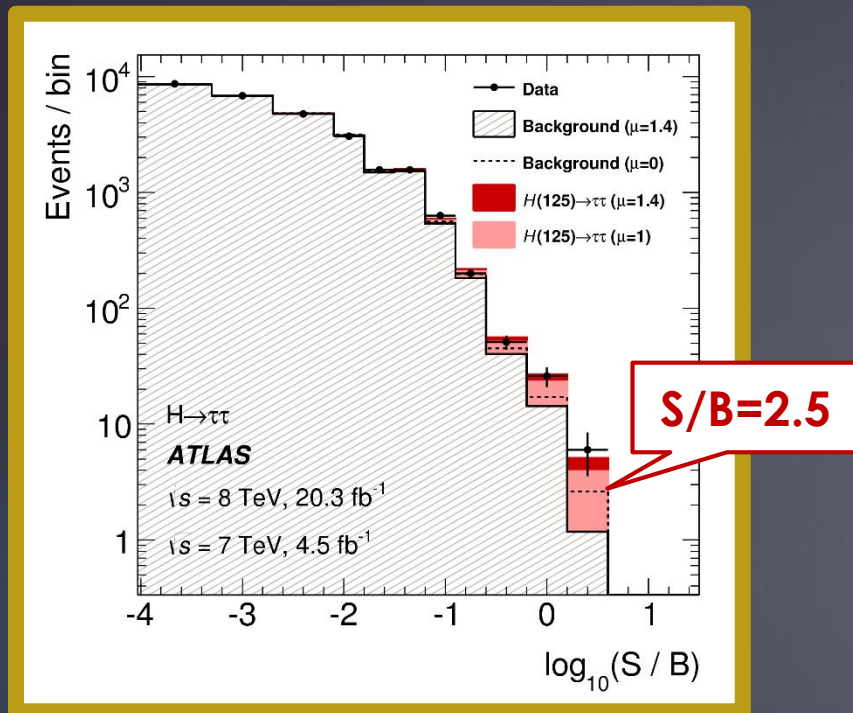
239

Invisibles 2015, Lydia Iconomidou-Fayard
16/06/2015



Channel and Category	Expected Significance (σ)	Observed Significance (σ)
$\tau_{lep}\tau_{lep}$ VBF	1.15	1.88
$\tau_{lep}\tau_{lep}$ Boosted	0.57	1.72
$\tau_{lep}\tau_{lep}$ Total	1.25	2.40
$\tau_{lep}\tau_{had}$ VBF	2.11	2.23
$\tau_{lep}\tau_{had}$ Boosted	1.11	1.01
$\tau_{lep}\tau_{had}$ Total	2.33	2.33
$\tau_{had}\tau_{had}$ VBF	1.70	2.23
$\tau_{had}\tau_{had}$ Boosted	0.82	2.56
$\tau_{had}\tau_{had}$ Total	1.99	3.25
Combined	3.43	4.54

H → $\tau\tau$: the ATLAS final result



Significance : 4.5 σ (3.4 σ expected)

Channel and Category	Expected Significance (σ)	Observed Significance (σ)
$\tau_{lep}\tau_{lep}$ VBF	1.15	1.88
$\tau_{lep}\tau_{lep}$ Boosted	0.57	1.72
$\tau_{lep}\tau_{lep}$ Total	1.25	2.40
$\tau_{lep}\tau_{had}$ VBF	2.11	2.23
$\tau_{lep}\tau_{had}$ Boosted	1.11	1.01
$\tau_{lep}\tau_{had}$ Total	2.33	2.33
$\tau_{had}\tau_{had}$ VBF	1.70	2.23
$\tau_{had}\tau_{had}$ Boosted	0.82	2.56
$\tau_{had}\tau_{had}$ Total	1.99	3.25
Combined	3.43	4.54

H- \rightarrow bb : the dominant

241

BR=58% at $M_H=125\text{GeV}$
But overwhelming QCD background

H- \rightarrow bb : the dominant

242

Invisibles 2015, Lydia Iconomidou-Fayard
16/06/2015

BR=58% at $M_H=125\text{GeV}$
But overwhelming QCD background

Use **associated Higgs production** $W(Z)H \rightarrow bb$
to increase the S/B ratio. Lower production
Xsection but easier signatures.

H- \rightarrow bb : the dominant

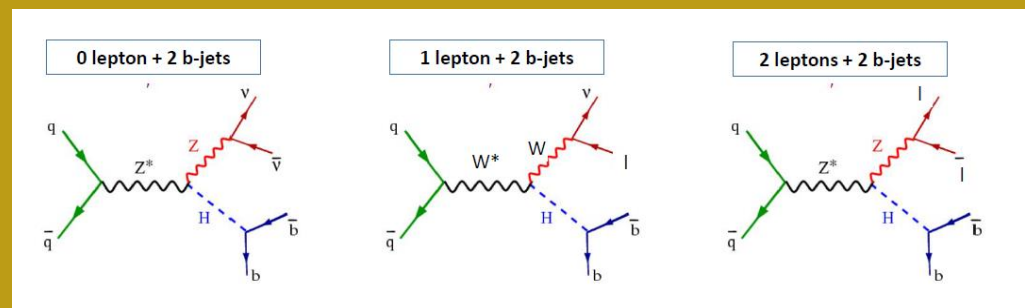
243

Invisibles 2015, Lydia Iconomidou-Fayard
16/06/2015

BR=58% at $M_H=125\text{GeV}$
But overwhelming QCD background

Use **associated Higgs production** $W(Z)H \rightarrow bb$
to increase the S/B ratio. Lower production
Xsection but easier signatures.

Requested signatures
 \rightarrow 0, 1 or two isolated and well identified leptons
(for the W or Z)
 \rightarrow 2 jets tagged as B



SIGNAL

H->bb : the dominant

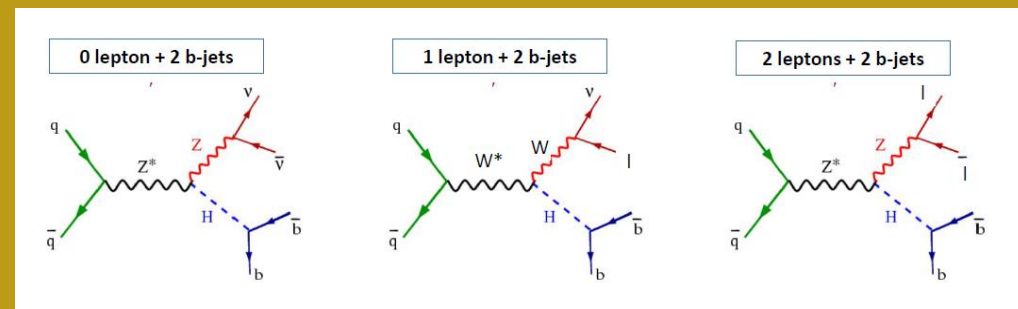
BR=58% at $M_H=125\text{GeV}$
But overwhelming QCD background

Use **associated Higgs production** $W(Z)H \rightarrow bb$
to increase the S/B ratio. Lower production
Xsection but easier signatures.

Backgrounds ;
Dibosons (WW, WZ, ZZ)
Bosons + jets
Ttbar, multijets

Backgrounds

Requested signatures
→ 0, 1 or two isolated and well identified leptons
(for the W or Z)
→ 2 jets tagged as B



SIGNAL

VH- \rightarrow bb

Require 2 b-tagged jets

245

Invisibles 2015, Lydia Iconomidou-Fayard
16/06/2015

VH- \rightarrow bb

Require 2 b-tagged jets

B-tagging algorithms, based on multivariate technics.

Inputs : track parameters and reconstruction of the secondary vertex

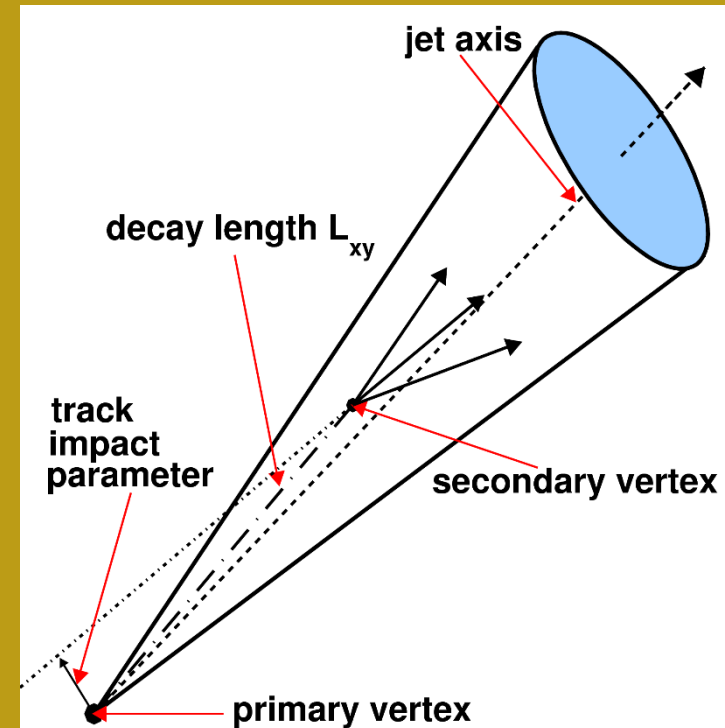
VH- \rightarrow bb

247

Require 2 b-tagged jets

B-tagging algorithms, based on multivariate technics.

Inputs : track parameters and reconstruction of the secondary vertex



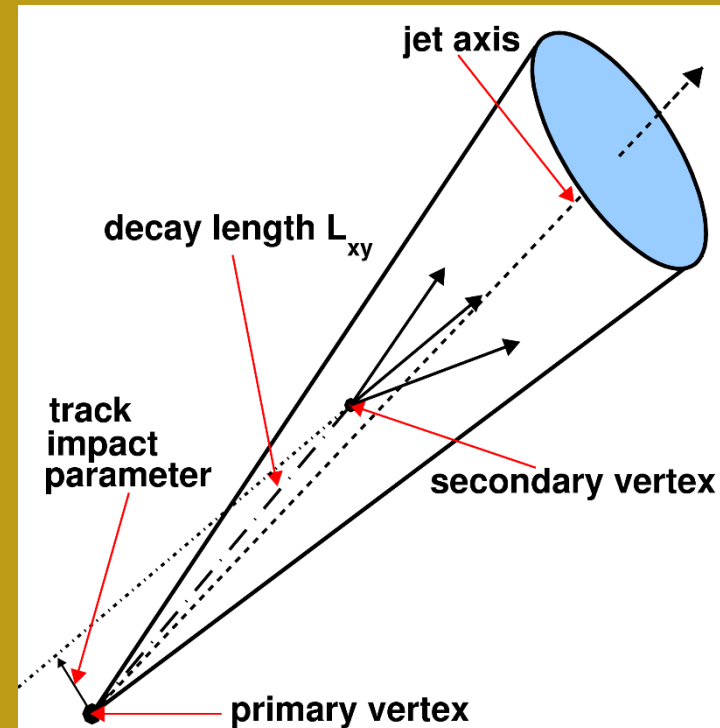
VH->bb

Require 2 b-tagged jets

B-tagging algorithms, based on multivariate technics.

Inputs : track parameters and reconstruction of the secondary vertex

Three b-tag working points;
Loose for 80% b-tag efficiency
Medium for 70% b-tag efficiency
Tight for 50% b-tag efficiency



VH- \rightarrow bb

249

A discriminant variable :
The bb invariant mass

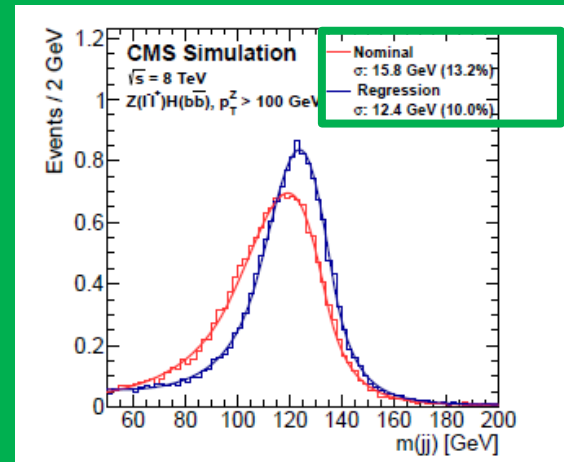
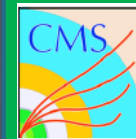
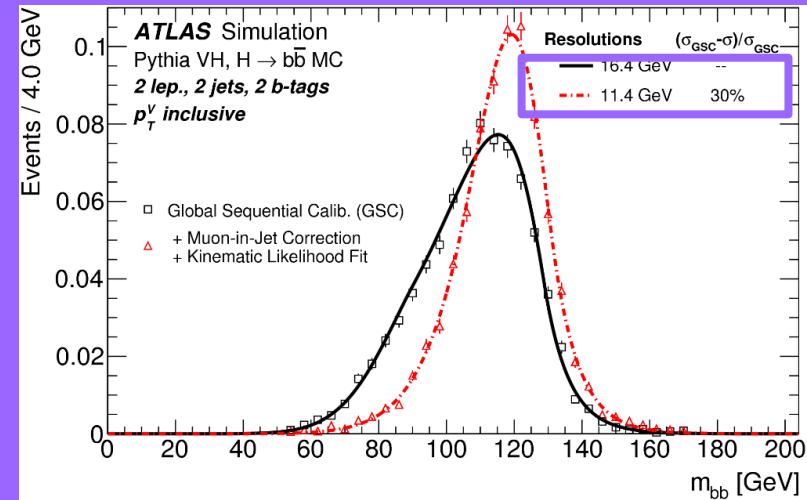
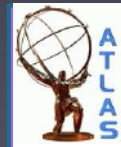
VH->bb

A discriminant variable :
The bb invariant mass

Improve the mass reconstruction

ATLAS: Add the muon momenta on top of the calorimetric jet energy.

CMS : MVA computation



VH->bb

A discriminant variable :
The bb invariant mass

Improve the mass reconstruction

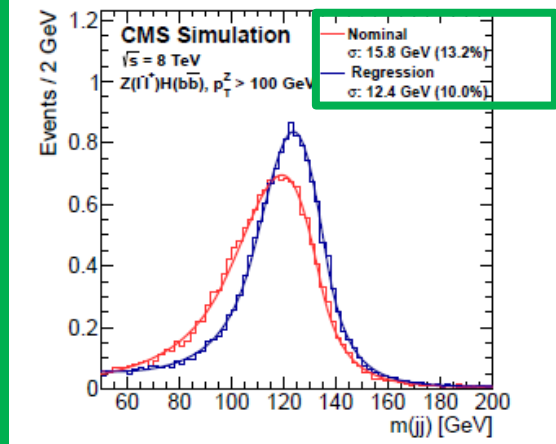
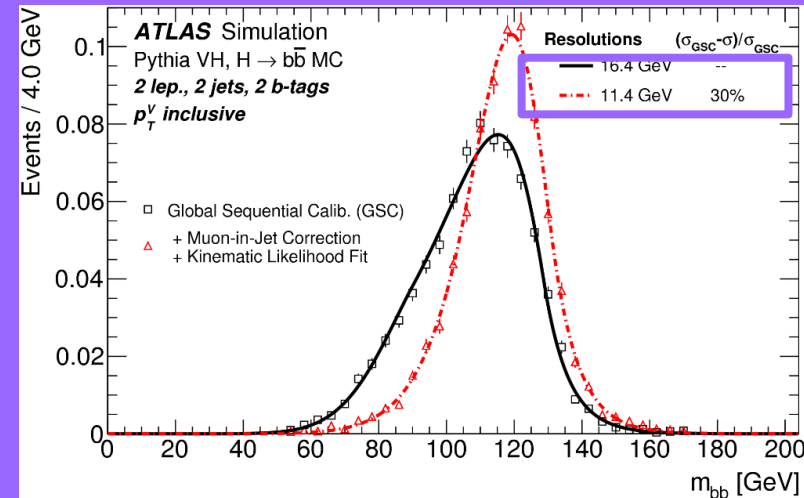
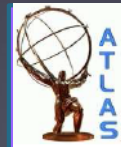
ATLAS: Add the muon momenta on top of the calorimetric jet energy.

CMS : MVA computation

Other discriminant variables : P_T^{ν} , ΔR (b1,b2)

Split in categories

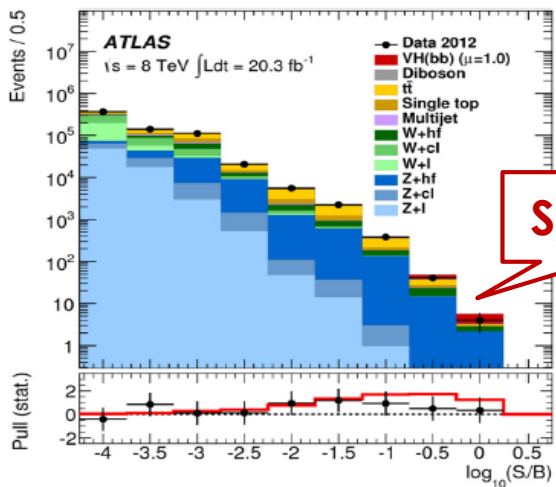
Use a Boosted Decision Tree to improve sensitivity



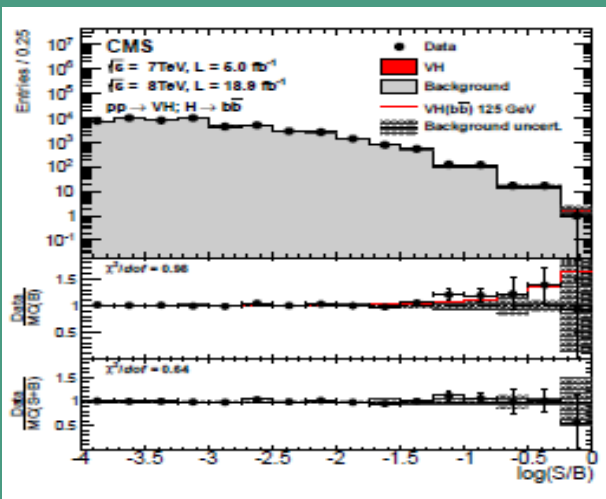
VH->bb : Can we see something?

252

Signal and Bkg in bins of S/B



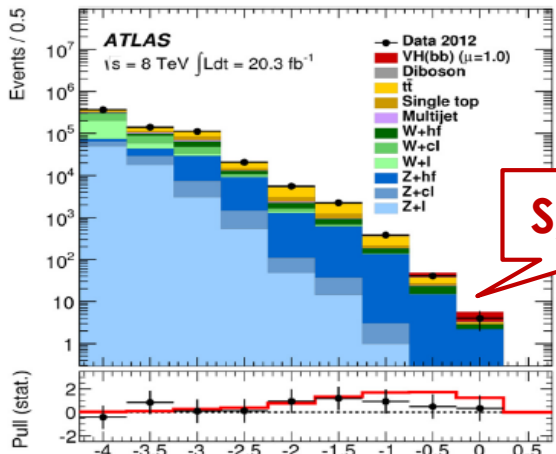
S/B=0.7



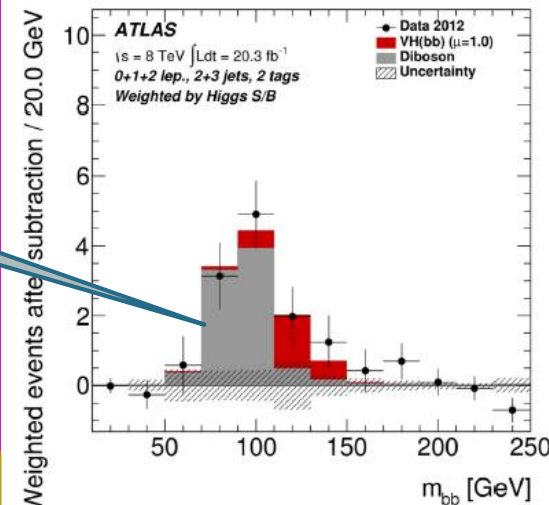
VH->bb : Can we see something?

Signal and Bkg in bins of S/B

Background subtracted data
Weighted by S/B

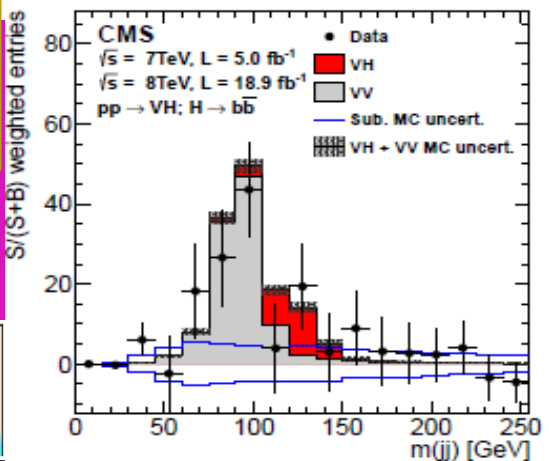
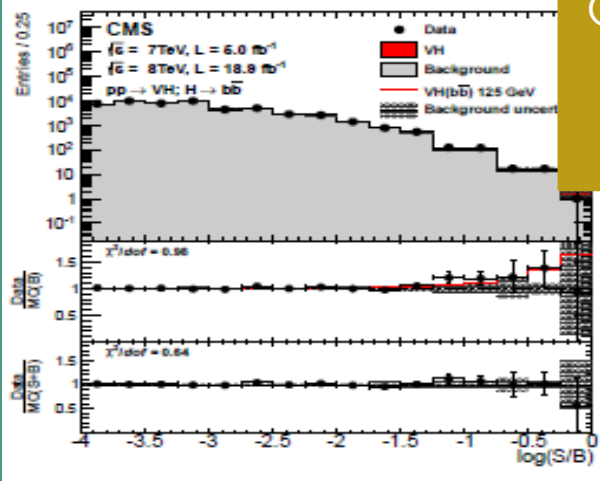


S/B=0.7



VZ

Observed (expected) significance:
ATLAS : 1.4 σ (2.6)
CMS : 2.1 σ (2.1)



The Scalar Boson Mass

Measured precisely in both, **diphoton and ZZ channels**.

Review here the challenges of the mass measurements and the combination.

H- \rightarrow ZZ* \rightarrow 4l mass measurement

255

Ingredients:

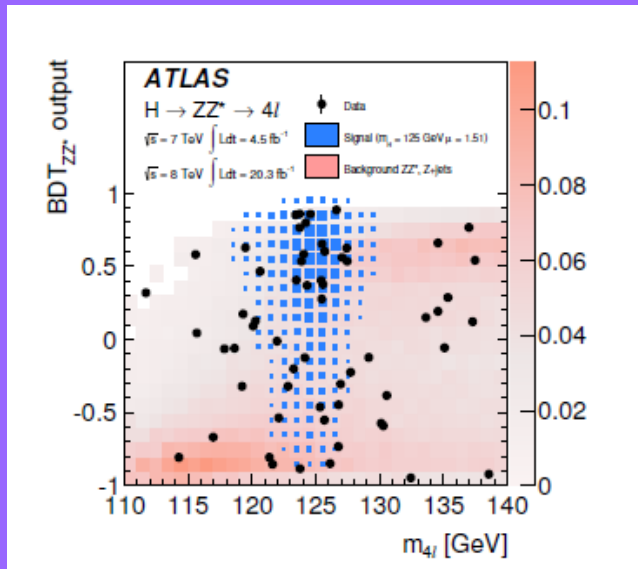
- Data
- Signal MC at 15 m_H values from 115- \rightarrow 130 GeV
- Background shape and yields from simulation (ZZ*) and data-driven measurements (Z+jets, ttbar..)
- Unbinned maximum likelihood of the 8 (m_{4l} , BDT) distributions (7 and 8 TeV data X 4 final modes).

H \rightarrow ZZ* \rightarrow 4l mass measurement

256

Ingredients:

- Data
- Signal MC at 15 m_H values from 115 \rightarrow 130 GeV
- Background shape and yields from simulation (ZZ*) and data-driven measurements (Z+jets, ttbar..)
- Unbinned maximum likelihood of the 8 (m_{4l} , BDT) distributions (7 and 8 TeV data X 4 final modes).

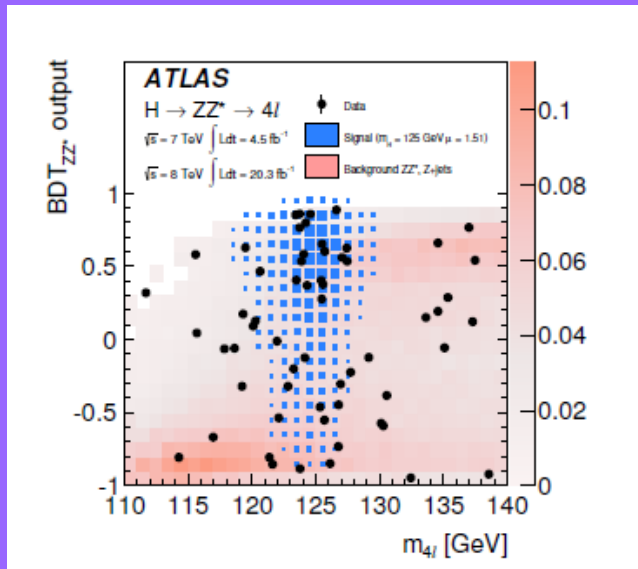


2D fit improves
by 8% the mass
statistical error

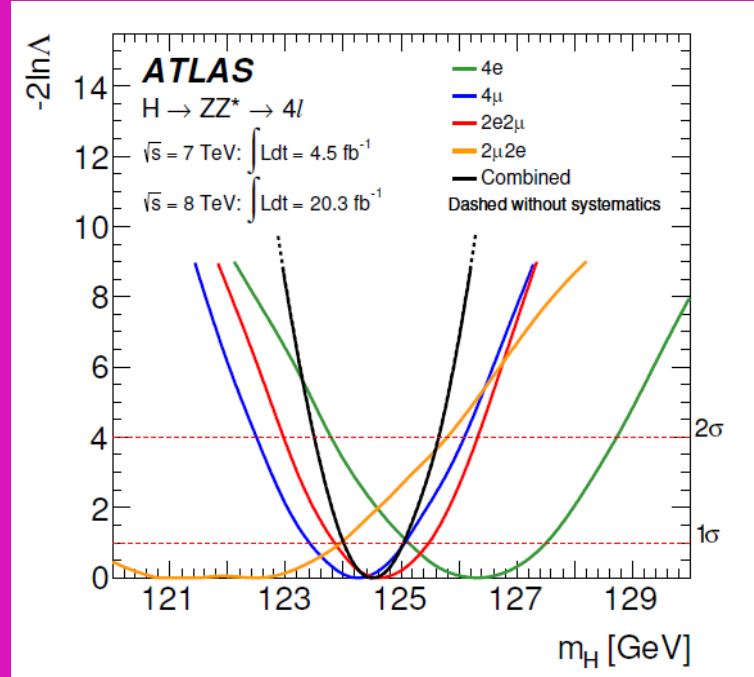
H \rightarrow ZZ* \rightarrow 4l mass measurement

Ingredients:

- Data
- Signal MC at 15 m_H values from 115 \rightarrow 130 GeV
- Background shape and yields from simulation (ZZ*) and data-driven measurements (Z+jets, ttbar..)
- Unbinned maximum likelihood of the 8 (m_{4l} , BDT) distributions (7 and 8 TeV data X 4 final modes).



2D fit improves by 8% the mass statistical error



$$M_H = 124.51 \pm 0.52 \text{ (stat)} \pm 0.06 \text{ (syst)}$$

Electron and muon energy scales



H- \rightarrow $\gamma\gamma$ mass measurement

258

Split data in
10 categories

Unconv. central low p_T
Unconv. central high p_T
Unconv. rest low p_T
Unconv. rest high p_T
Unconv. transition
Conv. central low p_T
Conv. central high p_T
Conv. rest low p_T
Conv. rest high p_T
Conv. transition

Unconverted photon
categories:
Better resolution than
converted



Central photons ($|\eta| < 0.75$):
Better resolution and smaller
energy scale uncertainties

H- \rightarrow $\gamma\gamma$ mass measurement

259

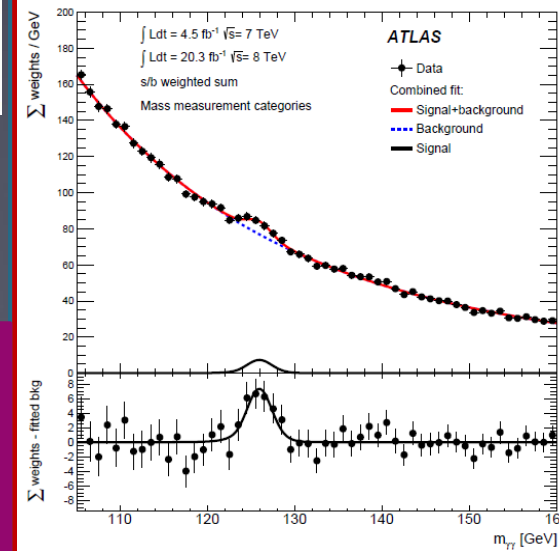
Split data in
10 categories

Unconv. central low p_T
Unconv. central high p_T
Unconv. rest low p_T
Unconv. rest high p_T
Unconv. transition
Conv. central low p_T
Conv. central high p_T
Conv. rest low p_T
Conv. rest high p_T
Conv. transition

Unconverted photon
categories:
Better resolution than
converted



Central photons ($|\eta| < 0.75$):
Better resolution and smaller
energy scale uncertainties



Invisibles 2015, Lydia Iconomidou-Fayard
16/06/2015

→ **Signal Modeling:** A Crystal-Ball + wider Gaussian to model tails

→ **Background modeling:** Analytical functions in 105-160 GeV tested in large dijet, jet+photon and diphoton simulated samples.

H- \rightarrow $\gamma\gamma$ mass measurement

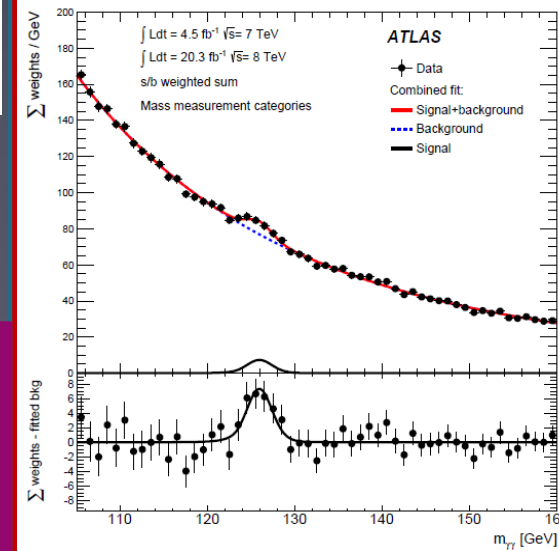
260

Split data in 10 categories

Unconv. central low p_T
Unconv. central high p_T
Unconv. rest low p_T
Unconv. rest high p_T
Unconv. transition
Conv. central low p_T
Conv. central high p_T
Conv. rest low p_T
Conv. rest high p_T
Conv. transition

Unconverted photon categories:
Better resolution than converted

Central photons ($|\eta| < 0.75$):
Better resolution and smaller energy scale uncertainties



Invisibles 2015, Lydia Iconomidou-Fayard
16/06/2015

→ **Signal Modeling**: A Crystal-Ball + wider Gaussian to model tails

→ **Background modeling**: Analytical functions in 105-160 GeV tested in large dijet, jet+photon and diphoton simulated samples.

$$M_H = 126.98 \pm 0.42(\text{stat}) \pm 0.28(\text{syst}) \text{ GeV}$$

Dominated by photon energy scale

H → $\gamma\gamma$ mass measurement

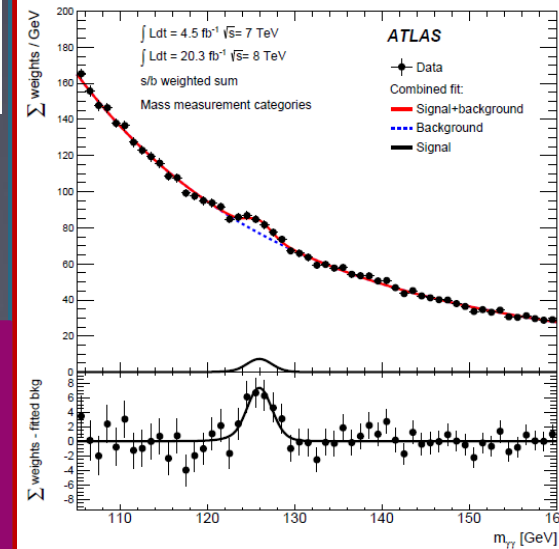
261

Split data in 10 categories

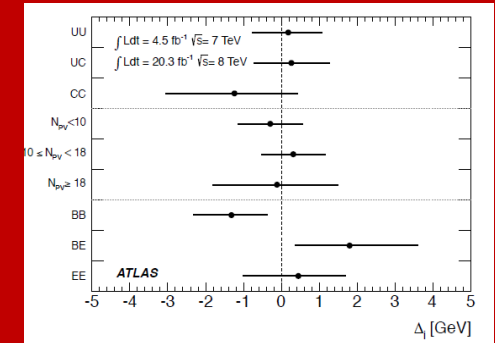
- Unconv. central low p_T
- Unconv. central high p_T
- Unconv. rest low p_T
- Unconv. rest high p_T
- Unconv. transition
- Conv. central low p_T
- Conv. central high p_T
- Conv. rest low p_T
- Conv. rest high p_T
- Conv. transition

Unconverted photon categories:
Better resolution than converted

Central photons ($|\eta| < 0.75$):
Better resolution and smaller energy scale uncertainties



Checks of M_H in other categories



→ **Signal Modeling**: A Crystal-Ball + wider Gaussian to model tails

→ **Background modeling**: Analytical functions in 105-160 GeV tested in large dijet, jet+photon and diphoton simulated samples.

$$M_H = 126.98 \pm 0.42(\text{stat}) \pm 0.28(\text{syst}) \text{ GeV}$$

Dominated by photon energy scale

Issues related to the $H \rightarrow \gamma\gamma$ and $H \rightarrow ZZ^* \rightarrow 4l$ mass combination

Systematic uncertainties on m_H^{4l} and $m_H^{\gamma\gamma}$
dominated by energy scale

Issues related to the $H \rightarrow \gamma\gamma$ and $H \rightarrow ZZ^* \rightarrow 4l$ mass combination

Systematic uncertainties on m_H^{4l} and $m_H^{\gamma\gamma}$
dominated by energy scale

- 1) Energy scale studies performed with electrons from $Z \rightarrow ee$
- 2) The obtained effects cross-checked for photons with a low statistics $Z \rightarrow \mu\mu\gamma$ data.
- 3) They are extrapolated to photons via simulations of the electron-photon differences (longitudinal shower shape, converted-unconverted etc)
→ Uncommon uncertainties

Issues related to the $H \rightarrow \gamma\gamma$ and $H \rightarrow ZZ^* \rightarrow 4l$ mass combination

Systematic uncertainties on m_H^{4l} and $m_H^{\gamma\gamma}$
dominated by energy scale

- 1) Energy scale studies performed with electrons from $Z \rightarrow ee$
- 2) The obtained effects cross-checked for photons with a low statistics $Z \rightarrow \mu\mu\gamma$ data.
- 3) They are extrapolated to photons via simulations of the electron-photon differences (longitudinal shower shape, converted-unconverted etc)
→ Uncommon uncertainties

Systematic	Uncertainty on m_H [MeV]
LAr syst on material before presampler (barrel)	70
LAr syst on material after presampler (barrel)	20
LAr cell non-linearity (layer 2)	60
LAr cell non-linearity (layer 1)	30
LAr layer calibration (barrel)	50
Lateral shower shape (conv)	50
Lateral shower shape (unconv)	40
Presampler energy scale (barrel)	20
ID material model ($ \eta < 1.1$)	50
$H \rightarrow \gamma\gamma$ background model (unconv rest low p_{Tl})	40
$Z \rightarrow ee$ calibration	50
Primary vertex effect on mass scale	20
Muon momentum scale	10
Remaining systematic uncertainties	70
Total	180

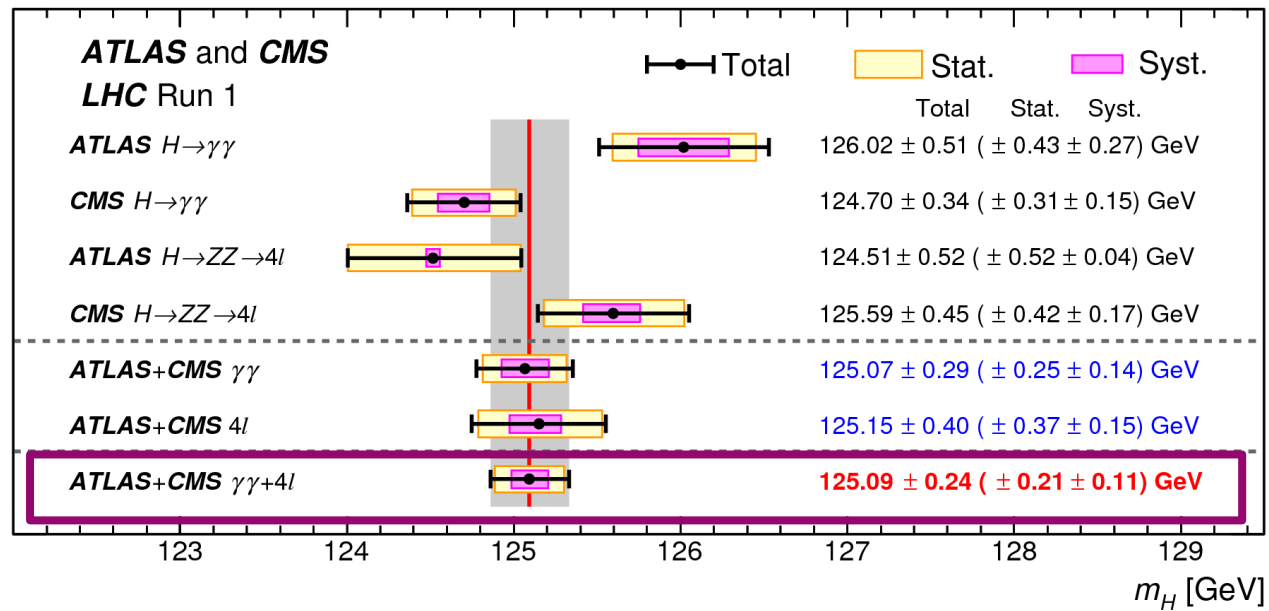
Energy Scale
related

Sources of final uncertainties on the Combined ATLAS mass.

The RUN1 Higgs mass combined measurement from ATLAS+CMS

265

Invisibles 2015, L
16/06/2015



ATLAS : $m_H = 125.36 \pm 0.41$ GeV



CMS : $m_H = 125.02 \pm 0.30$ GeV

m_H at Run1 known to 240MeV (<0.2% !)
Dominated by statistics

The New boson properties

Its quantum numbers, its width and its couplings
to fermions and bosons

The Spin and Parity

267

The observed decay of the $H \rightarrow \gamma\gamma$ restricts the possible Higgs spins to 0 and 2.

At LHC, analyses searched for several scenarios, implying

- Spin 2 resonances
- Pure 0^+ , or 0^- BSM Higgs Boson
- Mixture of 0^+ and 0^-

diakonomidou-fayard



The Spin and Parity

268

The observed decay of the $H \rightarrow \gamma\gamma$ restricts the possible Higgs spins to 0 and 2.

At LHC, analyses searched for several scenarios, implying

- Spin 2 resonances
- Pure 0^+ , or 0^- BSM Higgs Boson
- Mixture of 0^+ and 0^-

SPIN 2 Tensor-field $X^{\mu\nu}$ Lagrangian

$$\mathcal{L}_2 = \frac{1}{\Lambda} \left[\sum_V k_V X^{\mu\nu} \mathcal{T}_{\mu\nu}^V + \sum_f k_f X^{\mu\nu} \mathcal{T}_{\mu\nu}^f \right].$$

Couplings of $X^{\mu\nu}$: k_V to bosons k_f to fermions

Production via qq and $qg \rightarrow$ Study cases:

- 1) $k_g = k_q$ (universal coupling UC)
- 2) $k_g \neq k_q$: gives a characteristic high tail to the P_T of the resonance

The Spin and Parity

The observed decay of the H→γγ restricts the possible Higgs spins to 0 and 2.

At LHC, analyses searched for several scenarii, implying
 → Spin 2 resonances
 → Pure 0+, or 0- BSM Higgs Boson
 → Mixture of 0+ and 0-

SPIN 2 Tensor-field X^{μν} Lagrangian

$$\mathcal{L}_2 = \frac{1}{\Lambda} \left[\sum_V \kappa_V X^{\mu\nu} \mathcal{T}_{\mu\nu}^V + \sum_f \kappa_f X^{\mu\nu} \mathcal{T}_{\mu\nu}^f \right].$$

Couplings of X^{μν}: k_v to bosons k_f to fermions

Production via qq and qg→ Study cases:

- 1) k_g = k_q (universal coupling UC)
- 2) k_g ≠ k_q : gives a characteristic high tail to the P_T of the resonance

Spin 0 mixed CP Lagrangian for W and Z

$$\mathcal{L}_0^V = \left\{ c_\alpha \kappa_{SM} \left[\frac{1}{2} g_{HZZ} Z_\mu Z^\mu + g_{HWW} W_\mu^+ W^{-\mu} \right] - \frac{1}{4} \frac{1}{\Lambda} \left[c_\alpha \kappa_{HZZ} Z_{\mu\nu} Z^{\mu\nu} + s_\alpha \kappa_{AZZ} Z_{\mu\nu} \tilde{Z}^{\mu\nu} \right] - \frac{1}{2} \frac{1}{\Lambda} \left[c_\alpha \kappa_{HWW} W_{\mu\nu}^+ W^{-\mu\nu} + s_\alpha \kappa_{AWW} W_{\mu\nu}^+ \tilde{W}^{-\mu\nu} \right] \right\} X_0.$$

Couplings of X₀ : K_{SM} to standard model, k_{HVV} to BSM 0+ et k_{AVV} to BSM 0- interactions
 Mixing CP-states angle **α, s_α = sina, c_α = cosa**

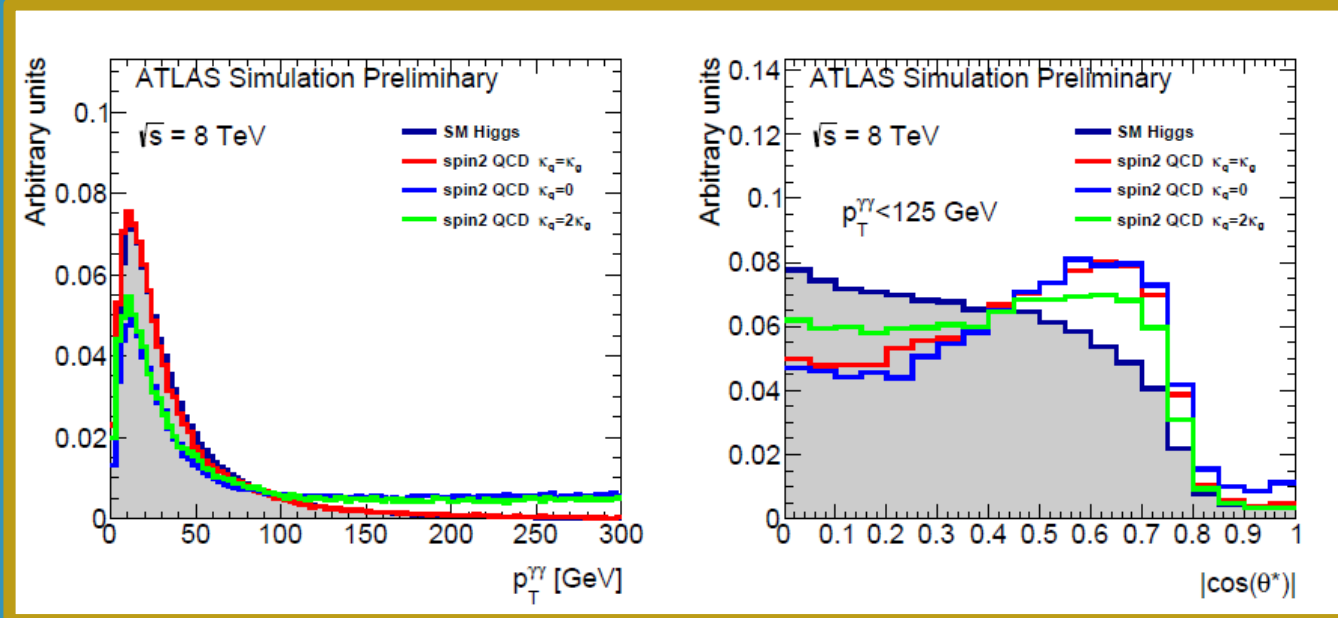
J ^P	Model	Choice of tensor couplings			
		κ _{SM}	κ _{HVV}	κ _{AVV}	α
0 ⁺	Standard Model Higgs boson	1	0	0	0
0 ⁺ _h	BSM spin-0 CP-even	0	1	0	0
0 ⁻	BSM spin-0 CP-odd	0	0	1	π/2



Spin 0 vs Spin 2 : tested with $H \rightarrow \gamma\gamma$, $H \rightarrow ZZ^* \rightarrow 4l$ and $H \rightarrow WW^* \rightarrow |v|v$

$H \rightarrow \gamma\gamma$: Use $P_T^{\gamma\gamma}$ and the angle in the Collins-Sopfer frame

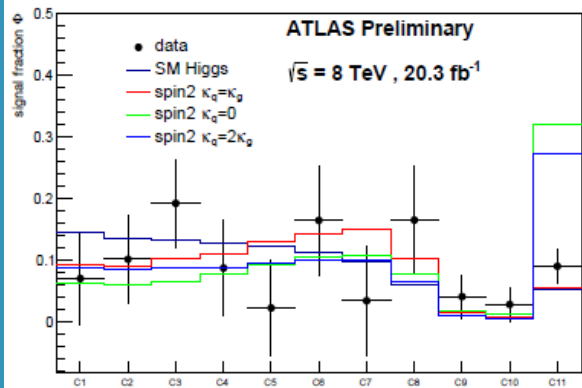
$$|\cos \theta^*| = \frac{|\sinh(\Delta\eta^{\gamma\gamma})|}{\sqrt{1 + (p_T^{\gamma\gamma}/m_{\gamma\gamma})^2}} \frac{2p_T^{\gamma 1} p_T^{\gamma 2}}{m_{\gamma\gamma}^2},$$



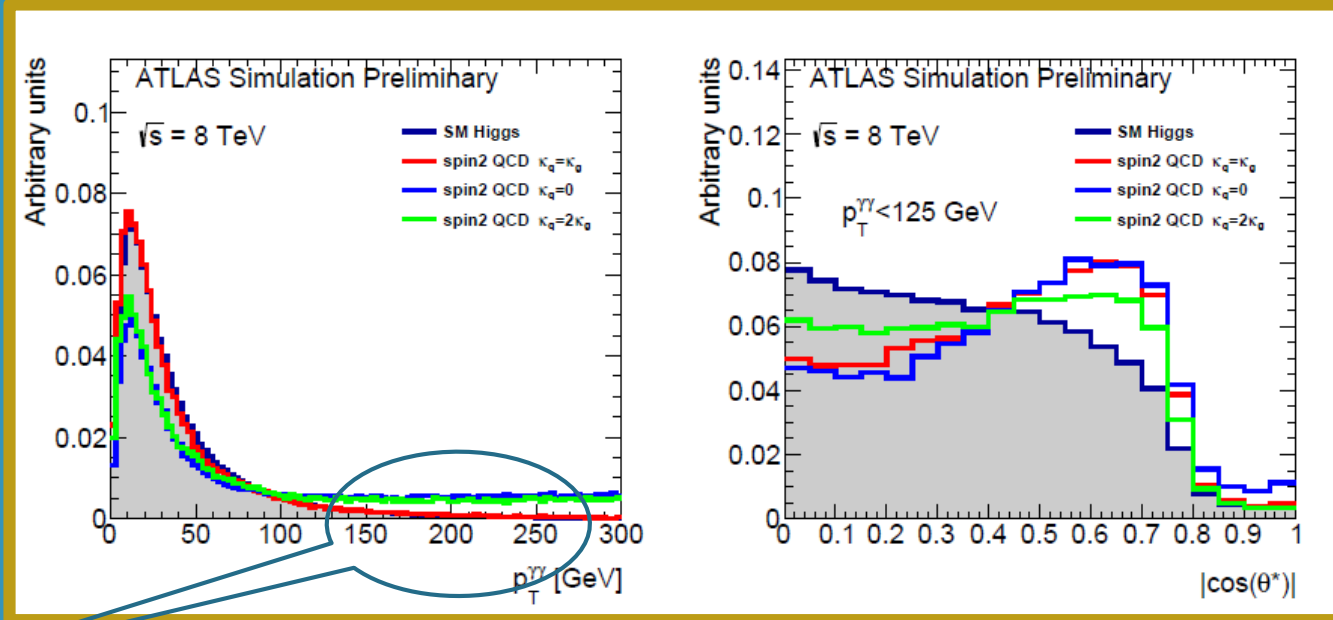
Spin 0 vs Spin 2 : tested with $H \rightarrow \gamma\gamma$, $H \rightarrow ZZ^* \rightarrow 4l$ and $H \rightarrow WW^* \rightarrow l\nu l\nu$

$H \rightarrow \gamma\gamma$: Use $P_T^{\gamma\gamma}$ and the angle in the Collins-Sopfer frame

$$|\cos \theta^*| = \frac{|\sinh(\Delta\eta^{\gamma\gamma})|}{\sqrt{1 + (p_T^{\gamma\gamma}/m_{\gamma\gamma})^2}} \frac{2p_T^{\gamma 1} p_T^{\gamma 2}}{m_{\gamma\gamma}^2},$$



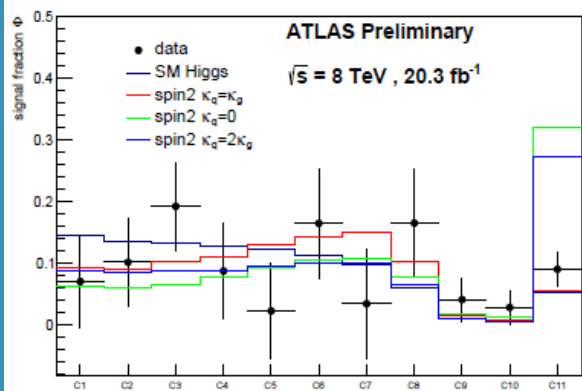
Nbin/Ntot in 10 $|\cos \theta^*|$ bins



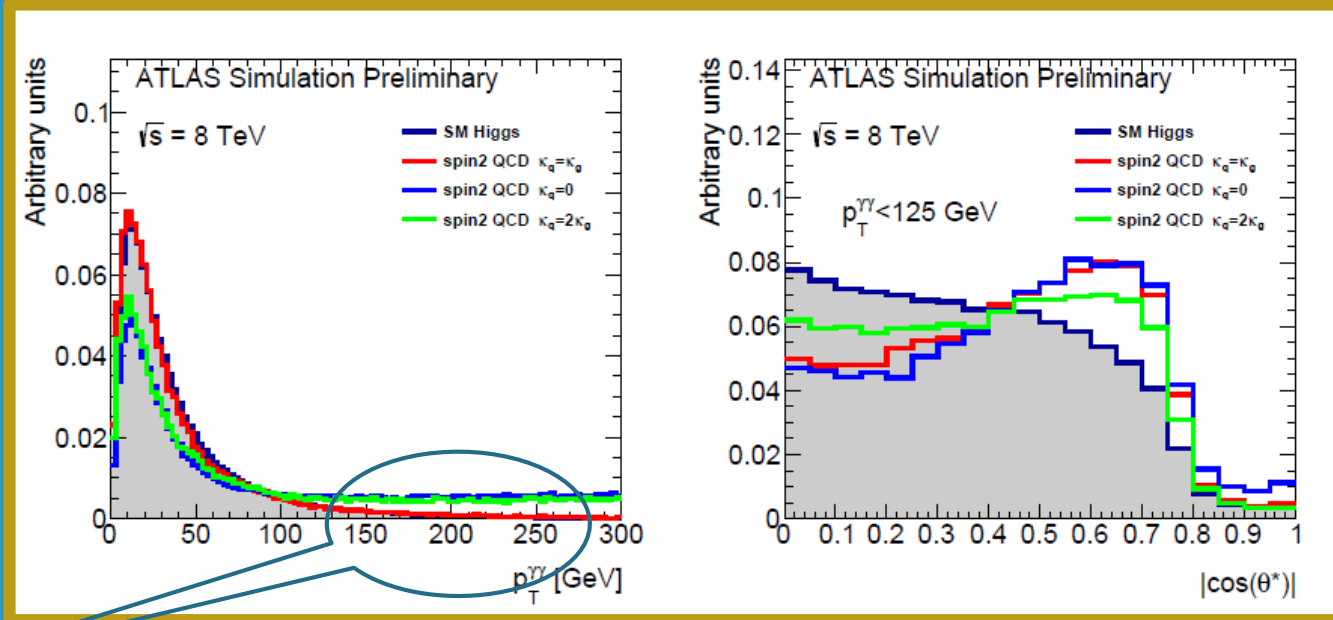
Spin 0 vs Spin 2 : tested with $H \rightarrow \gamma\gamma$, $H \rightarrow ZZ^* \rightarrow 4l$ and $H \rightarrow WW^* \rightarrow l\nu l\nu$

$H \rightarrow \gamma\gamma$: Use $P_T^{\gamma\gamma}$ and the angle in the Collins-Sopfer frame

$$|\cos \theta^*| = \frac{|\sinh(\Delta\eta^{\gamma\gamma})|}{\sqrt{1 + (p_T^{\gamma\gamma}/m_{\gamma\gamma})^2}} \frac{2p_T^{\gamma 1} p_T^{\gamma 2}}{m_{\gamma\gamma}^2},$$



Nbin/Ntot in 10 $|\cos\theta^*|$ bins



High $P_T^{\gamma\gamma}$ region:
Spin2 non-UC
scenarii strongly
disfavoured



Spin 0 vs Spin 2 : tested with $H \rightarrow \gamma\gamma$, $H \rightarrow ZZ^* \rightarrow 4l$ and $H \rightarrow WW^* \rightarrow l\nu l\nu$

$H \rightarrow ZZ^* \rightarrow 4l$

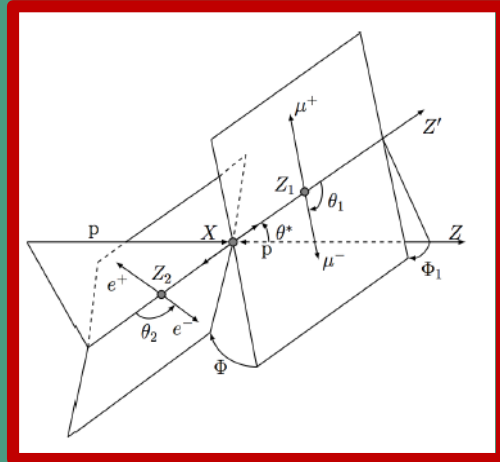
Profit from the information on various angles describing the production and decay.

Θ_1, Θ_2 : between l^- and Z s

Φ : angle of 2 decay planes

Φ_1 : leading lepton plane and Z_1

Θ^* : Z_1 angle in $4l$ -rest frame



Spin 0 vs Spin 2 : tested with $H \rightarrow \gamma\gamma$, $H \rightarrow ZZ^* \rightarrow 4l$ and $H \rightarrow WW^* \rightarrow l\nu l\nu$

$H \rightarrow ZZ^* \rightarrow 4l$

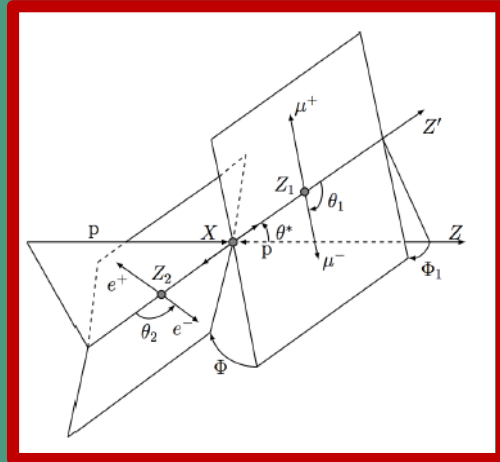
Profit from the information on various angles describing the production and decay.

Θ_1, Θ_2 : between l^- and Z s

Φ : angle of 2 decay planes

Φ_1 : leading lepton plane and Z_1

Θ^* : Z_1 angle in $4l$ -rest frame



$H \rightarrow WW^* \rightarrow l\nu l\nu$

Used variables: $m^{\parallel}, P_T^{\parallel}, m_T, \Delta P_T, \Delta\phi^{\parallel}, E_{ll\nu\nu}$

Combine them in 2 BDTs to test Spin and Parity

Spin 0 vs Spin 2 : tested with $H \rightarrow \gamma\gamma$, $H \rightarrow ZZ^* \rightarrow 4l$ and $H \rightarrow WW^* \rightarrow l\nu l\nu$

$H \rightarrow ZZ^* \rightarrow 4l$

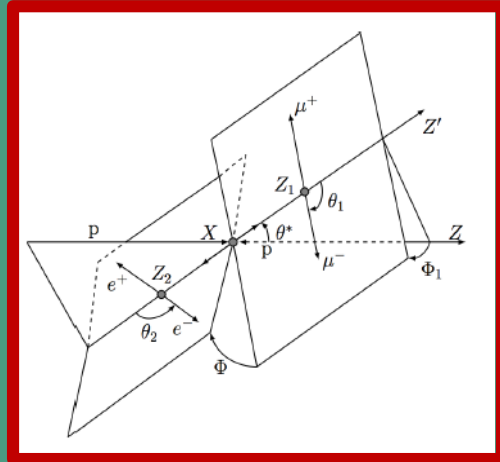
Profit from the information on various angles describing the production and decay.

Θ_1, Θ_2 : between l^- and Z s

Φ : angle of 2 decay planes

Φ_1 : leading lepton plane and Z_1

Θ^* : Z_1 angle in $4l$ -rest frame

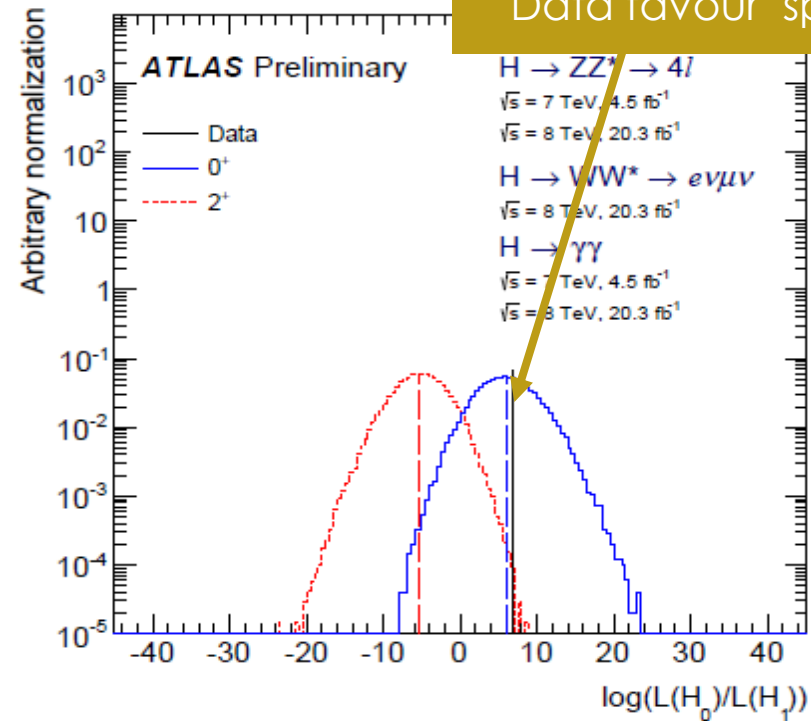


$H \rightarrow WW^* \rightarrow l\nu l\nu$

Used variables: $m^{\parallel}, P_T^{\parallel}, m_T, \Delta P_T, \Delta\phi^{\parallel}, E_{ll\nu\nu}$

Combine them in 2 BDTs to test Spin and Parity

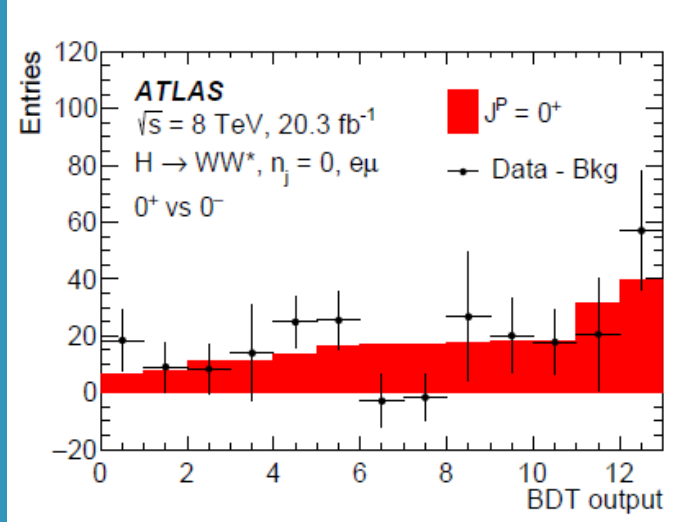
Combining 3 channels
Data favour spin 0



Spin 0, 0+ or 0-?

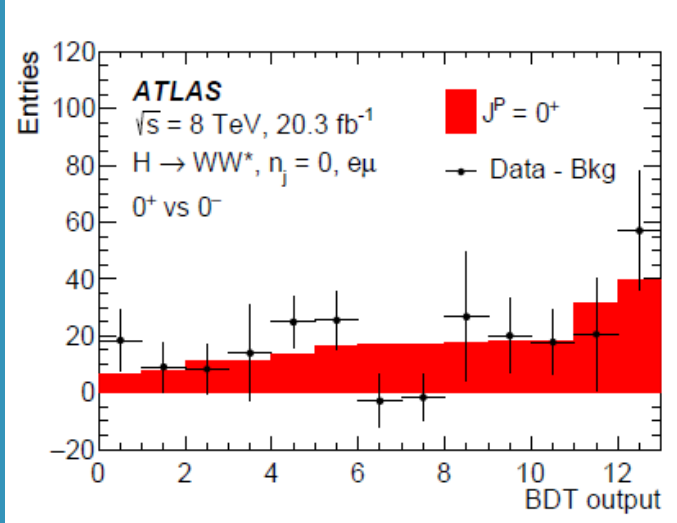
276

Exemple: $H \rightarrow WW^* \rightarrow l\nu l\nu$
BDT output and comparison with
scalar hypothesis



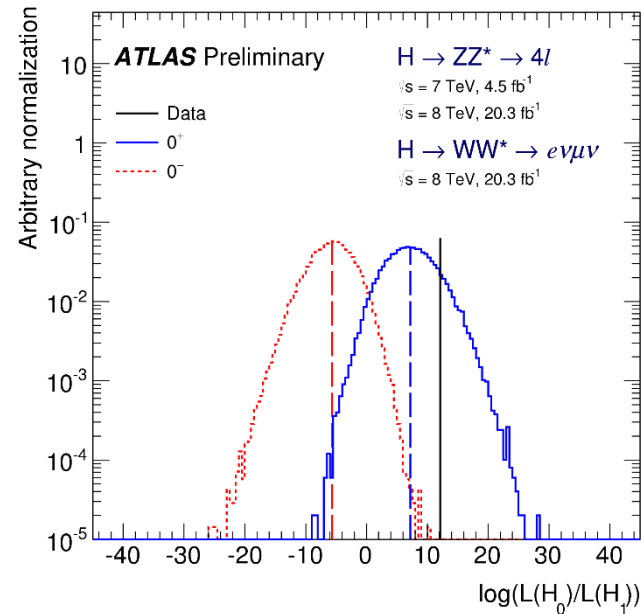
Spin 0, 0^+ or 0^- ?

Exemple: $H \rightarrow WW^* \rightarrow l\nu l\nu$
BDT output and comparison with
scalar hypothesis

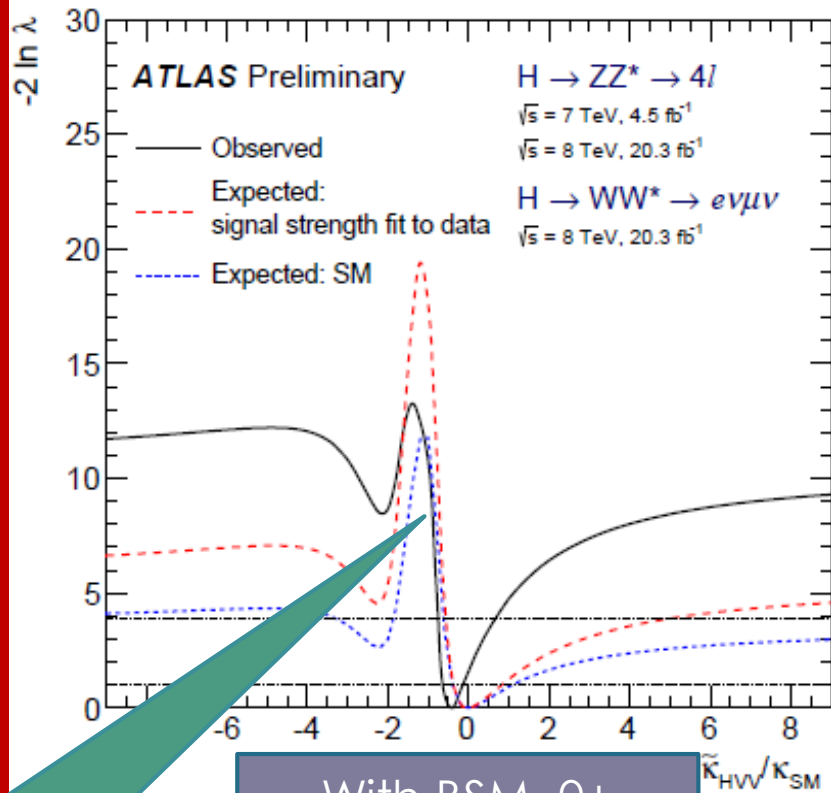


Data favour 0^+

Combined results using both
 $H \rightarrow ZZ^* \rightarrow 4l$ and $H \rightarrow WW^* \rightarrow l\nu l\nu$



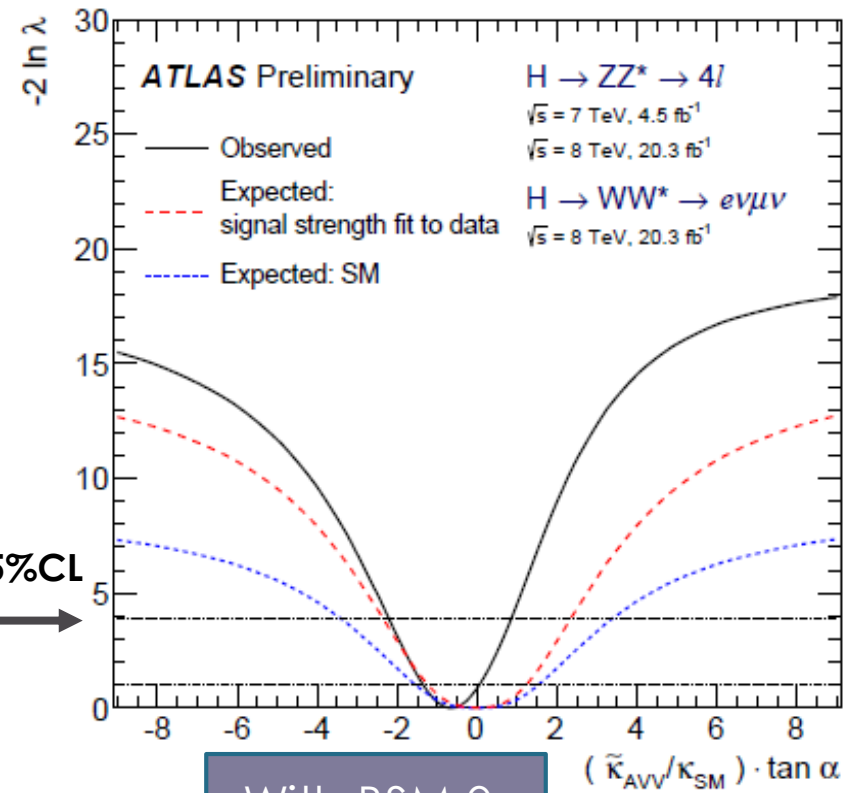
Spin 0^+ , pure or mixture with BSM?



With BSM 0^+
 <-0.7 and >0.6
 excluded

Interference effects
 between SM and BSM 0^+

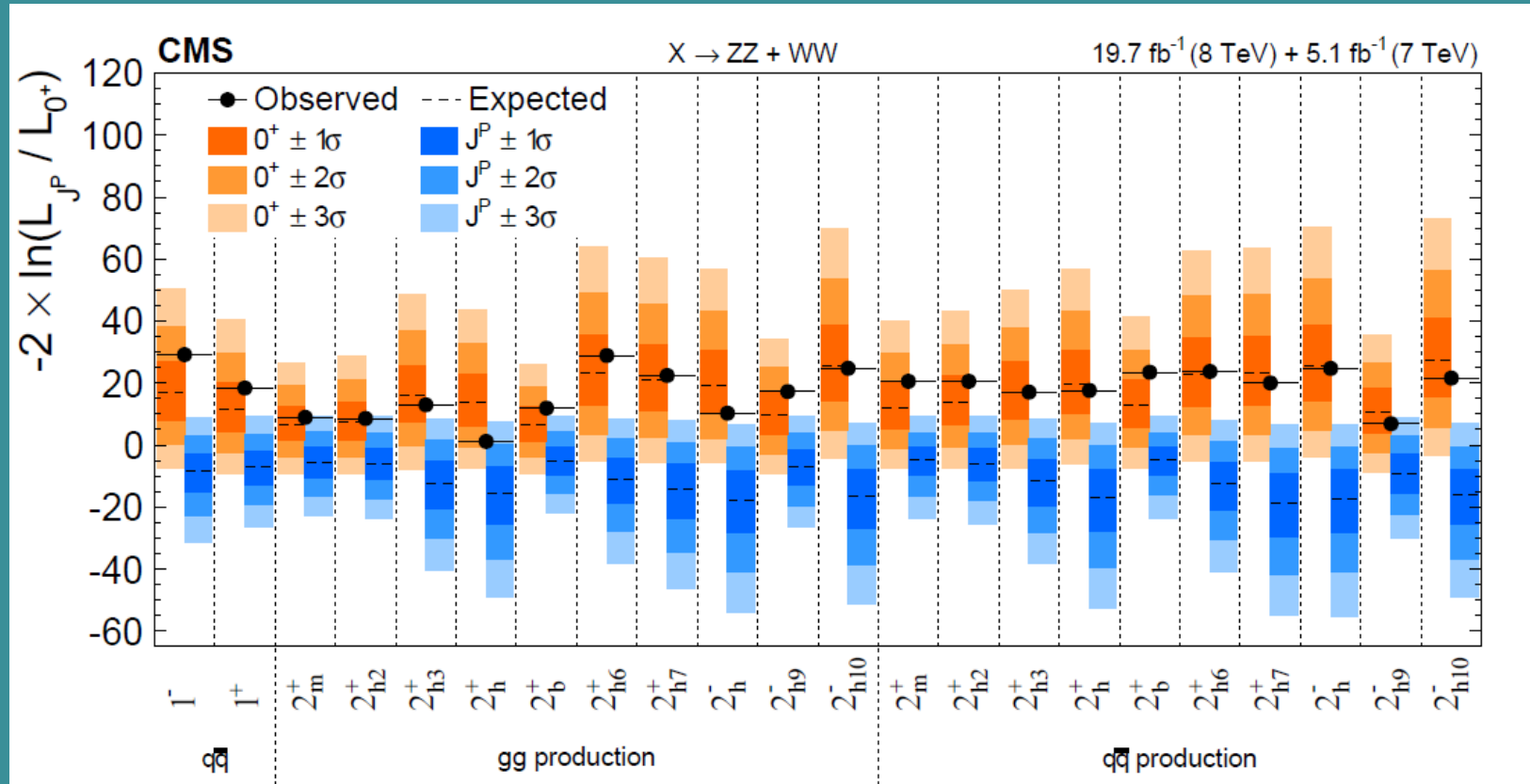
95%CL



With BSM 0^-
 <-2.2 and >0.8
 excluded

A long list of Spin-Parity models tested

279



Invisibles 2015, Lydia Iconomidou-Fayard
16/06/2015

→ Data points agree with the 0^+ SM prediction

The Scalar Boson Xsections and Branching ratios.

Analyses provide for each decay channel

- An observation significance (p_0)
- Constraints (or measurement) of the Higgs mass
- Constraints (or measurement) of the decay strength, often per production category

The Scalar Boson Xsections and Branching ratios.

Analyses provide for each decay channel

- An observation significance (p_0)
- Constraints (or measurement) of the Higgs mass
- Constraints (or measurement) of the decay strength, often per production category

Decay strength
expressed wrt SM
$$\mu = (\sigma \times \text{Br})_{\text{obs}} / (\sigma \times \text{BR})_{\text{SM}}$$

The Scalar Boson Xsections and Branching ratios.

Analyses provide for each decay channel

- An observation significance (p_0)
- Constraints (or measurement) of the Higgs mass
- Constraints (or measurement) of the decay strength, often per production category

Decay strength
expressed wrt SM

$$\mu = (\sigma \times \text{Br})_{\text{obs}} / (\sigma \times \text{BR})_{\text{SM}}$$

Important, since a deviation could be a sign of new physics (new channels, different couplings)

The Scalar Boson Xsections and Branching ratios.

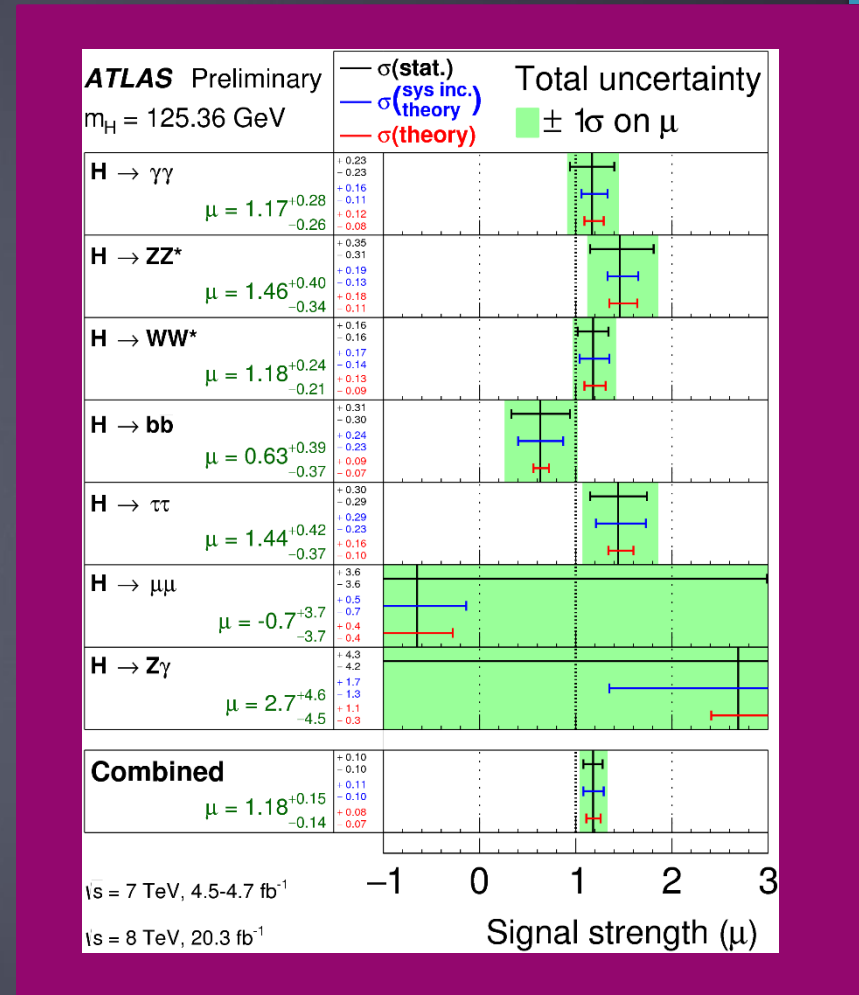
Analyses provide for each decay channel

- An observation significance (p0)
- Constraints (or measurement) of the Higgs mass
- Constraints (of measurement) of the decay strength, often per production category

Decay strength expressed wrt SM

$$\mu = (\sigma \times Br)_{obs} / (\sigma \times BR)_{SM}$$

Important, since a deviation could be a sign of new physics (new channels, different couplings)

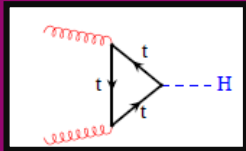


Combined Higgs global signal strength:
 $\mu = 1.18 + 0.15 - 0.14$

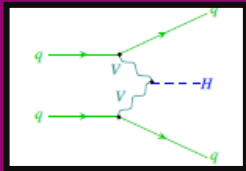
Signal strength for Higgs production mechanisms

284

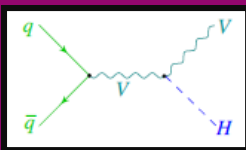
Invisibles 2015, Lydia Iconomidou-Fayard
16/06/2015



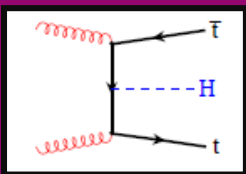
ggF



VBF

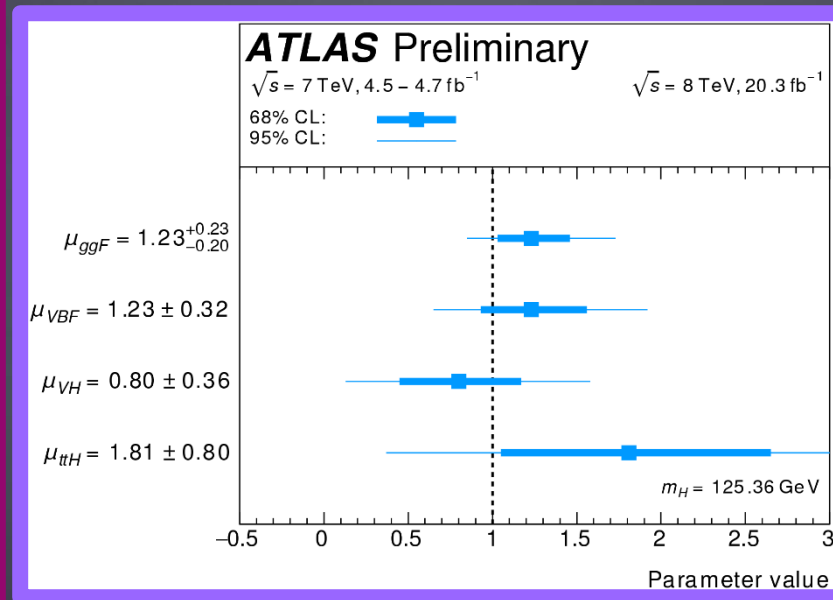
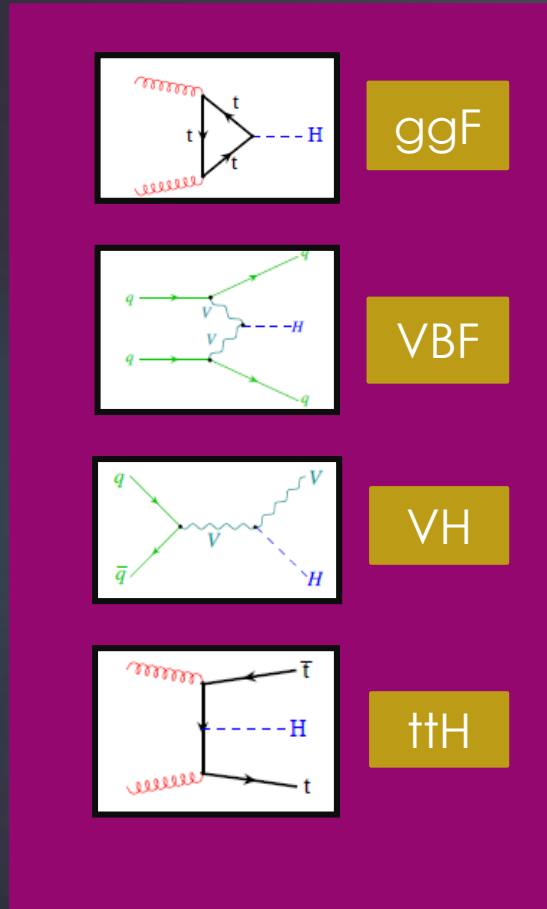


VH



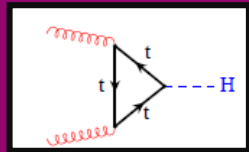
ttH

Signal strength for Higgs production mechanisms

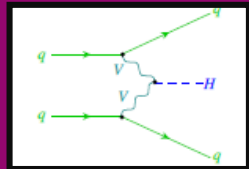


All decay channels together assuming SM Branching ratios

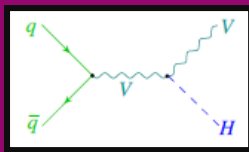
Signal strength for Higgs production mechanisms



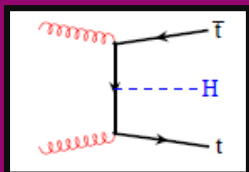
ggF



VBF

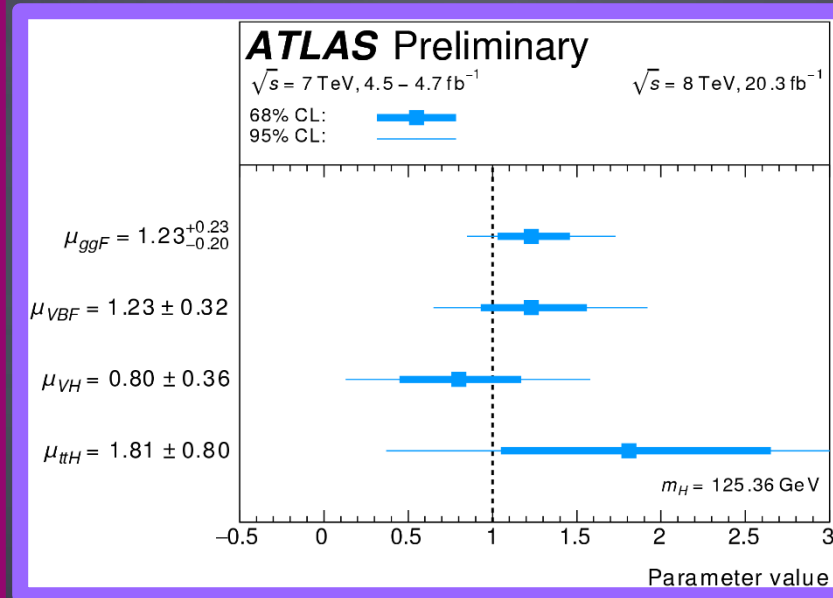


VH



ttH

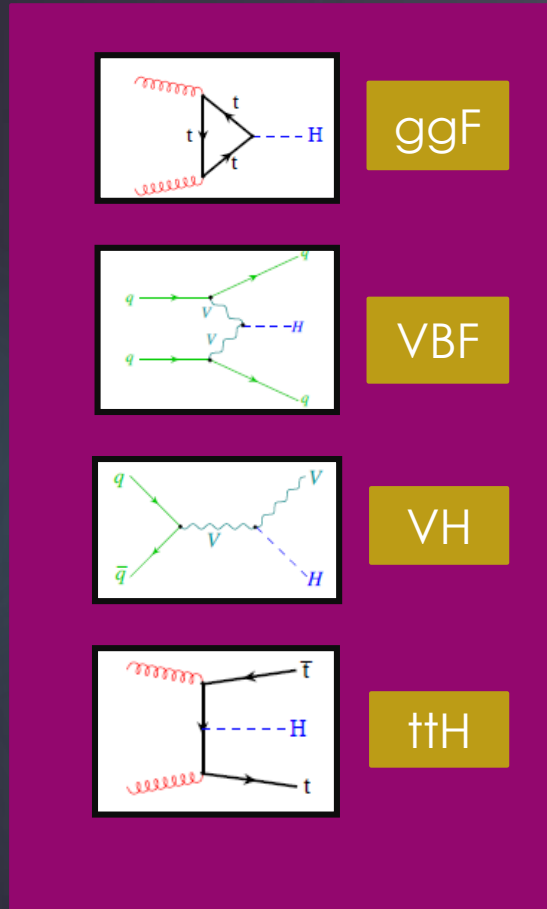
Coupling to Fermions :
ggF and ttH
Coupling to Bosons :
VBF and VH



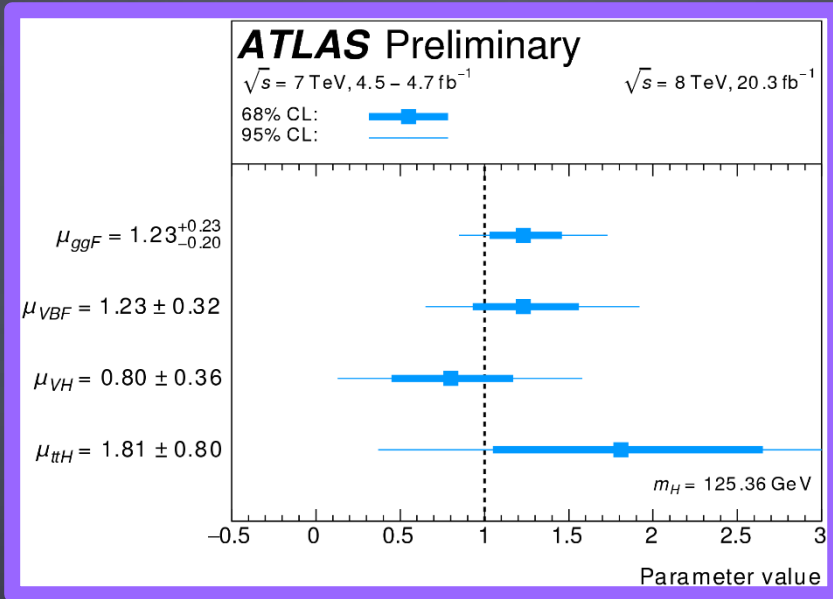
All decay channels together
assuming SM Branching ratios

Signal strength for Higgs production mechanisms

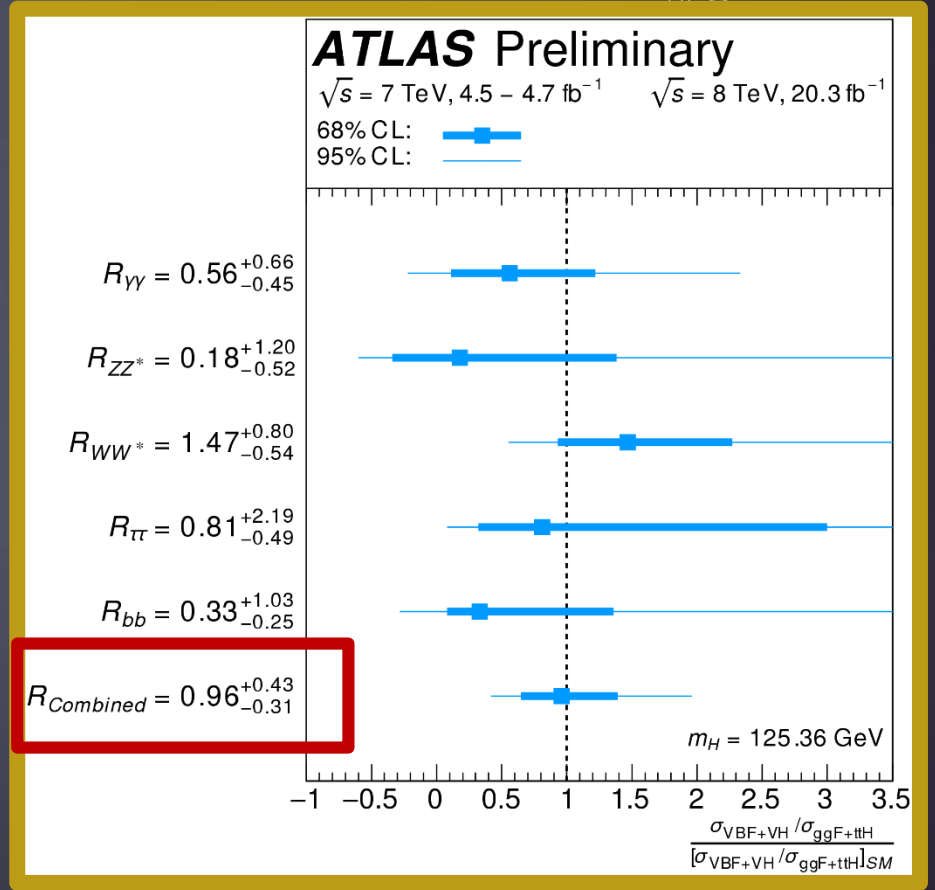
Bosonic & Fermionic coupling ratio
 $R = \mu_{\text{VBF+VH}} / \mu_{\text{ggF+ttH}} \rightarrow \text{decay channel}$



Coupling to Fermions :
 ggF and ttH
 Coupling to Bosons :
 VBF and VH



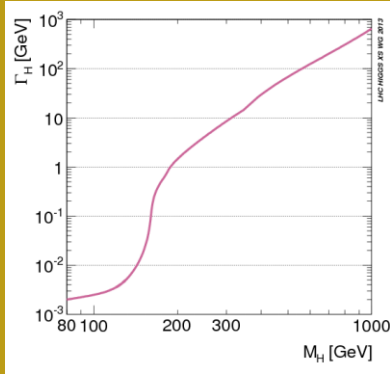
All decay channels together assuming SM Branching ratios



The Width of the Scalar Boson

288

Invisibles 2015, Lydia Ikonomidou-Fayard
16/06/2015



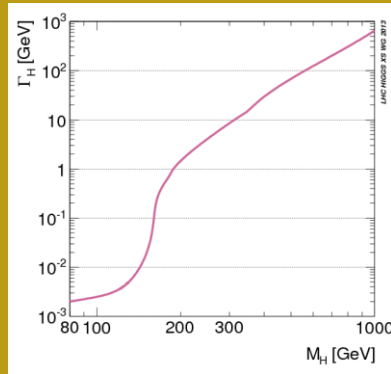
Higgs Width $\Gamma_H = f(M_H)$

For $M_H = 125$ GeV $\rightarrow \Gamma_H^{SM} \sim 4$ MeV

The Width of the Scalar Boson

289

Invisibles 2015, Lydia Ikonomidou-Fayard
16/06/2015

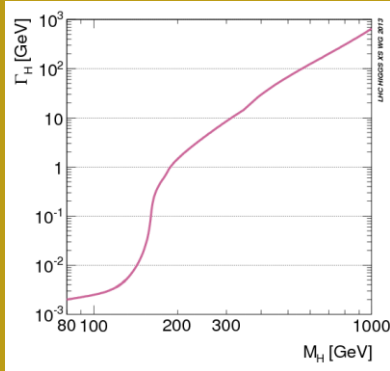


Direct measurement
impossible !
Exp resolution ~ 1.6 GeV

Higgs Width $\Gamma_H = f(M_H)$

For $M_H = 125$ GeV $\rightarrow \Gamma_H^{SM} \sim 4$ MeV

The Width of the Scalar Boson



Direct measurement
impossible !
Exp resolution ~ 1.6 GeV

Higgs Width $\Gamma_H = f(M_H)$

For $M_H = 125$ GeV $\rightarrow \Gamma_H^{SM} \sim 4$ MeV

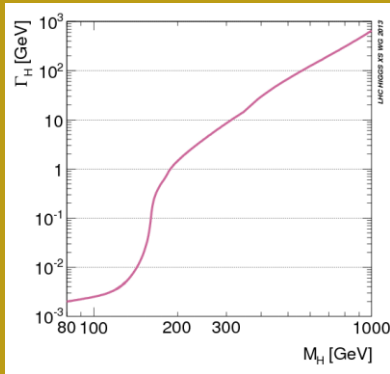
Derive the Width from Xsection
measurements on-shell?

$$\sigma_H \sim \frac{g_{H \rightarrow gg}^2 g_{H \rightarrow ZZ}^2}{\Gamma_H}$$

Ex: $H \rightarrow ZZ^*$

At a given measured Xsection, infinite
combinations for couplings and width

The Width of the Scalar Boson



Direct measurement impossible!
Exp resolution ~ 1.6 GeV

Higgs Width $\Gamma_H = f(M_H)$
For $M_H = 125$ GeV $\rightarrow \Gamma_H^{SM} \sim 4$ MeV

What about looking far (off-shell) from the Scalar Boson resonance?

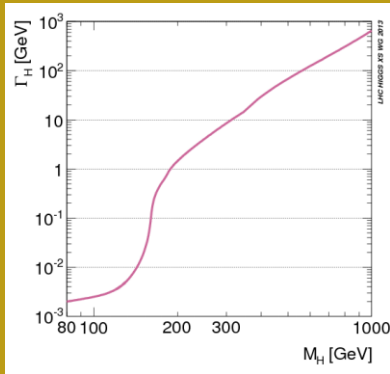
$$\sigma_{i \rightarrow H \rightarrow f} \sim \int ds \frac{g_i^2 g_f^2}{(s - m_h)^2 + m_h^2 \Gamma_h^2} \Big|_{s \gg m_h^2} \rightarrow \frac{g_i^2 g_f^2}{s}$$

Derive the Width from Xsection measurements on-shell?

$$\sigma_H \sim \frac{g_{H \rightarrow gg}^2 g_{H \rightarrow ZZ}^2}{\Gamma_H}$$

At a given measured Xsection, infinite combinations for couplings and width

The Width of the Scalar Boson



Direct measurement impossible!
Exp resolution ~ 1.6 GeV

Higgs Width $\Gamma_H = f(M_H)$
For $M_H = 125 \text{ GeV} \rightarrow \Gamma_H^{SM} \sim 4 \text{ MeV}$

What about looking far (off-shell) from the Scalar Boson resonance?

$$\sigma_{i \rightarrow H \rightarrow f} \sim \int ds \frac{g_i^2 g_f^2}{(s - m_h)^2 + m_h^2 \Gamma_h^2} \Big|_{s \gg m_h^2} \rightarrow \frac{g_i^2 g_f^2}{s}$$

$$\sigma_{\text{off}} \sim g_{H \rightarrow gg}^2 g_{H \rightarrow ZZ}^2 \sim \sigma_H \times \Gamma_H$$

$$\sigma_{\text{off}}^{SM} \sim \sigma_H^{SM} \times \Gamma_H^{SM}$$

$$\sigma_{\text{off}} \sim \sigma_{\text{off}}^{SM} \frac{\Gamma_H}{\Gamma_H^{SM}}$$

Derive the Width from Xsection measurements on-shell?

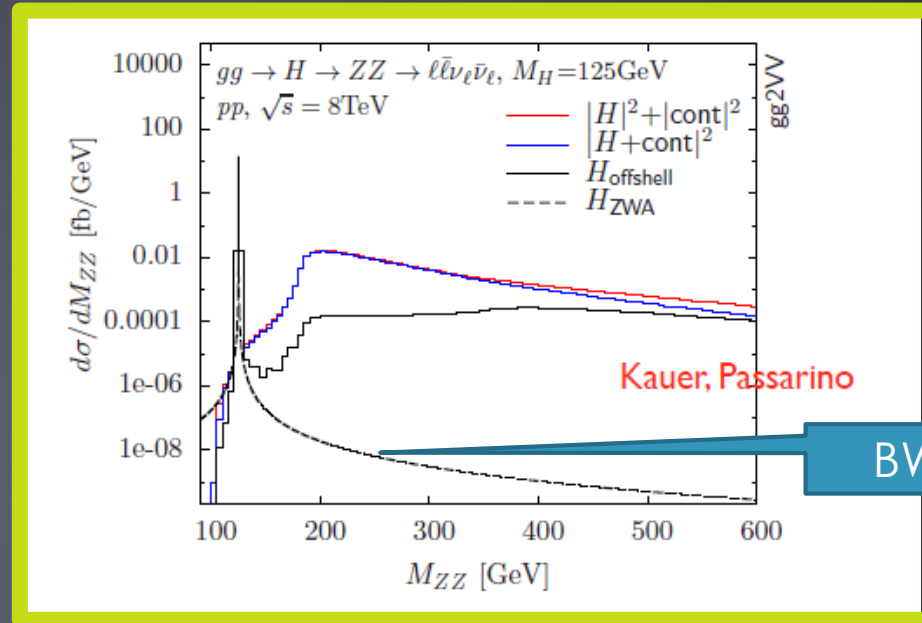
$$\sigma_H \sim \frac{g_{H \rightarrow gg}^2 g_{H \rightarrow ZZ}^2}{\Gamma_H}$$

At a given measured Xsection, infinite combinations for couplings and width

Caola, Melnikov
Kauer, Passarino
Campbell, Ellis, Williams

The Width of the Scalar Boson

The traces of Higgs(125) at high M_{ZZ}



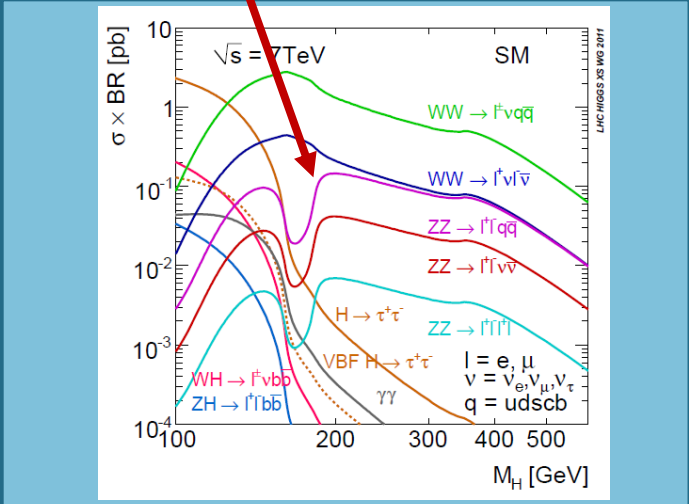
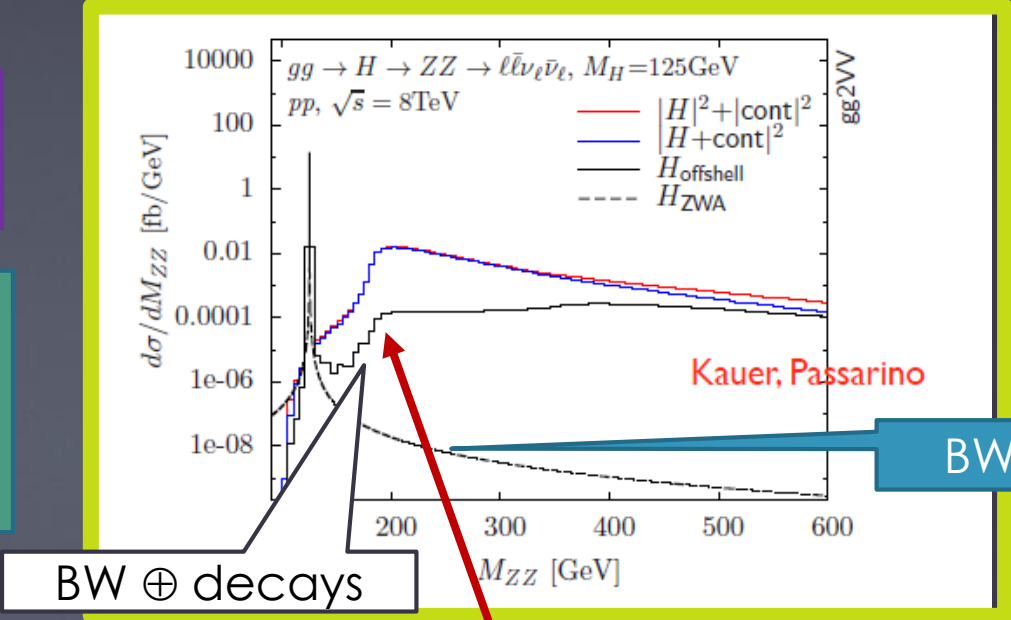
Invisibles 2015, Lydia Ikonomidou-Fayard
16/06/2015

Caola, Melnikov
Kauer, Passarino
Campbell, Ellis, Williams

The Width of the Scalar Boson

The traces of Higgs(125) at high M_{ZZ}

The Higgs Breit-Wigner high energy tail, is enhanced by the opening-up of the H->ZZ decays at $m_{ZZ} > 180\text{GeV}$



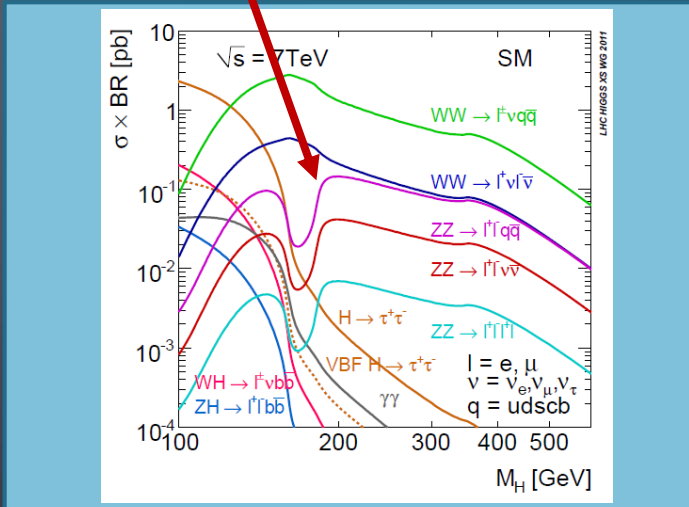
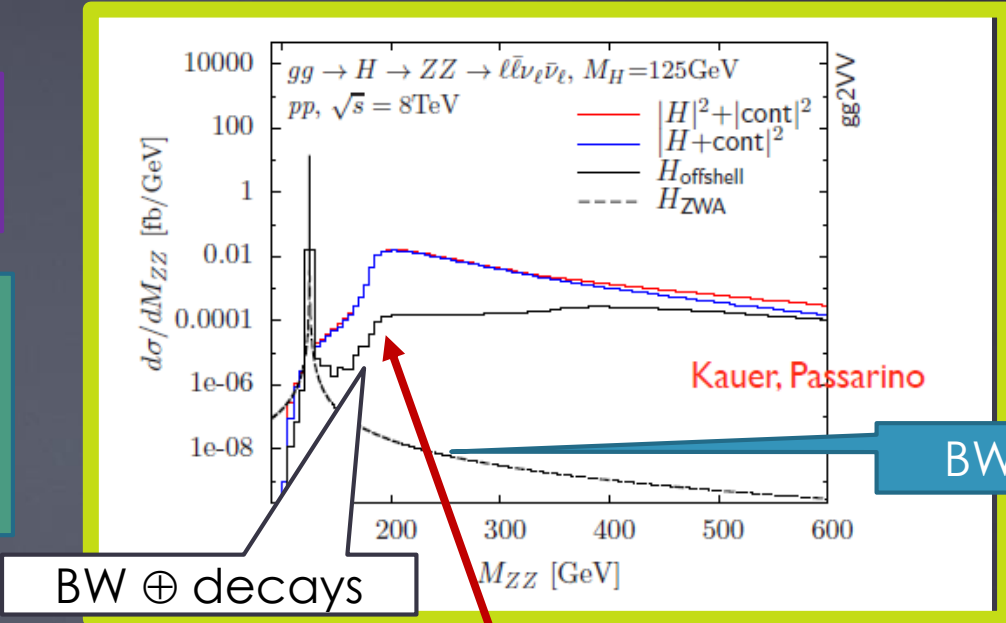
Caola, Melnikov
Kauer, Passarino
Campbell, Ellis, Williams

The Width of the Scalar Boson

The traces of Higgs(125) at high M_{ZZ}

The Higgs Breit-Wigner high energy tail, is **enhanced by the opening-up of the H->ZZ decays at $m_{ZZ} > 180\text{GeV}$**

This implies an increase of the number of expected events at $m_{ZZ} > 200\text{ GeV}$. Order few %



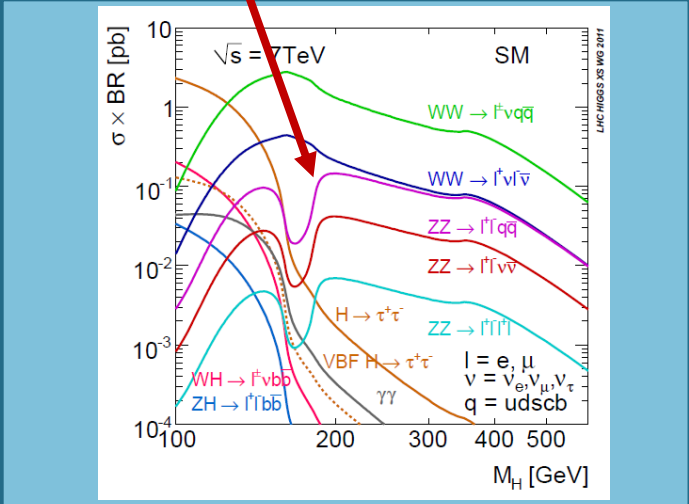
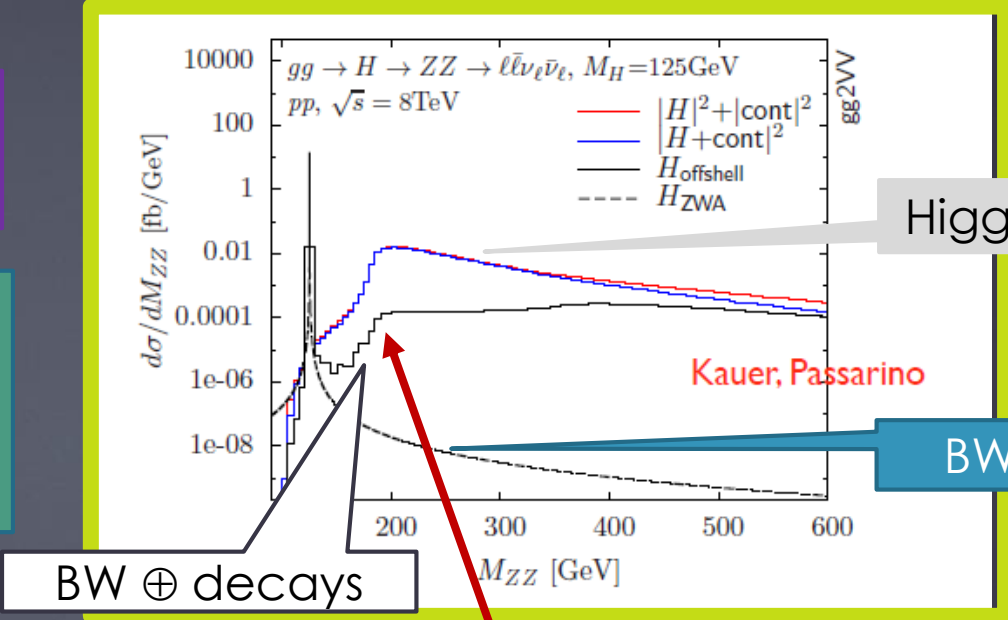
Caola, Melnikov
Kauer, Passarino
Campbell, Ellis, Williams

The Width of the Scalar Boson

The traces of Higgs(125) at high M_{ZZ}

The Higgs Breit-Wigner high energy tail, is enhanced by the opening-up of the H->ZZ decays at $m_{ZZ} > 180\text{GeV}$

This implies an increase of the number of expected events at $m_{ZZ} > 200\text{ GeV}$. Order few %
 Moreover: interference effects Between Higgs->ZZ and $gg \rightarrow ZZ$



Caola, Melnikov
 Kauer, Passarino
 Campbell, Ellis, Williams

The Width of the Scalar Boson

297

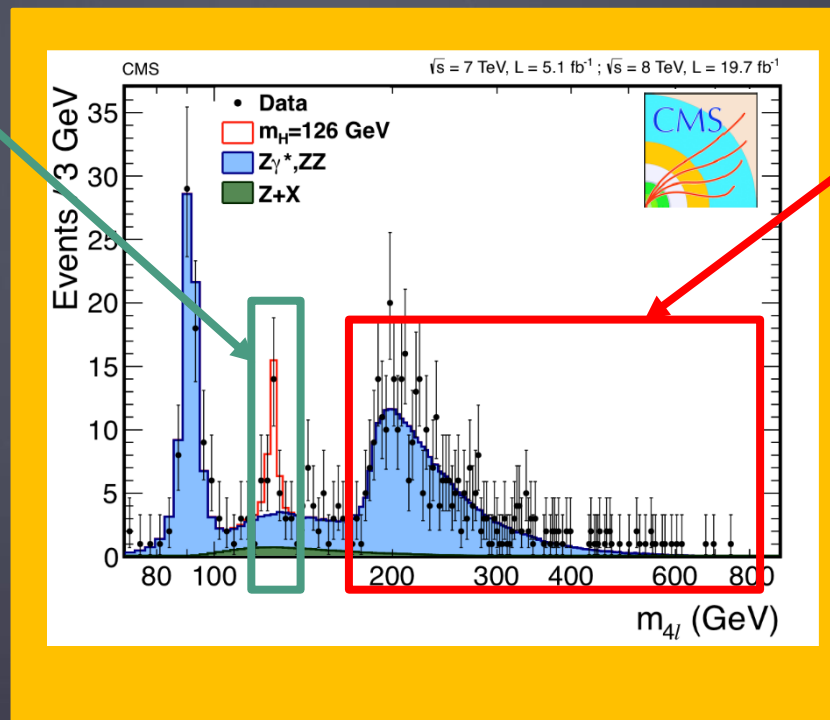
Invisibles 2015, Lydic
16/06/2015
M. Jou-Fayard

Measure OFF-SHELL vs ON-SHELL cross-sections with $H \rightarrow ZZ, WW$ decays in the clean leptonic channels

For ON-SHELL

$H \rightarrow ZZ \rightarrow 4l$

$H \rightarrow WW \rightarrow l\nu l\nu$



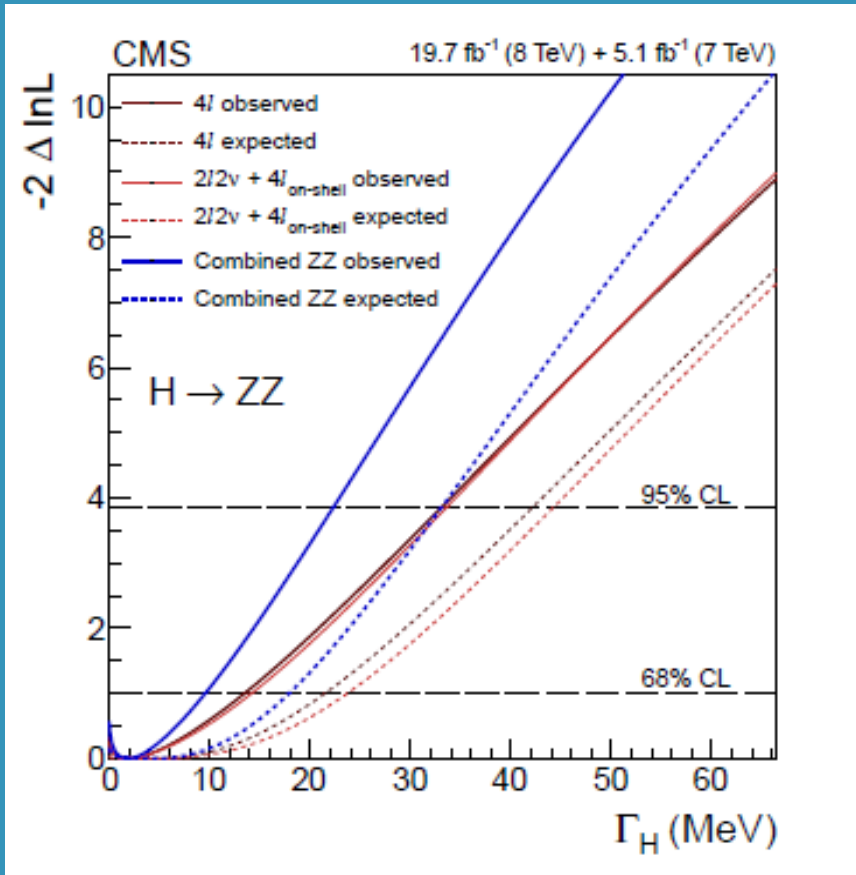
For OFF-SHELL

$H \rightarrow ZZ \rightarrow 4l$

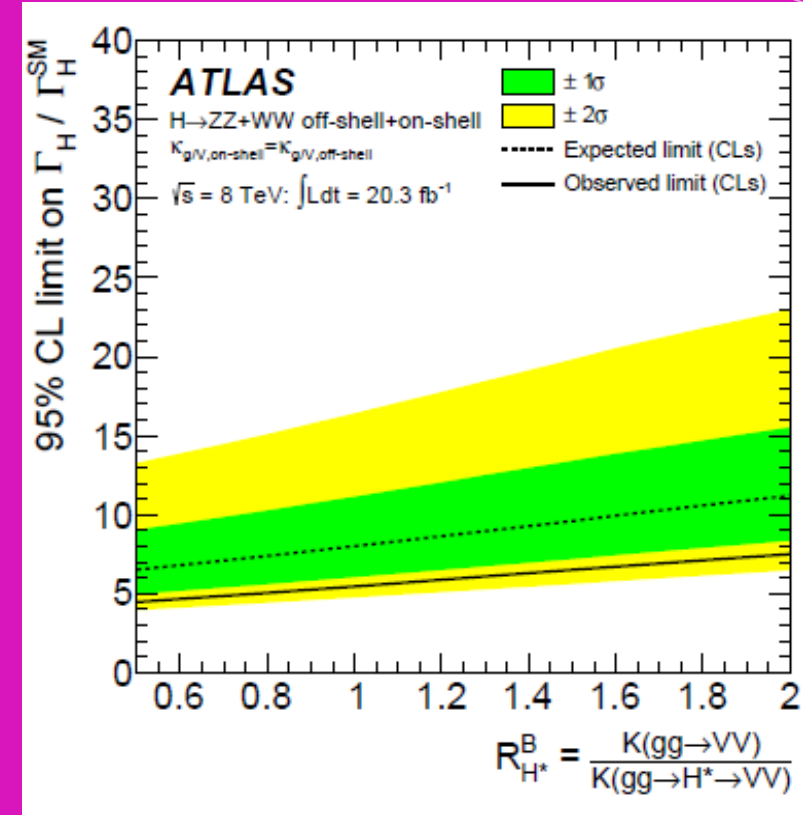
$H \rightarrow ZZ \rightarrow ll\nu\nu$

$H \rightarrow WW \rightarrow e\nu\mu\nu$

The Width of the Scalar Boson



$\Gamma_H < 22 \text{ MeV}$ (95% C.L.) ($\Gamma_{SM} \approx 4 \text{ MeV}$)



$\Gamma_H / \Gamma_{SM} < 5.5$ (95% CL)

16/17/2017, 11:00 AM

The Couplings

299

Invisibles 2015, Lydia Iconomidou-Fayard
16/06/2015

→ The total strengths look in agreement with SM (the various μ 's)

The Couplings

300

Invisibles 2015, Lydia Iconomidou-Fayard
16/06/2015

- The total strengths look in agreement with SM (the various μ 's)
- The μ 's imply simultaneously the couplings in production and in the decay

The Couplings

301

Invisibles 2015, Lydia Iconomidou-Fayard
16/06/2015

- The total strengths look in agreement with SM (the various μ 's)
- The μ 's imply simultaneously the couplings in production and in the decay
- Try to split down to “individual” Higgs couplings to initial and to final particles

The Couplings

302

Invisibles 2015, Lydia Iconomidou-Fayard
16/06/2015

- The total strengths look in agreement with SM (the various μ 's)
- The μ 's imply simultaneously the couplings in production and in the decay
- Try to split down to "individual" Higgs couplings to initial and to final particles

A series of assumptions are necessary
Built-up in common among the 2 experiments

Assumptions for benchmark models for testing the Higgs couplings

- 1) A single resonance has been discovered with a mass of 125 GeV
- 2) Higgs production and kinematics compatible with the SM one
- 3) Narrow width approximation \rightarrow
- 4) Assume CP-even scalar structure
- 5) Assume that the off-shell measurement depend on the coupling strengths and not on the Width
- 6) No running coupling constants

$$\sigma(i \rightarrow H \rightarrow f) = \frac{\sigma_i(\kappa_j) \cdot \Gamma_f(\kappa_j)}{\Gamma_H(\kappa_j)}$$

κ = coupling
 $\kappa=1$ for SM particles

$$\sigma^{\text{off}}(i \rightarrow H^* \rightarrow f) \sim \kappa_{i,\text{off}}^2 \cdot \kappa_{f,\text{off}}^2$$

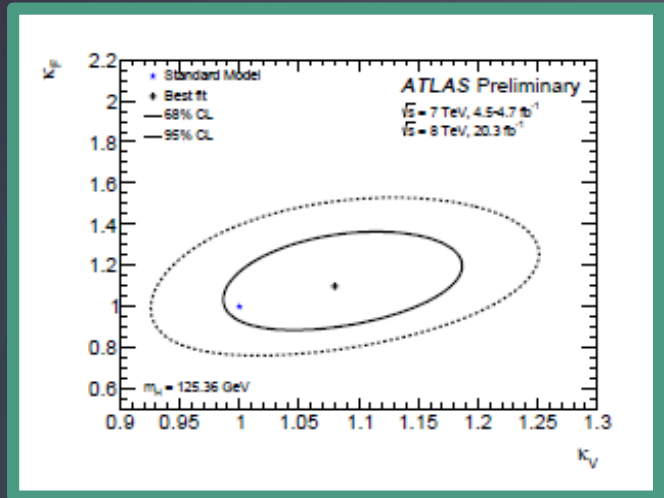
$$\kappa_{j,\text{off}} = \kappa_{j,\text{on}}$$

Fermionic vs Bosonic couplings

Assume

Bosons: $K_V = K_W = K_Z$

Fermions : $K_F = K_t = K_b = K_\tau = K_\mu = K_g$



$$K_V = 1.09^{+0.07}_{-0.07}$$

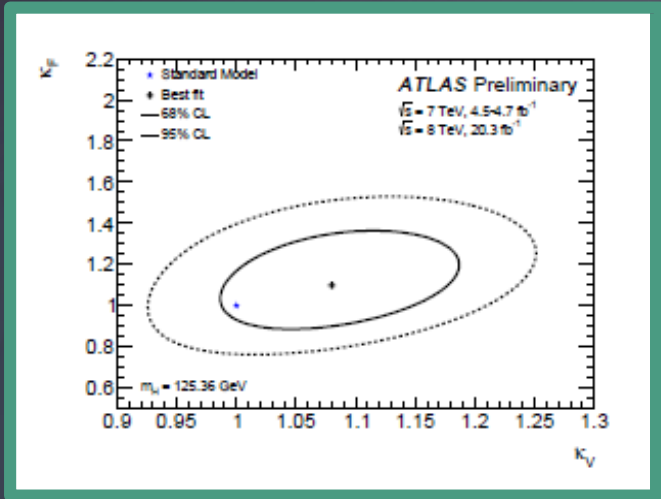
$$K_F = 1.11^{+0.17}_{-0.15}$$

Fermionic vs Bosonic couplings

Assume

Bosons: $K_V = K_W = K_Z$

Fermions : $K_F = K_t = K_b = K_\tau = K_\mu = K_g$



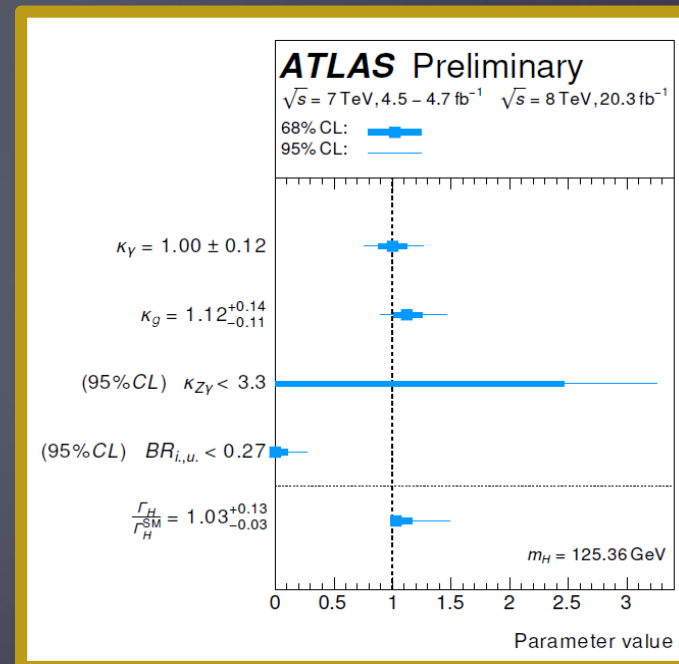
$$K_V = 1.09^{+0.07}_{-0.07}$$

$$K_F = 1.11^{+0.17}_{-0.15}$$

Anything else in the g and γ loops?

Assume

SM couplings for all particles, no constraint on the total Width

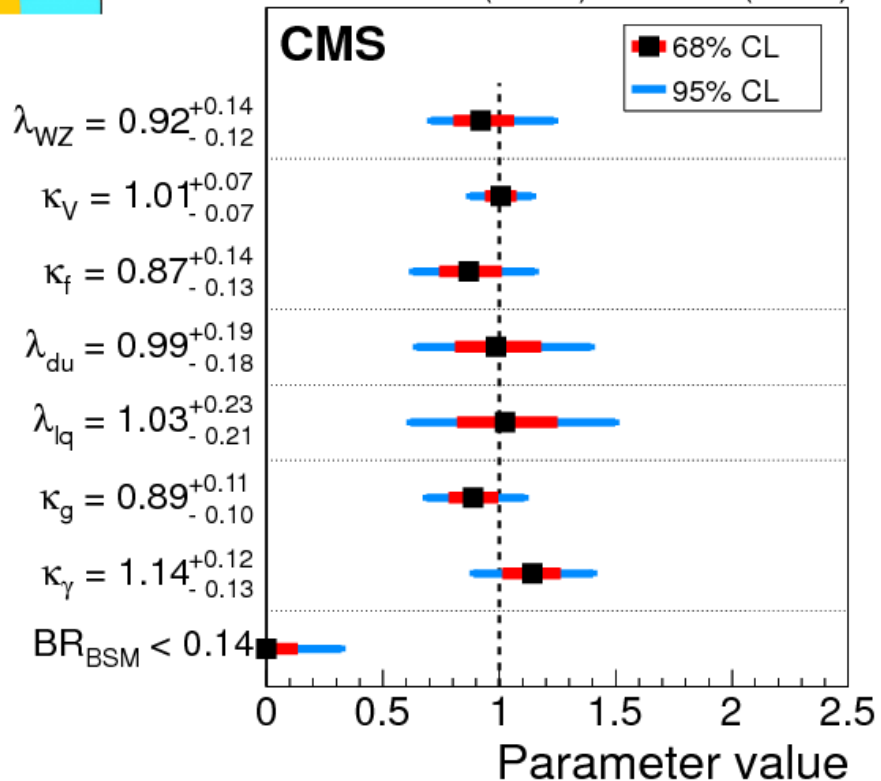


Invisible BR < 0.23 at 95%CL

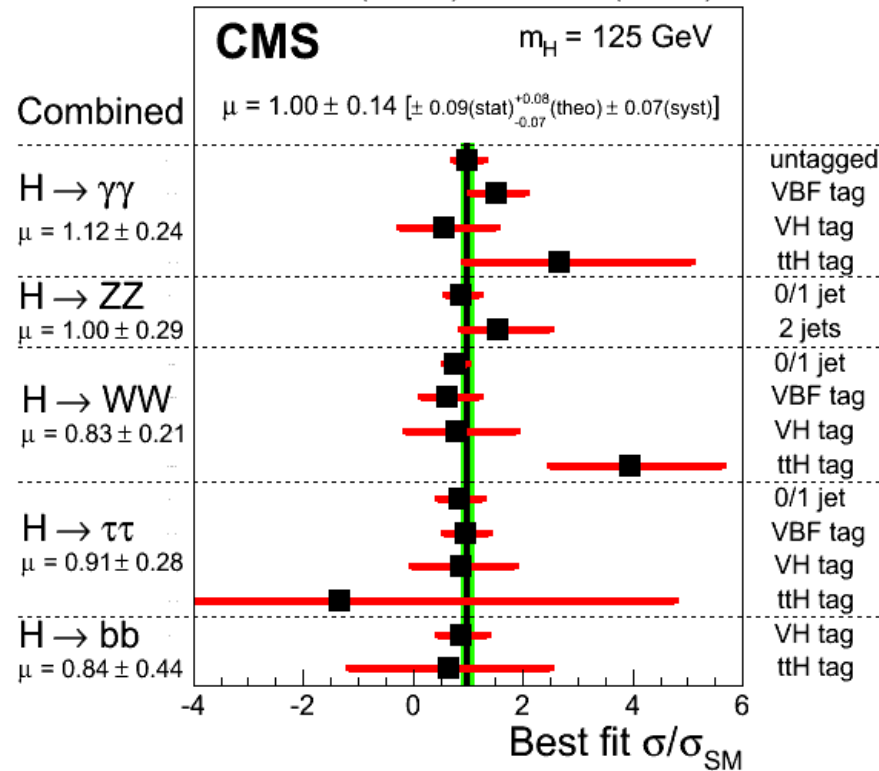
Again couplings..



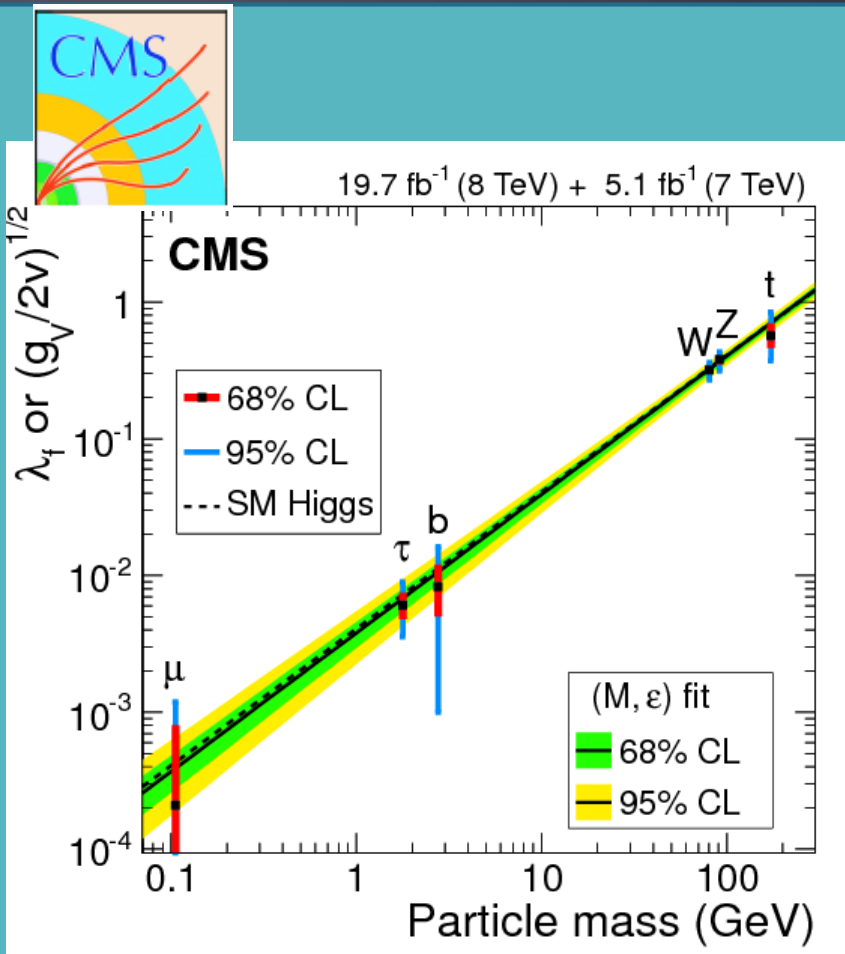
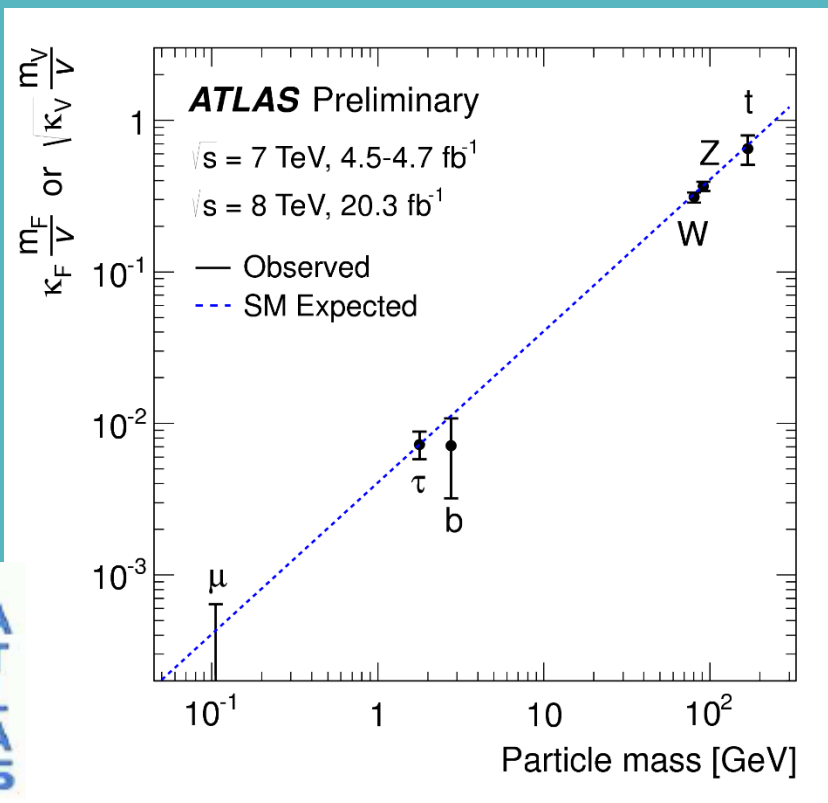
19.7 fb⁻¹ (8 TeV) + 5.1 fb⁻¹ (7 TeV)



19.7 fb⁻¹ (8 TeV) + 5.1 fb⁻¹ (7 TeV)



Coupling summary

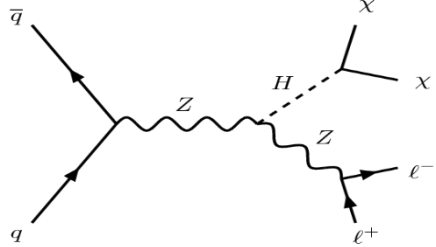


Higgs to invisible(s)?

308

Dark matter, long lived particles..

Look at ZH mode



Signature 1 : A leptonically decaying Z boson, not balanced in the transverse plane $\rightarrow E_T^{\text{miss}}$

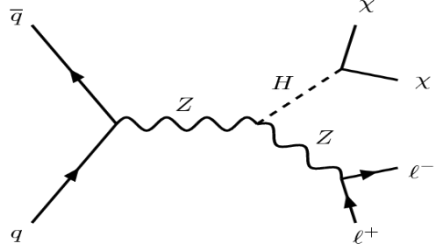
Higgs to invisible(s)?

309

Invisibles 2015, Lydia Iconomidou-Fayard
16/06/2015

Dark matter, long lived particles..

Look at ZH mode



Signature 1 : A leptonically decaying Z boson, not balanced in the transverse plane $\rightarrow E_T^{\text{miss}}$

Signal kinematics : Large E_T^{miss} , large $\Delta\phi(P_T^{\text{ll}}, E_T^{\text{miss}})$, small $\Delta\phi(l, l)$, no jets.

Dominant backgrounds: ZZ and WZ, ttbar, W+jets, multijets..

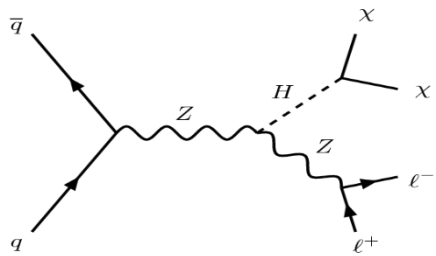
Higgs to invisible(s)?

310

Invisibles 2015, Lydia Iconomidou-Fayard
16/06/2015

Dark matter, long lived particles..

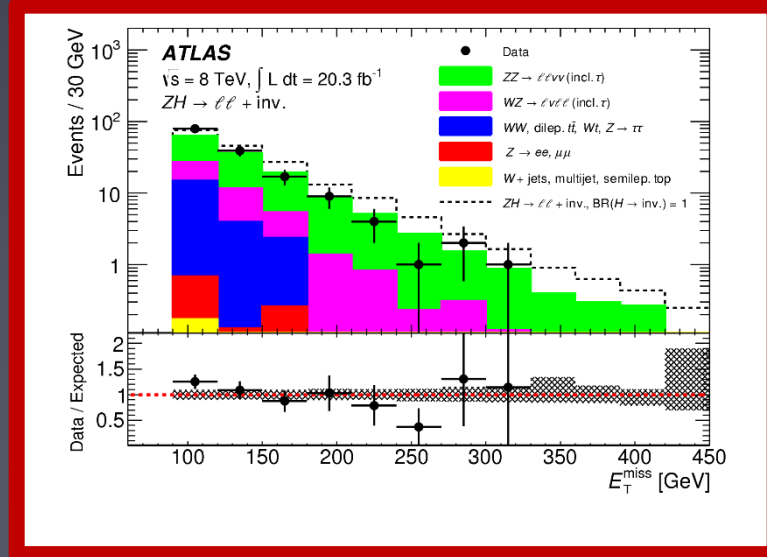
Look at ZH mode



Signature 1 : A leptonically decaying Z boson, not balanced in the transverse plane $\rightarrow E_T^{\text{miss}}$

Signal kinematics : Large E_T^{miss} , large $\Delta\phi(P_T^{\text{ll}}, E_T^{\text{miss}})$, small $\Delta\phi(l, l)$, no jets.

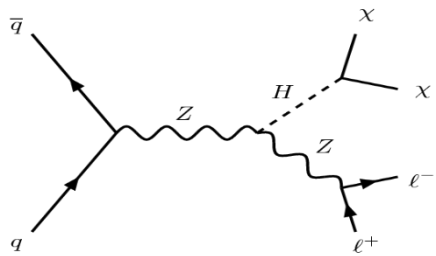
Dominant backgrounds: ZZ and WZ, ttbar, W+jets, multijets..



Higgs to invisible(s)?

Dark matter, long lived particles..

Look at ZH mode

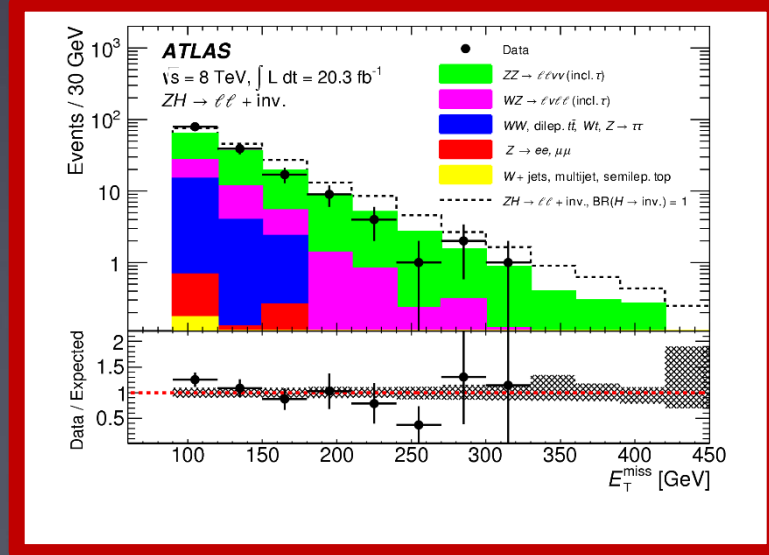


Signature 1 : A leptonically decaying Z boson, not balanced in the transverse plane $\rightarrow E_T^{miss}$

Signal kinematics : Large E_T^{miss} , large $\Delta\phi (P_T^{\parallel}, E_T^{miss})$, small $\Delta\phi(l, l)$, no jets.

Dominant backgrounds: ZZ and WZ, ttbar, W+jets, multijets..

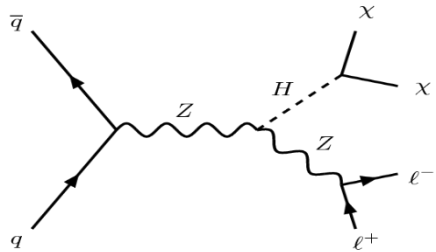
Observed 180 events (exp. 163 ± 10)
 $Br(H \rightarrow Invis) < 75\%$ at 95%CL



Higgs to invisible(s)?

Dark matter, long lived particles..

Look at ZH mode

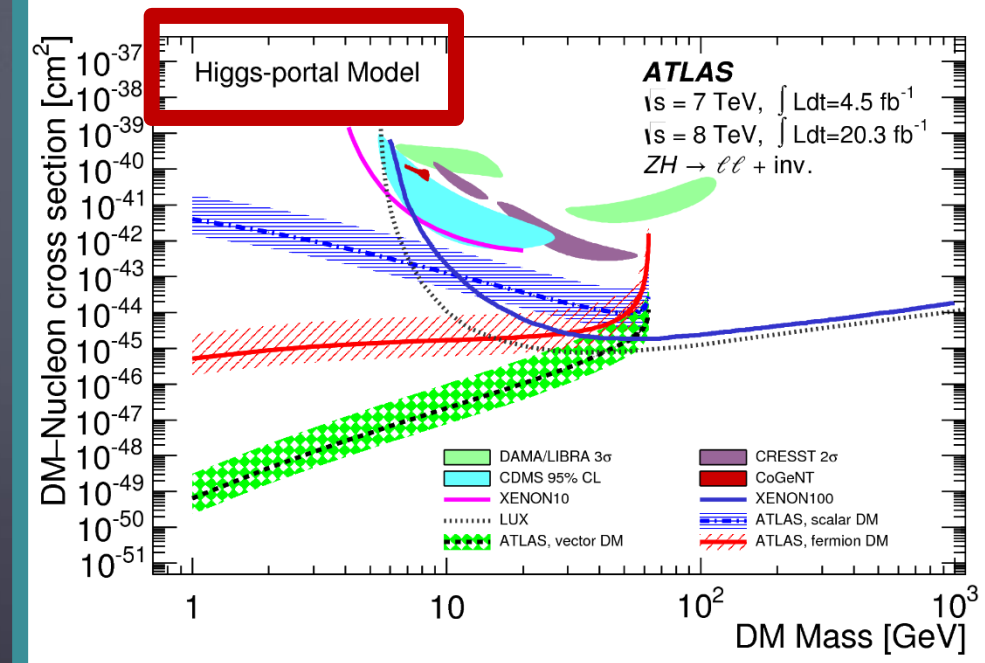
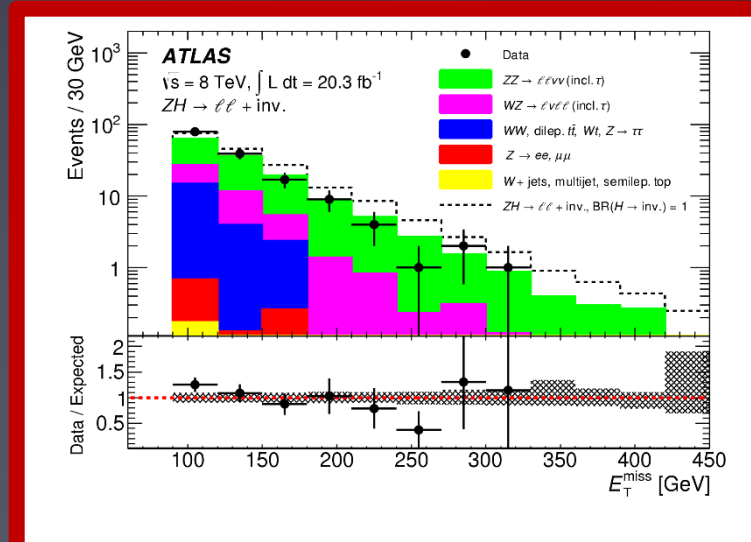


Signature 1 : A leptonically decaying Z boson, not balanced in the transverse plane $\rightarrow E_T^{\text{miss}}$

Signal kinematics : Large E_T^{miss} , large $\Delta\phi (P_T^{\parallel}, E_T^{\text{miss}})$, small $\Delta\phi(l, l)$, no jets.

Dominant backgrounds: ZZ and WZ, ttbar, W+jets, multijets..

Observed 180 events (exp. 163 ± 10)
 $\text{Br}(H \rightarrow \text{Invis}) < 75\%$ at 95%CL



Higgs to Invisible(s)?

Look at VH mode

Signature : Z/W bosons decaying in 2-jets, not balanced in the transverse plane

313

Invisibles 2015, Lydia Iconomidou-Fayard
16/06/2015

Higgs to Invisible(s)?

314

Look at VH mode

Signature : Z/W bosons decaying in 2-jets, not balanced in the transverse plane

Signal kinematics:

≥ 2 jets and large E_T^{miss} .
Categorize in E_T^{miss} regions.

Background : W/Z+jets, multijets, $t\bar{t}$...

Higgs to Invisible(s)?

Look at VH mode

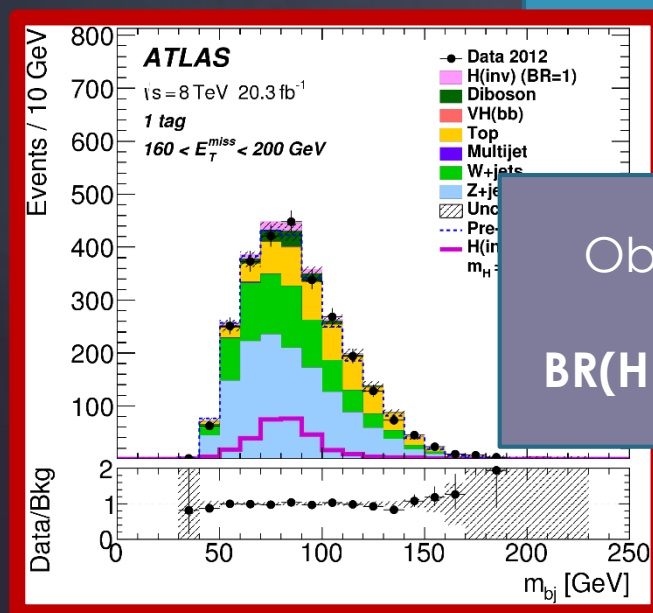
Signature : Z/W bosons decaying in 2-jets, not balanced in the transverse plane

Signal kinematics:

≥ 2 jets and large E_T^{miss} .
Categorize in E_T^{miss} regions.

Background : W/Z+jets, multijets, ttbar...

Observed 72022 events
(exp 72289 ± 534)
BR(H->Inv) < 78% (95% CL)



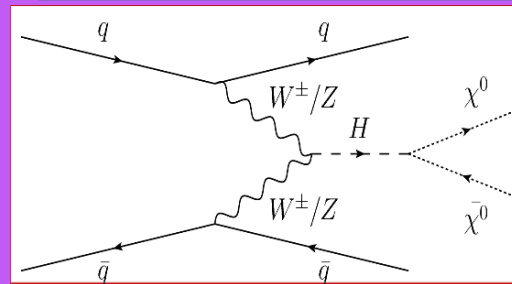
Higgs to Invisible(s)?

Look at VH mode

Signature : Z/W bosons decaying in 2-jets, not balanced in the transverse plane

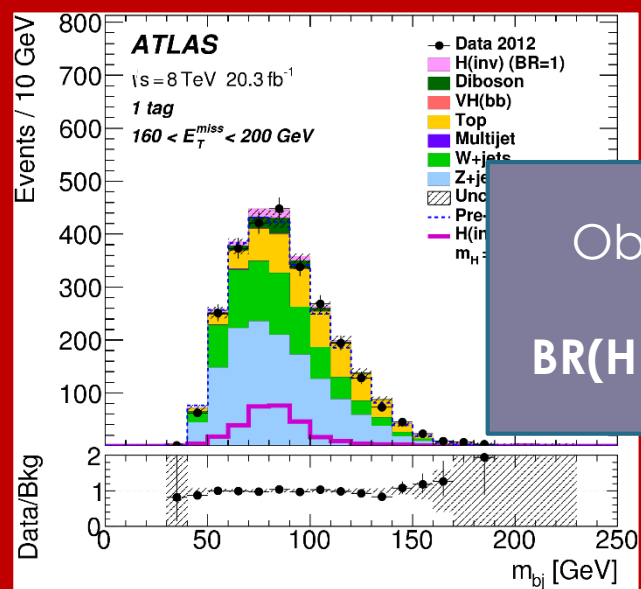
Signal kinematics:
 >=2 jets and large E_T^{miss} .
 Categorize in E_T^{miss} regions.
Background : W/Z+jets, multijets, ttbar...

Look at VBF mode



Signature:
 Two high energy, well separated-in-eta jets and large E_T^{miss}

G. Anagnostou-Fayard



Observed 72022 events
 (exp 72289 ±534)
BR(H->Inv) < 78% (95% CL)

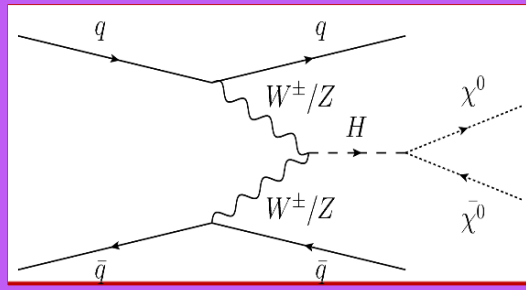
Higgs to Invisible(s)?

Look at VH mode

Signature : Z/W bosons decaying in 2-jets, not balanced in the transverse plane

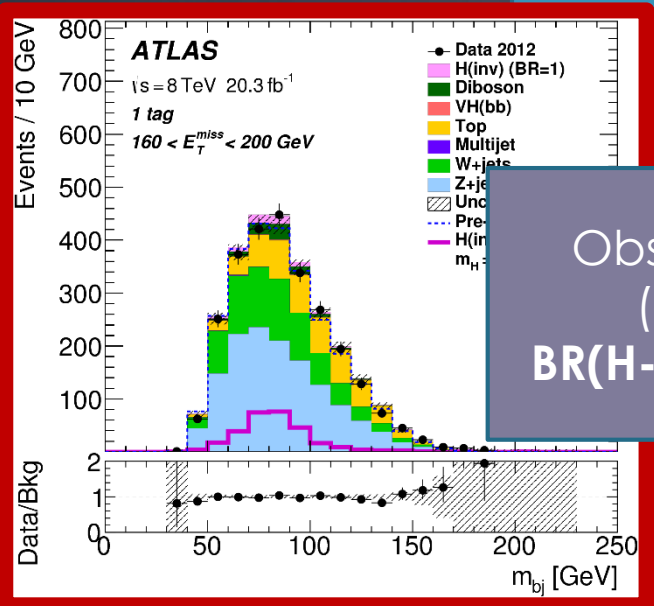
Signal kinematics:
 >=2 jets and large E_T^{miss} .
 Categorize in E_T^{miss} regions.
Background : W/Z+jets, multijets, ttbar...

Look at VBF mode



Signature:
 Two high energy, well separated-in-eta jets and large E_T^{miss}

Signal kinematics :
 → Two energetic jets with $PT > 75$ (50) GeV,
 $\Delta\eta$ (jet1, jet2) > 4.8 and $mass(jet1, jet2) > 1 TeV$
 → Large $E_{T}^{miss} > 150 GeV$
 → No leptons nor bjets in the event
Main backgrounds: W/Z+jets, multijets



Observed 72022 events
 (exp 72289 ± 534)
BR(H->Inv) < 78% (95% CL)

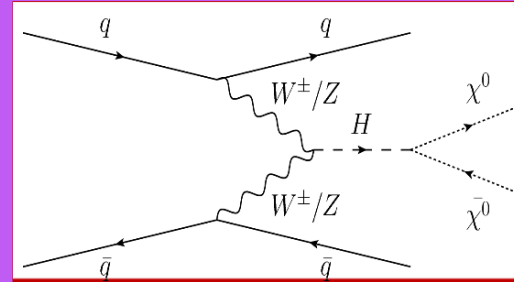
Higgs to Invisible(s)?

Look at VH mode

Signature : Z/W bosons decaying in 2-jets, not balanced in the transverse plane

Signal kinematics:
 >=2 jets and large E_T^{miss} .
 Categorize in E_T^{miss} regions.
Background : W/Z+jets, multijets, ttbar...

Look at VBF mode



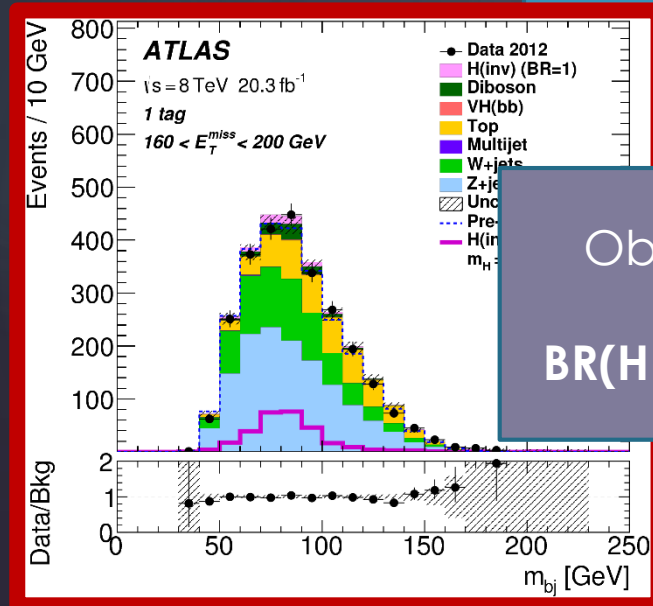
Signature:
 Two high energy, well separated-in-eta jets and large E_T^{miss}

Signal kinematics :
 → Two energetic jets with $PT > 75$ (50) GeV,
 $\Delta\eta$ (jet1, jet2) > 4.8 and $mass(jet1, jet2) > 1\text{TeV}$
 → Large $E_{T}^{miss} > 150\text{GeV}$
 → No leptons nor bjets in the event

Main backgrounds: W/Z+jets, multijets

Observed 539 events (exp: 576 ± 48)
Br(H->Invisible) < 29% (95% CL)

Observed 72022 events
 (exp 72289 ± 534)
BR(H->Inv) < 78% (95% CL)



Conclusions (1)

LHC Run1 was **a rare adventure**, with tremendous accomplishments, several euphoric moments, few distresses and an **unprecedented collective success**

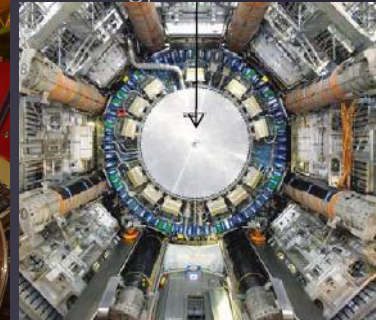
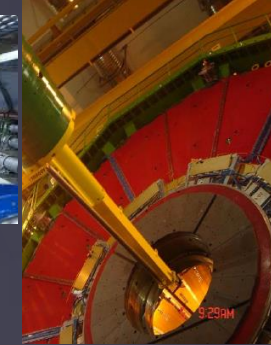


Conclusions (1)

320

LHC Run1 was **a rare adventure**, with tremendous accomplishments, several euphoric moments, few distresses and an **unprecedented collective success**

The long list of impressive results was realized **thanks to** the incredible ingenuity and long-term endeavor of the **accelerator and detector experts** who brought to completion these titanic challenging technological ensembles.



Invisibles 2015
16/06/2015

yard

Conclusions (1)

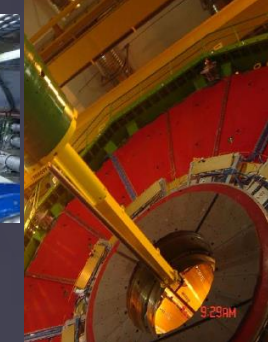
321

LHC Run1 was **a rare adventure**, with tremendous accomplishments, several euphoric moments, few distresses and an **unprecedented collective success**

The **long list of impressive results** was realized **thanks to** the incredible ingenuity and long-term endeavor of the **accelerator and detector experts** who brought to completion these titanic challenging technological ensembles.



Invisibles 2015
16/06/2015



yard



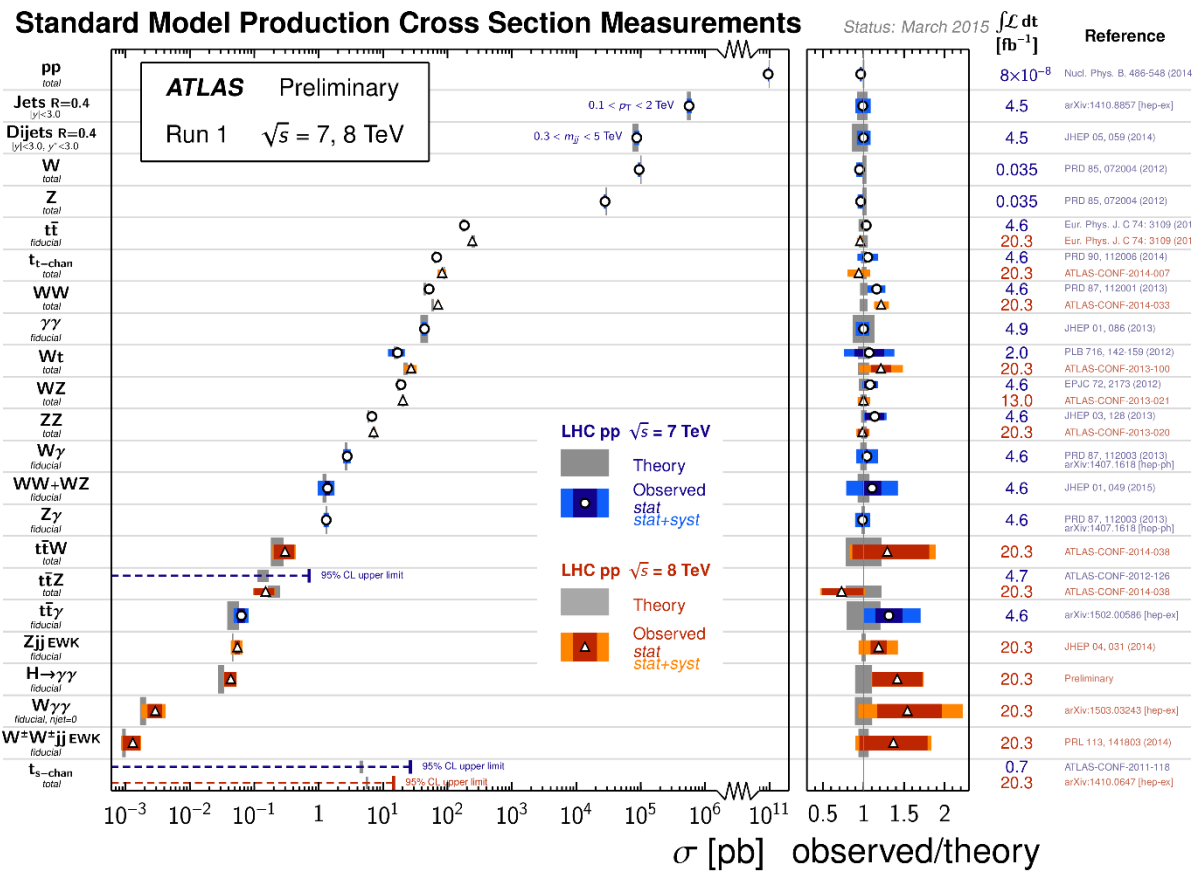
The **fast discovery of the Scalar Boson** was boosted by the fertile imagination of physicists. It was also the source of an **increasing cooperation and organization between the experimental and theory communities.**



LHC Higgs Cross-Section Working group

Conclusions (2)

From the abundant to rare:
Measurements over 14 orders of magnitude



ATLAS SUSY Searches* - 95% CL Lower Limits

Status: Feb 2015

Model	e, μ, τ, γ	Jets	E_T^{miss}	$\int \mathcal{L} dt$ [fb ⁻¹]	Mass limit	Reference
MSUGRA/CMSSM	0	2-6 jets	Yes	20.3	\tilde{g}, \tilde{g} 850 GeV, 1.7 TeV	$m(\tilde{g})=m(\tilde{g})$ 1405.7875
$\tilde{g}\tilde{g}, \tilde{g}\rightarrow q\bar{q}$	0	2-6 jets	Yes	20.3	\tilde{g} 250 GeV	$m(\tilde{g})=0$ GeV, $m(\tilde{g})=m(2^{\text{nd}} \text{ gen. } \tilde{g})$ 1411.1559
$\tilde{g}\tilde{g}, \tilde{g}\rightarrow q\bar{q}$ (compressed)	1 γ	0-1 jet	Yes	20.3	\tilde{g} 1.33 TeV	$m(\tilde{g})=m(\tilde{g}) = m(\tilde{c})$ 1405.7875
$\tilde{g}\tilde{g}, \tilde{g}\rightarrow q\bar{q}$	0	2-6 jets	Yes	20.3	\tilde{g} 1.2 TeV	$m(\tilde{g})=0$ GeV 1501.03555
$\tilde{g}\tilde{g}, \tilde{g}\rightarrow q\bar{q}, \tilde{g}\rightarrow q\bar{q}W^{\pm}\tilde{g}$	1 e, μ	3-6 jets	Yes	20	\tilde{g} 1.32 TeV	$m(\tilde{g})=300$ GeV, $m(\tilde{g})=0.5(m(\tilde{g})+m(\tilde{g}))$ 1501.03555
$\tilde{g}\tilde{g}, \tilde{g}\rightarrow q\bar{q}, \tilde{g}\rightarrow q\bar{q}W^{\pm}\tilde{g}$	2 e, μ	0-3 jets	-	20	\tilde{g} 1.6 TeV	$m(\tilde{g})=0$ GeV 1407.0603
GMSB (\tilde{g} NLSP)	1-2 $\tau + 0-1 \ell$	0-2 jets	Yes	20.3	\tilde{g} 1.28 TeV	$m(\tilde{g}) > 50$ GeV ATLAS-CONF-2014-001
GGM (bino NLSP)	2 γ	-	Yes	20.3	\tilde{g} 619 GeV	$m(\tilde{g}) > 50$ GeV ATLAS-CONF-2012-144
GGM (wino NLSP)	1 $e, \mu + \gamma$	-	Yes	4.8	\tilde{g} 900 GeV	$m(\tilde{g}) > 200$ GeV 1211.1167
GGM (higgsino-bino NLSP)	γ	1 b	Yes	4.8	\tilde{g} 690 GeV	$m(\text{NLSP}) > 200$ GeV ATLAS-CONF-2012-152
GGM (higgsino NLSP)	2 e, μ (Z)	0-3 jets	Yes	5.8	\tilde{g} 865 GeV	$m(\tilde{g})=1.8 \times 10^{-1}$ eV, $m(\tilde{g})=m(\tilde{g})=1.5$ TeV 1502.01518
Gravitino LSP	0	mono-jet	Yes	20.3	\tilde{g} 1.25 TeV	$m(\tilde{g})=400$ GeV 1407.0900
$\tilde{g}\rightarrow b\bar{b}$	0	3 b	Yes	20.1	\tilde{g} 1.1 TeV	$m(\tilde{g}) > 350$ GeV 1308.1841
$\tilde{g}\rightarrow t\bar{t}$	0-1 e, μ	3 b	Yes	20.1	\tilde{g} 1.34 TeV	$m(\tilde{g})=400$ GeV 1407.0600
$\tilde{g}\rightarrow b\bar{b}$	0-1 e, μ	3 b	Yes	20.1	\tilde{g} 1.3 TeV	$m(\tilde{g})=300$ GeV 1407.0600
$\tilde{b}_1, \tilde{b}_1 \rightarrow b\bar{b}$	0	2 b	Yes	20.1	\tilde{b}_1 100-620 GeV	$m(\tilde{b}_1)=90$ GeV 1308.2631
$\tilde{b}_1, \tilde{b}_1 \rightarrow b\bar{b}$	2 e, μ (SS)	0-3 b	Yes	20.3	\tilde{b}_1 275-440 GeV	$m(\tilde{b}_1)=2$ m(\tilde{b}_1) 1404.2500
$\tilde{t}_1, \tilde{t}_1 \rightarrow W\bar{b}t$	1-2 e, μ	1-2 b	Yes	4.7	\tilde{t}_1 110-167 GeV, 230-460 GeV	$m(\tilde{t}_1) = 2m(\tilde{b}_1), m(\tilde{t}_1)=55$ GeV 1209.2102, 1407.0583
$\tilde{t}_1, \tilde{t}_1 \rightarrow W\bar{b}t$ or $t\bar{t}$	2 e, μ	0-2 jets	Yes	20.3	\tilde{t}_1 90-191 GeV, 215-530 GeV	$m(\tilde{t}_1)=1$ GeV 1407.0583, 1406.1122
$\tilde{t}_1, \tilde{t}_1 \rightarrow t\bar{t}$	0-1 e, μ	1-2 b	Yes	20	\tilde{t}_1 90-240 GeV, 210-640 GeV	$m(\tilde{t}_1)=1$ GeV 1407.0608
\tilde{t}_1 (natural GMSB)	0	mono-jet/ ℓ -tag	Yes	20.3	\tilde{t}_1 150-580 GeV	$m(\tilde{t}_1)=m(\tilde{t}_1) < 85$ GeV 1403.5222
$\tilde{t}_1, \tilde{t}_1 \rightarrow t\bar{t}$	2 e, μ (Z)	1 b	Yes	20.3	\tilde{t}_1 290-600 GeV	$m(\tilde{t}_1)=150$ GeV 1403.5222
$\tilde{t}_2, \tilde{t}_2 \rightarrow t\bar{t} + Z$	3 e, μ (Z)	1 b	Yes	20.3	\tilde{t}_2 90-325 GeV	$m(\tilde{t}_2)=0$ GeV 1403.5294
$\tilde{t}_1, \tilde{t}_1 \rightarrow t\bar{t}$	2 e, μ	0	Yes	20.3	\tilde{t}_1 140-465 GeV	$m(\tilde{t}_1)=0$ GeV, $m(\tilde{t}_1, \tilde{t}_2)=0.5(m(\tilde{t}_1)+m(\tilde{t}_2))$ 1403.5294
$\tilde{t}_1, \tilde{t}_1 \rightarrow t\bar{t}$	2 e, μ	0	Yes	20.3	\tilde{t}_1 100-350 GeV	$m(\tilde{t}_1)=0$ GeV, $m(\tilde{t}_1, \tilde{t}_2)=0.5(m(\tilde{t}_1)+m(\tilde{t}_2))$ 1407.0350
$\tilde{t}_1, \tilde{t}_1 \rightarrow t\bar{t}$	2 τ	-	Yes	20.3	\tilde{t}_1 700 GeV	$m(\tilde{t}_1)=0$ GeV, $m(\tilde{t}_1, \tilde{t}_2)=0.5(m(\tilde{t}_1)+m(\tilde{t}_2))$ 1402.7029
$\tilde{t}_1, \tilde{t}_1 \rightarrow t\bar{t}$	3 e, μ	0	Yes	20.3	\tilde{t}_1 420 GeV	$m(\tilde{t}_1)=m(\tilde{t}_2), m(\tilde{t}_1)=0, m(\tilde{t}_1, \tilde{t}_2)=0.5(m(\tilde{t}_1)+m(\tilde{t}_2))$ 1403.5294, 1402.7029
$\tilde{t}_1, \tilde{t}_1 \rightarrow t\bar{t}$	2-3 e, μ	0-2 jets	Yes	20.3	\tilde{t}_1 250 GeV	$m(\tilde{t}_1)=m(\tilde{t}_2), m(\tilde{t}_1)=0, m(\tilde{t}_1, \tilde{t}_2)=0.5(m(\tilde{t}_1)+m(\tilde{t}_2))$ 1501.07110
$\tilde{t}_1, \tilde{t}_1 \rightarrow W\bar{b}t, h, \tilde{h} \rightarrow b\bar{b}(WW)/\tau\tau/\gamma\gamma$	e, μ, γ	0-2 b	Yes	20.3	\tilde{t}_1 620 GeV	$m(\tilde{t}_1)=m(\tilde{t}_2), m(\tilde{t}_1)=0, m(\tilde{t}_1, \tilde{t}_2)=0.5(m(\tilde{t}_1)+m(\tilde{t}_2))$ 1405.5086
$\tilde{t}_1, \tilde{t}_1 \rightarrow t\bar{t}$	4 e, μ	0	Yes	20.3	\tilde{t}_1 270 GeV	$m(\tilde{t}_1)=m(\tilde{t}_2)=160$ MeV, $m(\tilde{t}_1)=0.2$ ns 1310.3675
Direct \tilde{t}_1, \tilde{t}_1 prod., long-lived \tilde{t}_1	Disapp. trk	1 jet	Yes	20.3	\tilde{t}_1 832 GeV	$m(\tilde{t}_1)=100$ GeV, $10 \mu\text{s} < \tau(\tilde{t}_1) < 1000$ s 1411.6795
Stable, stopped \tilde{t}_1 R-hadron	trk	0-1 jets	Yes	27.9	\tilde{t}_1 1.27 TeV	$10 < \tau < 50$ 1411.6795
Stable \tilde{t}_1 R-hadron	trk	-	-	19.1	\tilde{t}_1 537 GeV	$2 < \tau < 3$ ns, SPSS model 1405.5542
GMSB, stable \tilde{t}_1	1-2 μ	-	-	19.1	\tilde{t}_1 435 GeV	$1.5 < \tau < 156$ nm, BR($\tilde{t}_1 \rightarrow t$), $m(\tilde{t}_1)=108$ GeV ATLAS-CONF-2013-092
GMSB, $\tilde{t}_1 \rightarrow \gamma \tilde{t}_1$, long-lived \tilde{t}_1	2 γ	-	Yes	20.3	\tilde{t}_1 1.0 TeV	$\lambda_{1,2} = 0.10, \lambda_{3,4} = 0.05$ 1212.1272
$\tilde{q}\tilde{q}, \tilde{q}\tilde{q} \rightarrow q\bar{q}q$ (RPV)	1 μ , displ. vtx	-	-	20.3	\tilde{q}, \tilde{q} 1.61 TeV	$\lambda_{1,2} = 0.10, \lambda_{3,4} = 0.05$ 1212.1272
LFV $pp \rightarrow \tilde{\nu}_\tau + X, \tilde{\nu}_\tau \rightarrow e + \mu$	2 e, μ	-	-	4.6	$\tilde{\nu}_\tau$ 1.1 TeV	$m(\tilde{\nu}_\tau)=m(\tilde{\nu}_\tau), \tau_{\tilde{\nu}_\tau} < 1$ mm 1404.2500
LFV $pp \rightarrow \tilde{\nu}_\tau + X, \tilde{\nu}_\tau \rightarrow e(\mu) + \tau$	1 $e, \mu + \tau$	-	-	4.6	$\tilde{\nu}_\tau$ 1.35 TeV	$m(\tilde{\nu}_\tau) > 0.2$ m($\tilde{\nu}_\tau$), $\lambda_{1,2} \neq 0$ 1405.5086
Bilinear RPV CMSSM	2 e, μ (SS)	0-3 b	Yes	20.3	\tilde{g}, \tilde{g} 450 GeV, 916 GeV, 850 GeV	$m(\tilde{g}) > 0.2$ m(\tilde{g}), $\lambda_{1,2} \neq 0$ 1405.5086
$\tilde{t}_1, \tilde{t}_1 \rightarrow W\bar{b}t, \tilde{t}_1 \rightarrow e\bar{e}\nu_\tau, q\bar{q}, \tilde{t}_1 \rightarrow t\bar{t}$	4 e, μ	-	-	20.3	\tilde{t}_1 490 GeV	$\text{BR}(\tilde{g})=\text{BR}(\tilde{g})=0$ ATLAS-CONF-2013-091
$\tilde{t}_1, \tilde{t}_1 \rightarrow W\bar{b}t, \tilde{t}_1 \rightarrow e\bar{e}\nu_\tau, \tilde{t}_1 \rightarrow t\bar{t}$	3 $e, \mu + \tau$	-	-	20.3	\tilde{t}_1 850 GeV	1404.250
$\tilde{g}\rightarrow q\bar{q}$	2 e, μ (SS)	0-3 b	Yes	20.3	\tilde{g} 490 GeV	$m(\tilde{g}) > 200$ GeV 1501.01325
$\tilde{g}\rightarrow t\bar{t}, \tilde{t}_1 \rightarrow b\bar{b}$	0	2 c	Yes	20.3	\tilde{g}	

*Only a selection of the available mass limits on new states or phenomena is shown. All limits quoted are observed minus 1σ theoretical signal cross section uncertainty.

Conclusions (3): “We got it”

323

The scalar Boson ID :

- Mass measured to 0.2%
- Properties compatible with the SM predictions
- It's a scalar (0^+)
- It's thin (width)
- It decays to EW vector bosons
- It decays to photons through loops
- Evidence for VBF production
- Evidence for decays to tau fermion pairs.

The new Scalar Boson it's a portal to more physics topics

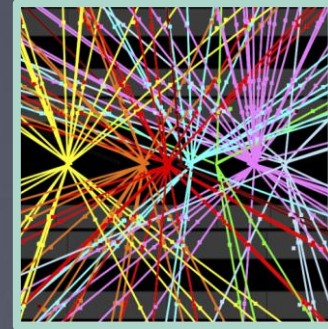
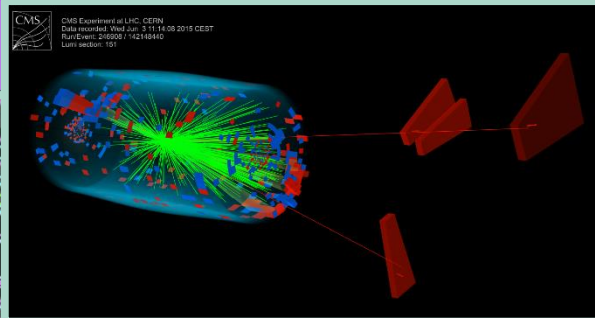
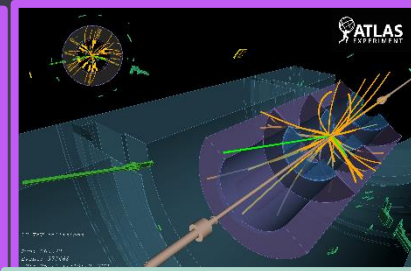
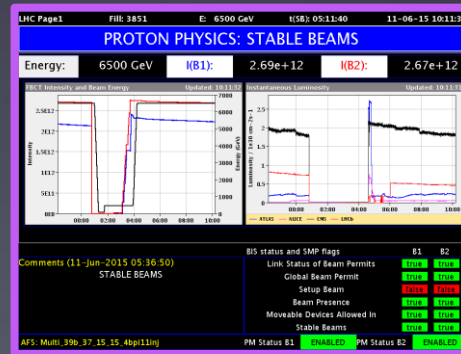
- Higgs couplings to fermions
- Differential cross sections
- Higgs self-couplings (HH, HHH)
- Rare Higgs decays

The new Scalar Boson it's a portal for New Physics

- Invisible Higgs decays
- BSM physics implying additional Higgses

Conclusion (4)

We are starting taking data at 13 TeV !
Expect 100 fb⁻¹ in Run2 (by 2018)



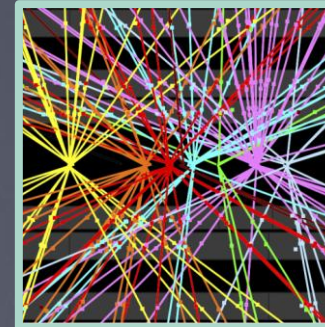
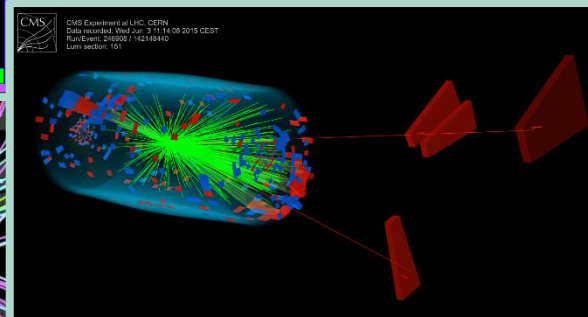
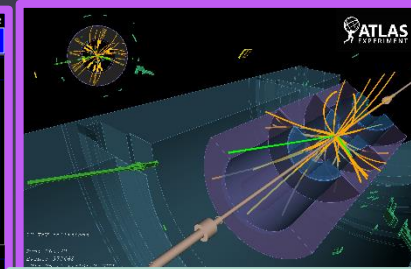
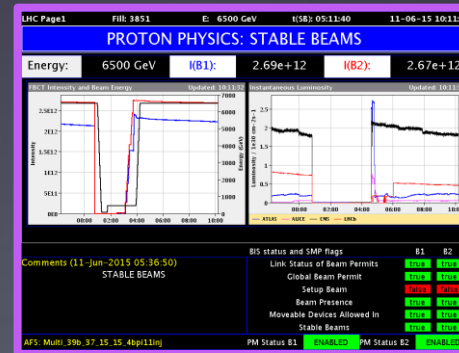
Conclusion (4)

We are starting taking data at 13 TeV !
Expect 100 fb⁻¹ in Run2 (by 2018)

In terms of possible discoveries:

nothing in the future of the LHC programme will match the step forward from 20 fb⁻¹ at 8 TeV to 100 fb⁻¹ at 13 TeV

M. Mangano LHCC, 3/6/15



Conclusion (4)

We are starting taking data at 13 TeV !
Expect 100 fb⁻¹ in Run2 (by 2018)

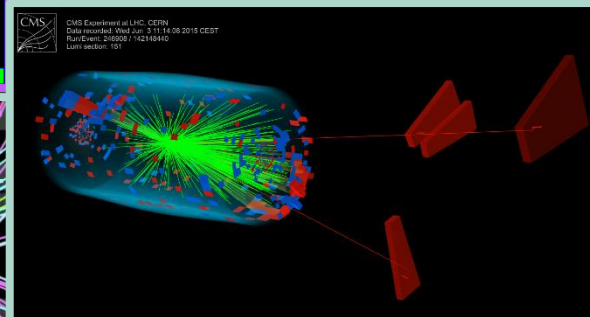
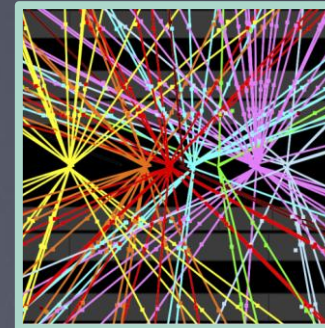
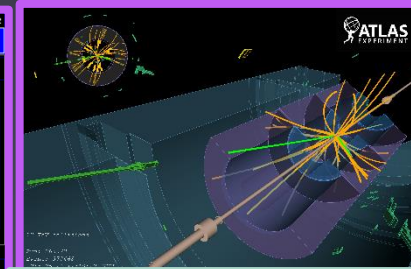
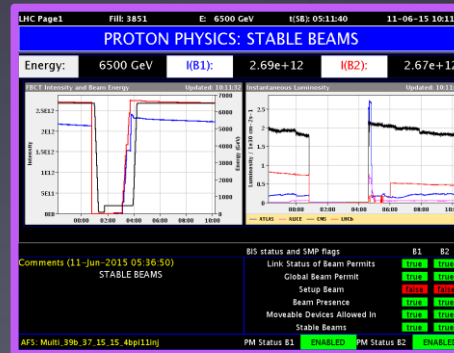
In terms of possible discoveries:

nothing in the future of the LHC programme will match the step forward from 20 fb⁻¹ at 8 TeV to 100 fb⁻¹ at 13 TeV

M. Mangano LHCC, 3/6/15

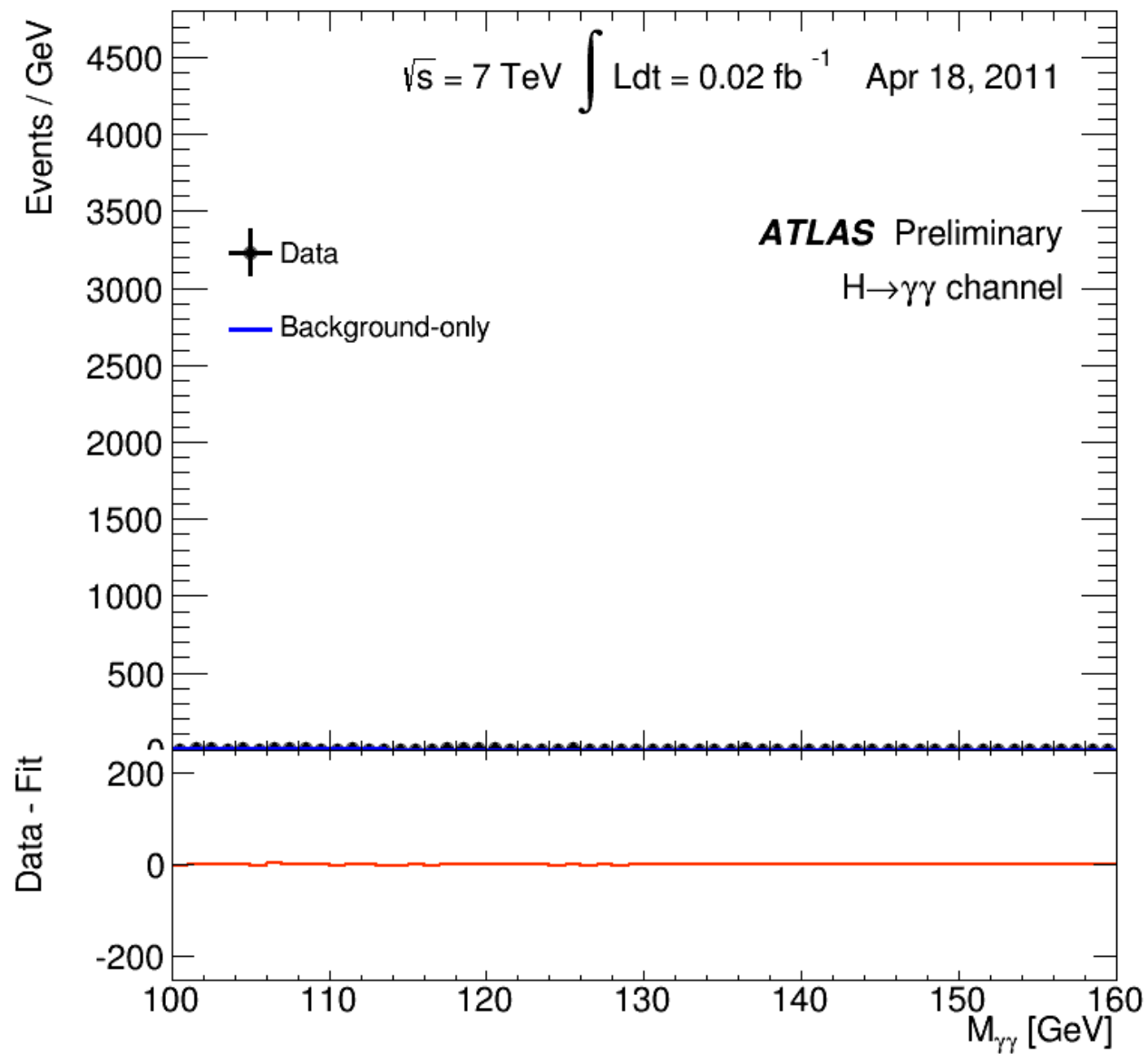
On the Higgs side:

- Observe H→bb, ttH, confirm H→ττ
- Gain in precision in the other channels
- Move from statistically limited to systematically limited measurements
- Theoretical work to improve the theory uncertainties



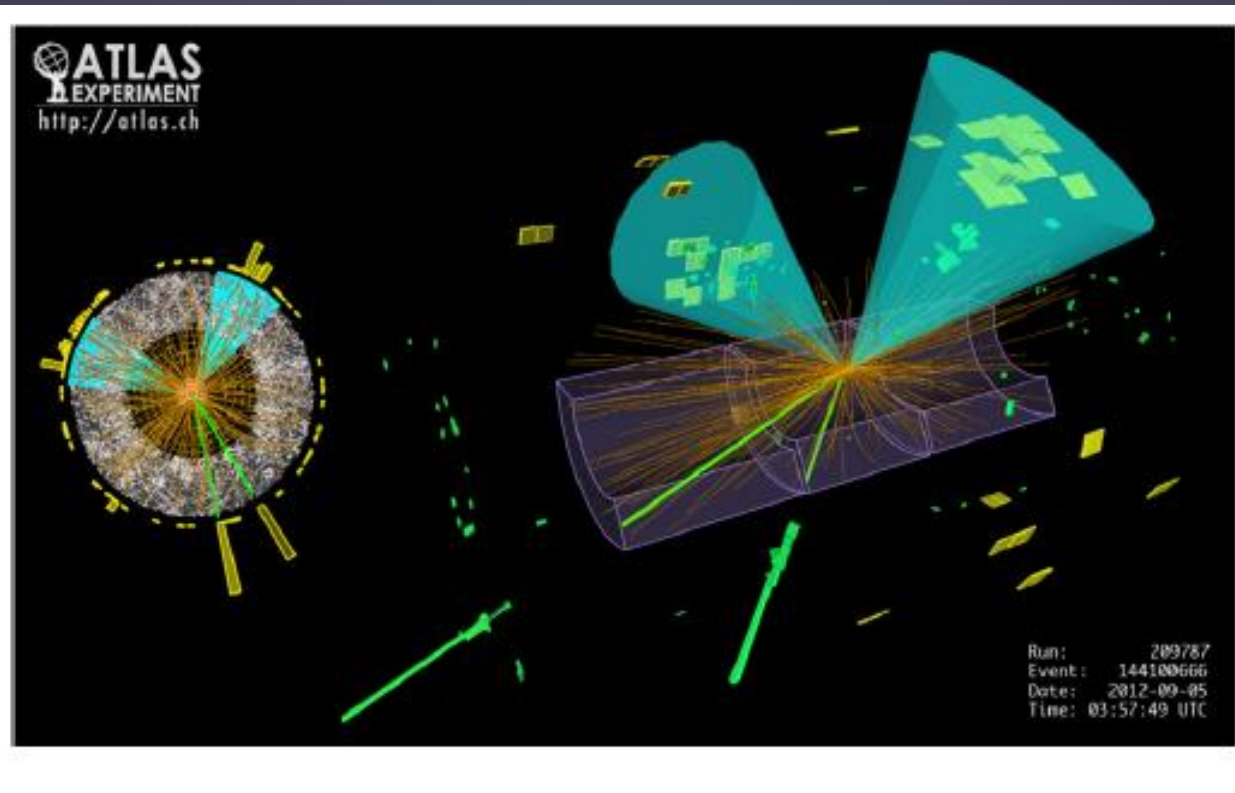
	$\sigma(8 \text{ TeV})$	$\sigma(13 \text{ TeV})$	ratio
gg→H	19.3	43.9	2.3
VBF	1.58	3.75	2.4
WH	0.70	1.38	2.0
ZH	0.42	0.87	2.1
ttH	0.13	0.51	3.9

From Higgs Cross Section WG, @m_H = 125 GeV



Let's hope for other
such new signals
coming out from Run2 !

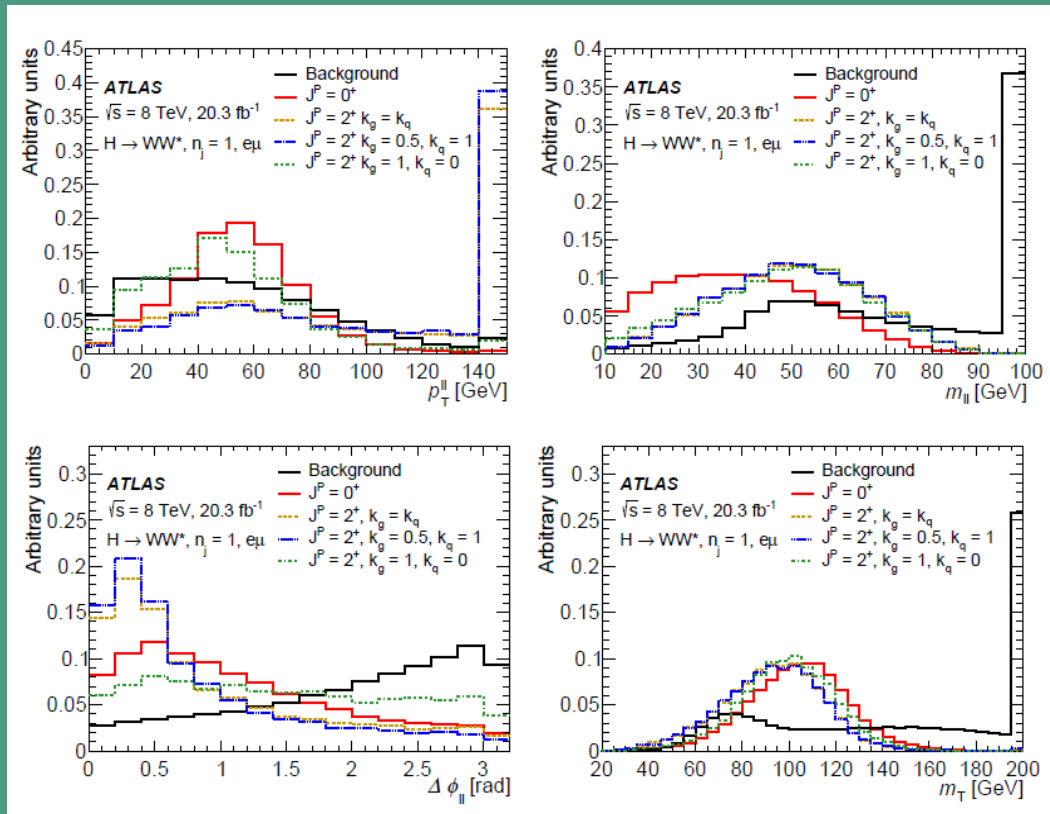
BACKUP



Spin 0 vs Spin 2 : tested with $H \rightarrow \gamma\gamma$, $H \rightarrow ZZ^* \rightarrow 4l$ and $H \rightarrow WW^* \rightarrow l\nu l\nu$

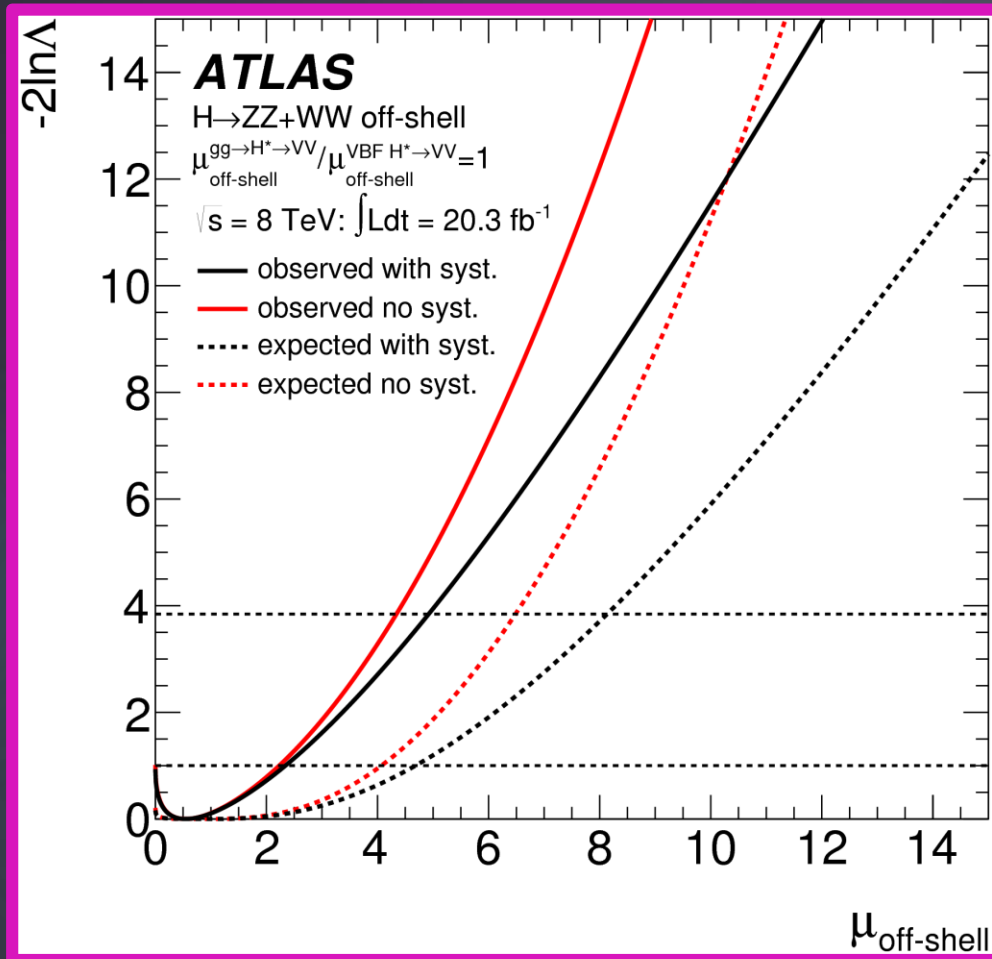
330

Invisibles 2015, Lydia Iconomidou-Fayard
 16/06/2015



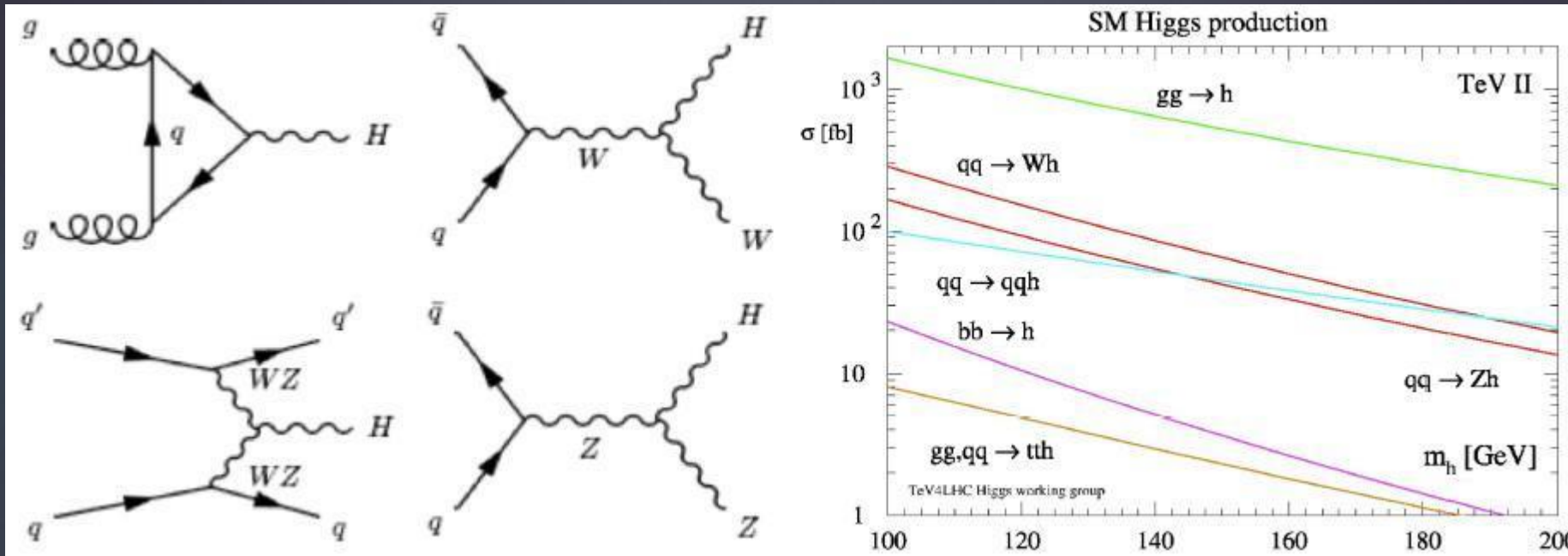
The off-shell strength

331



$\mu_{\text{off-shell}} < 6.2$ (8.1 expected) for standard $gg \rightarrow H^*$ and VBF strengths

Scalar boson production at Tevatron (ppbar machine, 1.96TeV)



H → $\tau\tau$

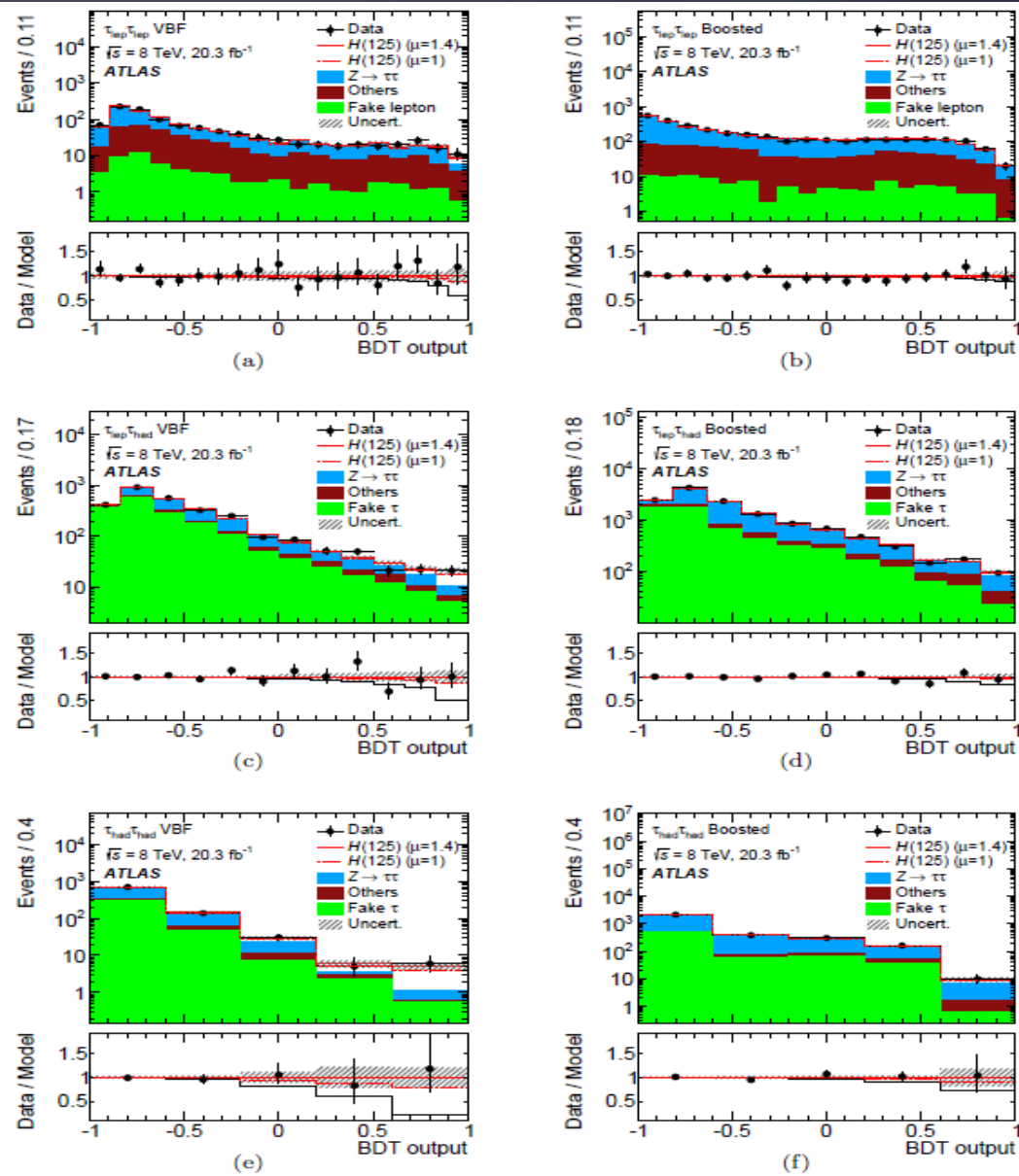
The 3 categories are split further:

--- VBF : + 2 high-pt jets with large separation in pseudorapidity

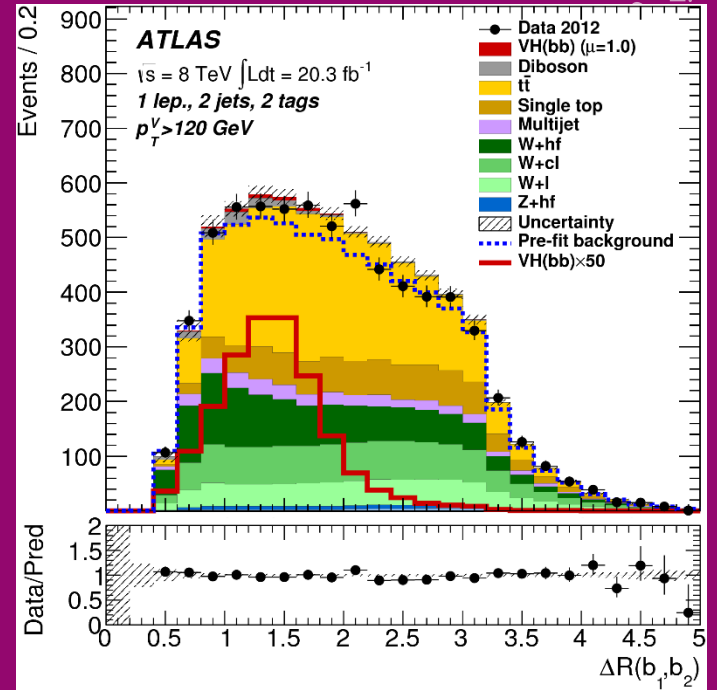
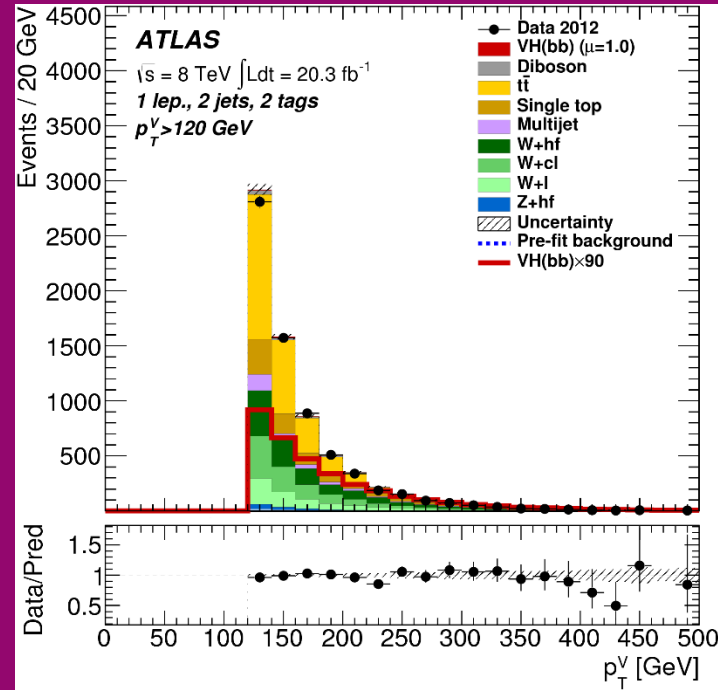
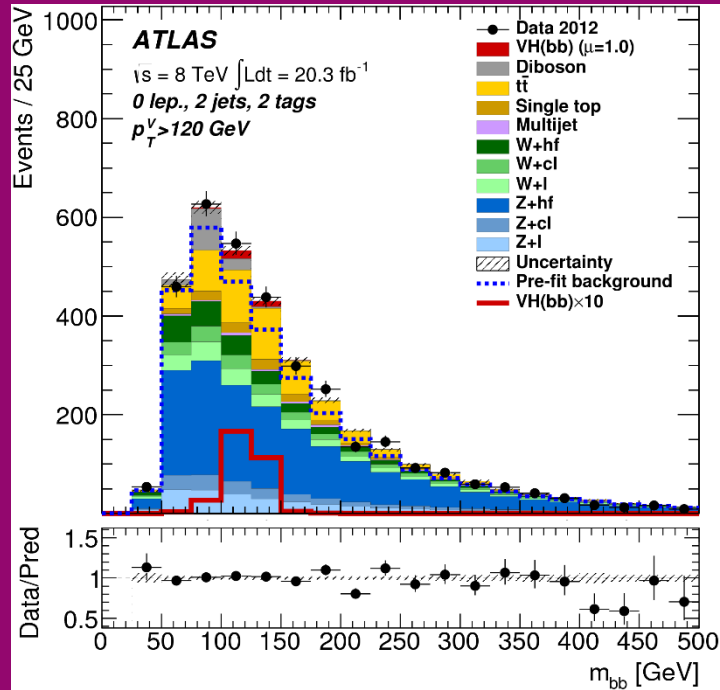
--- Boosted Higgs: no VBF but $P_{T^H} > 100$ GeV

Background checked in specific data control regions

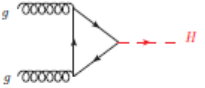
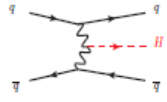
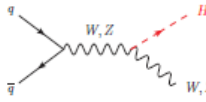
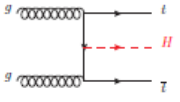
Final discriminant is a Boosted Decision Tree ran for all 6 categories



VH->bb



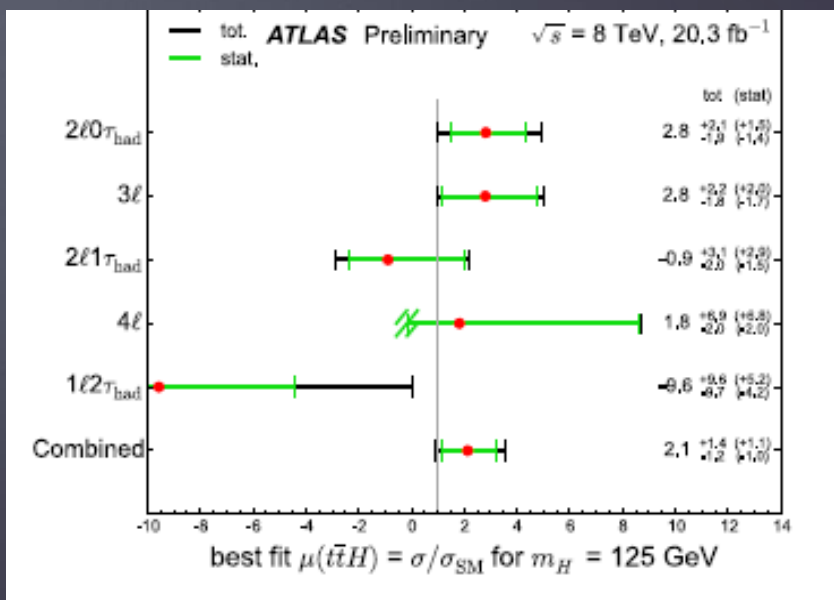
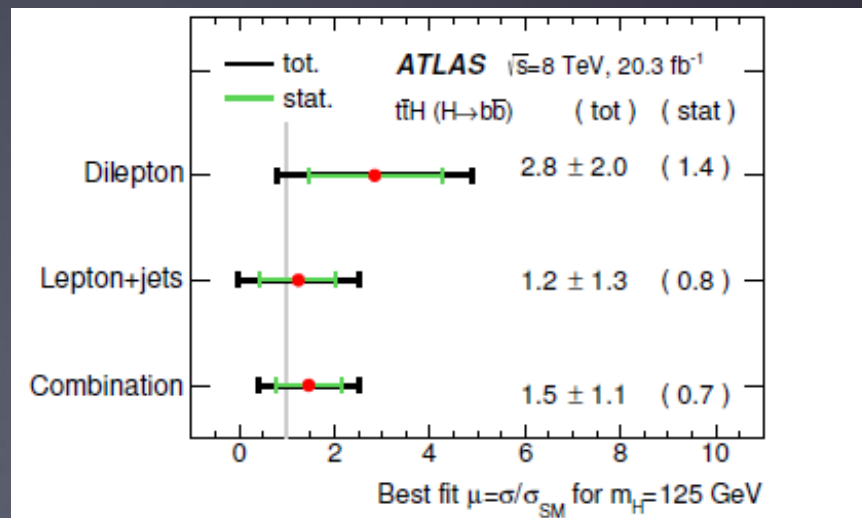
1/6/0
 Invis

Channel categories	ggF 	VBF 	VH 	ttH 
$\gamma\gamma$	✓	✓	✓	✓
ZZ (Hll)	✓	✓	✓	✓
WW (llνν)	✓	✓	✓	✓
$\tau\tau$	✓	✓	✓	✓
bb		✓	✓	✓
Zγ	✓	✓		
$\mu\mu$	✓	✓		
Invisible	✓ (monojet)	✓	✓	

ttH

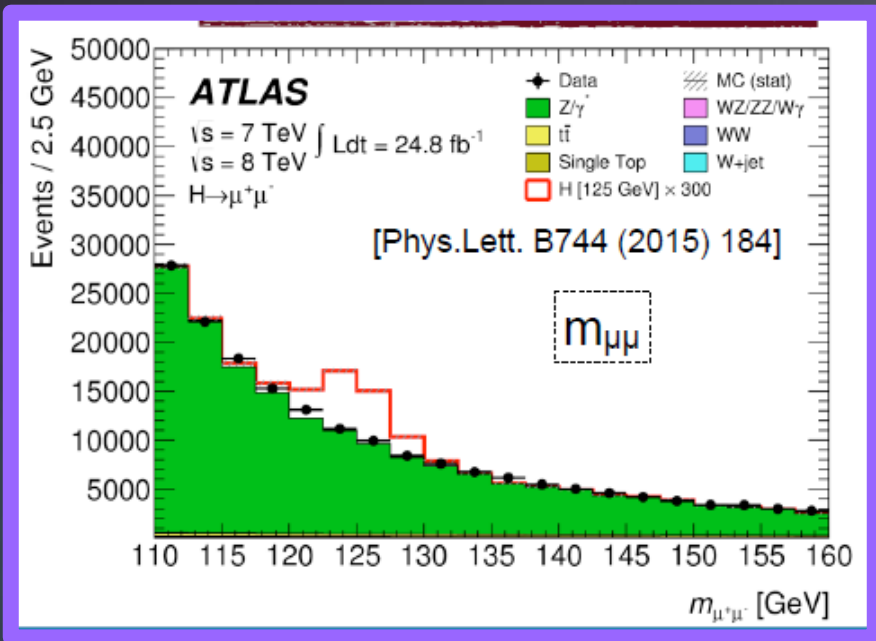
Use H Decay channels $H \rightarrow b\bar{b}$, $H \rightarrow WW^*/ZZ^*/\tau\tau$, $H \rightarrow \gamma\gamma$

Limits on ttH/SM production
 3.4(3.1) in bb channel at 95%
 4.7(3.7) in multiLepton channel at 95%
 6.7 (4.9) in $\gamma\gamma$ channel at 95%

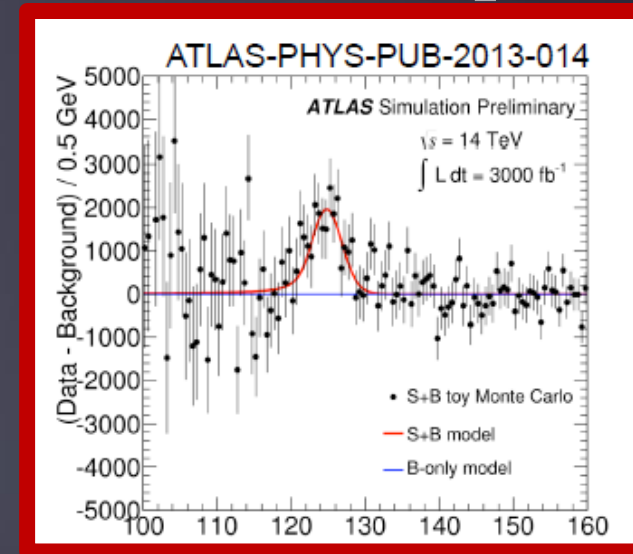


H → μμ

Expectations for next runs



$\mathcal{L} [\text{fb}^{-1}]$	300	3000
N_{ggH}	1510	15100
N_{VBF}	125	1250
N_{WH}	45	450
N_{ZH}	27	270
N_{tH}	18	180
N_{Bkg}	564000	5640000
$\Delta_{Bkg}^{sys} (\text{model})$	68	110
$\Delta_{Bkg}^{sys} (\text{fit})$	190	620
Δ_{stat}	750	2380
Signal significance	2.3σ	7.0σ
$\Delta\mu/\mu$	46%	21%



Invisibles 2011
 16/06/2015

Fill the LHC with protons

338

2808 bunches $\times 1.15 \cdot 10^{11} = 3 \cdot 10^{14}$ protons per beam
or, $6 \cdot 10^{14}$ protons for the two beams (1)

A small commercial hydrogen cylinder contains about 5 kg of gas. So the amount of hydrogen molecules is:

$$n = 5000/2 = 2500 \text{ moles}$$

$$2500 \times 6 \cdot 10^{23} = 1.5 \cdot 10^{27} \text{ molecules}$$

$$N = 2 \times 1.5 \cdot 10^{27} = 3 \cdot 10^{27} \text{ atoms}$$

Taking into account that the process yields about 70% protons we have:

$$0,7 \times 3 \cdot 10^{27} = 2.1 \cdot 10^{27} \text{ atoms}$$

With (1), this cylinder can be used:

$$2.1 \cdot 10^{27} / 6 \cdot 10^{14} = 3.5 \cdot 10^{12} \text{ times}$$

Since the LHC is filled every ten hours, this cylinder could be used for:

$$10 \times 3.5 \cdot 10^{12} = 3.5 \cdot 10^{13} \text{ hours}$$

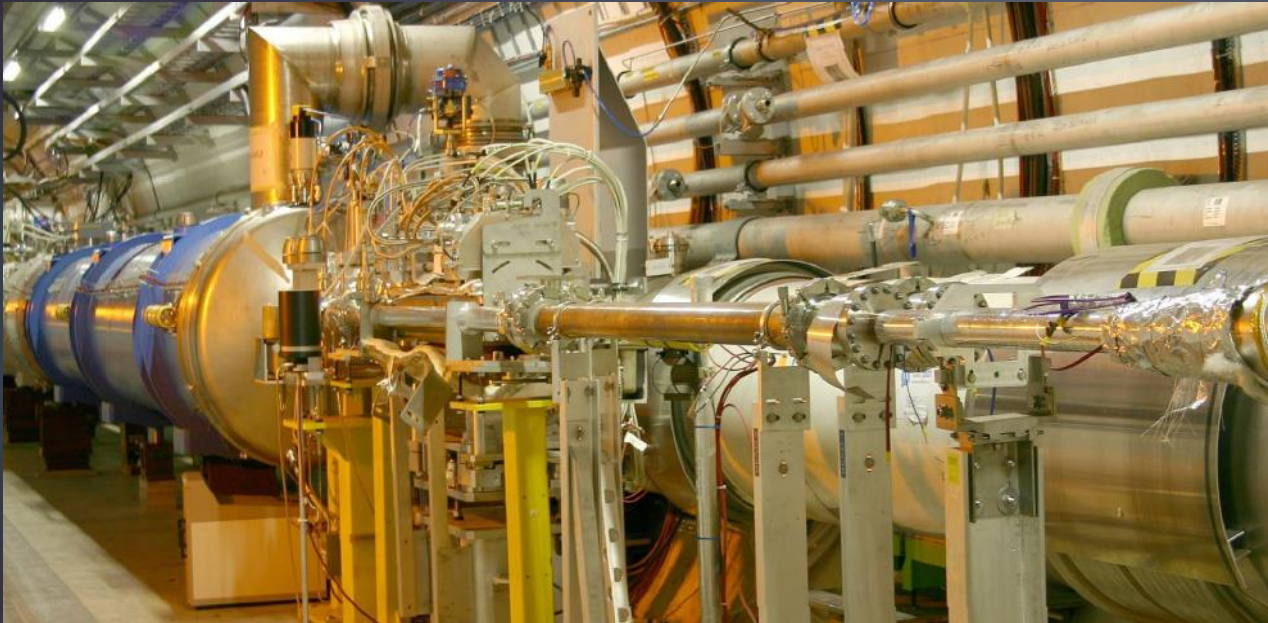
So, about $4 \cdot 10^9$ years

<http://www.lhc-closer.es/1/3/10/0>

From cold beam tube to Room Temperature beam tubes

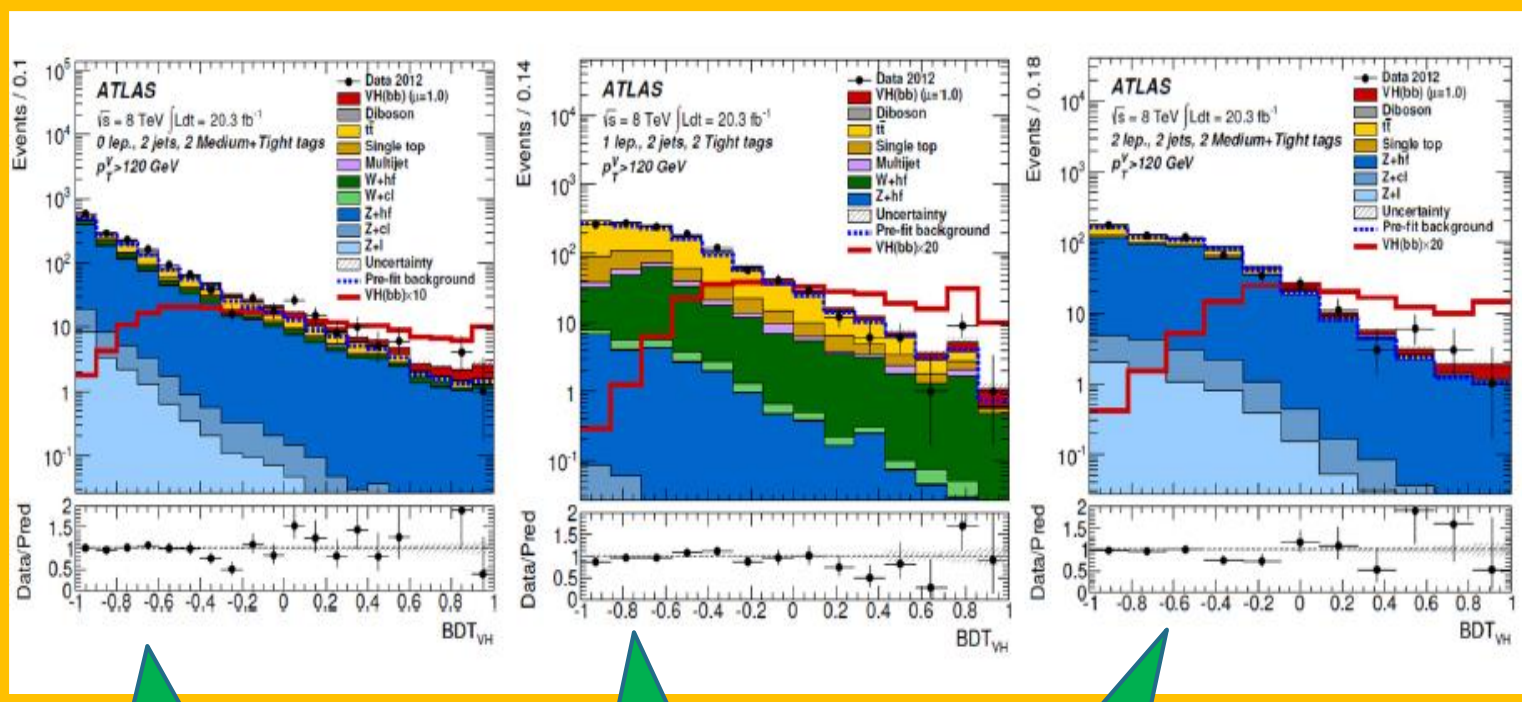
339

Invisibles 2015, L
16/06/2015



VH->bb

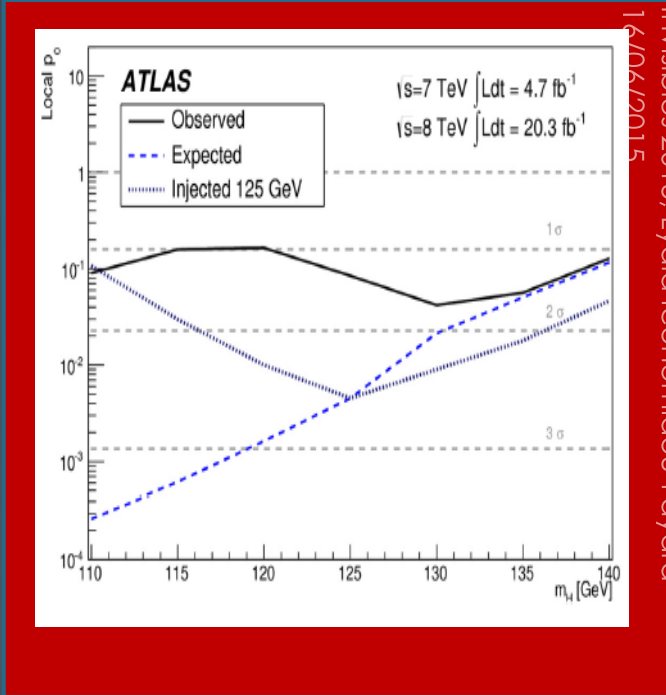
BDT score for the 3 final states



0 lepton - 2Jets

1 lepton - 2jets

2 leptons - 2jets



Observed (expected) significance:
ATLAS : 1.4σ (2.6)
CMS : 2.1σ (2.1)

LHC schedule (M.Lamont LHCC June 3)

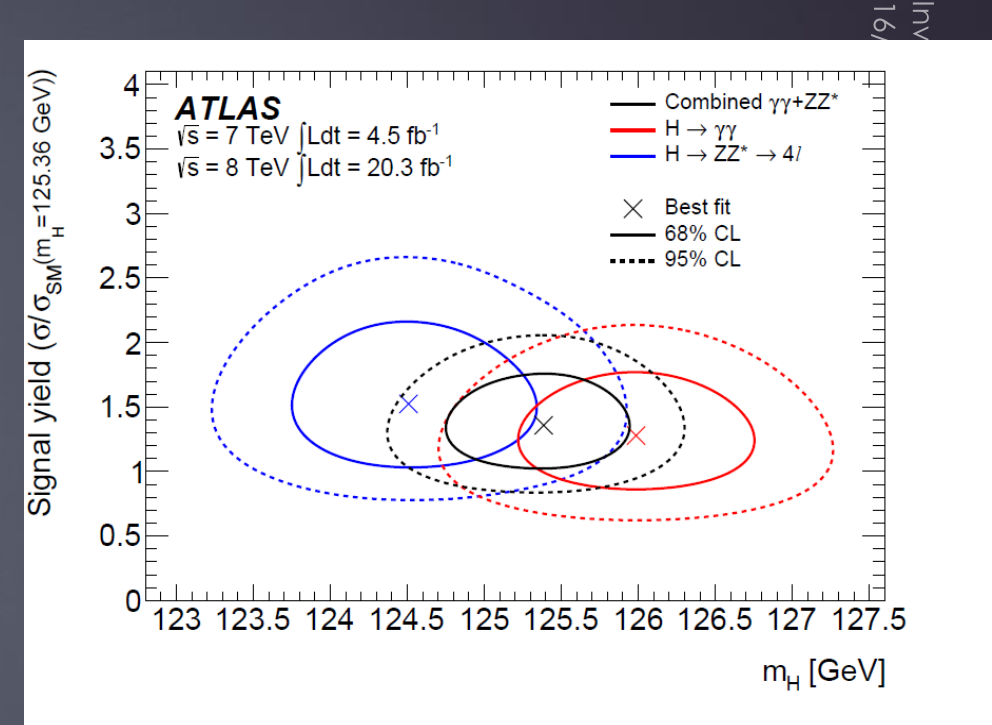
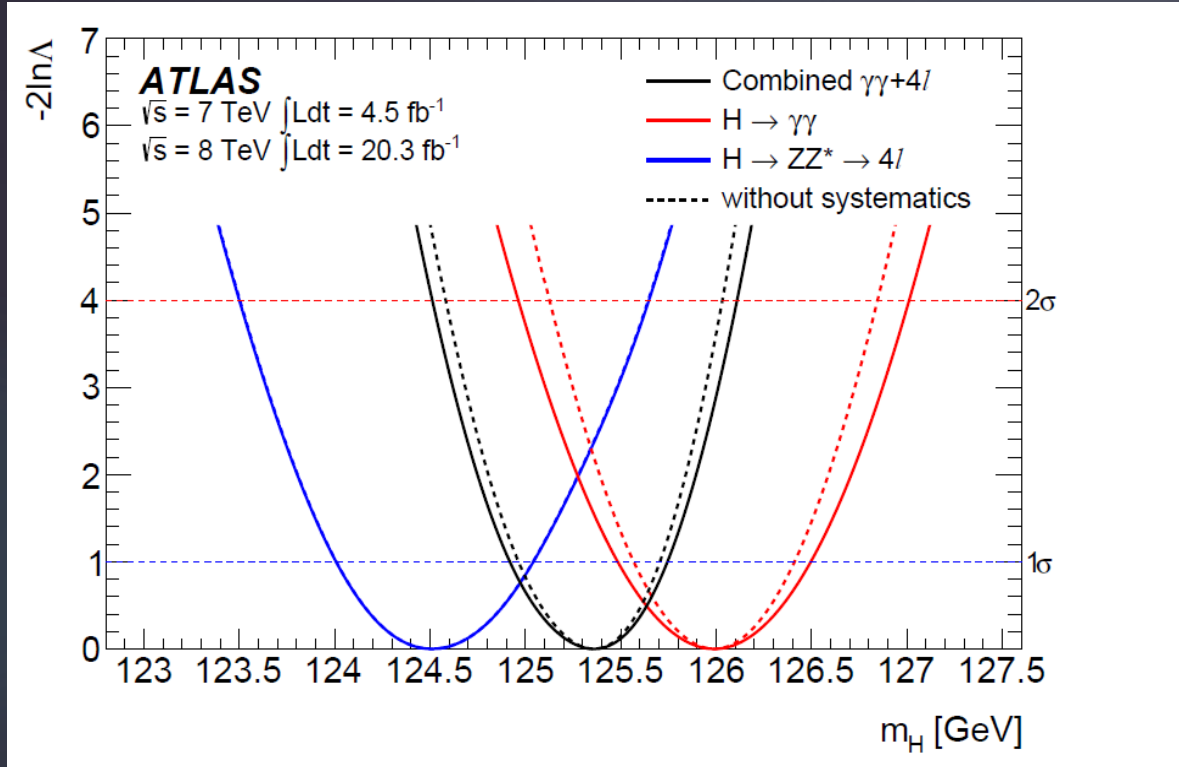
341

2015 – latest schedule

Phase	Days
Initial Commissioning	57
Scrubbing	23
Special physics run 1 (LHCf/VdM)	5
Proton physics 50 ns	9 + 21
Proton physics 25 ns	70
Special physics run 2 (TOTEM/VdM)	7
Machine development (MD)	15
Technical stops	15
Technical stop recovery	3
Ion setup/Ion run	4 + 24
Total	253 (36 weeks)

ATLAS Higgs mass

342

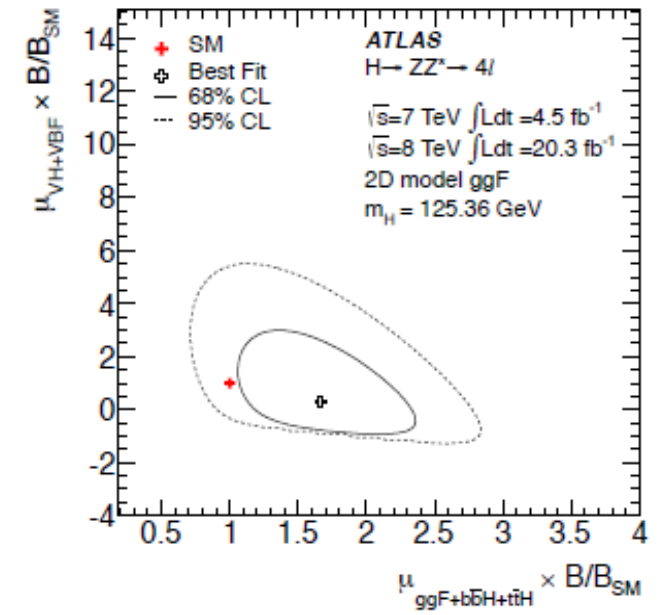
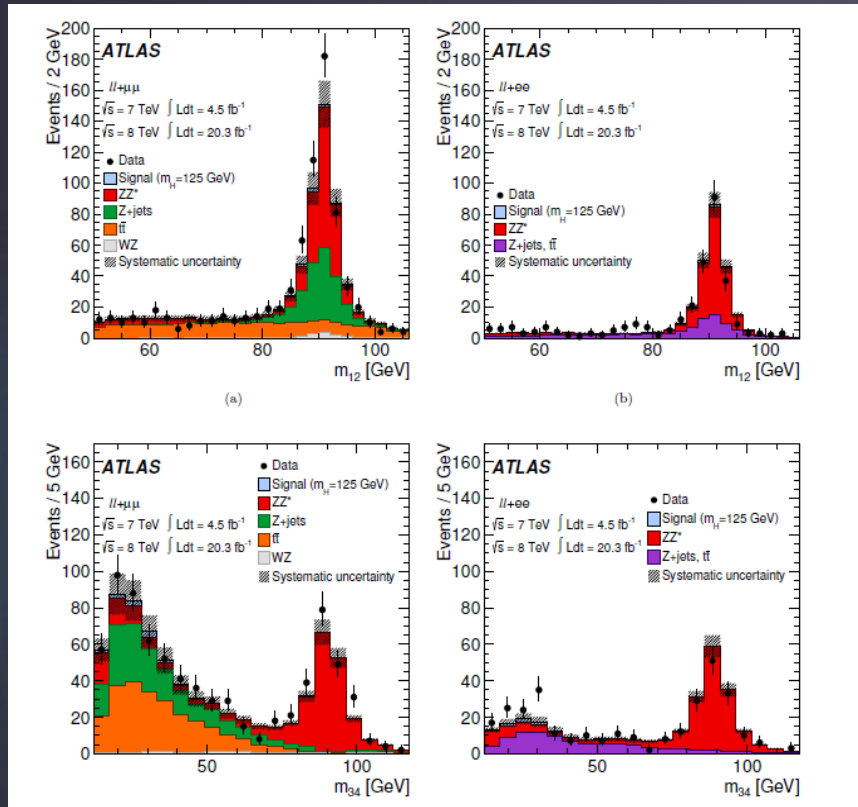


$\Delta m_H = 1.47 \pm 0.72 \text{ GeV} \quad 1.98 \sigma$

H → ZZ* → 4l

$$\mu_{\text{ggF}+b\bar{b}H+t\bar{t}H} \times B/B_{\text{SM}} = 1.66^{+0.45}_{-0.41} \text{ (stat)} \quad ^{+0.25}_{-0.15} \text{ (syst)}$$

$$\mu_{\text{VBF}+\text{VH}} \times B/B_{\text{SM}} = 0.26^{+1.60}_{-0.91} \text{ (stat)} \quad ^{+0.36}_{-0.23} \text{ (syst)}$$



VBF : Observe 1 event (exp 1.3)

Xsections & Br for $m_H=125.36$ GeV

Table 1: SM predictions of the Higgs boson production cross sections and decay branching ratios and their uncertainties for $m_H = 125.36$ GeV, obtained by linear interpolations from those at 125.3 and 125.4 GeV from Ref. [11] except for the tH production cross section which is obtained from Ref. [26]. The uncertainties on the cross sections are the quadratic sum of the uncertainties on the QCD scales, parton distribution functions and α_s . The uncertainty on the tH cross section is calculated following the procedure of Ref. [11].

Production process	Cross section (pb)		Decay channel	Branching ratio (%)
	$\sqrt{s} = 7$ TeV	$\sqrt{s} = 8$ TeV		
ggF	15.0 ± 1.6	19.2 ± 2.0	$H \rightarrow b\bar{b}$	57.1 ± 1.9
VBF	1.22 ± 0.03	1.57 ± 0.04	$H \rightarrow WW^*$	22.0 ± 0.9
WH	0.573 ± 0.016	0.698 ± 0.018	$H \rightarrow gg$	8.53 ± 0.85
ZH	0.332 ± 0.013	0.412 ± 0.013	$H \rightarrow \tau\tau$	6.26 ± 0.35
bbH	0.155 ± 0.021	0.202 ± 0.028	$H \rightarrow c\bar{c}$	2.88 ± 0.35
ttH	0.086 ± 0.009	0.128 ± 0.014	$H \rightarrow ZZ^*$	2.73 ± 0.11
tH	0.012 ± 0.001	0.018 ± 0.001	$H \rightarrow \gamma\gamma$	0.228 ± 0.011
Total	17.4 ± 1.6	22.3 ± 2.0	$H \rightarrow Z\gamma$	0.157 ± 0.014
			$H \rightarrow \mu\mu$	0.022 ± 0.001

Uncertainties on signal Strengths

Production process	Signal strength μ at $m_H = 125.36$ GeV			
	$\sqrt{s} = 8$ TeV	Combined $\sqrt{s} = 7$ and 8 TeV		
ggF	$1.23^{+0.25}_{-0.21}$	$\begin{bmatrix} +0.16 & +0.10 & +0.16 \\ -0.16 & -0.08 & -0.11 \end{bmatrix}$	$1.23^{+0.23}_{-0.20}$	$\begin{bmatrix} +0.14 & +0.09 & +0.16 \\ -0.14 & -0.08 & -0.12 \end{bmatrix}$
VBF	$1.55^{+0.39}_{-0.35}$	$\begin{bmatrix} +0.32 & +0.17 & +0.13 \\ -0.31 & -0.13 & -0.11 \end{bmatrix}$	1.23 ± 0.32	$\begin{bmatrix} +0.28 & +0.13 & +0.11 \\ -0.27 & -0.12 & -0.09 \end{bmatrix}$
VH	0.93 ± 0.39	$\begin{bmatrix} +0.37 & +0.20 & +0.12 \\ -0.33 & -0.18 & -0.06 \end{bmatrix}$	0.80 ± 0.36	$\begin{bmatrix} +0.31 & +0.17 & +0.10 \\ -0.30 & -0.17 & -0.05 \end{bmatrix}$
ttH	1.62 ± 0.78	$\begin{bmatrix} +0.51 & +0.58 & +0.28 \\ -0.50 & -0.54 & -0.10 \end{bmatrix}$	1.81 ± 0.80	$\begin{bmatrix} +0.52 & +0.58 & +0.31 \\ -0.50 & -0.55 & -0.12 \end{bmatrix}$

Invisibles 2015, Lydia Iconomidou-Fayard 16/06/2015

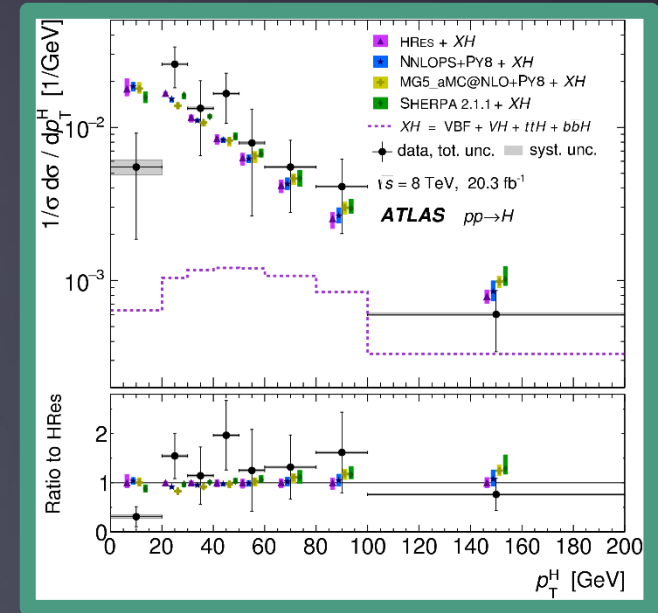
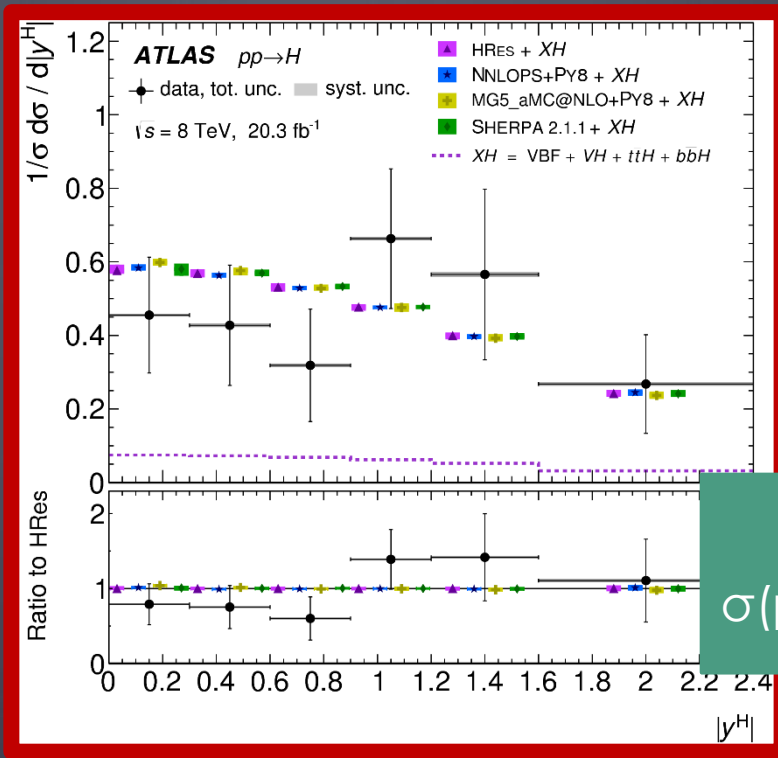
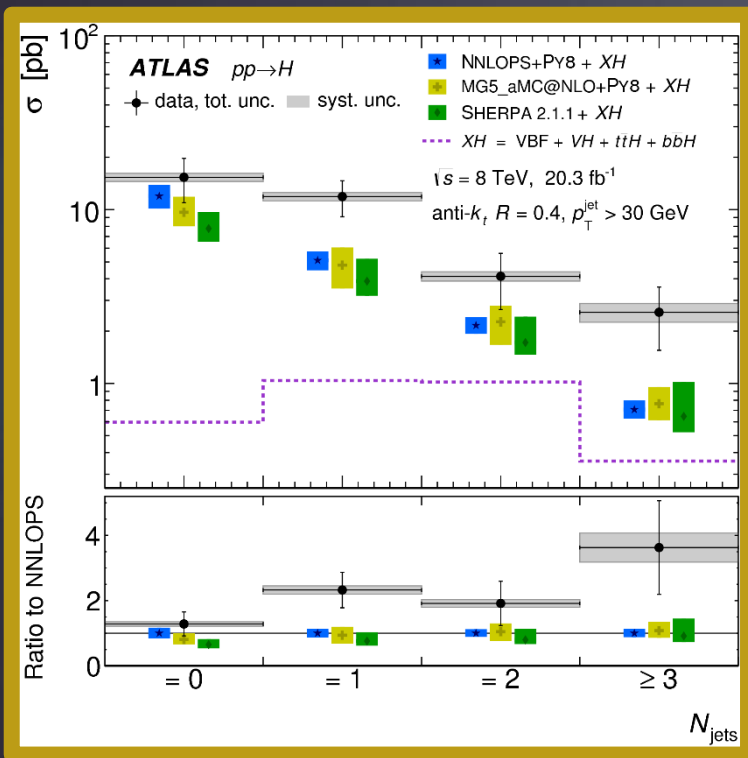
Statistical uncertainties

Experimental systematic uncertainties:
Signal and background modeling

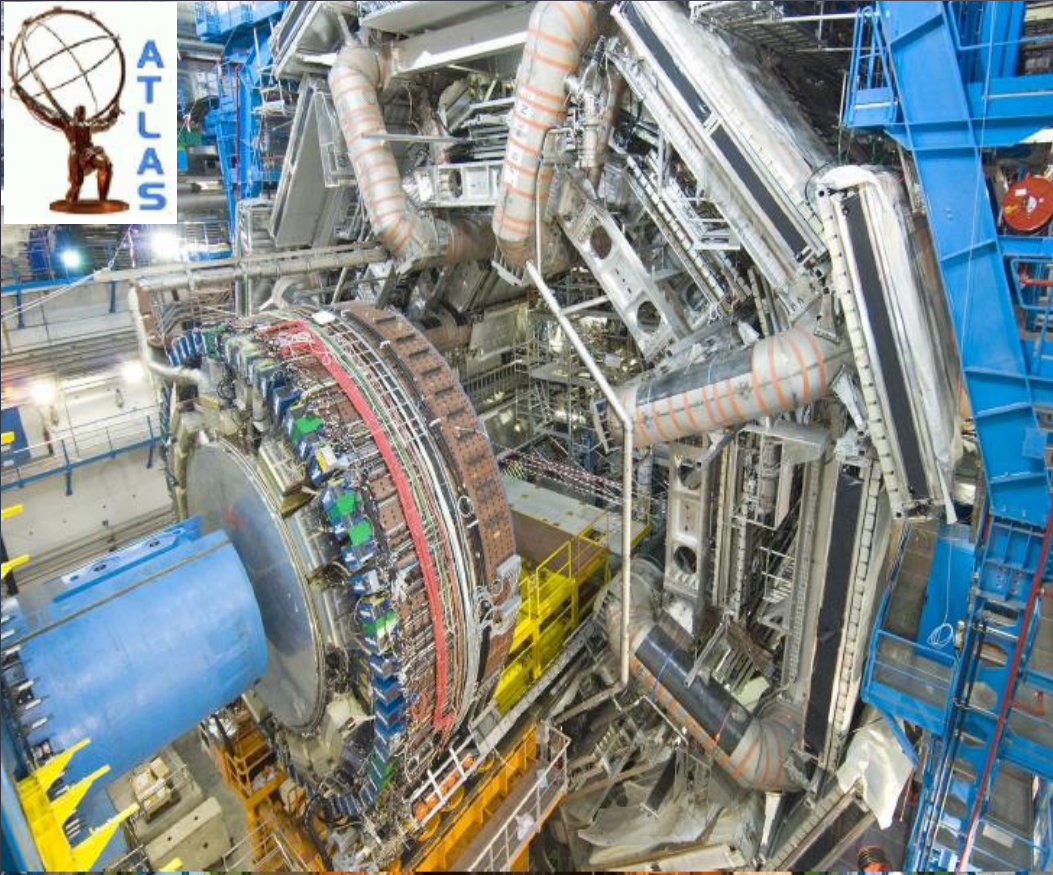
Theory uncertainties on production
Xsections, Br's, PDF's, QCD scale etc

Differential Cross sections vs p_T , rapidity, Nb of jets ...

Help at constraining QCD and PDF for ggF and VBF computations looking at different variables
 → Contribute to decrease uncertainties

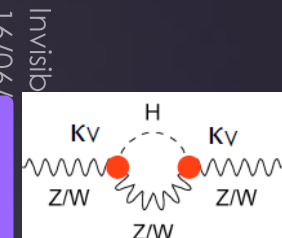
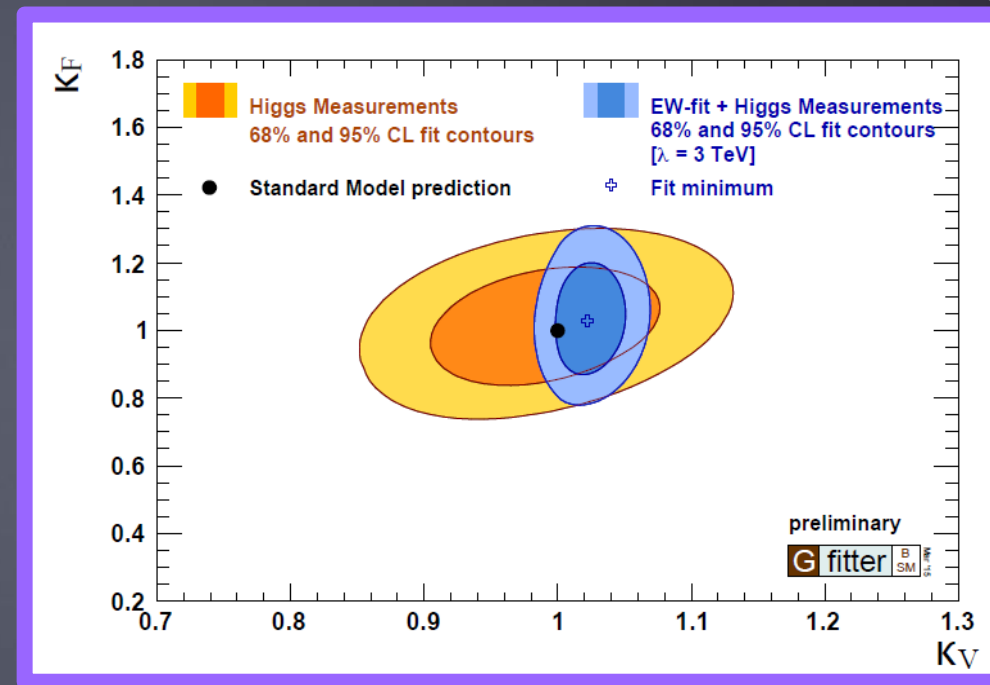


Total cross-section
 $\sigma(pp \rightarrow H) = 33.0 \pm 5.3(\text{stat}) \pm 1.6(\text{syst}) \text{ pb}$



Global EW fits

→ M_H [GeV]	125.14 ± 0.24	LHC
→ M_W [GeV]	80.385 ± 0.015	Tev.
Γ_W [GeV]	2.085 ± 0.042	
M_Z [GeV]	91.1875 ± 0.0021	LEP
Γ_Z [GeV]	2.4952 ± 0.0023	
σ_{had}^0 [nb]	41.540 ± 0.037	
R_ℓ^0	20.767 ± 0.025	
$A_{\text{FB}}^{0,\ell}$	0.0171 ± 0.0010	SLD
A_ℓ (*)	0.1499 ± 0.0018	
$\sin^2\theta_{\text{eff}}^\ell(Q_{\text{FB}})$	0.2324 ± 0.0012	SLD
A_c	0.670 ± 0.027	
A_b	0.923 ± 0.020	LEP
$A_{\text{FB}}^{0,c}$	0.0707 ± 0.0035	
$A_{\text{FB}}^{0,b}$	0.0992 ± 0.0016	
R_c^0	0.1721 ± 0.0030	
R_b^0	0.21629 ± 0.00066	
$\Delta\alpha_{\text{had}}^{(5)}(M_Z^2)$	2757 ± 10	low E
\bar{m}_c [GeV]	$1.27^{+0.07}_{-0.11}$	
\bar{m}_b [GeV]	$4.20^{+0.17}_{-0.07}$	
→ m_t [GeV]	173.34 ± 0.76	Tev.+LHC



16/06/2015
Invisibile
diakonimidou-Fayard

k_ν from fit = 1.03 ± 0.02
Much more precise than direct measurement

Definition of production categories

350

Invisibles 2015, Lydia Iconomidou-Fayard
16/06/2015

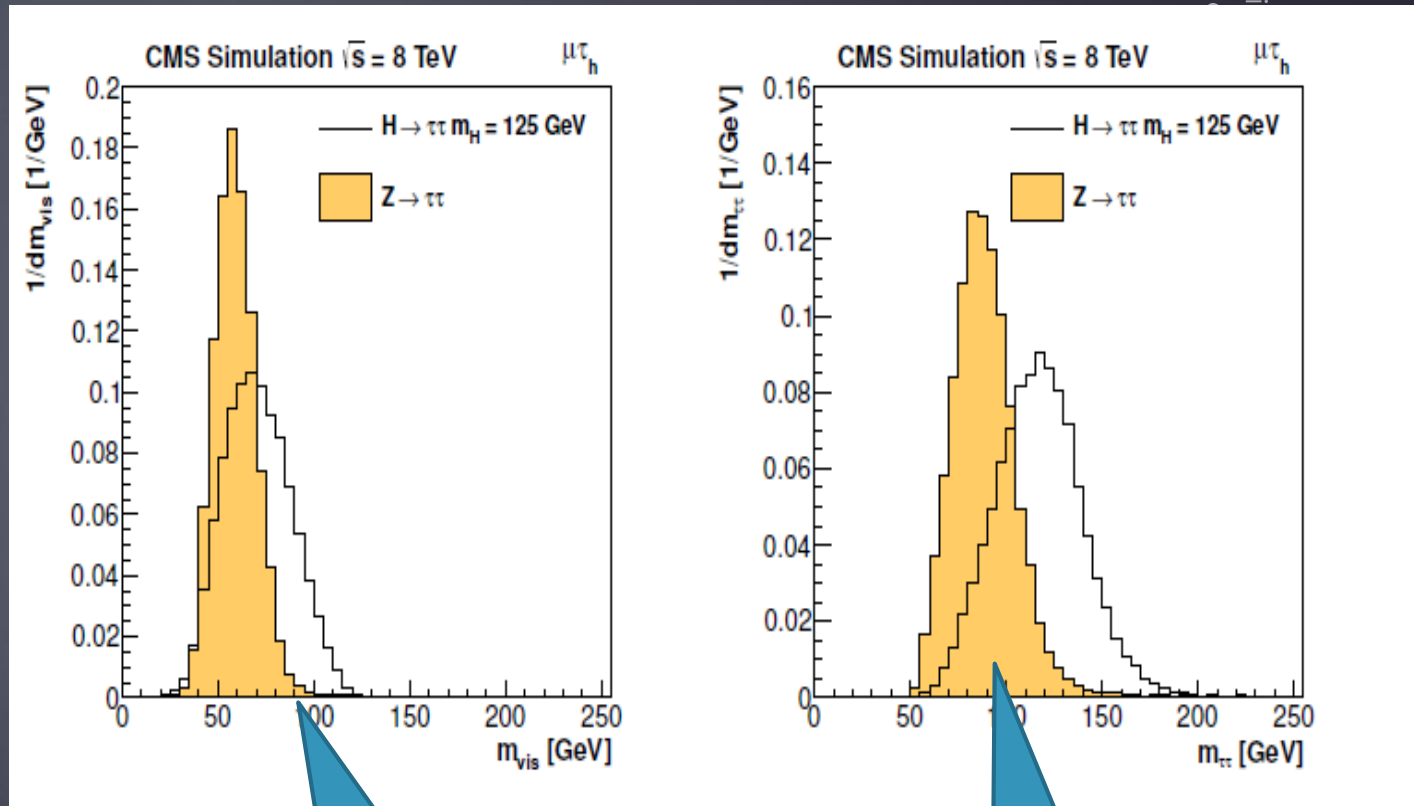
	H-> $\gamma\gamma$	H-> $ZZ^* \rightarrow 4l$	H-> WW^*	H-> $\tau\tau$	H-> bb
ggF	No VBF, no VH, no ttH.	No VBF no VH	2 OSleptons and 0,1, >=2 jets	$P_T^H > 160\text{GeV}$	
VBF	2 well separated high P_T jets.	2 well separated jets with $M_{jj} > 130\text{GeV}$	2leptons+ >=2 jets	2 well separated jets	
VH	One or two leptons, E_T^{miss} and hadronic decays for W,Z	If no VBF, and >1 lepton	Multileptons (2-3-4), E_T^{miss}		0,1,2 leptons for W/Z + 2 b jets
ttH	t->Wb Leptonic and hadronic decays for W. Btags				

H->tautau CMS

351

16/01
Invisi

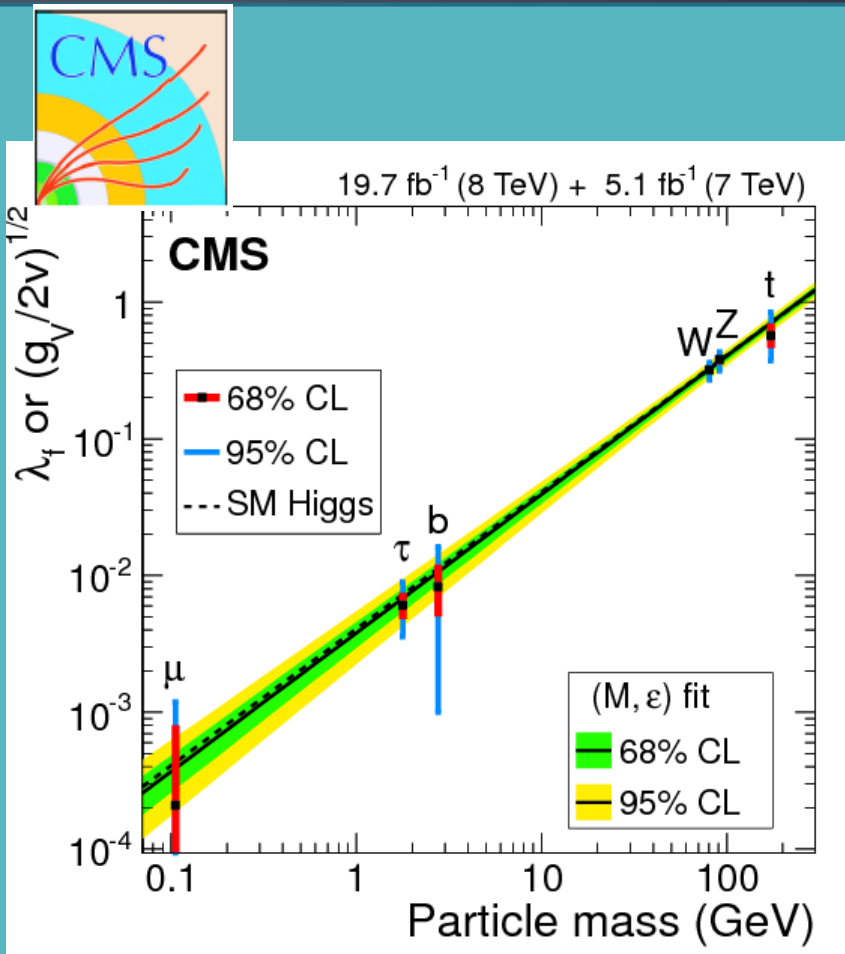
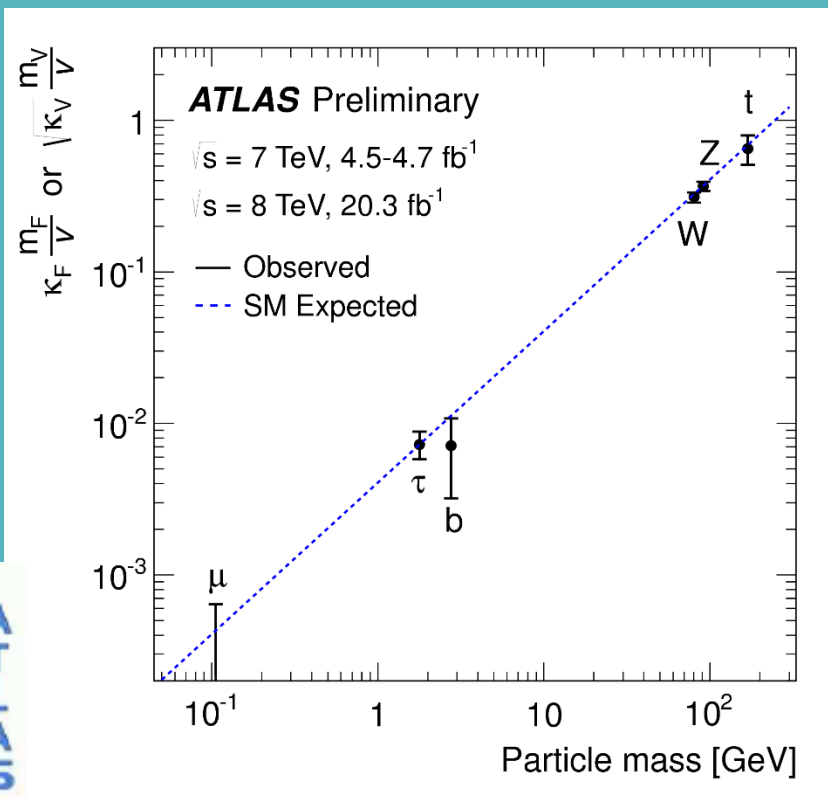
Resolutions on $M_{\tau\tau}$ mass:
10% on had-had
15% on lep-had
20% on lep-lep



Visible mass

After SVFit

Coupling summary



Energy stored in LHC

353

Energy stored in the magneters

$$E_{\text{dipole}} = 0.5 \times L_{\text{dipole}} \times I_{\text{dipole}}^2$$

For 1232 dipoles 9.4 GJ

1.9 Ton of TNT

Energy stored in the beams

2800 bunches/beam

Each containing 10^{11} protons

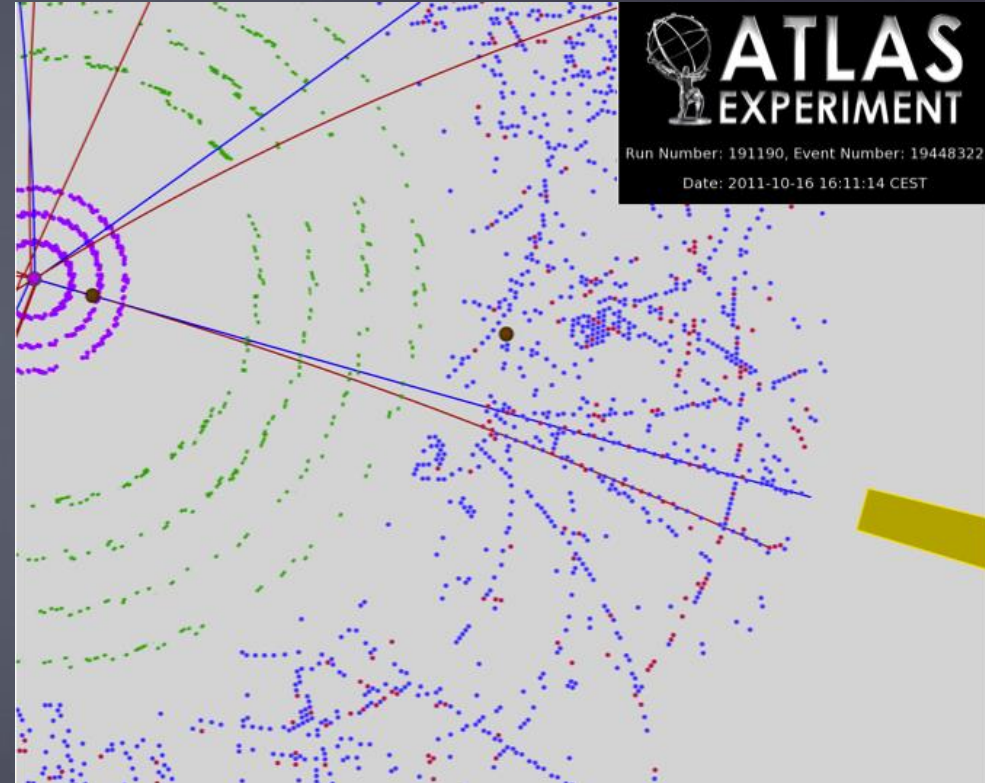
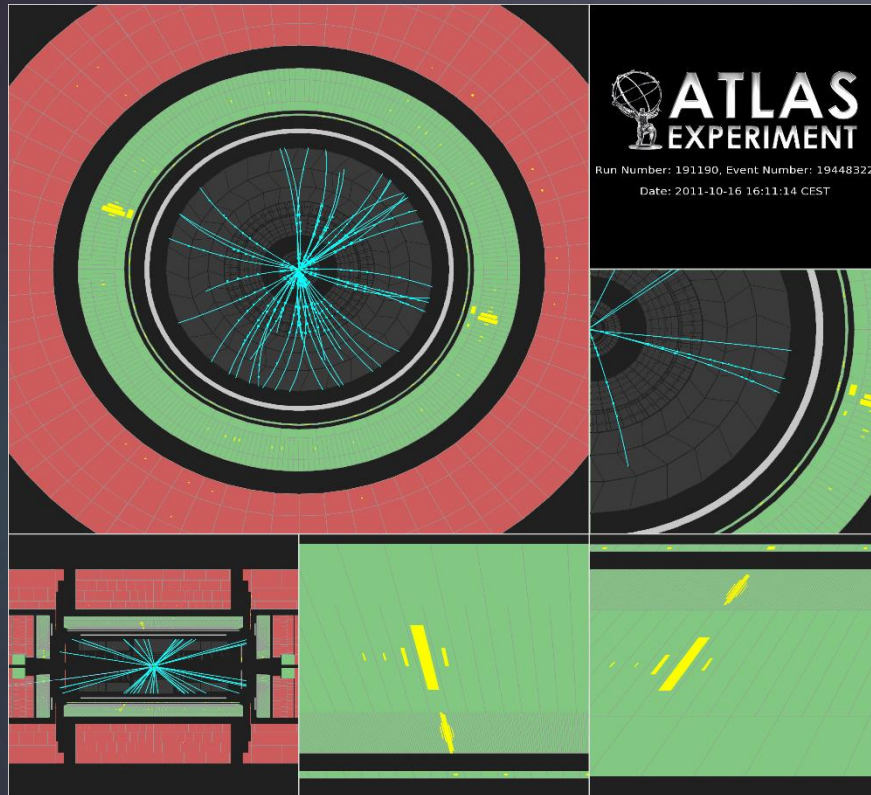
→ 3×10^{14} protons/beam

→ Stored energy for 7TeV

→ 362 MJ/beam

Display of a $H \rightarrow \gamma\gamma$ candidate with a converted photon

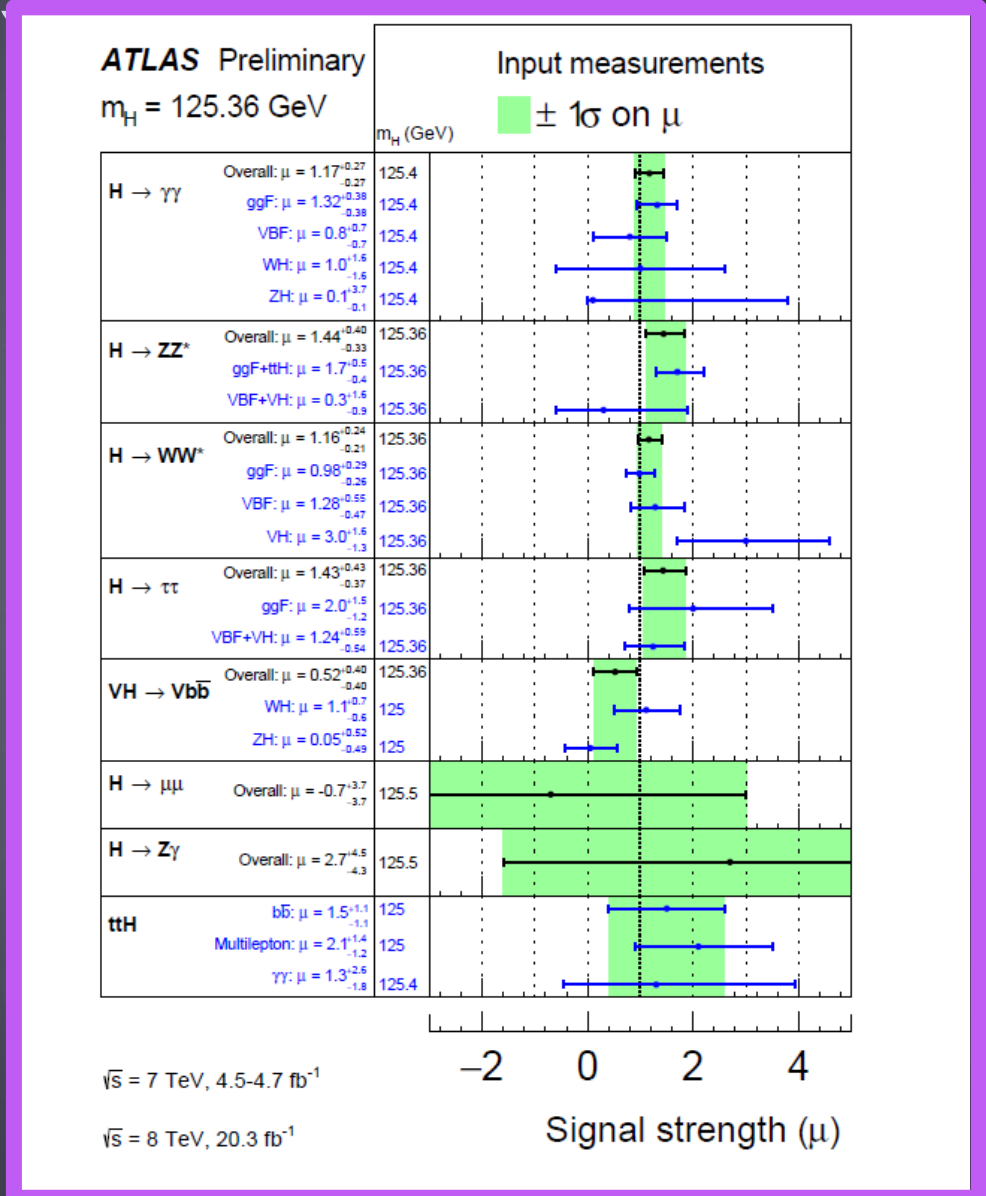
354



Invisibles 2015, Lydia Iconomidou-Fayard
16/06/2015

Analysis	Signal		$\int \mathcal{L} dt$ (fb ⁻¹)		
	Categorisation or final states	Strength	Significance [σ]	7 TeV	8 TeV
$H \rightarrow \gamma\gamma$ [12]		1.17 ± 0.27	5.2 (4.6)	4.5	20.3
$t\bar{t}H$: leptonic, hadronic				✓	✓
VH : one-lepton, dilepton, E_T^{miss} , hadronic				✓	✓
VBF: tight, loose				✓	✓
ggF: 4 p_{T1} categories				✓	✓
$H \rightarrow ZZ^* \rightarrow 4\ell$ [13]		$1.44^{+0.40}_{-0.33}$	8.1 (6.2)	4.5	20.3
VBF				✓	✓
VH : hadronic, leptonic				✓	✓
ggF				✓	✓
$H \rightarrow WW^*$ [14, 15]		$1.16^{+0.24}_{-0.21}$	6.5 (5.9)	4.5	20.3
ggF: (0-jet, 1-jet) \otimes ($ee + \mu\mu, e\mu$)				✓	✓
ggF: ≥ 2 -jet and $e\mu$					✓
VBF: ≥ 2 -jet \otimes ($ee + \mu\mu, e\mu$)				✓	✓
VH : opposite-charge dilepton, three-lepton, four-lepton				✓	✓
VH : same-charge dilepton					✓
$H \rightarrow \tau\tau$ [17]		$1.43^{+0.43}_{-0.37}$	4.5 (3.4)	4.5	20.3
Boosted: $\tau_{\text{lep}}\tau_{\text{lep}}, \tau_{\text{lep}}\tau_{\text{had}}, \tau_{\text{had}}\tau_{\text{had}}$				✓	✓
VBF: $\tau_{\text{lep}}\tau_{\text{lep}}, \tau_{\text{lep}}\tau_{\text{had}}, \tau_{\text{had}}\tau_{\text{had}}$				✓	✓
$VH \rightarrow Vb\bar{b}$ [18]		0.52 ± 0.40	1.4 (2.6)	4.7	20.3
0ℓ ($ZH \rightarrow \nu\nu b\bar{b}$): $N_{\text{jet}} = 2, 3, N_{\text{btag}} = 1, 2, p_{T1}^V > \text{and} < 120 \text{ GeV}$				✓	✓
1ℓ ($WH \rightarrow \ell\nu b\bar{b}$): $N_{\text{jet}} = 2, 3, N_{\text{btag}} = 1, 2, p_{T1}^V > \text{and} < 120 \text{ GeV}$				✓	✓
2ℓ ($ZH \rightarrow \ell\ell b\bar{b}$): $N_{\text{jet}} = 2, 3, N_{\text{btag}} = 1, 2, p_{T1}^V > \text{and} < 120 \text{ GeV}$				✓	✓
95% CL limit					
$H \rightarrow Z\gamma$ [19]			$\mu < 11$ (9)	4.5	20.3
10 categories based on $\Delta\eta_{Z\gamma}$ and p_{T1}				✓	✓
$H \rightarrow \mu\mu$ [20]			$\mu < 7.0$ (7.2)	4.5	20.3
VBF and 6 other categories based on η_μ and $p_{T1}^{\mu\mu}$				✓	✓
$t\bar{t}H$ production [21–23]				4.5	20.3
$H \rightarrow b\bar{b}$: single-lepton, dilepton			$\mu < 3.4$ (2.2)		✓
$t\bar{t}H \rightarrow$ multileptons: categories on lepton multiplicity			$\mu < 4.7$ (2.4)		✓
$H \rightarrow \gamma\gamma$: leptonic, hadronic			$\mu < 6.7$ (4.9)	✓	✓
Off-shell H^* production [24]			$\mu < 5.1 - 8.6$ (6.7 – 11.0)		20.3
$H^* \rightarrow ZZ \rightarrow 4\ell$					✓
$H^* \rightarrow ZZ \rightarrow 2\ell 2\nu$					✓
$H^* \rightarrow WW \rightarrow e\nu\mu\nu$					✓

List of individual signal strength measurements



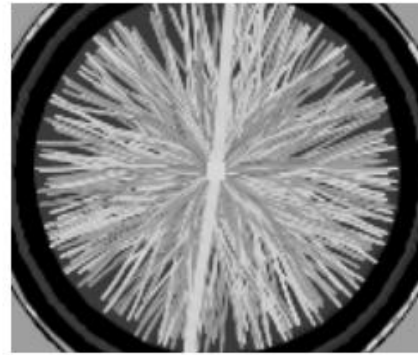
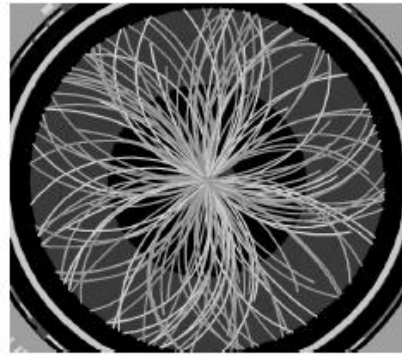
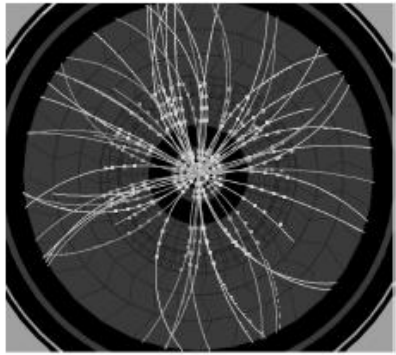
Pileup

357

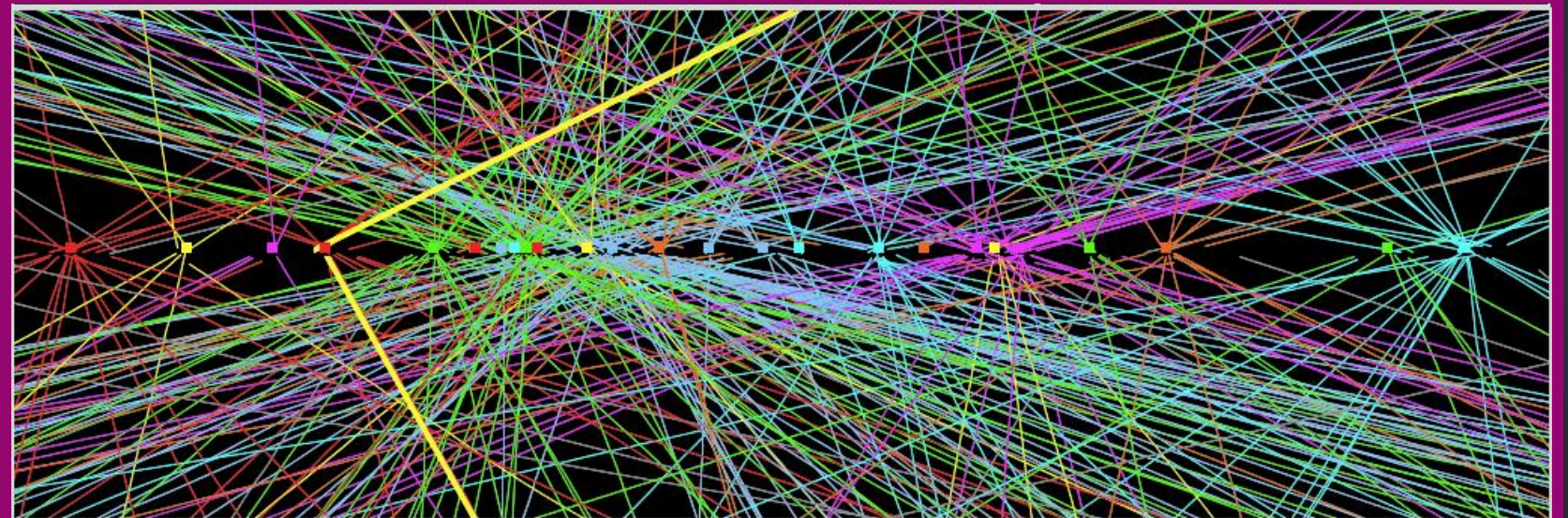
2010 (~2events)

2011 (~10events)

2012 (~30events)



Z- $\mu\mu$ event with 25
reconstructed vertices
2012 data



The niobium-titanium properties

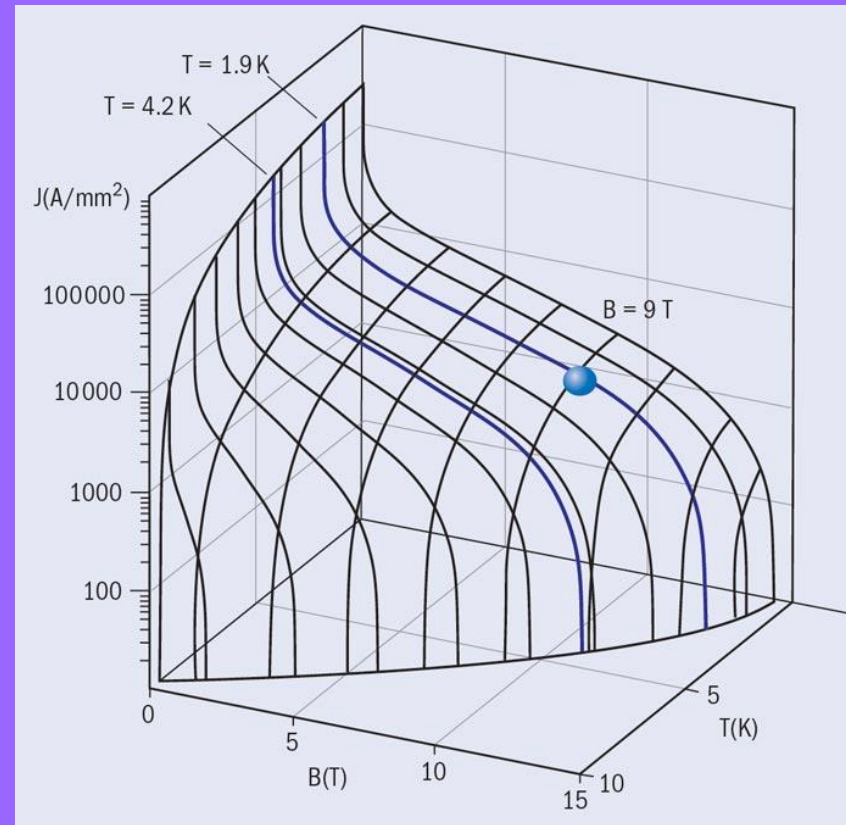
358

Invisibles 2015, Lydia Iconomidou-Fayard
16/06/2015

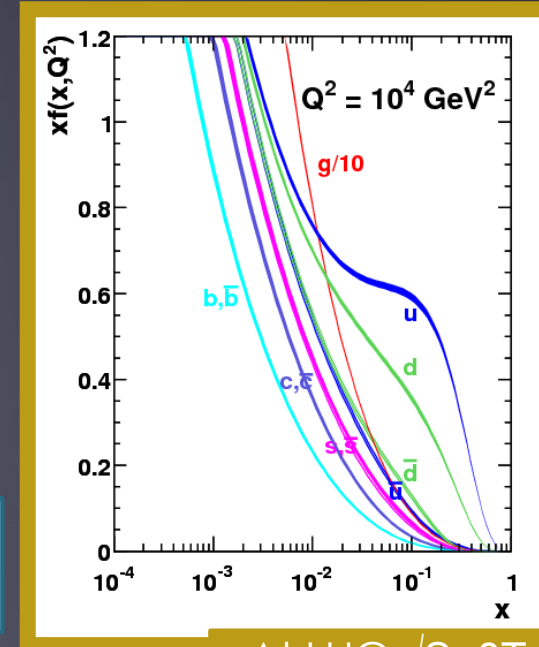
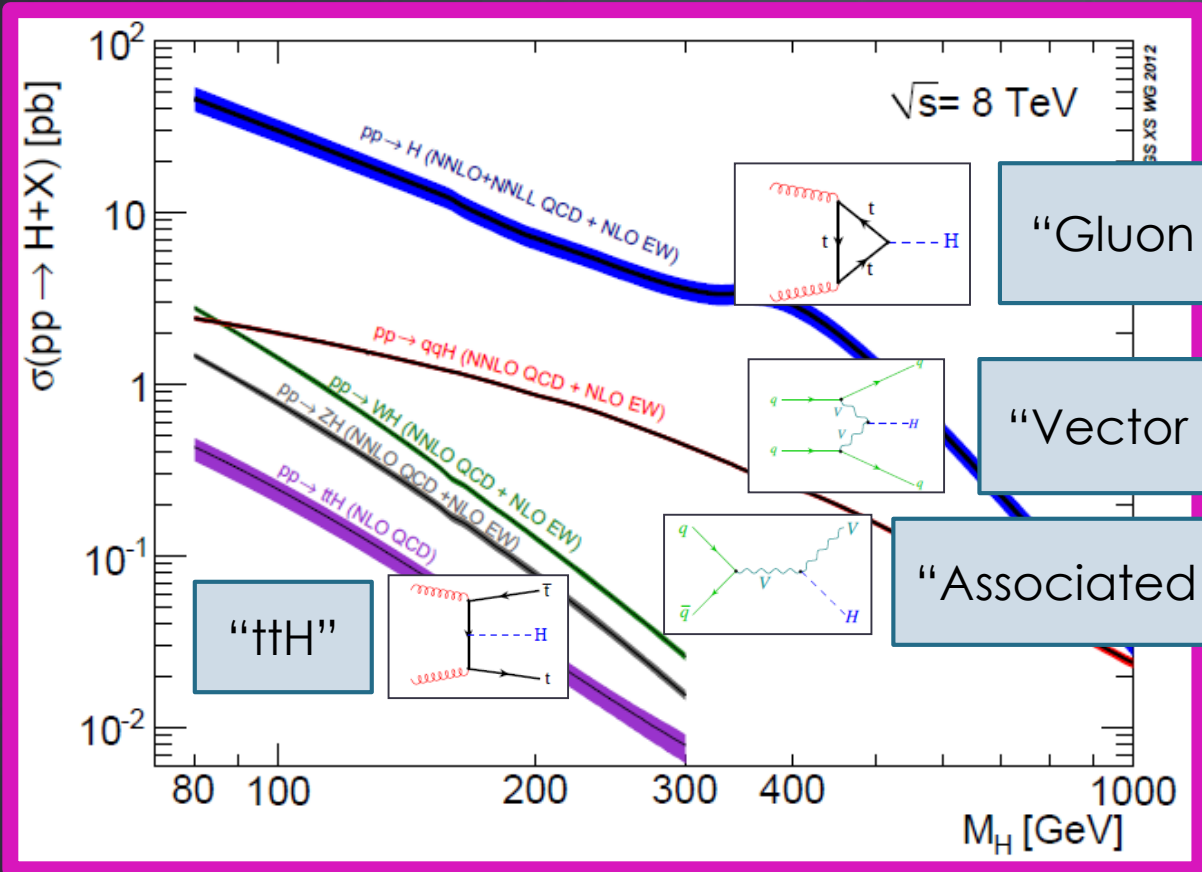
Alloy becoming superconducting
at low temperature = 10K.

For a given field, NbTi stands higher
currents at 1.9K than at 4.2K

LHC dipoles are kept
at 1.9-2 K



The production channels of the Scalar Boson



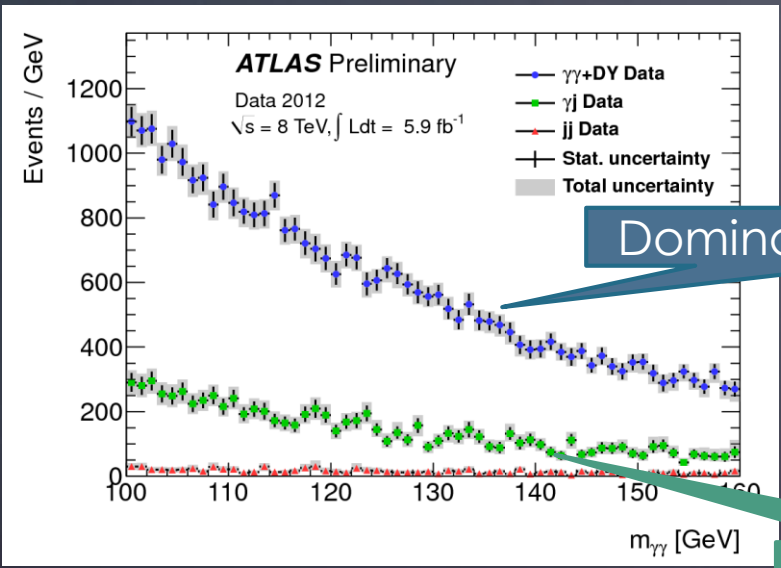
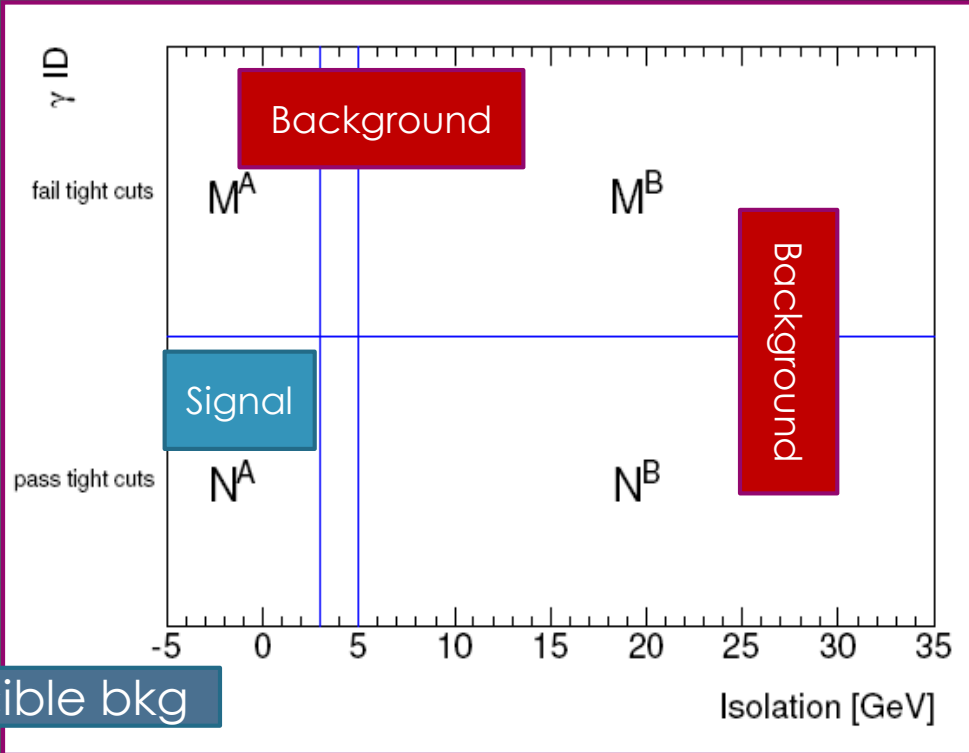
At LHC $\sqrt{s} \sim 8 \text{ TeV}$
 For $M \sim 100 \text{ GeV}$
 $x \approx M/\sqrt{s} = 0.01$

Measuring the fraction of fake photons

Principle

Genuine photons (signal) are ESSENTIALLY in Region NA
(Well isolated-satisfying tight selection criteria)

Fake photons are everywhere



Dominant irreducible bkg

Reducible bkg

In practice, one uses also MC to find the pure signal fraction

Constraints for the LHC and few numbers

361

- ▶ Use the existing LEP tunnel (27 Km long, ~100m under surface)
- ▶ Construct superconducting magnets to reach higher fields
- ▶ To reach high instantaneous and integrated Luminosities, make proton collisions (no proton-antiproton).
- ▶ Choice : Use two parallel rings in the same cold mass to let circulate the proton beams in opposite directions.
- ▶ Finally, 4 collision points along LHC to host ALICE, ATLAS, CMS and LHCb

Cost: ~5 Billion of Dollars

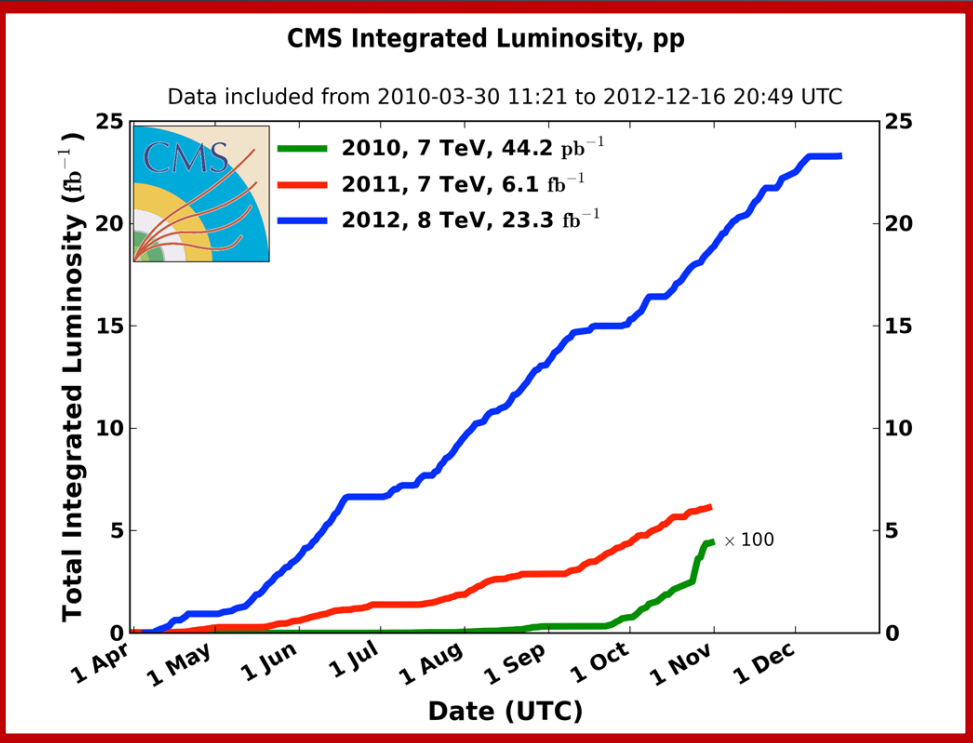
Peak magnetic field 8.3 Tesla

120 tons of Helium needed for cryogenic systems

Power Consumption: 120 MW, as for the Canton of Geneva: 19 MEuros/year

After repair: Restart in March 2010 .

Year	Overview	COM energy	Integrated luminosity [fb ⁻¹]
2010	Commissioning	7 TeV	0.04
2011	Exploring limits	7 TeV	6.1
2012	Production	8 TeV	23.1



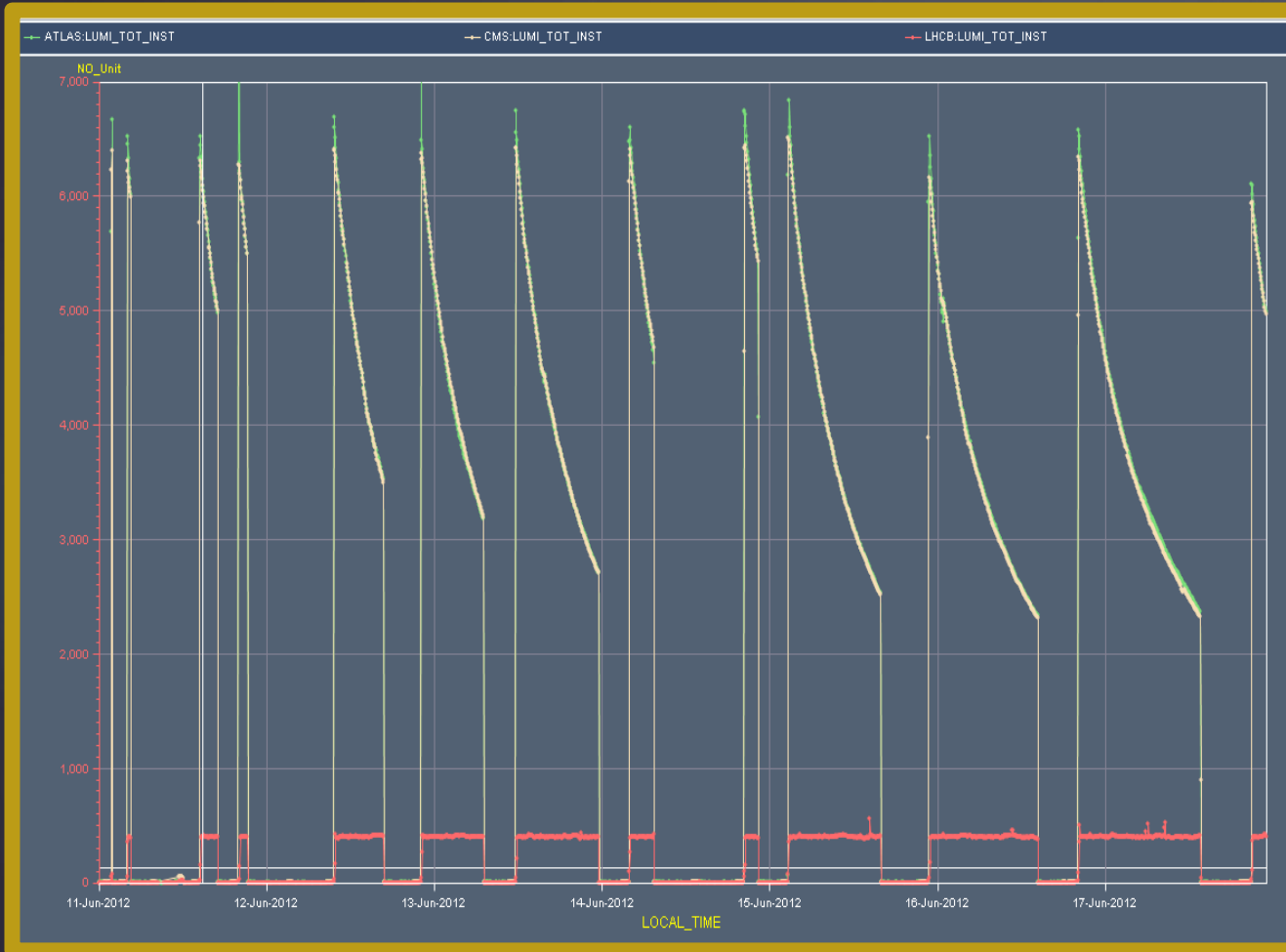
	2011	2012	Design
Energy Per beam	3.5TeV	4TeV	7TeV
Nb of bunches	1380	1380	2808
Bunch spacing (ns)	50	50	25
Beta* (CMS+ATLAS)	1.0	0.6	0.55
Nb of protons per bunch	1.45 x 10 ¹¹	1.7 x 10 ¹¹	1.15 x 10 ¹¹
Peak Luminosity	3.7 x 10 ³³	7.7 x 10 ³³	1 x 10 ³⁴
<nb _{collisions} > / bunchCross	~12	~30	19

Files 2014 / Media / Iconomidou-Foyard / 06/2015

Challenges for the beam lifetime

363

Invisibles 2014
16/06/2015



Fill	Duration	Ibeam	Lpeak [e30 cm-2s-1]	Lint [pb-1]	Dump
2723	2:26	2.03E+14	6406	46.06	Trip of RQX.A81B1, SEU?
2724	1:13	2.03E+14	6329	25.905	Electrical perturbation
2725	7:04	2.05E+14	6520	115.5	Trip of S81
2726	8:58	2.05E+14	6499	142.5	Electrical perturbation, FCMC
2728	11:41	2.06E+14	6525	171.5	Operator dump
2729	3:28	2.06E+14	6502	67.7	BLM self trigger
2732	1:52	2.06E+14	6592.5	40	QPS trigger RQX.R1, SEU?
2733	12:34	2.06E+14	6674	183	Triplet RQX.L2 tripped.
2734	15:33	2.01E+14	6257.5	203.5	Operator dump
2736	17:29	2.02E+14	6465.5	233	Operator dump
2737	3:36	1.99E+14	6021	66.1	RF Trip 2B2
Tot	51.1%			1301	

51% of time in stable beams; total **1.3 fb⁻¹** in one week

M. Lamont, 18 June 2012

The end point of the LHC beams

Want to dump the beams when

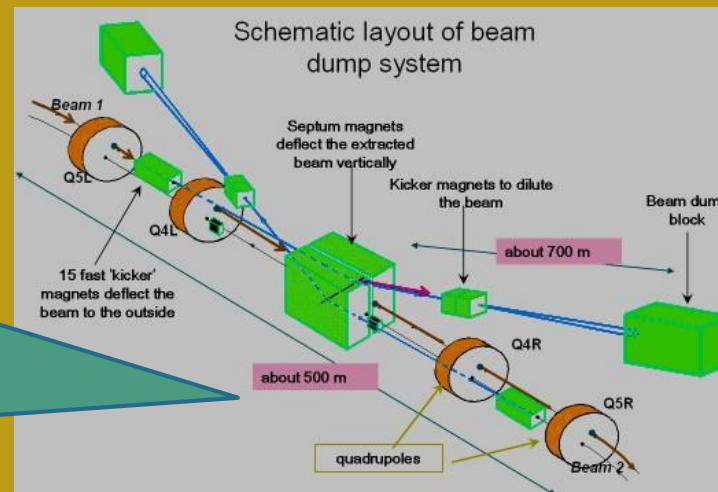
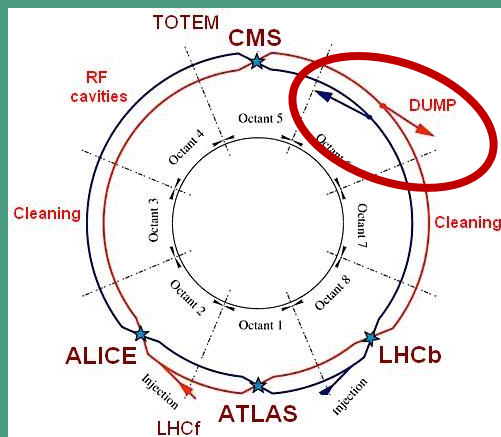
- 1) The beam quality has been deteriorated
- 2) the Beam loss monitors (BLM) installed along the machine detect activity beyond the safety threshold

During tests:
7MJ energy of a dipole released into a spot of the coil



© P.Pugnat

Invisibles 2015, Lydia Iconomidou-FC
16/06/2015



PROTON PHYSICS: BEAM DUMP

Energy:	3502 GeV	I(B1):	2.48e+09	I(B2):	9.43e+08
---------	----------	--------	----------	--------	----------

BTVDD.689339.B1 Updated: 17:10:36

BTVDD.629339.B2 Updated: 17:10:37

Comments 30-10-2011 17:12:49 :	BIS status and SMP flags	B1	B2
Dumped the last proton physics fill of the 2011	Link Status of Beam Permits	true	true
	Global Beam Permit	false	false
	Setup Beam	false	false
	Beam Presence	false	false
	Moveable Devices Allowed In Stable Beams	false	false

Preparing MD: ATS dry-run.

Combined M_H from $H \rightarrow \gamma\gamma$ and $H \rightarrow ZZ^* \rightarrow 4l$ channels, in ATLAS

Profiled Likelihood ratio

$$\Lambda(m_H) = \frac{L(m_H, \hat{\mu}_{\gamma\gamma}(m_H), \hat{\mu}_{4l}(m_H), \hat{\theta}(m_H))}{L(\hat{m}_H, \hat{\mu}_{\gamma\gamma}, \hat{\mu}_{4l}, \hat{\theta})}$$

Θ = " Nuisance parameter"
== systematic uncertainties



Example: the dominant uncertainties for $H \rightarrow \gamma\gamma$ mass (in %)

$$\hat{m}_H, \hat{\mu}_{\gamma\gamma}, \hat{\mu}_{4l}, \hat{\theta}$$

== **Maximum Likelihood Estimates (MLE)**, are the values of parameters that maximize $\Lambda(m_H)$.

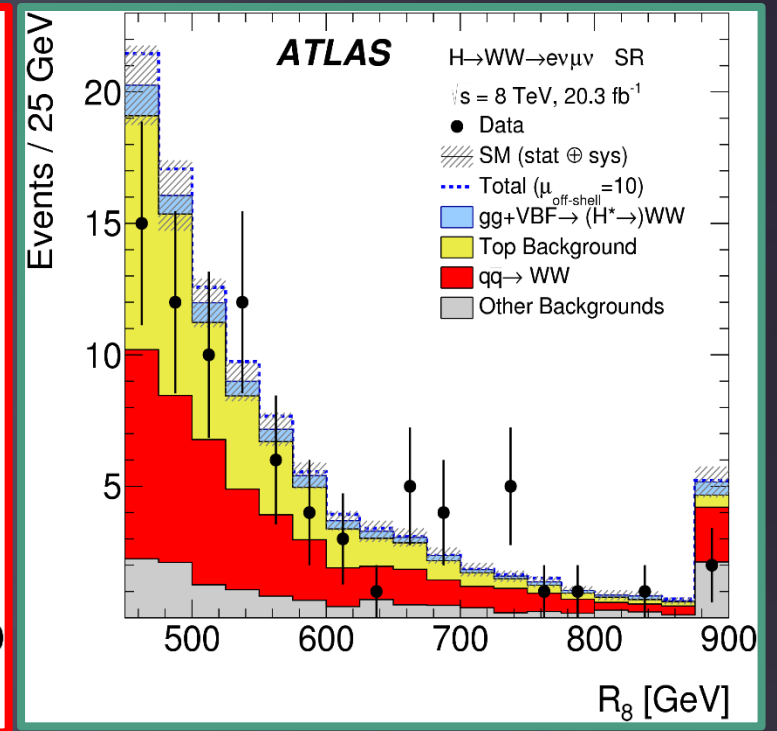
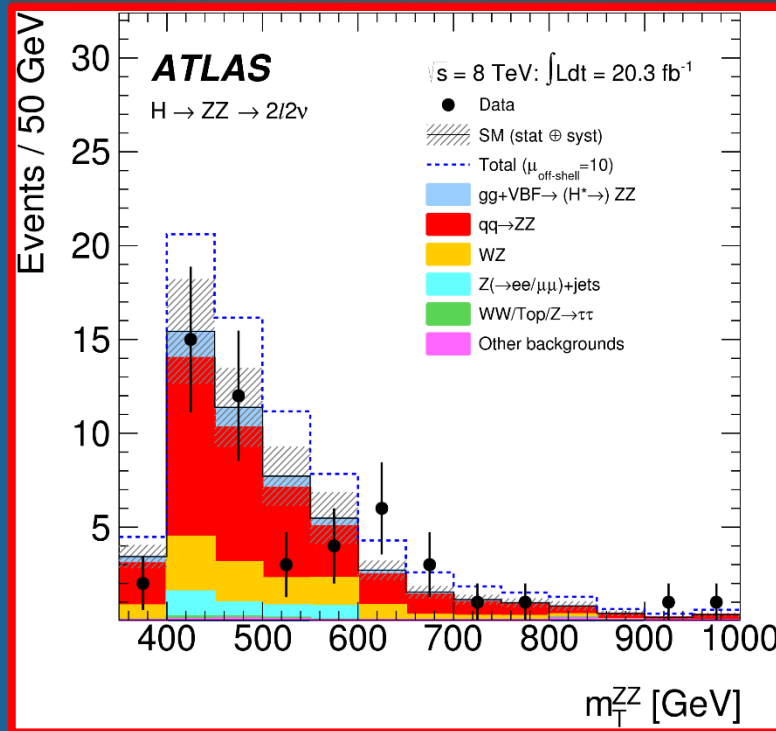
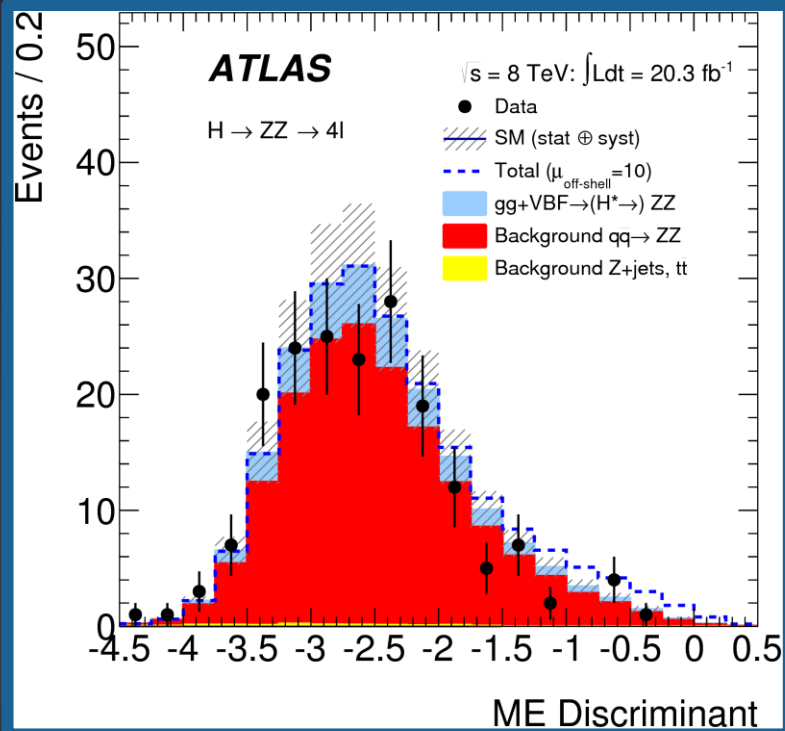
$$\hat{\mu}_{\gamma\gamma}(m_H), \hat{\mu}_{4l}(m_H), \hat{\theta}(m_H)$$

== **Conditional Maximum Likelihood Estimates (CMLE)** are the values of parameters that maximize $\Lambda(m_H)$ at fixed m_H

Class	Unconverted					Converted				
	Central		Rest		Trans.	Central		Rest		Trans.
	low p_{Tl}	high p_{Tl}	low p_{Tl}	high p_{Tl}		low p_{Tl}	high p_{Tl}	low p_{Tl}	high p_{Tl}	
$Z \rightarrow e^+e^-$ calibration	0.02	0.03	0.04	0.04	0.11	0.02	0.02	0.05	0.05	0.11
LAr cell non-linearity	0.12	0.19	0.09	0.16	0.39	0.09	0.19	0.06	0.14	0.29
Layer calibration	0.13	0.16	0.11	0.13	0.13	0.07	0.10	0.05	0.07	0.07
ID material	0.06	0.06	0.08	0.08	0.10	0.05	0.05	0.06	0.06	0.06
Other material	0.07	0.08	0.14	0.15	0.35	0.04	0.04	0.07	0.08	0.20
Conversion reconstruction	0.02	0.02	0.03	0.03	0.05	0.03	0.02	0.05	0.04	0.06
Lateral shower shape	0.04	0.04	0.07	0.07	0.06	0.09	0.09	0.18	0.19	0.16
Background modeling	0.10	0.06	0.05	0.11	0.16	0.13	0.06	0.14	0.18	0.20
Vertex measurement	0.03									
Total	0.23	0.28	0.24	0.30	0.59	0.21	0.25	0.27	0.33	0.47

Split the uncertainties of the 2 channels ($ZZ^* \rightarrow 4l$ and 2γ) in **correlated and uncorrelated nuisance parameters**

The Width of the Scalar Boson



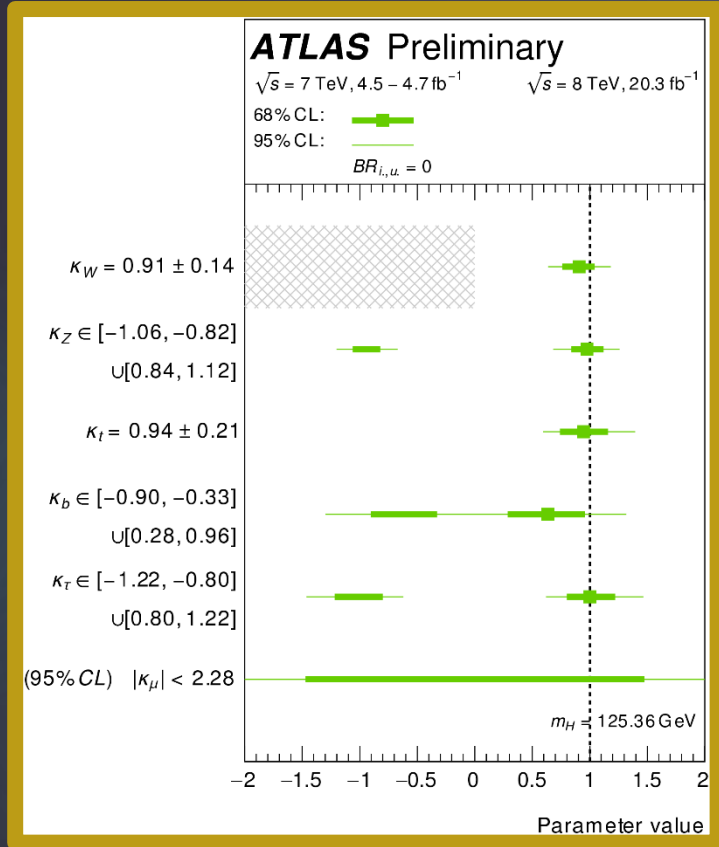
ZZ->4l
 ME discriminant combining
 8 variables for events
 With $220 \text{ GeV} < m_{4l} < 1000 \text{ GeV}$

ZZ->2l2nu
 Presence of neutrinos
 Look at m_T^{ZZ} in the region
 $380 \text{ GeV} - 1000 \text{ GeV}$

WW->ev mu nu
 Combine m_T^{WW} and m_{ll}

$$R_8 = \sqrt{m_{\ell\ell}^2 + (a \cdot m_T^{WW})^2}$$

Generic beyond SM models: individual couplings



Assumptions : Only SM particles in loops, no Invisibles → Check Kappas

